Characterizing the regulation of the inducible *HSP70* mRNA in yeasts and mammalian cells subjected to heat shock

Lokha Ranjani Alagar Boopathy

Department of Biochemistry

McGill University, Montreal

May 2024

A thesis submitted to McGill University in partial fulfillment of the requirements of the degree of Doctor of Philosophy

© Lokha Ranjani Alagar Boopathy, 2024

ABSTRACT

Cellular perturbations cause the proteins to misfold precluding their functions. In response to proteotoxic stress, cells downregulate gene expression by reducing cap-dependent translation. Concurrently, they upregulate the expression of a subset of molecular chaperones known as Heat Shock Proteins (HSPs) in charge of protein folding. The fast induction and rapid attenuation of the inducible HSP70 expression define the Heat Shock Response (HSR), which is critical for cell survival from stress. However, the ubiquitous expression of the inducible HSP70 is toxic and promotes tumorigenesis in mammalian cells. Thus, the fast degradation of the *HSP70* mRNA allows for tailoring the HSP70 synthesis to the misfolded protein load in the cell is vital.

Since the HSR is an evolutionarily conserved survival response, the induction and attenuation of the HSR have been studied in different model organisms. While the transcription of *HSP70* mRNA is well studied, our initial studies revealed an important difference between yeast and mammalian cells on *HSP70* mRNA translation. In yeast, the HSP70 synthesis peaks during heat shock, while in mammalian cells, it peaks during recovery. Based on this, we hypothesize that distinct regulatory elements in the sequence of the inducible *HSP70* mRNA in yeast and mammalian cells regulate its translation upon heat shock and recovery.

We discovered that in *Saccharomyces cerevisiae*, the coding sequence of the inducible *HSP70, SSA4,* is biased towards rare codons. These codons promote ribosome stalling and collisions on the mRNA that result in the control of Ssa4p expression by the ribosome quality control (RQC) mechanism. In RQC, the ribosomal protein Asc1p stabilizes the collided ribosomes triggering a series of downstream events to reduce translation and dissociate ribosomes. Our work elucidates the SSA4 coding sequence as a novel regulatory element and describes RQC as an

unexpected mechanism to restrain, rather than enhance, the synthesis of Ssa4p during heat shock. Interestingly, Asc1p also mediates decay of *SSA4* mRNA independently of RQC. Thus, Asc1p appears as a novel master regulator of the HSR.

The RQC-mediated regulation of inducible HSP70 synthesis is not conserved in mammals (Hspa1a) because it is rich in optimal codons. However, the 5' UTR forms a compact structure upon heat shock made of several stem loops suggesting a regulation at the level of translation initiation. We have found that the HSPA1A synthesis during heat shock, but not during recovery, is independent of the helicase eIF4A and the ternary complex factor eIF2α. Thus, we propose the 5' end of *Hspa1a* mRNA to regulate its translation by acting like an internal ribosome entry (IRES). However, assessing the functions of each stem-loop by causing the unzip mutation did not show a significant effect on HSP70 synthesis. Interestingly, using a CRISPR-cas9-based single-base editing approach, we defined specific nucleotides on the 5' UTR and CDS to regulate translation induction during heat shock. As a result of my thesis work, we have identified novel molecular mechanisms that regulate the translation of *Hspa1a* mRNA upon heat shock and its decay during recovery.

RÉSUMÉ

Les perturbations cellulaires entraînent un mauvais repliement des protéines, empêchant ainsi leurs fonctions. En réponse au stress protéotoxique, les cellules régulent à la baisse l'expression des gènes en réduisant la traduction dépendante de la coiffe. Parallèlement, ils régulent à la hausse l'expression d'un sous-ensemble de chaperons moléculaires appelés protéines de choc thermique (HSP) responsables du repliement des protéines. L'induction rapide et l'atténuation rapide de l'expression inductible de la HSP70 définissent la réponse au choc thermique (HSR), qui est essentielle à la survie des cellules en cas de stress. Cependant, l'expression omniprésente de la HSP70 inductible est toxique et favorise la tumorigenèse dans les cellules de mammifères. Ainsi, la dégradation rapide de l'ARNm de la HSP70 permet d'adapter la synthèse de la HSP70 à la charge protéique mal repliée dans la cellule, ce qui est vital.

Le HSR étant une réponse de survie conservée au cours de l'évolution, l'induction et l'atténuation du HSR ont été étudiées dans différents organismes modèles. Bien que la transcription de l'ARNm de HSP70 soit bien étudiée, nos premières études ont révélé une différence importante entre les cellules de levure et les cellules de mammifères en ce qui concerne la traduction de l'ARNm de HSP70. Chez la levure, la synthèse de la HSP70 atteint son maximum lors d'un choc thermique, tandis que dans les cellules de mammifères, elle culmine lors de la récupération. Sur cette base, nous émettons l'hypothèse que des éléments régulateurs distincts de la séquence de l'ARNm inductible de la HSP70 dans les cellules de levure et de mammifères régulent sa traduction lors d'un choc thermique et d'une reprise.

Nous avons découvert que chez Saccharomyces cerevisiae, la séquence codante de la HSP70 inductible, SSA4, est biaisée en faveur de codons rares. Ces codons favorisent le blocage des

ribosomes et les collisions sur l'ARNm, ce qui entraîne le contrôle de l'expression de SSA4p par le mécanisme de contrôle de la qualité des ribosomes (RQC). Dans le RQC, la protéine ribosomique Asc1p stabilise les ribosomes en collision, déclenchant une série d'événements en aval visant à réduire la traduction et à dissocier les ribosomes. Nos travaux élucident la séquence codante SSA4 en tant que nouvel élément régulateur et décrivent le RQC comme un mécanisme inattendu visant à restreindre, plutôt qu'à améliorer, la synthèse de SSA4p lors d'un choc thermique. Fait intéressant, Asc1p médie également l'ARNm de SSA4 indépendamment du RQC. Ainsi, ASC1p apparaît comme un nouveau régulateur principal du HSR.

La régulation de la synthèse de la HSP70 inductible par l'intermédiaire du RQC n'est pas conservée chez les mammifères (*Hspa1a*) car elle est riche en codons optimaux. Cependant, l'UTR 5' forme une structure compacte lors d'un choc thermique composée de plusieurs boucles de tige suggérant une régulation au niveau de l'initiation de la traduction. Nous avons découvert que la synthèse de HSP70 pendant le choc thermique, mais pas pendant la récupération, est indépendante de l'hélicase eIF4A et du facteur complexe ternaire eIF2α. Ainsi, nous proposons l'extrémité 5' de l'ARNm de *Hspa1a* pour réguler sa traduction en agissant comme une entrée interne du ribosome (IRES). Cependant, l'évaluation des fonctions de chaque tige-boucle en provoquant la mutation unzip n'a pas montré d'effet significatif sur la synthèse de HSPA1A. Fait intéressant, en utilisant une approche d'édition à base unique basée sur CRISPR-Cas9, nous avons défini des nucléotides spécifiques sur l'UTR 5' et le CDS pour réguler l'induction de la traduction lors d'un choc thermique. À la suite de mes travaux de thèse, nous avons identifié de nouveaux mécanismes moléculaires qui régulent la traduction de l'ARNm de *Hspa1a* lors d'un choc thermique et sa désintégration lors de la récupération.

ACKNOWLEDGEMENTS

I would like to express my deepest gratitude to Dr. Maria Vera Ugalde, my supervisor, for welcoming me to the lab and entrusting me with this extraordinary project. Her unwavering support has played a pivotal role in my every success and milestone. I am grateful for her visionary guidance, relentless encouragement and letting me realize my potential. Thank you for being an inspiring mentor and a driving force behind my journey.

I would like to express my gratitude to the members of my research advisory committee. First and foremost, thanks to Dr. Jerry Pelletier for always welcoming scientific discussions about the project. He offered support to our lab in terms of techniques and reagents. I was unfortunate to not to have the opportunity to thank him in person for all his letters of recommendation for my funding applications. He will be missed. Next, I would like to thank Dr. Selena Sagan for offering help and guidance with the project all along. Her valuable insights on the project eventually brought an opportunity to collaborate, which was an excellent experience working with her lab members. Finally, I would like to express my appreciation to Dr. Josée Dostie, for graciously agreeing to join my research advisory committee on short notice. Her last-minute insights and thoughts about the project were truly encouraging.

Thanks to Dr. Raquel Cuella-Martin from Department of Functional genomics for her collaboration, offering us the plasmids, reagents, and supervision for CRISPR-Cas9 cloning experiment. I extend my sincere appreciation to Dr. Rafael Cuesta Sanchez for his technical assistance, critical insights, and the time he dedicated to reviewing my research articles and presentation rehearsals. His suggestions for improvements and thoughtful questions have been invaluable.

I have a long list of current and previous lab members who either contributed to the project or being a moral support: Suleima Jacob-Tomas, Alan Ruochen Xiao, Sonya Madan, Maanasa Koripalli, Irene Garcia de Andres, Dr. Célia Alecki, Emma Beadle, Ryan Huang, Aitana Garcia-Bueno Rico, Kyla Edelmeier, Luca Lazzari, Idia Boncheva, Kevin Munoz Portocarrero, Stella Jiaming Xu, Dr. Mario Fernandez Comaduran, Talar Ghadanian, Jessamine Mattson, Alexandra Dimitrov, Jan Mak, Shruti Iyer, Iratxe Aldaba Gonzalez, Nathan Pilkey, and Evan Daynard. I thank them all for being a wonderful and fun colleagues, for their valuable feedback and discussions that helped prepare me for my PhD milestone presentations.

Particularly, I want to express gratitude to my students Emma, Ryan, Maanasa, Luca, Aitana, Delina, Kyla, Kevin, Jessamine, and Alexandra for their technical assistance. Special mention to Jessamine, Alexandra, Kevin and Shruti for their significant help with CRISPR-Cas9 cloning. I extend my heartfelt thanks to Stella, Luca, Talar, Alan, and Suleima for being an excellent source of moral support. I sincerely appreciate Célia for her contributions to the project and feedback.

I want to extend a heartfelt appreciation to my brother, Dr. Sethu Kovendhan Boopathy Jegathambal, for being a patient listener and an outstanding source of happiness and encouragement. Your presence, unconditional love, unwavering care and support hold immense value to me!!! I thank the rest of my family Dr. Komahan Boopathy and my mother Jegathambal Ramiah, and my father Boopathy Alagar Chetty for their care, understanding and encouragement.

I would like to thank my friends Dr. Zahraa Chorghay, Dr. Archita Rajasekaran, Dr. Senthil Kumar Duraisamy, Dr. Vincent Francis, Dr. John Thomas and Dr. Sathiyamoorthy Selladurai for their endless support and motivation. A special acknowledgment to Zahraa for her assistance in refining my funding applications.

Finally, I would like to appreciate my funding sources including Centre de Recherche en Biologie Structurale (CRBS), Fonds de recherche du Québec - Santé (FRQS), and the Department of Biochemistry. Their support in the form of tuition assistance, Graduate Research Enhancement and Travel Awards, McKinnell Travel Award, and the Arthur S. Hawkes Fellowship has been huge support and instrumental in my academic journey.

PREFACE

This thesis was written according to the McGill University's "Guidelines for Thesis Preparation". The candidate has chosen to present in a "Manuscript-based thesis" format by following these guidelines:

"As an alternative to the traditional format, a thesis may be presented as a collection of scholarly papers of which the student is the first author or co-first author. A manuscript-based doctoral thesis must include the text of a minimum of two manuscripts published, submitted or to be submitted for publication.

Manuscripts for publication in journals are frequently very concise documents. A thesis, however, is expected to consist of more detailed, scholarly work. A manuscript-based thesis will be evaluated by the examiners as a unified, logically coherent document in the same way a traditional thesis is evaluated."

The information of the published articles and manuscript in preparation are listed below. The contributions of all authors to each article are detailed in the "Contributions of authors" section.

Manuscripts included in this thesis:

1. **Lokha R Alagar Boopathy**, Suleima Jacob-Tomas, Célia Alecki, and Maria Vera. Mechanisms tailoring the expression of heat shock proteins to proteostasis challenges. J Biol Chem. 2022;298(5). doi: 10.1016/j.jbc.2022.101796.

2. **Lokha R Alagar Boopathy**, Emma Beadle, Aitana Garcia-Bueno Rico, and Maria Vera. Proteostasis regulation through ribosome quality control and no-go-decay. *WIREs RNA*. 2023;14(6):e1809. doi:10.1002/wrna.1809.

3. **Lokha R Alagar Boopathy**, Emma Beadle, Alan RuoChen Xiao, Aitana Garcia-Bueno Rico, Celia Alecki, Irene Garcia de-Andres, Kyla Edelmeier, Luca Lazzari, Mehdi Amiri, and Maria Vera. The ribosome quality control factor Asc1 determines the fate of HSP70 mRNA on and off the ribosome. Nucleic Acids Res. 2023;51(12):6370-6388. doi:10.1093/nar/gkad338.

4. **Lokha R Alagar Boopathy**, Shruti Iyer and Maria Vera. Characterization of *cis*- and *trans*-regulatory factors required for the translation *HSP70* mRNA during heat shock and recovery. *Manuscript In Preparation*

CONTRIBUTION TO ORIGINAL KNOWLEDGE

The contributions to original knowledge are listed below:

Chapter 2:

In yeast…

1. The coding sequence of inducible *HSP70* mRNA (*SSA4* in yeast) is highly non-optimal compared to constitutively expressed HSP70s.

2. Through the deletion of RQC factors Asc1p and Hel2p, we found that the coding sequence of *SSA4* mRNA is repressing the translation by ribosome quality control (RQC) during heat shock.

3. *SSA4*, the first endogenous mRNA characterized to undergo regulation by RQC.

4. During recovery, the *SSA4* mRNA is not being translated and so there is no regulation by RQC.

5. Optimizing the CDS of *SSA4* mRNAs enables them to escape the regulation by RQC.

6. The binding of Asc1p to the ribosome is required for the regulation of *SSA4* mRNA translation.

7. Codon optimized *SSA4* mRNA gets translated under permissive conditions. This suggests a different mechanism in action to regulate undesired Ssa4p expression upon leaky transcription under permissive conditions.

8. *SSA4* mRNA does not undergo clearance by RQC or No-Go Decay (NGD). Instead, Asc1p is solely responsible for the decay of the *SSA4* mRNA during recovery independently of ribosome binding activity.

9. Degradation of codon optimized *SSA4* mRNAs are also mediated by Asc1p during recovery.

10. Asc1p functions along with helicase Dhh1p and exonuclease Xrn1p, to mediate the decay of inducible *HSP70* mRNA during recovery.

11. Asc1p is a prosurvival factor and a new role as master regulator for the cells to survival during stress. The prosurvival activity of Asc1p is independent of its ribosome binding.

12. We identified novel RQC factors Rps28A and Rps19B functions alongside Asc1p during heat shock to regulate the Ssa4p expression.

13. Rps19B could be a generic RQC factor whereas Rps28A appears to be specific to certain substrate mRNAs (eg., *SSA4* mRNA) and/ or cell state specific (heat shock).

14. Collectively, Asc1p regulates the *SSA4* mRNA translation and decay by different pathways. For the effect on *SSA4* mRNA translation, Asc1p needs to bind to ribosome whereas for the decay no ribosome binding is needed.

Chapter 3:

In mammalian cells….

1. The translation efficiency of inducible *Hsp70* mRNA (*Hspa1a*) is higher during recovery than during heat shock.

2. The *Hspa1a* mRNA translation is independent of cap-dependent translation initiation factors-eIF4A and eIF2α during HS.

3. The translation of *Hspa1a* mRNA during recovery requires eIF4A and eIF2α.

4. Through knock down RACK1 (Asc1 ortholog), we identified that RQC of *Hspa1a* mRNA is not conserved in MEFs.

5. The *Hspa1a* mRNA does not require non-canonical translation factors RACK1 or eIF3d for its translation during HS or recovery.

6. The 5'UTR and 102 nts from CDS of *Hspa1a* mRNA is favoring the translation induction during HS.

7. The stem loop close to the 5' cap inhibits the binding of cap-recognition factors and thus the translation of *Hspa1a* mRNA under permissive conditions.

8. The stem loops described to be important (H1, H4 and H6) for *in vitro* structure formation by Pyle's lab did not constitute any significant effect on translation of *Hspa1a* mRNA *in vivo* during heat shock.

9. Through CRISPR-Cas9 single base editing technique, we identified certain nucleotides (146-147 and 179-181) on the *Hspa1a* mRNA to be important for its translation induction during HS.

10. The 5'UTR *Hspa1a* mRNA encompasses two binding sites for miRNA - Mir-30c-1-3p and RNA binding proteins such as PCBP1 and PCBP2 which could mediate structural changes on the mRNA and facilitate translation.

11. The formation of a temperature-induced RNA thermometer resembling HCV or CrPV IRES-like structure on the *Hspa1a* mRNA is still under investigation.

AUTHORS CONTRIBUTIONS

CHAPTER 1: INTRODUCTION

1. **Lokha R Alagar Boopathy**, Suleima Jacob-Tomas, Célia Alecki, and Maria Vera. Mechanisms tailoring the expression of heat shock proteins to proteostasis challenges. J Biol Chem. 2022;298(5). doi:10.1016/j.jbc.2022.101796.

   L.R.A.B and S.J.T conceptualization; L.R.A.B., S.J.T., and C.A drafted the manuscript; M.V. supervision; L.R.A.B., S.J.T., and M.V. revised the final manuscript.

2. **Lokha R Alagar Boopathy**, Emma Beadle, Aitana Garcia-Bueno Rico, and Maria Vera. Proteostasis regulation through ribosome quality control and no-go-decay. *WIREs RNA*. 2023;14(6):e1809. doi:10.1002/wrna.1809

   L.R.A.B conceptualization, L.R.A.B., E.B., and A.G.B.R., drafted the manuscript; M.V. supervision; L.R.A.B., E.B., and M.V., revised and edited the final manuscript.

CHAPTER 2:

Lokha R Alagar Boopathy, Emma Beadle, Alan RuoChen Xiao, Aitana Garcia-Bueno Rico, Celia Alecki, Irene Garcia de-Andres, Kyla Edelmeier, Luca Lazzari, Mehdi Amiri, and Maria Vera. The ribosome quality control factor Asc1 determines the fate of HSP70 mRNA on and off the ribosome. Nucleic Acids Res. 2023;51(12):6370-6388. doi:10.1093/nar/gkad338.

L.R.A.B and M.V. conceptualization; L.R.A.B., C.A and M.V drafted the manuscript; L.R.A.B., E.B., and A.R.X., performed western blotting and spot assay; A.G.B.R., I.G.A., and K.E., performed western blotting; A.R.X and M.V. performed codon optimization, smFISH and smFISH quantifications; L.R.A.B performed northern blots, growth assay and polysome profiling;

C.A., conducted coimmunoprecipitation and mass spectrometry data analysis. L.L., helped with a few RNA extractions. M.A. analyzed ribosome profiling data for ribosome pausing; M.V. supervision; L.R.A.B., C.A., and M.V. revised the final manuscript.

CHAPTER 3:

Lokha R Alagar Boopathy, Shruti Iyer and Maria Vera. Characterization of *cis*- and *trans*-regulatory factors required for the translation of inducible *HSP70* mRNA during heat shock and recovery. *Manuscript In Preparation*

L.R.A.B. and M.V. conceptualized and designed the study. L.R.A.B and S.I. generated stable cell lines expressing guide RNAs, screened the cell lines; L.R.A.B., performed western blots, smFISH, polysome profiling, northern blotting, qPCR, and quantification of the data. M.V. conducted the luciferase assays. L.R.A.B. and M.V. drafted and edited the manuscript.

TABLE OF CONTENTS

LIST OF FIGURES

LIST OF TABLES

LIST OF ABBREVIATIONS

4E-BP	Eukaryotic Initiation Factor 4E-Binding Protein
4EHP	Eukaryotic initiation factor 4E homologous protein
8-oxoG	8-oxoguanosine
AAQ	Ala-Ala-Gln (dominant negative mutation in eRF1)
ABCF1	ATP-binding cassette sub-family F member 1
Actb	Actin Beta
AD	Alzheimer's Disease
AFD	Amphid Neurons with Finger like Ciliated Ending
Ago2	Argonaute 2
ALS	Amyotrophic Lateral Sclerosis
APOBEC1	Apolipoprotein B mRNA Editing Enzyme Complex 1
AREs	AU-rich Elements
ASC-1	Activating Signal Cointegrator Complex
ASCC3	Activating Signal Cointegrator 1 Complex Subunit 3
ASM	Axonemal dynein heavy chain
ATE-1	Arginyltransferase-1
ATP	Adenosine Triphosphate
AU	Adenylate Uracil (AU)-rich Element
AUF1	ARE/poly(U)-binding/degradation factor 1
BAG1	BCL2-associated athanogene 1
BAG3	BCL2-associated athanogene 3
BiP	Binding immunoglobulin Protein
BSA	Bovine Serum Albumin
CAT	C-terminal alanine-threonine
Cdc48	Cell division cycle 48
cDNA	Complementary DNA
CDS	Coding Sequence
CFTR	Cystic Fibrosis Transmembrane Conductance Regulator
ChFP	Cherry Fluorescent Protein
CHIP	Carboxy-Terminus of HSP70-Interacting Protein
CO2	Carbon Dioxide
cpn60	chaperonin 60
CRISPR-Cas9	Clustered Regularly Interspaced Short Palindromic Repeats and CRISPR-associated protein 9
CrPV	Cricket Paralysis Virus
Cryo-EM	Cryo-Electron Microscopy
C-terminal	Carboxyl-terminal end of a protein or peptide
Cue2p	Coupling of Ubiquitin conjugation to ER degradation

DAPI	4',6-Diamidino-2-Phenylindole
DCP1/2	Decapping protein 1/2
DDX6	DEAD-box helicase 6
Ded1	DEAD-box Helicase 1
Dhh1p	DEAD box Helicase Homolog
DMEM	Dulbecco's Modified Eagle Medium
DNaseI	Deoxyribonuclease I
Doa1p	Degradation Of Alpha
Dom34	Duplication Of Multilocus region 34
DTT	Dithiothreitol
Dxo1	Decapping eXOnuclease 1
Eap1	eIF4E-associated protein 1
EDC3	Enhancer of mRNA decapping protein 3
EDF1	Endothelial differentiation-related factor
EDTA	Ethylenediaminetetraacetic acid
eEF1A1	Eukaryotic Elongation Factor 1 Alpha 1
eEF2	Eukaryotic elongation factor 2
EF-tu	Elongation factor thermo unstable
EGTA	Ethylene glycol-bis(2-aminoethylether)-N,N,N',N'-tetraacetic acid
eIF	Eukaryotic translation Initiation Factor
eIF2B	Eukaryotic translation Initiation Factor 2B
eIF2α	Eukaryotic translation Initiation Factor 2 alpha
eIF3	Eukaryotic translation Initiation Factor 3
eIF3D	Eukaryotic translation Initiation Factor 3D
eIF4A	Eukaryotic translation Initiation Factor 4A
eIF4B	Eukaryotic translation Initiation Factor 4B
eIF4E	Eukaryotic translation Initiation Factor 4E
eIF4F	Eukaryotic translation Initiation Factor 4F
eIF4G	Eukaryotic translation Initiation Factor 4G
EJC	Exon-Junction Complex
ER	Endoplasmic Reticulum
eRF1	Eukaryotic Release Factor 1
eRF3	Eukaryotic Release Factor 3
FACT	Facilitates Chromatin Transcription
FBS	Fetal Bovine Serum
FLUC	Firefly Luciferase
FTP	Flag-TEV-Protein A
G3BP1	Ras GTPase-activating protein(GAP)-binding protein 1
GCN2	General amino acid Control Nonderepressible 2
GDP	Guanosine diphosphate

GFP	Green Fluorescent Protein
GGQ	Glycine-Glycine-Glutamine (motif)
GIGYF2	GRB10 interacting GYF protein 2
gRNA	Guide RNA
GRP78	Glucose-regulated protein 78
GTP	Guanosine triphosphate
Gtpbp2	GTP-binding protein 2
HA	Hemagglutinin
Hbs1	Hsp70 subfamily B suppressor 1
HCV	Hepatitis C Virus
Hel2	Histone E3 Ligase 2
HeLa cells	Henrietta Lacks-derived cells
HEPES	4-(2-hydroxyethyl)-1-piperazineethanesulfonic acid
HGNC	HUGO Gene Nomenclature Committee
HIP	HSP70 Interacting Protein
His-tag	Histidine tag
HOP	HSP70/HSP90 Organizing Protein
HPLC	High-Performance Liquid Chromatography
HRI	Heme-regulated inhibitor kinase
HS	Heat Shock
HSC70	Heat Shock Cognate 70
HSE	Heat Shock Element
HSF1	Heat Shock Factor 1
HSP	Heat Shock Protein
HSP27	Heat Shock Protein 27
HSP60	Heat Shock Protein 60
HSP70	Heat Shock Protein 70
HSP82	Heat Shock Protein 82
HSP90	Heat Shock Protein 90
HSPA1A	Heat Shock Protein Family A Member 1A (gene)
HSPB8	heat shock protein family B (small) member 8
HSR	Heat Shock Response
HTT	Huntingtin gene
IGR	Intergenic Region
IP	Immunoprecipitation
IRES	Internal ribosome entry site
ISR	Integrated Stress Response
KCl	Potassium Chloride
kD	kilodalton
KO	Knockout

Ltn1	Listerin E3 ubiquitin ligase 1
m6A	N6-Methyladenosine
m7G	7-Methyl Guanosine
MAPK	Mitogen-activated protein kinase
Mbf1	Multi-protein bridging factor 1
MED12	Mediator Complex Subunit 12
Mex67	mRNA Export Factor 67
MG132	Proteasome inhibitor
miRNAs	microRNAs
mRNA	Messenger RNA
MRPL18	Mitochondrial Ribosomal Protein L18
MS	Mass Spectrometry
MS2V6	MS2 stemloop version 6
mtHSP70	Mitochondrial Heat Shock Protein 70
mTOR	Mammalian Target of the Rapamycin
Mtr2	mRNA Transporter 2
mut	Mutation
N4BP2	Nedd4-Binding Protein 2
NA	Numerical Aperture
nCas9	Cas9 nickase
ND	Neurodegenerative Disease
ND40	Nonidet P-40
NEF	Nucleotide Exchange factor
NEMF	Nuclear Export Mediator Factor
NGD	No-Go Decay
NIKS	Asparagine-Isoleucine-Lysine-Serine (motif)
nM	Nanomolar (a unit of concentration)
NMD	Nonsense-Mediated Decay
NONU1	Non-Uniform 1
NRD	Nonfunctional rRNA Decay
NSD	Non-Stop Decay
NTD	NucleoTide binding Domain
N-terminal	Amino-terminal end of a protein or peptide
nts	Nucleotides
OD	Optical Density
O-GlcNACylation	O-linked N-acetylglucosaminylation
ORF	Open Reading Frame
osmolality	Osmotic concentration
OTUD3	OTU deubiquitinase 3
PABP	Poly-A Binding Protein

PAM	Protospacer Adjacent Motif
PAN2/3	Poly(A)-specific ribonuclease complex 2/3
PARN	Poly(A) Ribonuclease
PB	Processing body
PBS	Phosphate Buffered Saline
PBSM	Phosphate Buffered Saline with Magnesium
PBST	Phosphate-Buffered Saline with Tween 20
PDB	Protein Data Bank
Pep-GFP	Truncated GFP peptides
PERK	PKR-like ER kinase
PFA	Paraformaldehyde
PGK1	Phosphoglycerate Kinase 1
pH	Potential of Hydrogen
PK-I	Pseudoknot I
PKR	Protein Kinase R
pl3	Nucleolar Protein 3
pLKO.1	Lentiviral Expression Vector
poly-A tail	Polyadenine tail
PQC	protein quality control
PRIDE	PRoteomics IDEntifications database
PTC	Premature Termination Codon
P-TEFb	Positive Transcription Elongation Factor b
PXD	ProteomeXchange Data
RACK1	Receptor for Activated C Kinase 1
RBPs	RNA Binding Proteins
RING domain	Really Interesting New Gene domain
RIPA	Radioimmunoprecipitation Assay
RLuc	Renilla Luciferase
RNA	Ribonucleic Acid
RNAPII	RNA Polymerase II
RNase R	Ribonuclease R
RNA-Seq	RNA Sequencing
RNC	Ribosome-Nascent Chain complex
RNP	Ribonucleoprotein
Rpl1B	Ribosomal protein L1B
RPM	Revolutions Per Minute
Rps19B	Ribosomal Protein S19B
Rps2	Ribosomal protein S2
Rps20	Ribosomal Protein S20
Rps28A	Ribosomal protein S28A

Rps7B	Ribosomal protein S7B
RQC	Ribosome Quality Control
RQT	Ribosome Quality Control Trigger
rRNA	Ribosomal RNA
RT	Room Temperature
RT-qPCR	Reverse Transcription Quantitative Polymerase Chain Reaction
S. cerevisiae	Saccharomyces cerevisiae
S6K	S6 kinase
SBD	Substrate Binding Domain
sCMOS	Scientific Complementary Metal-Oxide-Semiconductor
SDS-PAGE	Sodium Dodecyl Sulfate-Polyacrylamide Gel Electrophoresis
SG	Stress granule
SGO2	Shugoshin 2
sgRNA	Single Guide RNA
SHAPE	Selective 2'-Hydroxyl Acylation analyzed by Primer Extension
shRNA	Short Hairpin RNA
Sis1	Suppressor of Initiation of Transcription(SIT`)-Suppressor
Ski7	SuperKIller 7
Slh1	Ski2-like helicase
smFISH	Single-molecule Fluorescence In Situ Hybridization
SMR	Small MutS-Related
snoRNA	Small Nucleolar RNA
SQSTM1	Sequestosome 1
SSC	Saline Sodium Citrate
SV40	Simian virus 40
SWI/SNF	Switch/Sucrose Non-Fermentable
SYBR	SYBR Green
Syh1	Smy2p homolog in yeast
TAP	Tandem Affinity Purification
TAU	Microtubule-associated protein tau
TC	Ternary Complex
tmRNA	Transfer-messenger RNA
TPR	tetratricopeptide repeats
TRiC	T-complex protein Ring Complex
Trl1	tRNA ligase 1
tRNA	Transfer RNA
TSC1/2	Tuberous sclerosis complex 1/2
UBA	Ubiquitin Associated
UBP10	Ubiquitin-specific protease 10
Ufd1	Ubiquitin Fusion Degradation 1

uORF	Upstream Open Reading Frame
UPS	Ubiquitin-Proteasome System
USP10	Ubiquitin Specific Peptidase 10
USP21	Ubiquitin Specific Peptidase 21
UTR	Untranslated Region
UV	Ultraviolet
Vms1	VCP/Cdc48-associated Mitochondrial Stress-responsive
VRC	Vanadyl Ribonucleoside Complex
WT	Wild-Type
XRN1	Exoribonuclease 1
Ydj1	Yeast DnaJ homologue 1
YPD	Yeast Extract Peptone Dextrose
YRA1	Yeast RNA Annealing protein
YTHDC1	YTH Domain Containing 1
Zakα	sterile alpha motif and leucine zipper containing kinase AZK
ZNF598	Zinc Finger Protein 598
μM	Micromolar

CHAPTER 1: INTRODUCTION

1.1 Overview of cellular stress response and their key components

1.1.1 Stress and cellular damage

At the cellular level, stress can be defined as any perturbation in the internal or external cellular environment that challenges cellular functions and survival. This includes nutrient deprivation, shifts in pH, UV irradiation, osmolality changes, heavy metals presence, and temperature increases (1). Stressors damage most cellular macromolecules; proteins, nucleic acids, and lipids (2,3). Due to the conformational-dependent function of proteins and their high abundance, they are readily susceptible to stress, which results in protein denaturation and aggregation, threatening cells' ability to perform functions. Thus, failure to respond and resolve these perturbations ultimately leads to cell death (1). Depending on the intensity of the stress and level of cellular damage, cells attempt to restore to a homeostatic state and/or undergo transient adaptation or eliminate stressed cells (3,4).

1.1.2 Cellular adaptation and response to stress

In response to stress, cells exit the cell cycle and enter a state of quiescence where they downregulate transcription and translation to conserve energy and prevent the synthesis of protein that cannot achieve the native state (3,5). Thus, stress cells limit gene expression and cellular functions and metabolism, while solely upregulating the stress protective pathways (6,7). To limit the availability of mRNA regulatory proteins and mRNAs, stress includes the formation of membraneless organelles such as Stress Granules (SGs) and P bodies (PBs) by phase separation as part of the adaptation to stress (**Fig 1.1.1A)**.

SGs are assembled when global protein synthesis is inhibited (8). In general, phosphorylation of the translation initiation factor eIF2α triggers SG assembly. Alternatively, inhibition of another initiation factor, the RNA helicase eIF4A by pateamine or hippuristanol also induces the formation of SGs (1–4). In contrast to SGs, PBs are constitutively present in mammalian cells, however, they enlarge upon cellular stress (12). While SGs and PBs possess some shared components, they are markedly distinguished by unique core components (12–14). For example, PBs are enriched in mRNA decay factors in addition to non-translating mRNAs, and RNA binding proteins (RBPs) (12,15). SGs are composed of translation initiation factors, 40S ribosomal subunits, disordered proteins, non-translating mRNAs, and RBPs (9,11,13). These two cytoplasmic structures help to attenuate cellular functions by acting as a reservoir of protein and mRNAs serving to pause cellular metabolism. Remarkably, their fast dissociation during recovery allows cells to return to their constitutive functions (8,16).

The formation of SG and PB does not disrupt the upregulation of expression of genes involved in stress protection pathways; the unfolded protein response (UPR) protects proteins in the endoplasmic reticulum and the heat shock response (HSR) protects cytosolic and nuclear proteins (1,17–21). The HSR is the cellular stress response that triggers the expression of heat shock proteins (HSPs) and received this name because it was found upon exposing cells to temperatures higher than the homeostatic plateau that sustains life (22–24) (**Fig 1.1.1B)**. HSPs are molecular chaperones that alleviate the damage caused by stress by refolding misfolded proteins and preventing aggregation. The HSR is a universally conserved mechanism from prokaryotes to higher eukaryotic cells to cope with stress conditions (25–30). Therefore, in all organisms, the upregulation in the expression of HSPs in response to heat stress overcomes the general shut-down of cellular functions.

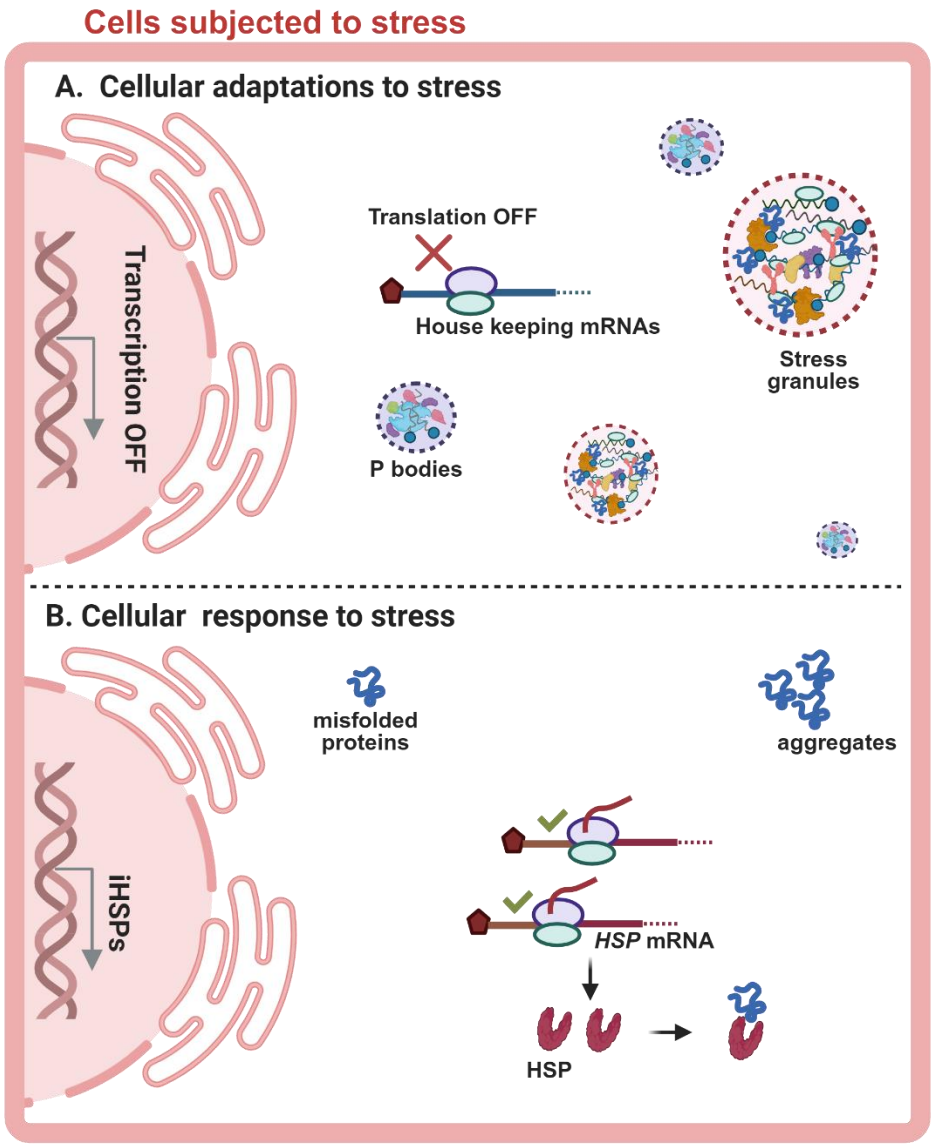

Figure 1.1.1. Overview of cellular adaptation and response to stress conditions. When cells experience stress, they adapt and respond to stress through the rapid formation of SG and PBs (A) and upregulation of HSP despite the general downregulation of gene expression (B). **A**. The formation of SGs and PBs recruit mRNAs, translation factors, decay enzymes, and RBPs that adapt the cells to stress. **B**. The upregulation of HSP protein synthesis in the cytosol is the cellular response to stress known as HSR. During stress, the load of misfolded protein increases triggering the upregulation of transcription and selective translation of HSPs to help with restoring the proteostasis.

1.1.3 The Heat Shock Response

The discovery of the Heat Shock Proteins

The discovery of HSPs dates to 1962 when geneticist Ferruccio Ritossa accidentally incubated the salivary gland cells of drosophila larvae at an elevated temperature (5 degrees higher than growth temperature, from 25 to 30 °C) (31). Upon exposure to heat, Ritossa observed a puffing pattern on the chromosomes and called it "chromosomal puffs" (31). This chromosomal pattern represents the transcriptional activation of several genes as a response to elevated temperature (31). From a decade of intensive research, the response to elevated temperature was termed the "heat shock response" (17). The genes induced by heat shock are known as "heat shock genes" and the resultant proteins are termed "heat shock proteins" (6,32–34). Subsequent studies in diverse model organisms confirmed that the HSR and some HSPs are highly conserved among organisms (4). Other stress conditions such as heavy metal (arsenite), high ethanol concentrations, and viral infection have also been shown to induce HSP expression (35–37). The discovery of the HSPs has been foundational in understanding the cellular response to stress, and how organisms maintain protein homeostasis under challenging conditions.

HSPs in protein homeostasis

HSPs play a pivotal role in maintaining cellular protein homeostasis (proteostasis) as they participate in all three machineries that embody the proteostasis network. First, HSPs mediate the folding of the nascent polypeptide chain by coordinating with the translation machinery. Second, HSPs ensure proper 3D conformation of the proteome as a component of folding machinery. Third, HSPs eliminate irreversibly misfolded proteins through degradation machinery or autophagy. Therefore, HSPs play a central role in escorting proteins from birth to their death.

Classification of HSPs

HSPs are classified based on their molecular weight into large HSPs (HSP90, HSP70, HSP60, HSP40), large (HSP110, HSP104) and small HSPs (HSP25, HSP10). All families of HSPs contain constitutive and stress-inducible members. This indicates that the functional importance of HSPs in protein folding extends beyond stress conditions to encompass general cellular protein folding processes. The housekeeping functions of HSPs include protein folding, transport, assembly and disassembly of protein subunits (38). The families of HSPs serve as holdases, foldases, disaggregases, or sequesterases and work as a network to maintain proteostasis in the cell (39). The HSP110 and HSP104 function in an ATP-dependent manner to disaggregate misfolded proteins by working with the HSP70-HSP40 complex. Metazoans lack HSP104, thus they rely exclusively on HSP110 for disaggregation (40). In yeast, targeting of aggregate proteins to HSP70-HSP104 complex is impaired in the absence of HSP110. This indicates that the function of HSP110 is essential for the efficient reactivation of misfolded proteins by HSP104 (40,41).

HSP60, also known as chaperonin (Cpn60 in chloroplasts), is the most conserved ATP-dependent chaperone expressed in archaea, bacteria, and eukaryotes (42). HSP60 forms two groups depending on the requirement of co-chaperone HSP10 (GROES in prokaryotes) Group I (HSP10-dependent) and Group II (HSP10-independent). The group I HSP60 functions in bacteria as GROEL-GROES complex and in eukaryotic organelles of bacterial origin (as HSP60-HSP10) (43–47). Group II HSP60 also known as TriC or CCT functions in archaea and cytosol of eukaryotes (48–50). The group I HSP60 forms a folding cage-like structure made of two heptameric rings with cochaperone HSP10 forming the lid of the cage. Although the assembly of cage formation differs in eukaryotic and bacterial systems, the substrate folding in both is achieved through the binding and hydrolysis of ATP, which induces conformation change in the cage that provides space

and time for the protein to fold by itself. The function of HSP60s is highly essential for the integrity of the mitochondrial respiratory chain as they mediate the folding and transportation of mitochondrial proteins. The group II HSP60 or TRiC assembles into a 1 Mda octameric complex with a double ring structure and an in-built lid (51). TriC allows 10% of the newly synthesized proteins to fold co-translationally either through direct interactions or handed over by other chaperones HSP40 or HSP70 (48).

In mammals, the HSP90 family has structurally similar members which are expressed in the cytosol (HSP90AA, HSP90AB), mitochondria (TRAP) or ER (GRP94). HSP90 is an ATP-dependent chaperone that functions as a homodimer. It possesses an N-terminal nucleotide-binding domain, a substrate binding middle domain, and a dimerization domain with a MEEVD motif in the C-terminus, which allows for the binding of TPR co-chaperones to form chaperone networks with HSP70s and HSP40s in the cytosol (52,53). A cycle of substrate binding, ATP hydrolysis, ADP and substrate release directs to the proper folding of client proteins. Almost 10% of the proteome are clients of HSP90 which includes actin, microtubule, intermediate filaments, steroid receptors, transcription factors, and kinases (6,18,19).

HSP70s are the main ATP-dependent chaperone that cooperates with other HSPs to promote cellular proteostasis. All these chaperones play a central role in the refolding of denatured proteins, preventing their aggregation and regulating apoptosis in response to stress.

1.1.4 The Heat Shock Protein 70 family

Family of HSP70

HSP70s are highly conserved through evolution (1). The human HSP70 protein shares 95%, 74%, 73%, and 50% identity to HSP70s of mice, yeast, Drosophila and *Escherichia coli* in

all eukaryotes possess multiple members with functional redundancy. In mammals, the members of the HSP70 family contain either organelle or tissue-specific functions and their expression is either transient or permanent (1,57). In humans, 13 independent genes code for HSP70. These HSP70s are categorized into two main groups, the stress-inducible HSP70s (such as *HSPA1A*, *HSPA1B*), and the constitutively expressed HSP70s (such as *HSPA8*) (58–60). HSP70 can be localized to various cellular compartments such as the nucleus (*HSPA1L*), ER (*HSPA5*), and mitochondria (*HSPA9*). GRP78 and mtHSP70 have a compartmental-specific role in maintaining proteostasis within the ER and mitochondria, respectively. The mitochondrial HSP70 is often involved in the import and folding of mitochondrial proteins by coordinating with mtHSP60 and cytoplasmic HSPs (58). The list of different members of the HSP70 family in yeast, mouse, and humans and their cellular localization are shown in **table 1.1.1**.

Cellular localization	Yeast	Mouse	Humans
Cytoplasm/ nucleus	*SSA1* *SSA2* *SSA3* *SSA4* *SSB1* *SSB2* *SSE1* *SSE2* *SSZ1*	*Hspa1a* *Hspa1b* *Hspa1l* *Hspa2* *Hspa4* *Hspa4l* *Hspa8* *Hspa13* *Hspa14* *Hsph1* *Hyou1*	*HSPA1A* *HSPA1B* *HSPA1L* *HSPA2* *HSPA4* *HSPA4L* *HSPA6* *HSPA7* *HSPA8* *HSPA13* *HSPA14* *HSPH1* *HYOU1*
Endoplasmic reticulum	*KAR2* *LHS1*	*Hspa5*	*HSPA5*
Mitochondria	*SSC1* *SSQ1* *ECM10*	*Hspa9*	*HSPA9*

Table 1.1.1: Tabulation of various HSP70 isoforms in yeasts, mice and humans functioning in cellular compartments such as cytoplasm/ nucleus, endoplasmic reticulum, and mitochondria.

HSP70 machinery

The structural features of HSP70 are highly conserved from bacteria (DNAK) to humans. HSP70 has two domains; a NucleoTide binding Domain (NTD) in the N terminal linked to a Substrate Binding Domain (SBD) with a C terminal EEVD motif for interacting with TPR co-chaperones **(Fig 1.1.2)**. HSP70 when bound to ATP has low affinity for substrates. The cochaperone HSP40, also known as DNAJ because they have a J-domain protein, stimulates the ATPase activity of HSP70 and brings the substrate to be folded. Now the ADP-bound HSP70 binds to its substrate with high affinity (61–65). A Nucleotide Exchange factor (NEF) binds at NBD to mediate the ADP-ATP exchange inducing the HSP70 conformational change and releasing the substrate. The cycle continues until the native state of the protein is reached or the protein is transferred to HSP90 by HOP or targeted to degradation by CHIP (61–63).

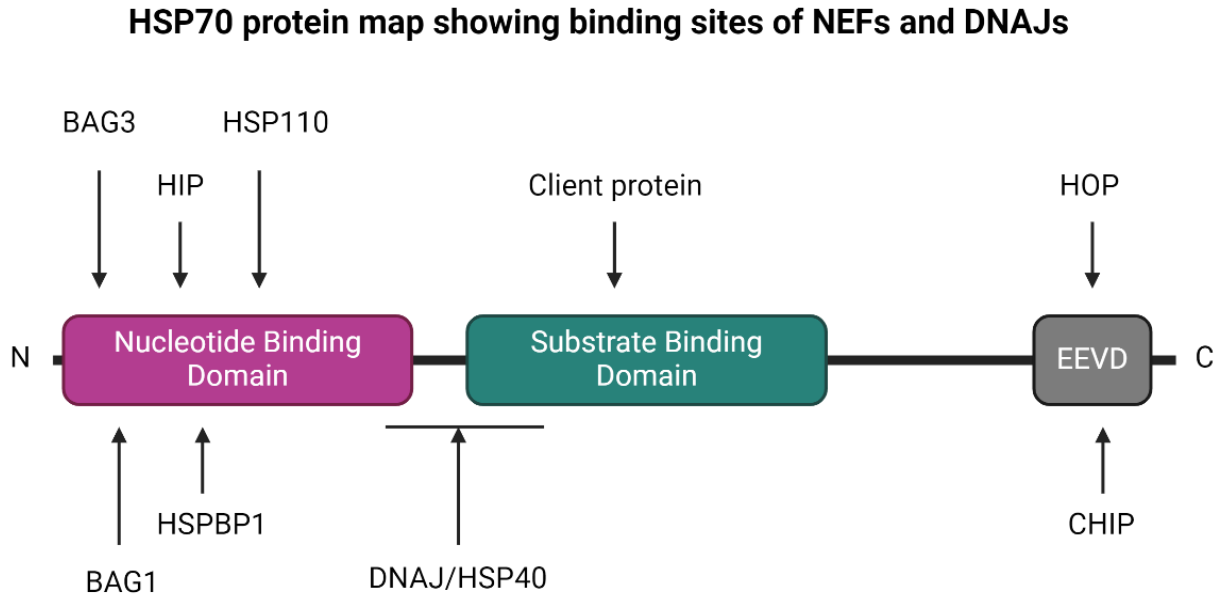

Figure 1.1.2. Domains of HSP70. The HSP70 has a nucleotide binding domain, substrate binding domain and EEVD motif. These domains harbor interaction sites for several co-chaperones to mediate the function of HSP70. The interaction sites for DNAJ/HSP40, NEFs (BAG1, BAG3, HIP, HSP110 and HSPBP1) (66), TPR cochaperones (HOP, CHIP) and client protein are shown.

Interacting partners or cochaperones of HSP70

The function of HSP70 solely relies on its interaction with several cochaperones or interacting partners. In fact, the interaction of HSP70 with cochaperones alters the fate of the substrate protein (**Figure 1.1.3**). The folding of client proteins is mediated by the interaction with DNAJs, NEFs and various other cochaperones. These cochaperones associate with either the NBD, the SBD or C-terminal EEVD motif of HSP70 **(Fig 1.1.2)**. The DNAJs interact at the interface between the NBD and the SBD of HSP70. They recognize the hydrophobic regions of the misfolded protein or nascent protein and provide the substrate to HSP70 (67–71). Despite the presence of several NEFs, they all have different binding affinities for HSP70. The first type of NEF, HSP110, catalyzes ADP-ATP exchange by binding to the NBD of HSP70. The association of HSP70 with HSP110 increases the folding activity of HSP70 and mediates protein disaggregation (72–74). The second common type of NEF is the BAG which has at least five members functioning in protein quality control (PQC). BAG1 has an intrinsic ubiquitin-like domain which serves as a signal for the Ubiquitin proteosome system (UPS). Thus BAG1 binding to HSP70 stimulates the ADP release and transfer of client protein to UPS for degradation (75–77). BAG3 on the other hand facilitates the degradation of substrate protein through the autophagosome-lysosome pathway (78,79). The third type of NEF comprises Fes/HSPBP1, which in addition to ADP release, directly prevents unproductive rebinding of the client protein to HSP70 (80,81). The cochaperone HIP alters the rate of the chaperone cycle of HSP70 by slowing down the release of ADP. Thus HIP favors the premature release of substrate protein while also preventing its aggregation and facilitating the substrate transfer to other chaperones or UPS (54,82).

Often, the HSP70 works with other chaperone machinery such as HSP60-HSP10/TriC and HSP90 to fold the protein to its native conformation. For the transport and folding of mitochondrial proteins, cytoplasmic HSP70 coordinates with the mitochondrial HSP60-HSP10 system (83). Likewise, HSP70 hands over the folding intermediate to either the TriC chaperonin system or HSP90 to complete folding (84). HSP70 substrates are handed to HSP90 by the action of cochaperone HOP. HOP has a tetratricopeptide repeats (TPR) domain which recognizes the EEVD motifs of both HSP70 and HSP90 chaperones. Thus HOP acts as a bridge and facilitates the transfer of client proteins from HSP70 to HSP90 (52). Steroid receptors, kinases, p53, and HSF1 are examples of proteins whose biological activity is controlled by transient interactions with HSP90 and HSP70 (85). The EEVD domain harbors binding for another TPR domain protein CHIP. CHIP often competes with HOP for the EEVD motif on HSP70 and HSP90. CHIP contains E3 ubiquitin ligase activity which adds ubiquitin molecules to the substrate for degradation through UPS (86). Thus, the activity of HSP70 and the fate of the substrate protein depends on the interacting cochaperones.

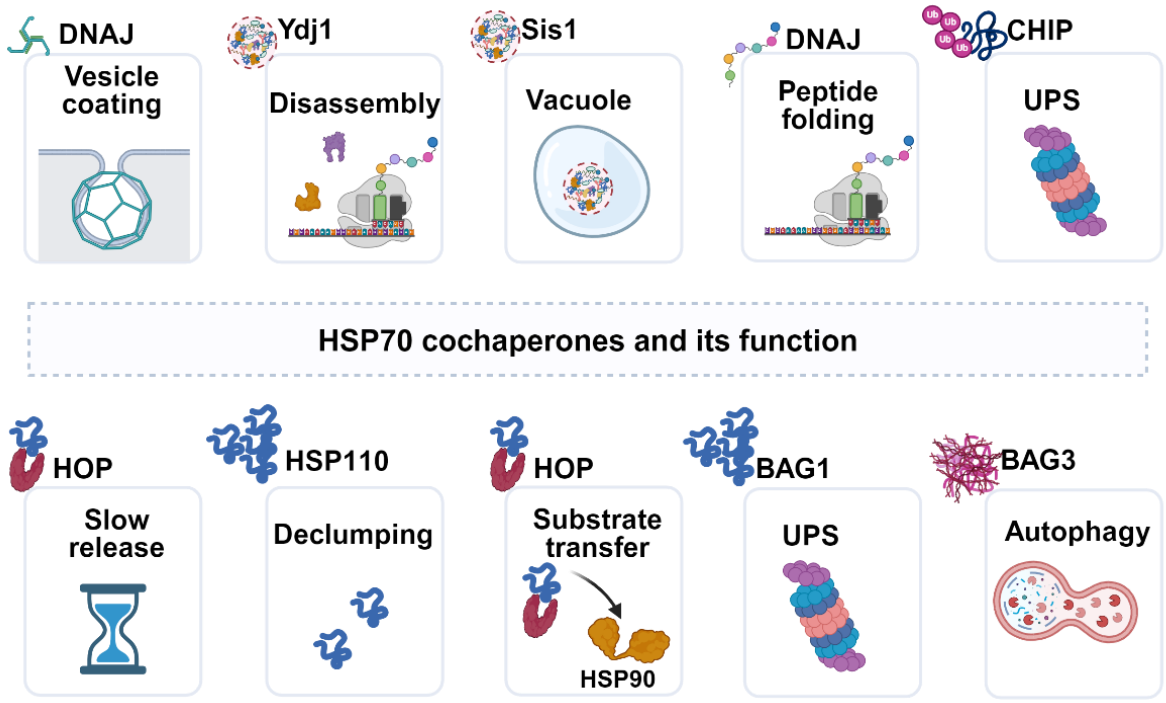

Figure 1.1.3. Cochaperones of HSP70 and their function. The HSP70 interacts with several cochaperones to alter the fate of the client protein. Depending on the cochaperone, HSP70 could mediate clathrin assembly and disassembly on vesicles, disassemble SGs and resume translation of mRNAs, target the SGs to the vacuole, nascent polypeptide chain folding, mark misfolded proteins with ubiquitin for degradation (Top, left to right); slow down the substrate release, disaggregate misfolded proteins, transfer substrate to other chaperones, target aggregates to UPS and degrade aggresome by autophagy.

Client proteins of HSP70

HSP70 requires DNAJ/HSP40 cochaperones to assist in binding and releasing substrates (61–65). The DNAJ/HSP40 binds to the hydrophobic region of the substrate protein that needs to be folded and presents the client protein to HSP70. HSP70 interaction requires recognition of hydrophobic residues on client proteins by HSP40s (68–71). Generally, regions of proteins enriched in hydrophobic residues (around 5-7) need assistance to fold into proper conformation (67–71). During stress, the misfolded proteins often expose their hydrophobic regions, and they interact with each other forming aggregates (87–89). As HSP70 has a broader role to play in the

cells, it also has a wide range of client proteins (90,91). Some general clients are stress-induced misfolded proteins, nascent polypeptides, and terminally misfolded proteins. The nascent polypeptide chain at the ribosome exit tunnel interacts with HSP70 for assistance with protein folding (92,93). The absence of this interaction during stress mediates translation pausing at the stage of elongation (92,93). Disassembly of protein complexes such as clathrin for vesicle formation requires HSP70 (94). Certain mitochondrial proteins and ER localizing proteins that are being imported need assistance from HSP70 (89–91).

1.1.5 Function of HSP70 in stress alleviation

HSP70 has several critical functions in the cellular stress response **(Fig 1.1.4)**. Firstly, HSP70 provides cytoprotection by mitigating the damage caused by stress and promotes cellular recovery once the stress stimulus is removed (95,96). This was discovered by subjecting the yeast, *saccharomyces cerevisiae*, to a mild heat shock at 39°C prior to a lethal heat shock at 42°C (97–99). Yeast that experienced a mild heat shock overexpress HSP70s which condition them to survive better to the lethal heat shock than the yeast kept at homeostatic temperatures (99). Thus, HSP70 fits yeast cells to survive a lethal heat shock (97–99). This phenomenon of cytoprotection is conserved from yeasts to mammals (95–97,100–102).

Secondly, HSP70 promotes cellular recovery by mediating the disassembly of SGs formed during stress (10). In yeast, it has been shown that several members of the HSP70 family (SSA1, SSA2, and SSA4) and HSP40 (Sis1 and Ydj1) colocalize with SGs, whose disassembly depends on the ATPase activity of HSP70 (10,16). Depending on the interaction with Sis1 or Ydj1, the fate of SGs tends to change. While Ydj1 promotes the SGs disassembly and translation, Sis1 accumulates SGs in a vacuole and limits SGs disassembly. In mammalian cells, a minor portion of SGs are targeted directly to autophagy for clearance (16). The majority of SGs undergo

dissociation where the defective ribosomal proteins and other misfolded proteins are sorted to the perinuclear region by their interaction with HSPB8 inside SGs. The HSPB8 facilitates the recruitment of the BAG3-HSP70 complex to target only the misfolded client proteins for autophagy (78,103). This ensures that the components of SGs are disassembled while targeting only misfolded protein for degradation (104).

Thirdly, the HSP70-HSP40 complex, along with HSP110 is involved in the disaggregation and refolding of misfolded proteins. This was demonstrated in a cell-free system by creating aggregates of GFP and luciferase through heat deactivation or urea-denaturation, respectively. The aggregates were then incubated with purified HSP70/HSP110 from mammalian cells or yeast for refolding-mediated functional reactivation. The activity of GFP or luciferase was measured as a readout to determine the refolding kinetics mediated by the chaperones (73,105). From the experiments, the function of each chaperone in protein disaggregation was identified. HSP70/HSP40/HSP110 failed to rapidly refold in the absence of the yeast HSP104 (105). In cell-free system, the absence of HSP104, HSP70/HSP40/HSP110 complex failed to rapidly refold the amyloid substrates or alpha-synuclein. This suggests that the combined activity of HSP110 and HSP104 is required to reactivate the aggregated proteins (40).

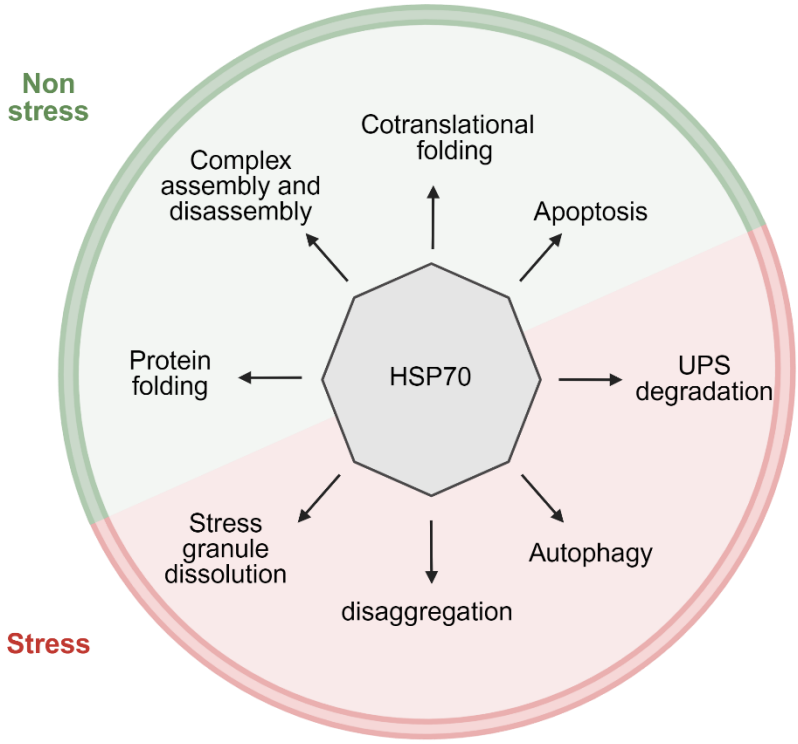

Figure 1.1.4. Cellular functions of HSP70 under non stress and stress conditions. The HSP70 has constitutive housekeeping functions (green) as well as stress-related functions (red). The housekeeping functions include protein folding, assembly of multimeric protein complexes and their disassembly, cotranslational folding of nascent polypeptides and apoptosis. The stress-related functions of HSP70 include the dissolution of SGs, disaggregation of misfolded protein aggregates, autophagy and UPS-mediated clearance of terminally misfolded protein aggregates.

Finally, in the case of irreversibly damaged proteins, HSP70 initiates their clearance through the proteasome or triggers autophagy to eradicate the terminally damaged cell. The association with an E3 ubiquitin ligase CHIP or NEF BAG1 with HSP70 mediates degradation of the client protein (such as actin, Tau, histone, alpha crystalline, misfolded CFTR) by proteasome (54,86,106–110). Alternatively, when the amount of misfolded protein exceeds the capacity of the chaperone-refolding and proteasome system, then aggregates of misfolded proteins form a perinuclear structure called the aggresome (78). In this case, the HSP70 is directed to aggresome by BAG3 through microtubule reorganization. The BAG3 recruits autophagic receptor p62

(SQSTM1) which is recognized by autophagosome-lysosomal for fusion and degradation (79,111–113).

1.1.6 Regulation of HSP70 expression

The inducible member of the HSP70 family, HSPA1A (SSA4 in yeast), is the most stress-inducible of all HSPs. The tight regulation of HSP70 induction relies on the master transcription regulator, Heat shock Factor 1 (HSF1). The HSF1 is sequestered as monomers in the cytoplasm by chaperones HSP70 and HSP90 under physiological conditions. The misfolded proteins caused by stress dilute the chaperones thereby liberating the HSF1. HSF1 undergoes trimerization and relocation to the nucleus. In the nucleus, HSF1 is activated by several post-translational modifications (PTMs) and binds to Heat Shock Elements (HSE) to induce the transcription of the downstream heat shock genes (covered more in detail in **section 1.3**). Thus, the stress upregulates both constitutive (HSPA8 in mammals and SSA2 in yeast) and inducible HSP70s. Upon entering the cytoplasm, the *Hspa1a* mRNA encounters a translation-deficient environment as canonical translation initiation factors are depleted during stress (covered in section 1.4).

Despite the downregulation of global translation, cells preferentially translate only the inducible *HSP70* mRNAs. In contrast to the inducible HSPA1A, the constitutive *HSP70* mRNAs undergo only slight upregulation at the level of transcription and translation. During stress, splicing is downregulated which further reduces the processivity of newly transcribed constitutive *HSP70* mRNA in mammals. Thus, reducing the availability of constitutive *HSP70* mRNA for translation in mammalian cells. Soon after the removal of stress, inducible *HSP70* mRNAs are rapidly cleared from the cell to attenuate the HSR (114,115). The cells tightly control the inducible *HSP70* mRNA levels during heat shock and recovery to avoid the potential cytotoxic effect of these proteins (114). All organisms conserve the process of transcriptional induction, selective translation and

degradation upon stress and recovery, respectively. Investigations conducted over past decades have identified the significance of the 5'UTR in selective translation and 3'UTR in selective degradation of inducible HSP70s. Interesting to note that the length and composition of 5'UTR of inducible *HSP70* mRNA varies between organisms (116–118). In yeast, the 5'UTR of inducible *HSP70* mRNA is 72% AT-rich and shorter compared to mammalian cells. In addition to the difference in the 5'UTR, the CDS of inducible *HSP70* in yeast, are highly non-optimal (53%) while the mouse CDS are less non-optimal (~20%). These differences suggest the possibility of variations in the regulation of *HSP70* mRNA translation from lower to higher eukaryotes.

Therefore, my thesis work was directed towards gaining insights into the gene expression regulation encoding in the sequence of the inducible *HSP70* mRNAs in yeast and mammals. In yeast, the non-optimal codons of inducible *HSP70* mRNA caused ribosomes to stall and collide. Thereby, controlling the translation of inducible *HSP70* mRNA by a mechanism of ribosome quality control (RQC) expression. However, in mammalian cells, we found that the translation regulation of inducible *HSP70* mRNA relies on the structural and sequence elements involving the 5'UTR and CDS. In the upcoming review, I will provide background on the mechanisms of HSR and RQC both involved in maintaining proteostasis. In chapter 1.2, I will focus on how the cell downregulates the global gene expression during cellular stress. This section will emphasize the importance of prompt activation of HSR followed by timely attenuation in promoting cell recovery from stress. In Chapter 1.3, I will focus on the RQC mechanisms, including examining processes such as the inhibition of translation initiation, degradation of problematic mRNA through No Go Decay (NGD), ribosomal subunit recycling, and the degradation of truncated polypeptides. This section will provide a deeper understanding of how cells maintain the fidelity of protein synthesis

and prevent the accumulation of aberrant proteins, thus safeguarding cellular function and viability.

1.2: Mechanisms tailoring the expression of heat shock proteins to proteostasis challenges.

Lokha R. Alagar Boopathy[1*], Suleima Jacob-Tomas[1*], Dr. Célia Alecki[1], and Dr. Maria Vera[1]**.

[1]Department of Biochemistry, McGill University, Montreal, QC H3G 1Y6, Canada.

**Corresponding author: maria.veraugalde@mcgill.ca

* Authors have equal contributions

1.2.1 Abstract

All cells possess an internal stress response to cope with environmental and pathophysiological challenges. Upon stress, cells reprogram their molecular functions to activate a survival mechanism known as the heat shock response, which mediates the rapid induction of molecular chaperones such as the heat shock proteins (HSPs). This potent production overcomes the general suppression of gene expression and results in high levels of HSPs to subsequently refold or degrade misfolded proteins. Once the damage or stress is repaired or removed, cells terminate the production of HSPs and resume regular functions. Thus, fulfillment of the stress response requires swift and robust coordination between stress response activation and completion that is determined by the status of the cell. In recent years, single-cell fluorescence microscopy techniques have begun to be used in unravelling HSP-gene expression pathways, from DNA transcription to mRNA degradation. In this review, we will address the molecular mechanisms in different organisms and cell types that coordinate the expression of HSPs with signaling networks that act to reprogram gene transcription, mRNA translation, and decay and ensure protein quality control.

1.2.2 Introduction

For organisms to grow and function properly, they must maintain specific internal cellular conditions that allow proteins to acquire their functional conformations and cells to achieve protein homeostasis (proteostasis) (1). Maintaining proteostasis becomes critical when facing abrupt changes in the external conditions, such as an increase in temperature, which can lead to protein misfolding and aggregation, and consequently, cellular dysfunction (2). Thus, organisms must sense, rapidly respond, and adapt to new environmental conditions for survival. Organisms from bacteria to mammals have evolved similar and varying stress responses to cope with protein misfolding and maintain proteostasis successfully. Some of these strategies include modulations of signaling cascades, changes in transcriptional programs, and regulation of translation, posttranslational modifications, and the dynamic assembly of RNA and protein condensates (ribonucleoprotein [RNP] granules) through liquid–liquid phase separation (1, 3, 4, 5, 6, 7). Several of these molecular mechanisms converge to sustain proteostasis in response to sudden and acute changes in environmental conditions.

Increases in the environmental temperature is a universal proteostasis challenge encountered by most organisms. For historical reasons, thermal stress has been used as a paradigm to study the stress response. Nowadays, these studies have an additional relevance due to the increased exposure of organisms to heatwaves derived from climate change (8, 9, 10). Increased thermal energy in the cells can result in heat-induced denaturation of proteins and thermally altered metabolic activity leading to an increase in reactive oxygen species, which can damage all biological macromolecules, including proteins (11). Cells cope with an increased load of unfolded and misfolded proteins by modulating the expression of specific molecular chaperones, also known as heat shock proteins (HSPs) (12, 13, 14, 15). The heat shock response (HSR) refers to the

activation of the expression of HSPs, and it is the most common and widely studied cell response to thermal stress. HSPs play a central role in the lifecycle of proteins because they promote the folding of nascent polypeptides into their native/functional configurations and prevent protein misfolding and aggregation (12, 15, 16). HSPs also collaborate with the quality control mechanisms, the ubiquitin-proteasome system, and autophagy, to target misfolded proteins and aggregates whose native functional state cannot be recovered for degradation (5, 17).

Given that HSPs are central to the cellular proteostasis network, cells undertake several gene expression adaptations to favor the synthesis of HSPs at the expense of decreasing most cellular functions **(Fig. 1.2.1)**. Biochemical and molecular biology approaches highlight the unique regulation of HSP gene expression. The spatiotemporal resolution of such precise regulation is now being uncovered using high-resolution quantitative fluorescence microscopy. Gene expression adaptions during stress act together to protect macromolecules and promptly resume the cytoplasmic and nuclear activities once permissive conditions are restored (3). The regulation of HSP expression coordinates with other cell protective mechanisms, like the formation of RNP condensates and the activation of the integrated stress response (ISR) to repress translation initiation. HSPs are grouped into families based on an apparent molecular weight (18, 19). The HSP70 and HSP90 families are the most functionally relevant HSPs in the cell (15, 20).

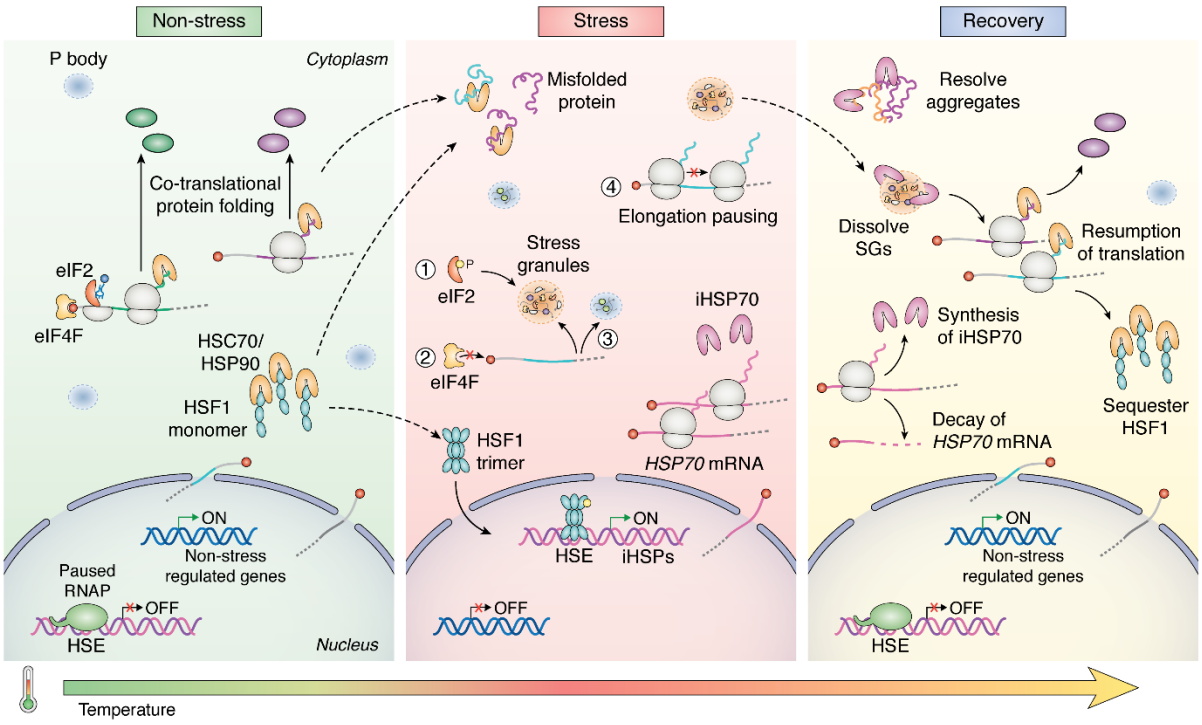

Figure 1.2.1. Overview of the cellular response to heat stress. Cells under nonstress conditions keep the transcription of the inducible HSPs inactive. A paused polymerase occupies their promoter, and the transcription factor HSF1 is sequestered in monomeric form by constitutive chaperones HSC70/HSP90 in the cytoplasm. Constitutive chaperones also assist in protein folding and preserving protein homeostasis. Under physiological conditions, nonstress–regulated genes are transcribed, and their mRNAs undergo canonical cap-dependent translation. Exposure to heat stress induces protein misfolding, which titrates out the HSC70/HSP90 and allows HSF1 to trimerize and translocate to the nucleus, where it binds to the HSE in the promoter of HSPs and activates transcription. Concomitant to the HSR activation, there is a global transcriptional and translational repression. The translation is repressed by (1) phosphorylation of eIF2α (2); inhibition of eIF4F complex formation (3); recruitment of untranslated mRNAs and regulatory proteins in stress granules (SGs) and processing bodies (PBs) (4); and translation arrest at the stage of elongation. The inducible HSP mRNAs, especially HSP70, skip translation repression and are translated through a cap-independent mechanism to increase the number of available chaperones needed to cope with the abundant misfolded proteins and prevent their toxic aggregation. Once the temperature returns to being permissive, the newly synthesized HSPs favor recovering proteostasis and functionality by folding misfolded proteins and disabling SGs. The resumption of regular translation and transcription coincides with the decay of HSP mRNAs and silencing of their transcription. HSEs, heat shock elements; HSF1, heat shock factor 1; HSP, heat shock protein.

They are ATP-dependent chaperones that cooperate with small HSPs and HSP110. Cochaperones of the J-domain family of proteins modulate HSP70 activity by accelerating ATP hydrolysis,

participating in substrate recognition and substrate folding or refolding (**Fig. 1.2.2**) (21, 22, 23, 24, 25, 26, 27). HSPs are further categorized as constitutive or inducible based on their steady-state expression levels. The expression of all inducible and some constitutive HSPs is upregulated to some extent upon heat stress. Among them, the inducible HSP70 genes are the fastest and most upregulated (23, 24, 27).

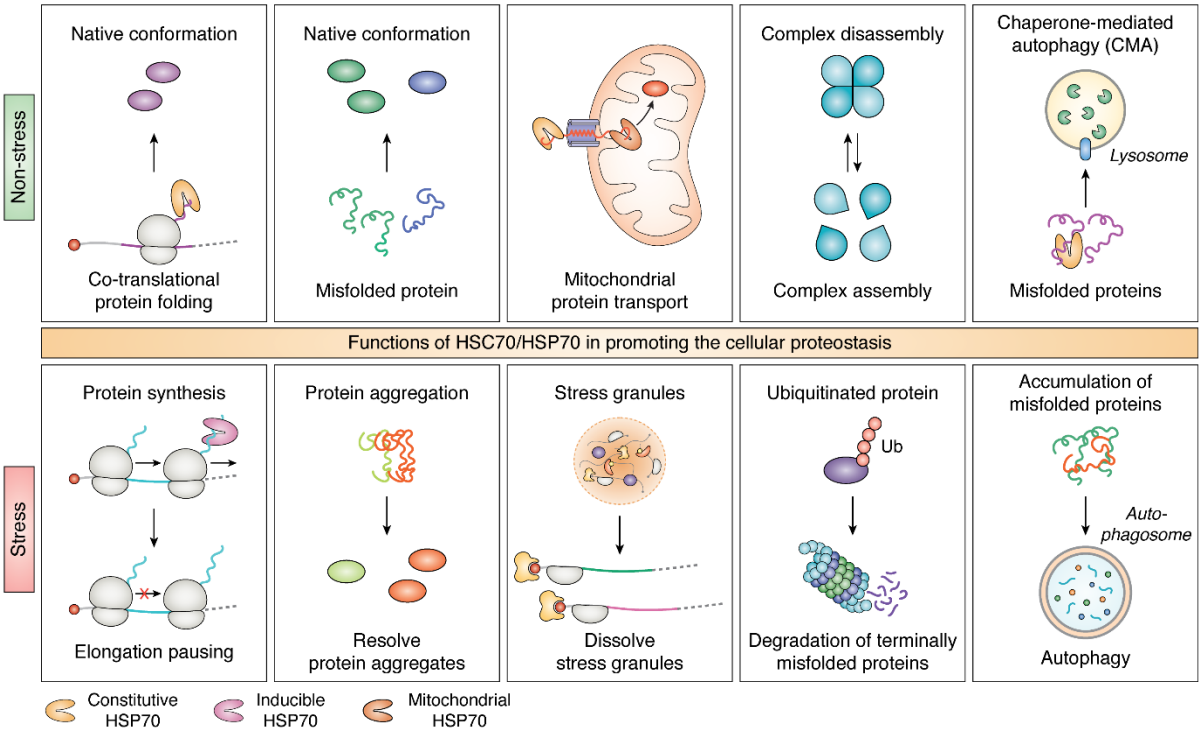

Figure 1.2.2. The function of HSC70/HSP70 in retaining the cellular proteostasis. The illustration depicts the significant tasks of the HSP70 chaperone network inside the cell to maintain proteostasis. (Starting from the top left tile) Under nonstress conditions, HSC70 provides cotranslational folding of the nascent polypeptide to obtain native conformation; helps to refold misfolded proteins; transports nascent polypeptide from the cytoplasm to the mitochondria where it is assisted by mitochondrial HSP70 (mtHSP70) and HSP60 to attain functional conformation; involved in protein complex assembly and/or disassembly; and leads specific proteins for their degradation by the lysosome through chaperone-mediated autophagy (236, 237). (Continuing bottom left tile) During stress, the lack of HSP70 at the exit of the ribosome tunnel represses the translation at the elongation stage. HSP70 and HSP90 prevent protein aggregation, and HSP70 also resolves stress granules so that the sequestered mRNAs can resume their translation during recovery from stress; targets terminally misfolded protein for proteasomal degradation; and mediates autophagy by autophagosome. HSP, heat shock protein.

Interestingly, they are highly conserved among species having an amino acid similarity of 50% between *Homo sapiens* and *Escherichia coli*, while some domains are 96% similar, which highlights its vital role in cell adaption to changing environmental conditions (28).

In this review, we frame the molecular regulation of the HSR to the context of the gene expression changes undertaken by eukaryotic cells in response to an increase in temperature. We compare the response mounted by different organisms and cell types and suggest new technological approaches to overcome the gap in our knowledge on the HSPs expression.

1.2.3 Transcriptional regulation of inducible HSPs versus constitutive genes

Transcriptional upregulation of stress-inducible HSPs

The robust transcriptional induction of genes of the HSP70 family is one of the main and fastest response to heat stress. Their transcriptional induction occurs at the expense of a general transcriptional downregulation of constitutively expressed genes. Most inducible HSP70 genes are short (around 2500 nucleotides) and intronless, and their promoter contains one or more binding sites, known as heat shock elements (HSEs), for the association of the master transcription factor heat shock factor 1 (HSF1) (29). Under physiological conditions, the inducible HSP70 genes are not expressed. However, their loci are neither present in a compact heterochromatin domain nor marked by repressive epigenetic histone modification. The promoter and 3′ end of HSP70 gene is nucleosome-free while its gene body is covered by nucleosomes. The promoter is bound by a paused RNA polymerase II (RNAPII) (30). These characteristics prevent the stable transcriptional repression of HSP70 genes and facilitate their prompt activation in response to the binding of HSF1.

Under physiological conditions, HSF1 shuttles between the nucleus and cytoplasm, and it is kept as an inactive monomer by constitutive members of HSP90 and HSP70 families. Upon stress, HSF1 is released from HSPs, trimerizes, and localizes in the nucleus where it binds to the HSE, which is comprised of at least three nGAAn repeats organized head to tail in the promoters of genes encoding HSPs and other gene products (31, 32) **(Fig. 1.2.3)**. HSF1 has three domains, an oligomerization domain next to the DNA binding domain at the N terminus, a trans-activation domain at the C terminus that induces transcription initiation and elongation, and a regulatory domain in the middle that negatively regulates the function of the trans-activation domain in nonstress conditions. By forming a trimer, the affinity of HSF1 for the HSE increases as each HSF1 of the trimer binds to a nGAAn repeat through its DNA binding domain. The binding of HSF1 to HSE is not sufficient to activate transcription and has to be accompanied by extensive posttranslational modifications. HSF1 undergoes hyperphosphorylation of serine and threonine residues that cover up to 90% of the regulatory domain (33, 34, 35, 36). However, only a few of these phosphorylation sites, like serines 230 or 326, are necessary for the activity of HSF1 (35, 37). Concomitantly, sumo groups that have an inhibitory effect on transcription are removed from HSF1 (38). HSF1 acetylation at lysines 116 and 118 favors its transcriptional activity, whereas acetylation at several other lysine residues regulates its nuclear localization and oligomerization (31). Acetylation of HSF1 occurs a few hours after heat shock to decrease its DNA affinity and the transcriptional response (39). In summary, HSF1 undergoes extensive posttranslational modifications, which are regulated under various stresses. Although the function of some of these modifications has been identified, the role of many others, as well as the proteins responsible for their regulation, remains to be elucidated.

The combination of posttranslational modifications and titration of HSPs by misfolded proteins have been demonstrated to activate HSF1. Recent work in the yeast, Saccharomyces cerevisiae, has allowed building a simple mathematical model that points to the dissociation of HSP70/HSP90 from HSF1 as the first "switch on" step to activate HSP70 transcription, which feedback to HSF1 to switch it off or repress it (40, 41). Zheng et al. (41) identified 70 phosphorylation sites on HSF1 upon heat shock and were able to model that these phosphorylations have no effect on HSF1 activation but instead increase its transcriptional activity by favoring its association with the mediator complex. Additionally, the translation factor eEF1A and the noncoding RNA HSR1 are among the factors activating HSF1. They act together to form a nucleoprotein complex with HSF1 and stimulate HSF1 trimerization (42). Following heat shock, HSF1 recruits multiple cofactors to HSE (43, 44, 45, 46), including SGO2, which recruits the subunit mediator complex MED12, essential for the strong transcriptional induction of HSPs genes (47). SGO2 binding to hypophosphorylated RNAPII targets it to the promoter of HSP genes by forming a complex with HSF1. Transcription is then induced by other transcription factors like P-TEFb, recruitment of which are mediated by HSF1 (48). P-TEFb is sufficient to induce the phosphorylation of the serine 2 in the C-terminal domain of RNAPII, which leads to transcription elongation (48, 49). However, a strong transcriptional induction requires the nucleosomes positioned along the HSP70 gene body to be removed. The chromatin remodelers SWI/SNF in mammals and FACT together with the histone chaperone Spt6 in *Drosophila melanogaster (D. melanogaster*) are recruited by HSF1 to the HSP70 genes within minutes after heat shock to remove the nucleosomes (31).

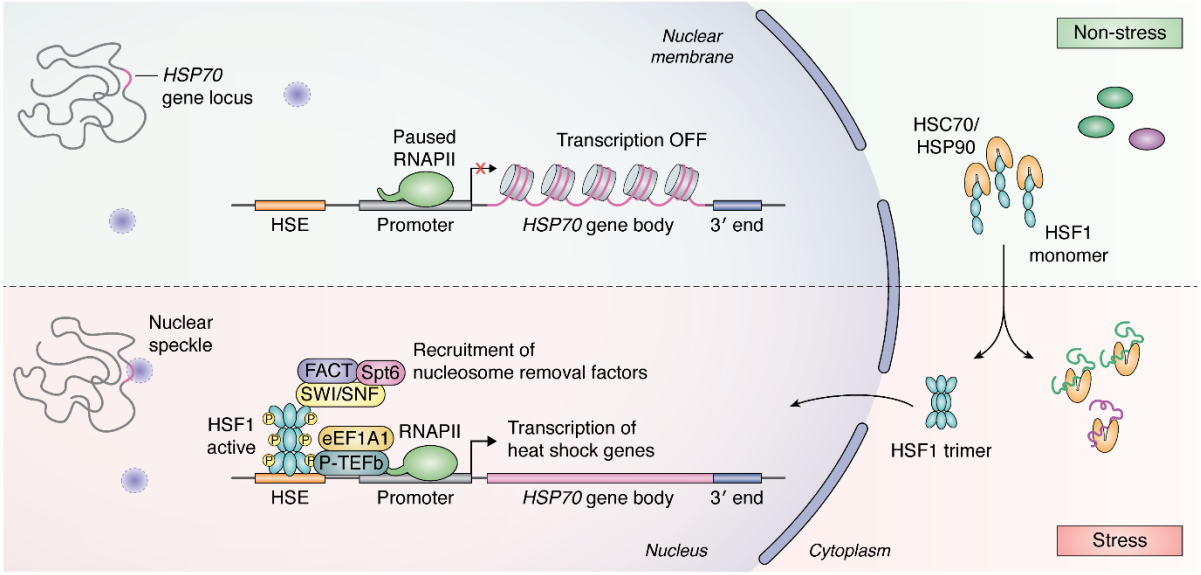

Figure 1.2.3. Chromatin remodeling and transcriptional activation of HSP genes. The figure represents the changes in the chromatin region and the promoter of heat shock genes under nonstress and stress conditions in mammalian cells. Under physiological conditions, HSF1 is sequestered in the cytoplasm by constitutive chaperones HSP90 and HSC70. RNAPII is bound to the open promoter region of HSP genes and remains paused/transcriptionally inactive, and the HSP70 gene locus is located close to the membrane. Under stress, the HSP70 locus moves to the nuclear speckle. The chaperones bound to HSF1 now bind misfolded protein, thereby releasing HSF1, which trimerizes and localizes to the nucleus where it binds to the heat shock elements (HSEs) in the HSP gene promoter. Multiple posttranslational modifications activate the HSF1 trimer, resulting in the recruitment of transcription factors (P-TEFb) and nucleosome removal factors (FACT, SWI/SNF, Spt6) to the site causing chromatin remodeling and favoring transcription elongation. HSF1, heat shock factor 1; HSP, heat shock protein; RNAPII, RNA polymerase II.

Besides the activation of HSF1, heat shock induction of HSP70 in mammalian cells depends on the relocation of the HSP70 loci from the nuclear membrane to speckles (50, 51). The rapid, active, and unidirectional movement of HSP70 loci is mediated by nuclear actin polymerization. The association of the HSP70 locus with speckles depends on the promoter sequence and determines the robust transcriptional activation of HSP70 upon heat shock stress. Although speckles contain serine 2–phosphorylated RNAPII and other components of the transcriptional machinery, the specific speckle factors critical for the transcriptional activation of HSP70 have not been yet identified. In yeast, genes encoding for different HSPs coalesce in discrete spots in the nucleus

upon transcription stimulation. This interallelic clustering leads to the interaction between HSP104 and HSP12 loci and depends on the activation of their transcription. This result suggested the presence of specific transcriptional factories formed in response to heat stress, which could be coregulated by HSF1 (52).

Transcriptional downregulation of nonstress genes

The transcriptional induction of HSP genes during heat stress is accompanied by the upregulation of other non-HSP genes encoding for cytoskeleton and oxidative stress proteins and a massive downregulation of thousands of genes (For review: (53)). Detailed analysis of the position of the RNA polymerases, chromatin modifications, and domains in *D. melanogaster* and mammalian cells suggest that changes in the chromatin landscape cannot explain the rapid changes in transcriptional preferences upon heat shock (54, 55).

Heat shock does not induce a global chromatin remodeling nor modifications of topology associated domains in human or *D. melanogaster* S2 cells (56) or rearrangements of topology associated domain borders in *D. melanogaster* Kc167 cells (57). The addition of DTT to induce protein unfolding in *D. melanogaster* S2 cells did not trigger a global decrease in nucleosome occupancy over the induced genes, their promoters, or enhancers, as detected by micrococcal nuclease sequencing (54). However, the accessibility of the chromatin is increased at upregulated genes as measured with ATAC-seq. These results could be explained by nucleosomes undergoing an increased turnover due to their increased acetylation and ongoing transcription. Mueller et al. also reported a decrease in nucleosome occupancy and an increase in accessibility in a few genes, like the constitutively expressed chaperone HSC70. Similar observations were done in human K562 cells following 30 minutes of heat shock. The level of histone 3 lysine 27 acetylation (H3K27Ac) increased at the promoter of all transcribed genes, which also experienced an increase

in RNAPII occupancy in the promoter and to a lesser extent in the gene body (55). Conversely, a decrease of polymerase occupancy is observed along the gene body of constitutively expressed genes whose transcription is downregulated upon stress. Hence, it is suggested that the extra available RNAPII quickly replaced the RNAPII undertaking transcription elongation in stress-regulated genes.

Additionally, noncoding RNAs have been shown to be a transcriptional repressor of non-HSP genes during heat shock. For instance, noncoding transcripts such as Alu RNA derived from short interspersed nuclear elements bind to RNAPII during heat shock to inhibit transcription of other mRNAs, such as actin (58, 59, 60). Interestingly, it has recently been shown that the long noncoding RNA, heat-enhanced antisense transcript (Heat) binds to HSF1 in vitro and in vivo via a trans-acting manner to attenuate the expression of stress genes. Experiments on mouse embryonic fibroblasts suggest that Heat uses HSF1 as a carrier by forming an RNP complex to target stress genes. While the exact mechanism by which Heat suppresses transcription is not known, Ji et al. (61) suggest the attenuation of the HSR by Heat involves an m6A modification and the nuclear m6A reader protein YTHDC1. Furthermore, the global downregulation of transcription induced by heat shock is suggested to be caused by activation of cryptic intronic polyadenylation sites in introns. Intronic polyadenylation sites led to premature transcriptional termination and new short mRNAs accumulating in the nucleus (62). Thirty percent of the stress-induced genes have HSF1 bound to the promoter. Several genes upregulated by heat stress but not bound by HSF1 are frequently contacted by distal regions bound by HSF1 as shown by chromosome conformation capture techniques, Hi-C performed in human and Drosophila cells (56). However, the regulatory mechanisms that coordinate the transcriptional induction of HSF1-dependent and -independent genes with the transcriptional repression of more than 6000 genes in

humans remains to be uncovered. Overall, heat shock and other stresses dramatically affect global transcriptional regulation, leading to potent induction of genes encoding for prosurvival proteins.

1.2.4 Translational regulation during the HSR

To preferentially synthesize HSPs during stressful events, cells have adapted a mechanism whereby non-HSP transcripts are retained in the nucleus, and HSP transcripts are selectively exported to and translated in the cytoplasm. The exact mechanism of this selective process is not known. However, work conducted on S. cerevisiae has shown that nuclear export of non-HSP mRNA involves RNA adaptor proteins, Npl3, Gbp2, Hrb1, and Nab2, cotranscriptionally loaded onto the pre-mRNA, which then recruits Mex67–Mtr2 (TAP–p15 in humans), an essential heterodimeric receptor mRNA export factor (63). These adaptor proteins have an mRNA quality control function that prevents the nuclear export of incorrect, possibly improperly processed or assembled mRNAs (64). During stress, Mex67 and the adaptor proteins are dissociated from non-HSP transcripts to prevent nuclear export. However, HSP transcripts do not require adaptive proteins and are loaded directly with Mex67 via HSF1 (64). Thus, HSP transcripts bypass the adaptor–protein–mediated quality control mechanism to be rapidly exported and translated.

The newly synthesized HSP mRNAs encounter a cytoplasmic environment in which translation is repressed. Cells sense the load of misfolded proteins and repress translation by different pathways to decrease the load of unfolded and misfolded proteins. However, the translation of mRNA encoding for specific HSPs, such as the inducible HSP70, HSP82, and HSP27, is specifically favored (65). Regulation of translation enables the cells to rapidly adapt their proteome to stress conditions (66). From the three stages of translation: initiation, elongation, and termination, stress conditions repress cap-dependent translation initiation and elongation (67). The association of translation initiation factors (eIF4A, eIF4B, Ded1) and ribosomal proteins with mRNAs is

decreased immediately upon stress (68). Additionally, stress conditions promote the recruitment of translation factors and regulatory RNA binding proteins to stress-induced cytoplasmic structures known as stress granules (SGs) and processing bodies (PBs), limiting their availability (69, 70, 71) **(Fig. 1.2.1).**

Regulation of translation initiation and elongation

Eukaryotic translation initiation is a highly regulated multistep process and the rate-limiting step in translation. It involves the assembly of the ternary complex (TC) and binding of the eIF4F complex to the 5′ m7G cap structure in the mRNA. Both steps are downregulated during stress by different signaling pathways (72).

The TC, GTP-eIF2α-initiator methionine tRNA, preloaded with eIF1, eIF1A, eIF3, and eIF5, assembles on the 40S ribosomal subunit to form the 43S preinitiation complex (73, 74, 75). Stress precludes the formation of the TC by the reversible phosphorylation of the Ser51 in eIF2α. This phosphorylation event limits the pool of available eIF2α for the TC formation. (Fig. 1). The phosphorylation of eIF2α in response to stress is part of the ISR (76). Depending on the stress stimulus, one of four serine-threonine kinase enzymes catalyzes the phosphorylation of Ser51. These kinases are the heme-regulated inhibitor and the general control nonderepressible 2, which are conserved in eukaryotes, the protein kinase R (PKR), which is specific to vertebrates, and the PKR-like ER kinase, which is absent in fungi. Heme-regulated inhibitor is activated to cope with heme deficiency in red blood corpuscles, heat and osmotic shock, oxidative and mitochondrial stress, cytosolic protein aggregation, and arsenite treatment in cells other than red blood corpuscles (66, 77, 78, 79, 80, 81, 82). General control nonderepressible 2 phosphorylates eIF2α in conditions of nutrient depletion (83) and UV irradiation (84, 85). PKR mediates the phosphorylation of eIF2α in response to the detection of double-stranded viral RNA and hyperosmotic stress (dsRNA) (82,

86). PKR-like ER kinase activates upon ER stress, aggregation of misfolded proteins in the ER lumen, hypoxia, hypoglycemia, ischemia, oxidative stress, and perturbation in Ca2+ levels (87, 88). The conversion of the eIF2-GDP binary complex to the translation competent eIF2-GTP is mediated by the eIF2-specific guanine nucleotide exchange factor, eIF2B (80, 89). Two copies of eIF2B forms an active decameric complex that interacts with eIF2 and loads a molecule of GTP on eIF2. Phosphorylated eIF2α acts as a noncompetitive inhibitor by sterically hindering the access of eIF2 to the catalytic domain of eIF2B and sequestering it. Consequently, the recycling of eIF2α is decreased, which in turn decreases the abundance of TC (80, 90, 91) and impairs cap-dependent translation promoting metabolic dormancy to survive through the stress (92).

In addition to eIF2α phosphorylation, the binding of the eIF4F complex to the 5′ m7G cap structure is impaired by different means. The eIF4F complex is made of the cap recognizing factor eIF4E, the scaffold protein eIF4G, and the ATP-driven RNA helicase eIF4A that unwinds secondary structures in the 5′ untranslated region (UTR) of mRNAs (75, 93). The binding of eIF4E to the cap is partially regulated by the mammalian target of the rapamycin (mTOR) pathway (93, 94, 95, 96). mTOR is a kinase that phosphorylates the downstream targets eIF4E binding protein 1, preventing its binding to eIF4E, which allows its binding to the cap under favorable conditions (93, 97). During stress, mTOR is inactivated by TSC1/2, leading to the dephosphorylation of eIF4E binding protein 1, which readily sequesters eIF4E and suppresses the eIF4F complex formation (98, 99, 100, 101). Additionally, the newly synthesized HSP27 binds eIF4G with high affinity preventing the formation of the eIF4F complex (102). Together, these mechanisms prevent the assembly and binding of eIF4F to the m7G cap structure and cap-dependent translation.

The elongation step of translation is also regulated to enforce the translation repression of nonstress mRNAs during conditions that challenge protein homeostasis. During translation elongation, the

GTP-bound elongation factor eEF1A brings the aminoacyl-tRNA corresponding to the codon in the ribosomal A site, and eEF1A-GDP is released upon codon–anticodon base pairing. The ribosomal RNA in the peptidyl transfer center catalyzes the peptide bond formation, and the translocase eEF2–GTP triggers the mRNA–tRNA movement with the expense of GTP, and eEF2-GDP is released (103, 104, 105). Stress regulates translation elongation by a major downstream effector of mTORC1, the S6 kinase. The S6 kinase phosphorylates Ser366 of the eEF2 kinase and inactivates it (106). Inhibition of mTORC1 upon stress leads to the activation of eEF2 kinase that phosphorylates eEF2 at Thr56 of the GTP binding domain, pausing translation elongation (107, 108, 109, 110, 111, 112, 113). It should be noted that the regulation of eEF2 and its kinase is more complex than what we have described here, as they can be phosphorylated at different residues through different pathways (111, 114).

Besides eEF2 regulation, studies from two independent laboratories have identified chaperone-mediated regulation of translation elongation during stress. The cytoplasmic chaperone HSP70 and HSP90 interact with nascent polypeptides, favoring their cotranslational folding as they emerge out the ribosome exit tunnel (115, 116) (Fig. 1). During severe stress, the prevalence of unfolded proteins titrates out the chaperones leaving the nascent polypeptides unassisted for cotranslational folding. Hence, an arrest in elongation was observed after the synthesis of the first 65 amino acids, which corresponds to the length of the nascent polypeptide that fits in the ribosome exit tunnel. Consequently, stalled ribosomes were observed in several different mRNAs at nucleotide position 195. The lack of chaperone–ribosome interaction impairs the cotranslational folding of nascent polypeptides accounting for the elongation pausing and global translation repression during severe heat stress (117, 118). Overall, HSP encoding mRNAs should be equipped to overcome the several steps at which translation is shut by the cell.

SGs and PB formation

Translation repression is accompanied by changes in the physical properties of the cytoplasmic milieu. Stress triggers RNAs and proteins to phase separate and form SGs and PBs that contain untranslated, long, and highly unstructured mRNAs and proteins that participate in translation, transcription, splicing, and decay (71, 119, 120, 121). SGs and PBs are dynamic membraneless structures assembled by liquid–liquid phase transition that favor stress tolerance and promote cellular fitness (122, 123, 124, 125, 126). While the number and size of PBs increase upon stress, SGs are formed under stress conditions that invoke arrest in translation initiation (127). SGs and PBs have different mRNA and protein compositions. PBs are made of RNA processing factors (e.g., eIF4E, DDX6, and Ded1p), decapping and deadenylation enzymes, exoribonucleases, and factors mediating mRNA stability (For review: (124, 125)). Based on their enrichment in decay-related factors, PBs were believed to be mRNA degradation sites. However, mRNAs retained in PBs can return to the cytoplasm and engage in translation (124, 128). Thus, it is widely accepted that PBs could serve as a reservoir of nontranslating mRNAs and inactive decay enzymes (129, 130).

SGs form under stress conditions that induce eIF2α phosphorylation (131, 132), but they can also form independently of eIF2α phosphorylation. For example, puromycin treatment and inhibition of eIF4A with hippuristanol stimulate SG assembly (133, 134, 135, 136, 137). SGs are enriched in translation initiation factors, mRNA binding proteins, 40S ribosomal subunit, and mRNAs encoding for house-keeping genes (131, 132, 138, 139). mRNAs recruited to SGs are translationally repressed and undergo compaction as the elongating ribosomes are released from the transcripts (140, 141). The SGs were speculated to function in blocking protein synthesis by trapping several initiation factors and stabilizing translationally inactive constitutive mRNAs so

that they can reengage in translation upon recovery (136, 142, 143, 144). Certain mRNAs are shown to have paused ribosomes at the start codon to quickly re-initiate the protein synthesis as the cells recover from stress (145). Even so, the lack of SGs does not change mRNA translational repression or stability (142). Additionally, mRNAs-encoding stress-regulated proteins like activating transcription factor 4 have been shown to translate inside the SGs (146). HSP mRNAs skip the localization in SGs and PBs as their ongoing translation prevents them from condensating (119, 147).

Translation of HSP70 mRNAs under stress conditions

Several inducible HSP mRNAs are highly translated in spite of the general repression of translation during heat stress (148). Among them, the inducible HSP70 is the most synthesized HSP, as shown in 3H-leucine pulse labeling experiments (65). Hence, the *HSP70* mRNA should have specific features favoring its translation. In 1985, Klemenz et al. (149) were the first to indicate that the 5′UTR of the *HSP70* mRNA is required for its preferential translation during heat stress. McGarry and Lindquist also reported that the 5′ leader sequence of the *HSP70* mRNAs is the region detected by *D. melanogaster* cells to preferentially translate it during heat stress (150). Given that both deletions and insertions within the 5′ UTR rendered *HSP70* mRNA untranslated during heat stress and actively translated during recovery from stress, the authors suggested the presence of a secondary structure in the 5′ UTR (150). However, it was not until 1988 that the internal ribosome entry sites (IRESs) were discovered to mediate the translation of picornaviral mRNAs (151, 152), and until 1991 that the first cellular IRES was identified in the mRNA encoding for the immunoglobulin heavy chain binding-protein BiP or GRP78 (153). GRP78 is indeed an HSP70 that localizes and functions in the ER. Unlike the picornavirus mRNAs, the GRP78 mRNAs are capped, and their translation is favored when cap-dependent translation is

halted under conditions of stress (149, 154, 155). Studies in HeLa cells also indicated that the factors eIF4E and eIF4G are dispensable for translation of *HSP70* mRNA, suggesting a cap-independent mechanism of translation initiation (156). Following these discoveries, several labs have attempted to characterize the IRES structure and trans-regulatory factors required to translate *HSP70* mRNA in different organisms (157, 158, 159). However, those attempts were unsuccessful in finding an IRES in the 5′ UTR of *HSP70* mRNA and provided early evidence of an *HSP70* mRNA cap-independent translation mechanism (160). Overall, these studies indicated that the mammalian *HSP70* mRNA translation has reduced dependence on the eIF4F cap-binding complex during stress, *HSP70* mRNA is translated in a cap-independent manner upon mTOR inhibitions, and the 5′ UTR is required for *HSP70* mRNA translation during heat stress (157, 161) **(Fig. 1.2.4)**.

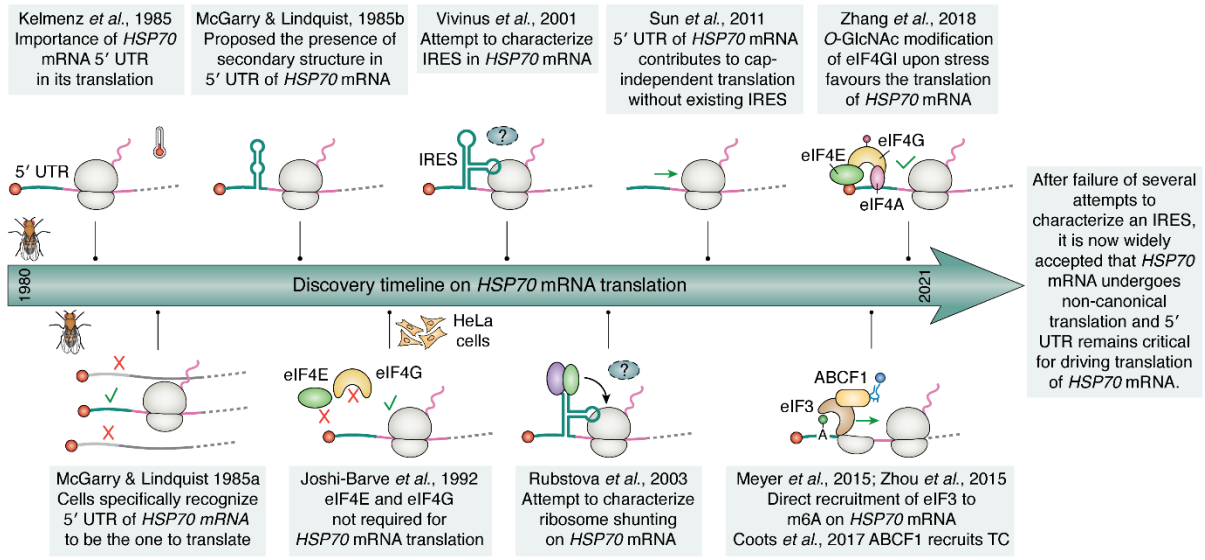

Figure 1.2.4. Milestones on the discovery of *HSP70* mRNA translation. Timeline of the discoveries made toward elucidating the translation mechanism of *HSP70* mRNA. Since the discovery of internal ribosome entry site (IRES)–mediated cap-independent translation, several studies have attempted to characterize an IRES in 5′ UTR of *HSP70* mRNA. While no studies have reported an IRES so far, they have emphasized the significance of the 5′ UTR of *HSP70* mRNA. It is now widely accepted that *HSP70* mRNA undergoes IRES-independent noncanonical translation. UTR, untranslated region.

Two different translational initiation control mechanisms have been suggested for the mammalian *HSP70* mRNA: ribosome shunting (157) and recruitment of eIF3 by N6-methyladenosine (m6A) modification (161, 162). During ribosome shunting, the 40S ribosomal subunit skips a large portion of the HSP70 5′ UTR and shunts to a region proximal to the canonical start codon when the cap-dependent translation is inhibited during heat shock (157, 159). More recently, it was found that *HSP70* mRNAs are cotranscriptionally imprinted at adenosine 103 of their 5′UTR by methylation, m6A (161, 162). This methylation supports translation initiation by binding to the initiation complex eIF3, which recruits the ribosome to the mRNA. A follow-up paper concluded that cells activate m6A-mediated translation through the factor ABCF1. ABCF1 serves as an alternative recruiter for the TC to *HSP70* mRNA during noncanonical translation upon heat shock (163). Further, heat-stress–mediated O-GlcNACylation of eIF4GI has been reported essential for the translation of *HSP70* mRNAs (164). Additionally, the escape of *HSP70* mRNA from the shutoff of global protein synthesis was explained by the existence of specialized stress ribosomes. These ribosomes bear the cytoplasmic version of a mitochondrial protein, MRPL18, synthesized upon stress and might facilitate the recruitment of factors involved in translation elongation (165). The main caveat of these publications is the timing at which translation of *HSP70* mRNA was studied. They used 4 h of recovery following 1 h of heat stress. At this time point, cap-dependent translation resumes, and SGs are resolved. Hence, they provide solid evidence on the regulation of *HSP70* mRNA translated during recovery. Whether the same factors participate in its translation during stress remains to be elucidated **(Fig. 1.2.4)**.

A relevant outcome of this research is the suggestion of cotranscriptionally imprinting of the mRNA that provides an advantage for its translation in the cytoplasm (163, 165). Paradigm shifting studies in yeast support the role of the HSE sequence in the promoter of HSP genes in

determining the translation of inducible HSP mRNAs in the cytoplasm of glucose-starved yeast (166). We have previously reported that eEF1A1 links HSP70 transcription to translation in mammals, implicating the evolutionary conservation of this “remote control” mechanism of translational regulation (167). Hence, newly synthesized HSP mRNAs might arrive at the cytoplasm equipped for translation. These factors, together with the intrinsic characteristics of the 5′UTR, allow HSP mRNAs to engage in translation at the expense of housekeeping mRNAs. For example, the Ded1 helicase is recruited to condensates upon heat stress, precluding the translation of housekeeping mRNAs with secondary structures and favoring the translation of HSP mRNAs that have little structure in yeast (168). However, the 5′UTR sequence varies among HSP70 inducible genes and species. While *D. melanogaster* contains mostly AU-rich (70%) sequence and no secondary structure formation, like in yeast (158), the mammalian sequence has higher GC content (63%) which is likely to favor a formation of stable secondary structures. Even though we have not yet put together all the regulatory elements and the cascade of events that lead to the preferential synthesis of the inducible HSP70 during stress, they might differ among species.

1.2.5 Recovery from stress and the degradation of HSP70 mRNA

The newly synthesized HSP70 allows cells to resume their normal functions gradually by recovering proteostasis through the folding of misfolded proteins, which also prevents their aggregation, and by participating in the disassembly of SGs (169, 170). Accordingly, the synthesis of a nonfunctional HSP70 or inhibition of *HSP70* mRNA translation during stress delays the recovery of global translation in *D. melanogaster* cells (148, 171, 172, 173). However, the synthesis of HSP70 should be repressed when cells return to optimal conditions. The persistent expression of the inducible HSP70 under nonstress conditions causes growth defects in *D. melanogaster* (174) and promotes malignancy in mammalian cells (175). Hence, the HSP

transcription repression is accompanied by the rapid degradation of their mRNAs during recovery (171, 176). *HSP70* mRNAs are the first to undergo translational repression and degradation. The timing and rate of its degradation during recovery depends on the severity and duration of heat treatment (176, 177). When cells are returned to optimal conditions following heat shock, they restore global protein synthesis, and constitutive mRNAs engage in translation (176, 177).

In mammalian cells, *HSP70* mRNA transitions from being a stable mRNA during heat stress to a short-lived mRNA with a half-life of around 50 min during recovery from heat shock (172, 178, 179, 180). While the instability of *HSP70* mRNA is also characteristic of nonstress cells, other stresses like incubation of cells with sodium arsenite or inhibition of protein synthesis initiation with pactamycin also stabilize *HSP70* mRNA. Therefore, it has been suggested that a trans-regulator synthesized by the cells under nonstress or recovery conditions could destabilize *HSP70* mRNA by binding to its 3′ UTR. Deletion of the *HSP70* mRNA 3′UTR or substitution with that of the alcohol dehydrogenase (adh) 3′UTR sequence stabilizes the transcript during recovery from stress (173, 177, 181). In mammalian cells, PKR directly or indirectly, for example through AUF1 protein, associates to the 3′UTR of *HSP70* mRNA through its AU-rich elements (AUUUA) that destabilize the transcript during recovery (182). However, AU-rich elements become dispensable for the fast deadenylation of HSP70 transcripts during recovery in *D. melanogaster* cells, which suggests that RNPs mediating *HSP70* mRNA stability might differ among species (183). Like most cellular mRNAs, most HSP70 transcripts undergo a fast deadenylation mediated by the CCR4-NOT complex followed by decapping and degradation by the exonuclease Xrn1 in the 5′-to-3′ direction, as described in *D. melanogaster*. *HSP70* mRNA fragments shorter than the full-length mRNAs were identified by northern blot suggesting that some molecules might

undergo degradation after an endonucleolytic cleavage by the exosome in the 3′-to-5′ direction (183) **(Fig1.2.5)**

How does the cell recognize the HSP70 transcripts as the ones to be degraded? Within minutes of heat shock, hundreds of these mRNAs are synthesized, and when the conditions become optimal, they are selectively degraded with high efficiency. Is there a link between the translational status of the cell and HSP mRNA turnover? Polysome fractionation to study the translational profile of *HSP70* mRNA in *D. melanogaster* and mammalian cells show a fraction of transcripts retained in higher polysomes while a subset of them is translationally inactivated (177). Are both populations degraded by the exact decay mechanism? It might also be possible that RNPs associated with *HSP70* mRNA undergo posttranslational modifications, like arginylation, mediated by ATE-1, to regulate the stability of HSP transcripts, providing protection to cells upon heat shock (184).

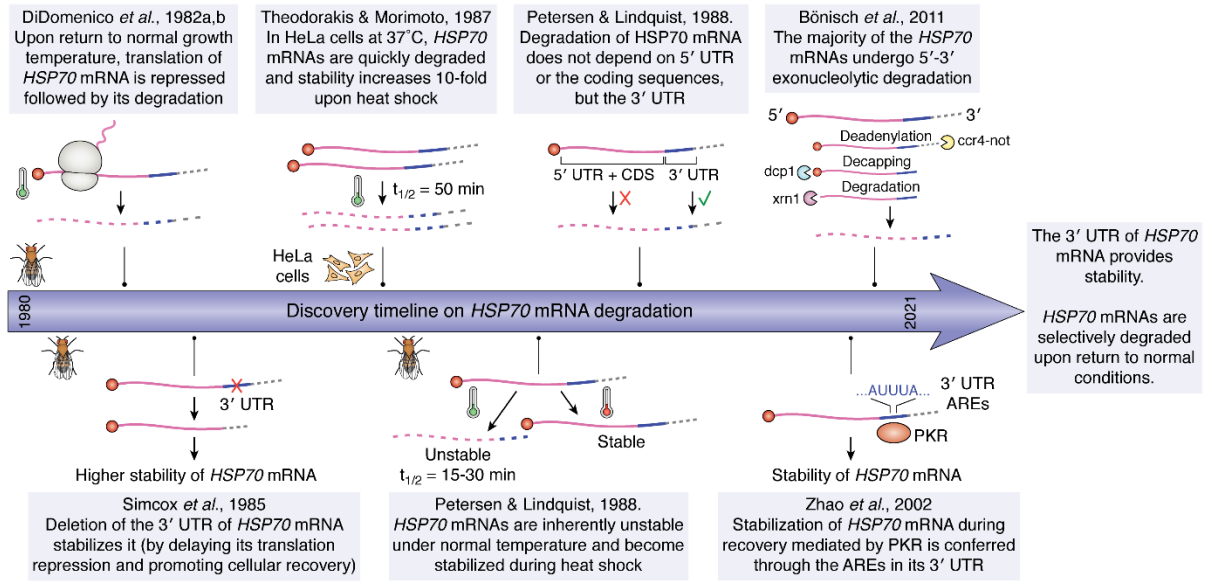

Figure 1.2.5. Milestones on the discovery of *HSP70* mRNA degradation. Stress stabilizes the *HSP70* mRNA. However, soon after the removal of stress stimulus, the cells rapidly and selectively degrade the *HSP70* mRNA. The figure indicates the crucial discoveries made toward elucidating the mechanism of degradation of *HSP70* mRNA. Various studies have reported that the 3′ UTR of *HSP70* mRNA coordinates its stability or turnover. AREs, AU-rich elements; HSP, heat shock protein; UTR, untranslated region.

1.2.6 Proteostasis on specific organisms, cell types, and conditions

While the HSR is a universal survival response to changes in the environment, there are variations in the regulation of the HSR among species and even within cell types of the same organisms. Additionally, the adaptation to abrupt or long-term changes influence the cellular response differently (8, 16, 181, 182, 183).

Variation of the HSR among organisms

The number of genes encoding for HSPs and cochaperones has increased over evolution, probably reflecting the increased number of proteins and complexity of functions undertaken by more evolved cells (185, 186). Multicellular organisms have not only expanded on the HSPs encoded in the genome of unicellular organisms but also adapted them to their proteostasis needs. For example, the mammalian genome lacks the disaggregase HSP104 present in S. cerevisiae (in eubacteria ClpB), which reverses stress-induced protein aggregation (187, 188, 189) and has been suggested to serve as a potential therapeutic agent to disaggregate toxic misfolded aggregates characteristic of neurodegenerative diseases (NDs) (187). While it is unknown why mammalians lack HSP104, in vitro data have shown that protein disaggregation in humans (and other metazoans such as nematodes) relies on the molecular machinery comprised of HSP70, HSP110, and J-proteins (188, 190, 191). These J-proteins are critical in driving HSP70–HSP110–based disaggregase by concomitantly interacting with both substrates and HSP70 partner proteins via single or mixed cooperating J-protein cochaperones of class A and B which relocalize to protein aggregates following heat shock promote specific or broad-range aggregate targeting (188, 190, 191, 192). Overall, the core chaperones of the HSP70 and HSP90 families are similar among species and their organization as constitutive or inducible HSPs depends on their basal expression level **(Table 1.2.1).**

There is a variation in the temperature threshold needed to activate the HSF1 and the HSR across multicellular and unicellular eukaryotic species (193, 194) (Table 1). For example, while *D. melanogaster* induces the HSR at 30 °C, humans do so at 40 °C. This variability in temperature threshold has been suggested to be based on the environmental temperature of the organism and its capacity to maintain a constant body temperature (195, 196). Indeed, organisms occupying moderate variable thermal environments can modify the constitutive levels of HSPs and adjust their HSR to a higher onset temperature. In contrast, those organisms from a stable or highly variable thermal environment are not as capable of readjusting the levels of their HSPs or onset temperature as they are already meeting their maximum thermal limit.

An interesting example is multicellular organisms lacking the induction of an HSR, like the Antarctic marine invertebrate ciliates and the Antarctic fish of the suborder *Notothenioidei* (8, 197). The absence of the HSR is suggested to be due to these animals living in a highly stabilized cold environment; thus, they evolved to adapt to this nontransient environment. However, this is the opposite of the *Notothenioidei* cold-temperate relatives in New Zealand, which have been shown to induce an HSR following heat stress. Another example of an animal with no HSR is the freshwater cnidarian species *Hydra oligactis*, which is also highly sensitive to minor thermal variations. Its congener, *Hydra vulgaris*, can tolerate greater thermal ranges because it induces thermal tolerance following induction of HSPs synthesis (8, 197). Despite the lack of expression of inducible HSPs, these organisms express constitutive HSPs. They might have adapted the expression of their constitutive HSPs to help them overcome challenges faced in their environmental niche (8, 198). Thus, constitutive HSPs might play an essential role in overcoming proteostasis challenges without an inducible HSR. Examining the potential coordinated network

of constitutive and inducible HSPs in promoting a competent HSR would provide a better understanding of the network of HSPs participating in the adaptation to changes in temperature.

Table 1.2.1. Comparison of HSP genes and ranges of temperatures across different organisms

	Yeast		C. elegans		Drosophila		Mammals		E. coli	
										
Temperature range of HSR	30-37 °C(238) ΔT: 7 °C		29-35 °C (239) ΔT: 6 °C		29-38 °C (35-37)(239) ΔT: 9 °C (2 °C)		41-45 °C (240,241) ΔT: 4 °C		37-50 °C ΔT: 9 °C (13 °C)	
Number of HSP genes	63(238)		21(242)		87		>142(18)		~3 (243)	
Transcription of HSPs	Initiation (244)	Peak (241)	Initiation (239)	Peak (239)	Initiation (245)	Peak (246)	Initiation (247)	Peak (167)	Initiation (248)	Peak (248)
	1-5min at 37 °C	15min at 37 °C	Hsp70 and Hsp80 60min at 35 °C	Hsp70 and Hsp80 2hr at 35 °C	Hsp70 4min at 37 °C	1-2 min at 37 °C	~2.5-12 min at 42 °C	1 hr at 43 °C	Hsp70 (DnaK) 1-4 min at 42 °C	Hsp70 (DnaK) 5-6 min at 42 °C
Translation of HSPs	Temp Initiation (249)	Temp Peak (250)	Temp Initiation (239)	Temp Peak (239)	Temp Initiation (65)	Temp Peak (65)	Temp Initiation (251)	Temp Peak (251)	Temp Initiation (252)	Temp Peak
	Hsp38, 100, and 90 ~4min at 36 °C	HSP70 10-15min at 37 °C	Hsp16: 29 °C Hsp18: 29 °C Hsp19: 35 °C Hsp29: 35 °C Hsp81: 35 °C Hsp70: 29 °C	Hsp16: 33 °C Hsp18: 33 °C Hsp70: 35 °C	Hsp23: 33 °C Hsp26: 33 °C Hsp82: 26 °C Hsp70: 26 °C	Hsp23: 35 °C Hsp26: 35 °C Hsp82: 33 °C Hsp70 37 °C	Hsp70 ~6min at 42 °C	Hsp70 30min at 42 °C	Hsp60 (GroEL) and Hsp70 (DnaK): ~3-5 min at 42 °C	Hsp60 (GroEL) (188) and Hsp70 (DnaK) (256): 5-10min at 42 °C

Multicellular endothermal organisms tolerate higher ranges in temperature than unicellular or stenothermal multicellular organisms. However, endothermal organisms required a lower increase over their body temperature to induce the HSR (Table 1). There are unicellular organisms from the Archaeal species that can tolerate extreme temperatures such as those between 50 °C to

70 °C (thermophiles) and 80 °C or higher (hyperthermophiles) before the HSR is induced (199). In addition to the HSR, bacteria rely on a structural liability in response to temperature changes which create biological temperature sensors, such as DNA- and RNA-based environmental temperature sensors. Temperature changes will alter gene expression at transcriptional and posttranscriptional steps via DNA and RNA thermosensors to maintain proteostasis. Furthermore, changes in the secondary or tertiary structure can also be used by "RNA thermometers" in bacteria to regulate the translation efficiency of heat shock mRNAs. In this RNA 'zipper-like' thermosensory mechanism, the mRNA will adopt a thermolabile stem-loop structure in the 5′UTR which will either close to block translation at low temperatures or open at high temperatures to favor ribosome binding and translation (3, 10). These RNA thermosensing mechanisms are also important in the translation control of some HSPs in eukaryotic cells when cap-dependent translation initiation is inhibited (3, 10). For example, HSP90 mRNA in *D. melanogaster* becomes actively translated in response to heat shock but is inefficient in normal growth temperatures. It has been suggested that the HSP90 mRNA translation is substantially activated by heat shock due to the presence of a long stem in the AUG initiation proximal half of the 5′UTR, which serves as a heat-sensitive inhibitory element in the UTR that impedes access to the initiation codon (200). However, in heat stress, the stem undergoes a thermal destabilization, which allows the ribosomal subunits to recognize the region (200). While the expression of HSP90 has been shown to be essential for restoring folding yield when HSP70 levels are high, excess HSP90 (as well as HSP70) produced during heat shock may be detrimental to folding (201). Thus, the presence of a thermosensor is critical in mediating the translation of HSPs that are important for protein folding during heat shock. This preferential heat shock translation occurs in a similar translation mechanism as in bacteria wherein the start codon (AUG) will respond to differences in temperature

similarly to bacterial RNA thermosensors. A similar mechanism of translation control has been proposed for *HSP70* mRNA in human cells but has yet to be examined (3). These examples suggest that multicellular organisms conserved some of the modes of adaptation to heat stress used by bacteria, but they have changed the regulatory factors sustaining them.

Additionally, endothermal organisms readjust their physiology to increasing temperatures (197). The repeated exposure to elevations in core temperature due to natural environmental heat stress causes heat acclimatization (202). An increase in temperature is associated with a change in the pattern of HSPs expressed is due to proteins being able to adapt their structures to varying temperatures, e.g., altering hydrophobicity, charge, noncovalent interactions, volume, and cooperativity. Indeed, patterns of adaptive variation in the structural and functional properties of proteins from organisms that have adapted to different temperatures have been reported (203, 204). A similar phenomenon has been recently described in the yeast *S. Cerevisiae* in response to a long-term temperature shift (205). Interestingly, a key feature of long-term temperature adaptation is the disappearance of protein aggregates, whereas acute heat shock induces protein aggregates. Thus, yeast may have adapted to persistent high temperatures by reducing the load of thermolabile proteins and relocating some proteins to minimize protein misfolding/unfolding at high temperatures (205). These findings have important implications in the context of global climate change as the current temperature changes we are experiencing can be considered as long-term temperature adaptation to the constant heat.

Variation of the HSR among cell types

The requirements of cellular proteostasis also vary across cell types in multicellular organisms, which maintain a relatively stable internal environment to sustain proteostasis among specialized tissues and organs (1, 2, 206). These multicellular organisms have highly specialized

functions performed by distinct proteomes, in which proteostasis, assisted by a network of core and cell-specific chaperones, becomes challenging (186, 206). There are two hypotheses as to how multicellular organisms maintain proteostasis following an environmental perturbation like temperature. The first is that molecular chaperones are expressed in all cell types to guide folding and prevent misfolding, and thus, they can buffer unexpected folding challenges. This hypothesis requires all cells to invest energy to have a reserve of chaperones for emergencies (1, 197, 205, 206, 207, 208). As described in this review, the constitutive HSPs provide immediate assistance in coping with misfolded proteins upon acute stress (197, 206). Whereas de novo synthesized HSPs favor recovery from stress and fit the cell to overcome subsequent and more detrimental stress stimuli. This phenomenon, known as stress-preconditioning, is used for medical purposes and suggests that cells have a certain buffer of HSPs to handle mild changes in environmental conditions (205, 207, 209, 210, 211, 212).

The second hypothesis states that cells do not store excess chaperones. Instead, the cellular concentration of the chaperones is regulated precisely according to the immediate cellular requirements. Hence, the folding environment in the cell is delicate, with little capacity for a flux of non-native species. This hypothesis requires the HSR to be rapidly tailored to the proteostatic demands of the cell (206). Additionally, cell types and tissues would need to exchange information on the status of internal cellular proteostasis to coordinate proteostasis at the organismal level (2). The second hypothesis is demonstrated in Caenorhabditis elegans, wherein the thermosensory amphid neurons with finger-like ciliated endings (AFDs) detect changes in the ambient temperatures and coordinate the response. This coordinated response involves communication between the different tissues of *C. elegans* and is regulated by neurons. More specifically, AFDs sense heat shock stress in the environment; these stress signals are then sent via neuroendocrine

fashion to tissues such as muscle and intestinal cells to regulate their HSR by activating HSF1 and promoting the induction of HSP70 (C12C8) (2, 213). At the same time, muscle and intestine cells have a transcellular chaperone signaling between nonneuronal tissues that sense local proteotoxic stress and enhance chaperone signaling at a distance by signaling back to the neurons. These AFD neurons along with their postsynaptic cells, AIY interneurons, further regulate the temperature-dependent behavior of these organisms, such as growth and reproduction (206, 213). Similar activation of HSF1 through neuroendocrine signaling from the hypothalamic–pituitary–adrenal axis operates in rats (214).

As neurons play an important role in this organismal-level coordination in eukaryotes, it is important to mention the current literature on neuronal proteostasis. Neurons are highly polarized cells that have the capacity to tune their proteome locally, at axons, dendrites, and synapses, through the regulation of local protein synthesis, degradation, and posttranslational modifications (215). However, it is not fully understood how proteostasis is sustained in different neuronal subcompartments under heat stress conditions. Rodent hippocampal and motor neurons exhibit a lower HSR activation than nonneuronal cells (206, 216). This impaired HSR could make neurons vulnerable to the toxic accumulation of misfolded proteins that underlie age-related NDs (216, 217, 218, 219). Hence, a potential therapeutic strategy for NDs is to promote the activation of the HSR in neurons (220, 221, 222, 223). The overexpression of HSP70 in a mouse model of Alzheimer's Disease exerted cytoprotective roles and ameliorated physiological and behavioral deficits (220, 221, 222, 223). Promoting the activation of HSF1 has long been considered a promising treatment for NDs. However, the threshold to activate HSF1 in motor neurons is higher than in somatic nonneuronal cells (216). The chromatin environment of HSP genes in neurons does not favor the binding of HSF1, and the treatment with histone deacetylases can enhance the

transcriptional activity of HSF1 in motor neurons undergoing specific stresses (224). Hence, neurons might have been wired differently to handle proteostasis challenges and rely on other quality control mechanisms, like ubiquitin-proteasome system and autophagy, to sustain a healthy and functional proteome (218, 225, 226, 227, 228, 229).

The induction of HSPs represents the first line of defense toward an increase in protein unfolding (230). To date, the regulation of HSPs expression has been mostly studied by ensemble measurements in cultured cell lines and yeast. This extensive research has provided detailed information on the kinetics of HSPs transcription and mRNA translation and degradation and has identified regulatory factors involved in each step of the life cycle of HSP mRNAs. In the last decade, single-cell microscopy approaches have granted the spatial resolution needed to investigate changes in the localization of HSP loci upon stress (50) as well as the subcellular localization of newly synthesized mRNAs (166, 167). These latest studies indicate that the fate of HSP mRNAs is decided cotranscriptionally. Therefore, a finely tuned communication between the nucleus and the cytoplasm under stress conditions could enable cells to identify HSP mRNAs as the ones to be translated. These results also suggest that each step in the life cycle of HSP mRNAs highly influences the next one. Given that hundreds of HSP mRNAs molecules are rapidly synthesized, translated, and degraded, the use of single-molecule fluorescence microscopy techniques to detect single mRNAs and de novo protein synthesis will mind the gap of our knowledge in the impact of HSP mRNAs translation on decay and the localization of mRNA degradation (231, 232, 233).

1.2.7 Conclusion and perspectives

Activation of the HSR requires a mechanism to sense the damage and gene expression reprogramming to prioritize the expression of HSPs. The transcription factor HSF1 directs the

upregulation of HSPs transcription. Activation of HSF1 occurs in all eukaryotes under a wide range of stresses (31, 230, 234). Together with HSF1 activation, cells attempt to minimize protein unfolding by blocking general translation elongation (230, 235). It is possible that besides the increased load of unfolding proteins, this general ribosome stalling signals to HSF1 by a still unknown mechanism (166). Identifying the mechanisms that act to orchestrate a competent HSR will provide the means to interrogate neurons in their stunt HSR and relate it with the neuronal vulnerability to accumulate misfolded proteins. In this case, using pathophysiological conditions relevant to the neuronal activity will provide a better understanding of the neuronal response to proteostasis challenges. Expanding the pioneering research done in *C. elegans* to other multicellular organisms will provide the means to integrate the response of the nervous system into the organism effort to sustain proteostasis (213). A comprehensive analysis of the cellular response to stress in the context of the organism will open new windows to study the etiology of diseases derived from the loss of protein homeostasis, like cancer and neurodegeneration.

1.3: Proteostasis regulation through Ribosome Quality Control and No-Go-Decay

Authors

Lokha Ranjani Alagar Boopathy1, Emma Beadle1, Aitana Garcia-Bueno Rico1, Maria Vera1.

1. Department of Biochemistry, McGill University, Montreal, Canada.

1.3.1 Abstract

Cell functionality relies on the existing pool of proteins and their folding into functional conformations. This is achieved through the regulation of protein synthesis, which requires error-free mRNAs and ribosomes. Ribosomes are quality control hubs for mRNAs and proteins. Problems during translation elongation slow down the decoding rate, leading to ribosome halting and the eventual collision with the next ribosome. Collided ribosomes form a specific disome structure recognized and solved by Ribosome Quality Control (RQC) mechanisms. RQC pathways orchestrate the degradation of the problematic mRNA by No-Go Decay and the truncated nascent peptide, the repression of translation initiation, and the recycling of the stalled ribosomes. All these events sustain protein homeostasis and return valuable ribosomes to translation. As such, cell homeostasis and function are maintained at the mRNA level by preventing the production of aberrant or unnecessary proteins. It is becoming evident that the crosstalk between RQC and the protein homeostasis network is vital for cell function, as the absence of RQC components leads to the activation of stress response and neurodegenerative diseases. Here, we review the molecular events of RQC discovered through well-designed stalling reporters. Given the impact of RQC in proteostasis, we discuss the relevance of identifying endogenous mRNA regulated by RQC and their preservation in stress conditions.

1.3.2 Graphical/Visual Abstract and Caption

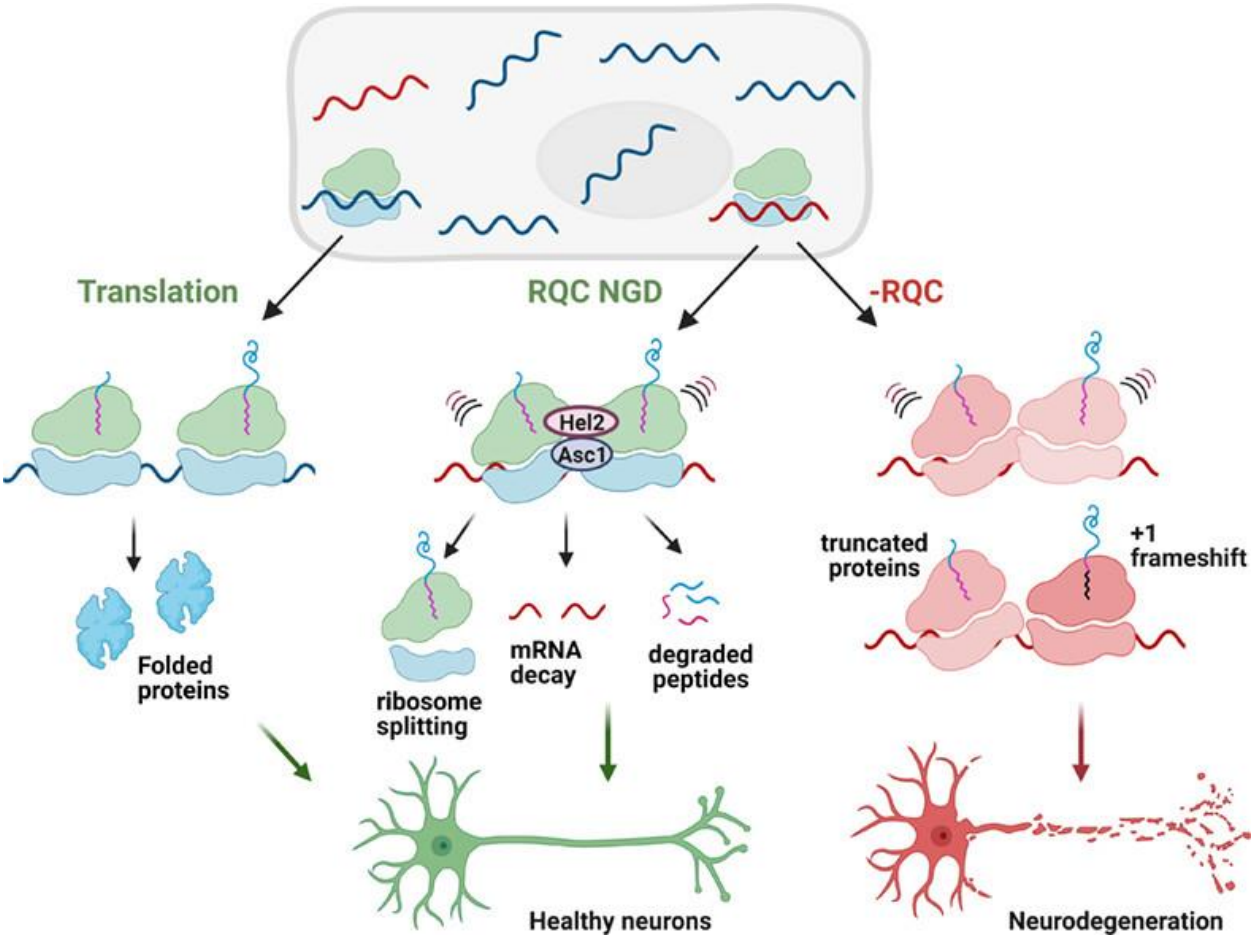

Cells identify and solve mRNAs with stalling sequences among their translation pool through the ribosome quality control mechanisms (RQC). RQC is linked to the No-Go-Decay (NGD) mRNA surveillance pathway to solve ribosome collisions and prevent problematic mRNAs from entering subsequent translation rounds. RQC prevents the accumulation of truncated nascent peptides, recycles ribosomes, and supports cell proteostasis. The absence of RQC/NGD factors or their saturation by stress leads to proteostasis collapse, for which neurons are especially vulnerable.

1.3.3 Introduction

Several cellular processes, such as cell proliferation, differentiation, and adaptation to changing environmental conditions, require the tight regulation of gene expression. The timed control of gene expression is facilitated by the cell's capacity to rapidly modify the pool of cytoplasmic mRNAs and control their translation. Cellular mRNAs are subjected to multiple checkpoints, co- and post-transcriptionally, before entering the cytoplasm and engaging in protein synthesis (As previously reviewed by (Brewer, 2001; de Almeida & Carmo-Fonseca, 2010; Karamyshev & Karamysheva, 2018; Keene, 2007)). As a result of these primary quality control checkpoints, mRNAs with serious aberrations, such as the lack of 5' cap or the poly-A tail, are retained and degraded within the nucleus through nuclear mRNA surveillance mechanisms (Shoemaker & Green, 2012). Additionally, cells have co-translational quality control mechanisms to detect mRNAs bearing subtle defective sequences, such as the insertion of or mutation of a stop codon (Bengtson & Joazeiro, 2010; Choe et al., 2016; Dimitrova et al., 2009; Powers et al., 2020; Shoemaker & Green, 2012). Translation of faulty mRNAs results in the synthesis of aberrant, nonfunctional proteins that disrupt protein homeostasis and challenge cell fitness, function, and survival (Shoemaker & Green, 2012). Thus, ribosomes recognize errors in the mRNA during translation elongation, which halt their elongation and activate ribosome quality control (RQC) mechanisms (Brandman et al., 2012; Choe et al., 2016; Matsuo et al., 2017; Pisareva et al., 2011; Shoemaker et al., 2010; Shoemaker & Green, 2011). RQC encompasses mRNA surveillance and protein quality control to repress their translation and triggers the degradation of problematic mRNAs and truncated nascent peptides (Ito-Harashima et al., 2007; Juszkiewicz & Hegde, 2017; Matsuo et al., 2017; Simms et al., 2017; Sitron et al., 2017; Sundaramoorthy et al., 2017). Translation and ribosome biogenesis are energy-expensive processes, as they require the

coordination of rRNA transcription, modification of rRNAs, and translation of ribosomal proteins to achieve ribosome assembly (Hershey et al., 2019; Holcik & Sonenberg, 2005; Z. Li et al., 2009; Young & Guydosh, 2022). Thus, RQC also enables cells to rescue and recycle ribosomes from problematic mRNAs to make them available to translate appropriate mRNAs (Ikeuchi et al., 2019; Juszkiewicz et al., 2018; Juszkiewicz & Hegde, 2017; Matsuo et al., 2017; Sitron et al., 2017; Sundaramoorthy et al., 2017). This highlights the relevance of degrading the faulty mRNAs to prevent them from engaging in subsequent rounds of translation, which would waste valuable ribosomes by producing aberrant proteins.

Cells have three mRNA surveillance mechanisms to ensure the quality of mRNAs being translated: nonsense-mediated decay (NMD), non-stop decay (NSD), and no-go decay (NGD) (Bengtson & Joazeiro, 2010; Dimitrova et al., 2009; Doma & Parker, 2006; Shoemaker et al., 2010; Simms & Zaher, 2016). While the mRNA substrate for each of these processes has defining features, all three mechanisms are triggered by the presence of a stalled ribosome on an mRNA. Although a few mRNAs rely on NMD to regulate their cytoplasmic lifecycle, NGD is unique as it does not require the mRNA to hold a mutation to signal its decay (Maquat, 2004; Shoemaker & Green, 2012). Instead, it recognizes ribosome collisions resulting from elongating ribosomes that stall due to an aberrant decoding slowdown. If a ribosome is stalled for an extended period, a second elongating ribosome can collide with the initially stalled ribosome forming a disome. The disome structure provides a hub to recruit the mRNA decay factors. Thus, NGD has the potential to degrade mRNAs based on the characteristics of their coding sequence (CDS) or their translation efficiency. For example, changes in the pool of available tRNAs dictate translation elongation rates, and a higher translation initiation increases the chances of ribosome collisions (Park & Subramaniam, 2019). As such, NGD is intimately related to RQC and arises as a mechanism to

adjust the pool of cytoplasmic mRNAs according to internal or external cell clues. NGD also prevents the stalled ribosomes from frameshifting and the subsequent synthesis of aberrant proteins (Simms et al., 2019). Interestingly, the depletion of NGD factors leads to the activation of the integrated stress response (ISR) as a mechanism to lessen general translation initiation to maintain proteostasis (Yan & Zaher, 2021). Here, we review the cytoplasmic mRNA surveillance mechanism of NGD and its close relation with RQC, with particular emphasis on its components and mechanical processes involved in its execution. We briefly discuss the techniques and reporters used to study RQC and NGD and ultimately provide the molecular, cellular, and organismal implications of these mechanisms in safeguarding proteostasis and possible implications for neurodegenerative conditions.

1.3.4 General mRNA decay versus surveillance mRNA mechanisms

In eukaryotic cells, mRNA turnover is critical for the tight regulation of protein expression. Regulation of mRNA turnover reduces the pool of mRNAs, efficiently diminishing the synthesis of their encoded proteins. The degradation pathways of eukaryotic mRNAs have been well characterized in *Saccharomyces cerevisiae* and are highly conserved in metazoans (Bönisch et al., 2007; Decker & Parker, 2002). The unique features of eukaryotic mRNAs – the 7-methyl guanosine (m7G) cap co-transcriptionally added to the 5' end and the long stretch of adenine residues post-transcriptionally incorporated to the 3' end termed poly-A tail – are crucial for nuclear export, translation, and protection from cytoplasmic exonucleases (Decker & Parker, 2002). Hence, the decay machinery targets the 5' cap and/or 3' tail of mRNAs to adjust the proteome according to cellular needs (Bönisch et al., 2007). In yeast, the general mRNA turnover begins with the shortening of the poly-A-tail, which leads to two pathways; the 5’-3' exonuclease-mediated decay (which is predominant in yeast) or the 3’-5' exosome-mediated decay (Anderson

& Parker, 1998; Decker & Parker, 2002; Tucker & Parker, 2000). Deadenylation renders the mRNA translation incompetent by precluding the RNA-binding of the poly-A binding protein (PABP), which interacts with the eukaryotic translation initiation factor eIF4G favoring the translation initiation (Tharun & Parker, 2001). Additionally, deadenylation provides access to decapping enzymes and exposes the mRNAs for degradation. The deadenylation process is highly conserved from yeast to mammals and relies on the large multimeric CCR4-CAF1-NOT and PAN2/3 complexes. Vertebrates possess an additional enzyme, Poly(A) Ribonuclease (PARN), that is involved in deadenylation (Figure 1A) (Garneau et al., 2007; Łabno et al., 2016). In the 5'-3' degradation pathway, soon after deadenylation, the mRNA is decapped by DCP1p/2p, and then transcript degradation proceeds in the 5'- 3' direction by the conserved exoribonuclease XRN1 (Cougot et al., 2004; Hsu & Stevens, 1993; Muhlrad et al., 1994, 1995; Vidya & Duchaine, 2022). In the 3'-5' degradation or exosome-mediated pathway, following deadenylation, an RNA exosome complex degrades the transcripts in 3'-5' direction while the mRNA is simultaneously decapped by Dcs1p. Decapping in the 5'-3' pathway liberates m7GDP, whereas the 3'-5' pathway releases m7GMP (Figure 1B) (Anderson & Parker, 1998; Cougot et al., 2004; Liu et al., 2002; Vidya & Duchaine, 2022). It has recently become evident that the speed of ribosome decoding influences mRNA decay. Transcripts with low decoding kinetics require the Ccr4-Not complex for degradation and are specifically deadenylated by the exonuclease Caf1.

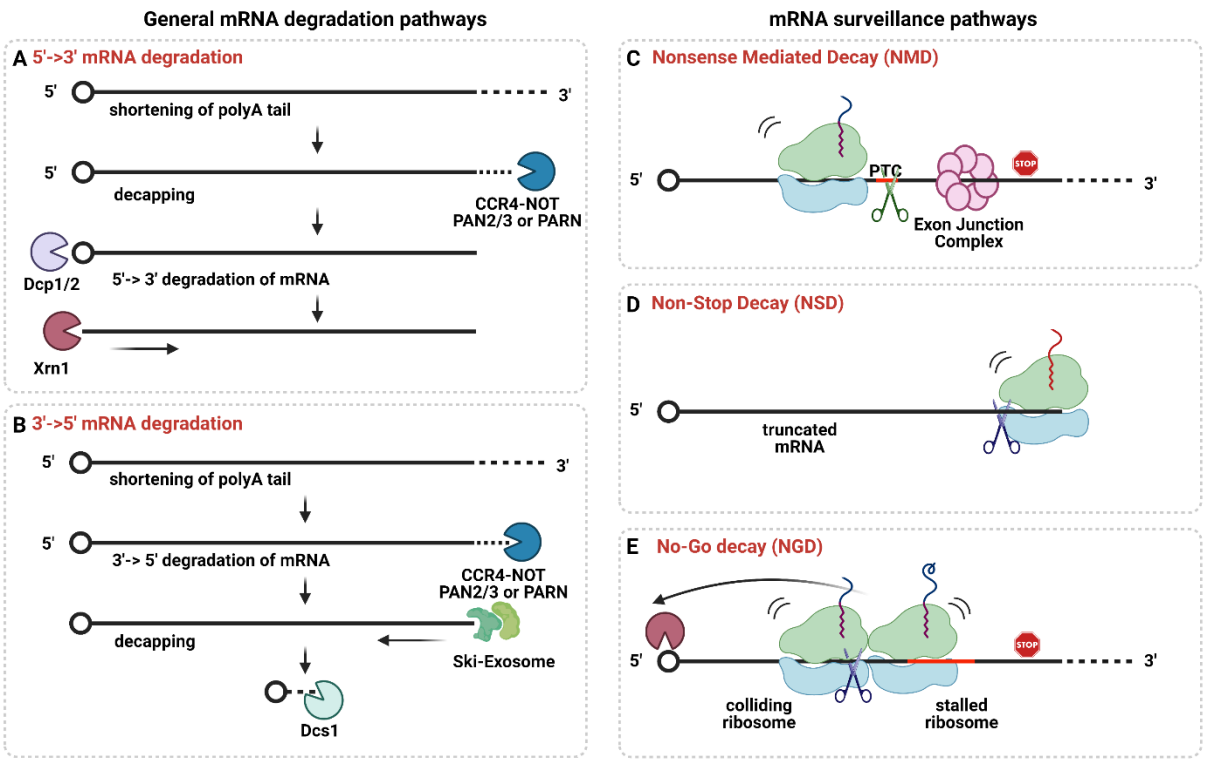

Figure 1.3.1. mRNA degradation and surveillance pathways. Left panels: General mRNA degradation pathways. (**A**) mRNA undergoes 5' to 3' degradation by shortening of the polyA tail (represented as dotted lines) by CCR4-NOT and PAN2/3 or PARN, followed by 5' decapping of the m7G cap by Dcp1/2, which exposes the 5' end to Xrn1 exonuclease degradation. (**B**) mRNA undergoes 3' to 5' degradation by shortening of the polyA tail by CCR4-NOT and PAN2/3 or PARN, which exposes the 3' end to the Ski-Exosome complex for degradation, and simultaneously the 5' end is decapped by Dcs1p. Right panels: mRNA surveillance pathways. (**C**) In Nonsense Mediated Decay, a translating ribosome encounters a premature termination codon (PTC). Proximity to an exon junction complex serves as the recognition signal for endonucleolytic cleavage and degradation of the mRNA. (**D**) In Non-Stop Decay, a translating ribosome stalls at the end of the truncated mRNA, which recruits the exosome complex to release the ribosomal subunits and the mRNA is degraded. (**E**) In No-Go Decay, translating ribosome collides with a stalled ribosome upstream, which signals for endonucleolytic cleavage of the mRNA or the degradation by Xrn1, release of the stalled ribosomes, and degradation of the nascent peptide.

The Not5 subunit of Ccr4-Not complex recognizes ribosomes slow enough to have dissociated the E-site tRNA without having occupied the A-site with a cognate tRNA. In this case, the E-site is recognized by the N-terminus of Not5, which bring Ccr4-Not for deadenylating and the follow-up decapping and Xrn1- mRNA degradation (Buschauer et al., 2020; Webster et al., 2018). In addition to the turnover of cytoplasmic mRNA, three surveillance mechanisms NMD, NSD, and NGD

coordinate the degradation of mRNAs with stalled ribosomes. They rely on the meticulous inspection of translation by elongating ribosomes, but each recognizes a specific type of error in an mRNA (Karamyshev & Karamysheva, 2018; Morris et al., 2021). In NMD, the ribosome recognizes mRNAs harboring premature termination codons (PTC), which triggers rapid degradation of these transcripts (Maquat, 2004; Shoemaker & Green, 2012). Otherwise, the truncated protein products of these mRNAs may have deleterious dominant-negative or gain-of-function effects (Unterholzner & Izaurralde, 2004). In eukaryotes, intron splicing is a key step in mRNA maturation. Errors in splicing can leave an in-frame stop codon (premature stop codon (PTC)) upstream of the correct stop codon (Green et al., 2003). During splicing, the exon-junction complexes (EJC) bind the mRNA near the exon-junction site, which is typically upstream of the stop codon (Hoek et al., 2019). Normally the EJC is removed by the ribosome as it translates (Hoek et al., 2019). However, if the mRNA had a splicing defect resulting in a PTC, the EJC remains on the mRNA (Hoek et al., 2019). This serves as a signal that recruits several factors involved in either exonucleolytic degradation of the mRNA or SMG6-mediated endonucleolytic cleavage followed by further processing of mRNA fragments (Figure 1C) (Eberle et al., 2009; Gatfield & Izaurralde, 2004; Hoek et al., 2019; T. Li et al., 2015; Morris et al., 2021; Schmidt et al., 2015). A small portion of mRNAs have another exon-exon junction downstream of the stop codon, and many of these mRNAs are natural NMD substrates (Mendell et al., 2004). NSD targets transcripts lacking an in-frame stop codon for decay, primarily affecting mRNAs with a short poly-A tail (Frischmeyer et al., 2002; van Hoof et al., 2002). They arise due to point mutations within the stop codon or premature poly-adenylation. Further, mRNAs harboring mechanical breakage or enzymatic cleavage inside the CDS are substrates that trigger NSD (Arribere & Fire, 2018; Bengtson & Joazeiro, 2010; Dimitrova et al., 2009; Klauer & van Hoof, 2012). While premature

transcription might yield mRNAs lacking a stop codon, it is more likely that the lack of a polyadenylation site will target such transcripts for degradation inside the nucleus. In NSD, the ribosome translates through the 3'UTR and stalls at the 3' end of the mRNA as the absence of a stop codon prevents release factors from entering the A-site (Bengtson & Joazeiro, 2010; Dimitrova et al., 2009; Frischmeyer et al., 2002; Ito-Harashima et al., 2007; Klauer & van Hoof, 2012; van Hoof et al., 2002). The stalled ribosome recruits an exosome complex which releases the ribosomal subunits and results in mRNA degradation (Klauer & van Hoof, 2012). In addition, its peptidyl-tRNA has a suboptimal conformation for peptide bonding, and the poly-lysine tail electrostatically interacts with the ribosomal proteins in the exit tunnel, and both events contribute to stalling and subsequent ribosomal collisions (explained in section 3.1 and Figure 3 below) (Chandrasekaran et al., 2019; Ikeuchi et al., 2019; Klauer & van Hoof, 2012).

NSD shares key factors with and elicits a very similar response to the most recently discovered RNA surveillance mechanism, NGD **(Figure 1.3.1D)**. NGD recognizes ribosome collisions caused by ribosomes that aberrantly slow down and pause translation elongation for an extended period. Since stall-inducing mRNAs may yield incomplete or truncated proteins, cells eliminate such truncated peptides and mRNAs through RQC and NGD, respectively. Ribosomal pausing is common during translation elongation and can be caused by various factors, including RNA secondary structures, codon optimality, amino acid charge, and tRNA availability to favor proper protein folding (Charneski & Hurst, 2013; Kim et al., 2015; Tsao et al., 2011; Weinberg et al., 2016; Yu et al., 2015). Therefore, for ribosome collisions to initiate NGD, specific structural characteristics of the disome (made by the stalling and colliding ribosomes) are recognized. We refer to these disomes as "RQC-disomes" to differentiate them from disomes formed in mRNAs that transiently pause translation elongation. Stabilization of RQC-disomes leads to four

interconnected mechanisms to solve the problem: translational repression, endonucleolytic cleavage of the mRNA and degradation of mRNA fragments by Xrn1 and Ski2, degradation of the nascent peptide, and ribosome recycling **(Figure 1.3.1E)**.

1.3.5 No-Go Decay mRNA clients, players, and the RQC-disome

The RQC, NGD, and ribosome recycling pathways are coupled and share many common factors. In recent years, studies involving genetic screening and stalling reporters, as well as cryo-EM and ribosome footprinting, have led to the identification of these factors, molecular events, and structural features of the NGD mechanisms and the RQC-disome (Ikeuchi et al., 2019; Juszkiewicz et al., 2018; Matsuo et al., 2020; Narita et al., 2022; Pochopien et al., 2021; Saito et al., 2022; Tesina et al., 2020; Zhao et al., 2021) **(Figure 1.3.2)**.

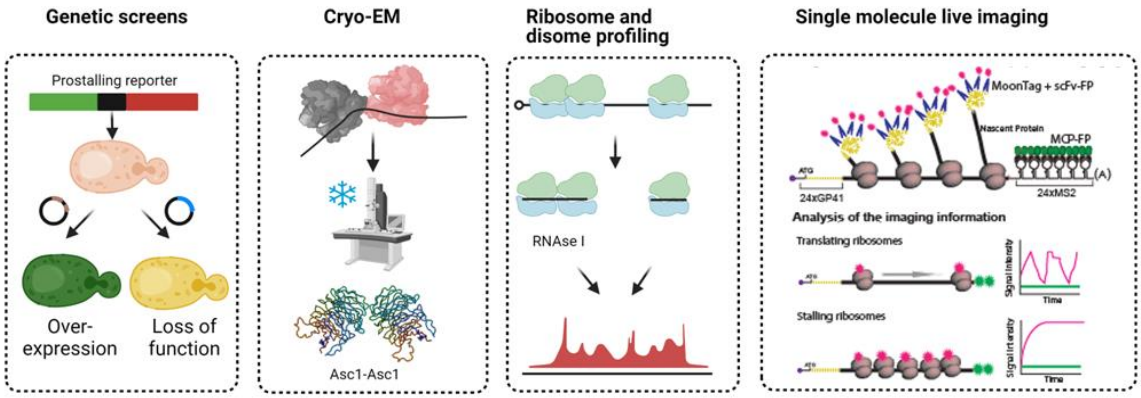

Figure 1.3.2. Summary of techniques used to study NGD. Genetic screens using reporters have identified NGD factors and determined their functions in the pathway. Cryo-EM studies provide the structural characteristics of the RQC-disome, for example the interaction between two Asc1 molecules. Ribosome profiling studies have identified stalling codons and sequences based on the frequency of such sequences in deep sequencing analyses. Future studies with single molecule imaging could provide dynamics of on-going translation elongation and initiation rates in live cells.

1.3.5.1 What are the features of mRNAs targeted by NGD?

The features of mRNAs which lead to stalling and NGD were initially studied in *S. cerevisiae* using *in vitro* translation assays and stalling reporters (Figure 3). Obstructive secondary structures, such as large stem loops, were known to physically block the translation machinery from passing, leading to stalling and collisions (Hosoda et al., 2003). At the discovery of the NGD mechanism, Roy Parker's laboratory used GAL1-induced reporter constructs to express the Phosphoglycerate Kinase 1 PGK1 mRNAs bearing in its CDS stalling structures, such as stable stem-loop or pseudoknot, or sequences, such as rare and proline codons **(Figures 1.3.3A and 1.3.3B)** (Doma & Parker, 2006). Due to its imino-structure, Proline is incorporated inefficiently by the ribosome, specifically at the peptidyl transfer step, thus halting elongating ribosomes (Artieri & Fraser, 2014; Muto & Ito, 2008; Pavlov et al., 2009). Specific peptides containing polybasic repeats can slow and stall elongation by charge-specific interaction of the nascent chain with the ribosome **(Figures 1.3.3C and 1.3.3D)** (Lu & Deutsch, 2008). For example, long stretches of Lys and Arg residues have been shown to destabilize reporter mRNAs (Ito-Harashima et al., 2007). Indeed, the PGK1-stem-loop reporter was modified to remove the stem-loop, replacing it with an array of Arg (12x CGN) that cause stalling due to inefficient decoding of the wobble pair I-A and resulted in a translational arrest (Gamble et al., 2016; Letzring et al., 2010; Matsuo et al., 2017). Ribosome stalling in the endogenous SDD1 mRNA in S. cerevisiae occurs on the CGA-CGA dicodon in the context of KRRKK polybasic, indicating that the surrounded sequences influence ribosome stalling probably due to inefficient decoding and low tRNA availability **(Figure 1.3.3E)** (Matsuo et al., 2020). Recent Cryo-EM studies on ribosomes stalled in stretches of AAA encoding to Lys (like the polyA sequence) have also demonstrated that these AAA stretches reconfigure the decoding center, which precludes the incoming of new aminoacyl tRNAs.

The poly-lysine encoded by Poly-A slows elongation by resulting in suboptimal peptidyl-tRNA conformation in the peptidyl-transferase center and stabilizing the rRNA-mRNA interaction in the decoding center. This interaction alters the decoding center, making the engagement with the next aminoacyl tRNA unlikely to occur and causing elongation to stall (Chandrasekaran et al., 2019; Ikeuchi & Inada, 2016; Ito-Harashima et al., 2007; Klauer & van Hoof, 2012). Non-optimal codons generally have a lower corresponding tRNA concentration in the cell, thus increasing the duration of the A-site vacancy. This might be an important mechanism during stress as oxidative stress decreases charged tryptophan tRNA availability, resulting in ribosomal stalling at tryptophan repeats (Rubio et al., 2021). Aside from the availability of tRNAs and low-frequency codons, ribosome elongation rate can be affected by codon-pair (such as CGA-CGA pair) bias and codon context, which depends on the cell's inner and external conditions (Alexaki et al., 2019; Gamble et al., 2016; Lanza et al., 2014; Wolf & Grayhack, 2015). For example, the non-optimal sequence of the SSA4 mRNA leads to RQC regulation of its translation during heat stress. This regulation is abolished by optimizing the SSA4 codon sequence (Alagar Boopathy et al., 2022).

Stalling also occurs on aberrant mRNAs, such as those with chemical damage. In yeast, ribosomal stalling has been observed at sites of depurination. Using an inducible translation system, the half-life of the Brome mosaic virus RNA was decreased in cells expressing a ribosome-inactivating protein known to depurinate the virus mRNA. This study used toe-printing analysis to show that ribosomes stalled at points of depurination, and suggested NGD as the mechanism of RNA decay following stalling **(Figure 1.3.3F)** (Gandhi et al., 2008). Oxidation of mRNAs has also been demonstrated in bacteria to reduce the decoding rate (Simms et al., 2014). In an in vitro translation system showed that mRNAs with oxidized nucleotides, specifically 8-oxoguanosine (8-oxoG), stall and are subsequently targeted for NGD. Since 8-oxoG can base-pair with

adenosine, near-cognate aminoacylated-tRNAs attempt to bind oxidized codons, but this decoding is inefficient and results in stalling (Simms et al., 2014). Likewise, site-specific oxidative damage triggers the degradation of the damaged mRNA and alkylative damage, resulting in nucleotides such as m1A, m3C, and m1G disrupting base-pairing precluding tRNA decoding and increasing ribosomal stalling (Yan et al., 2019).

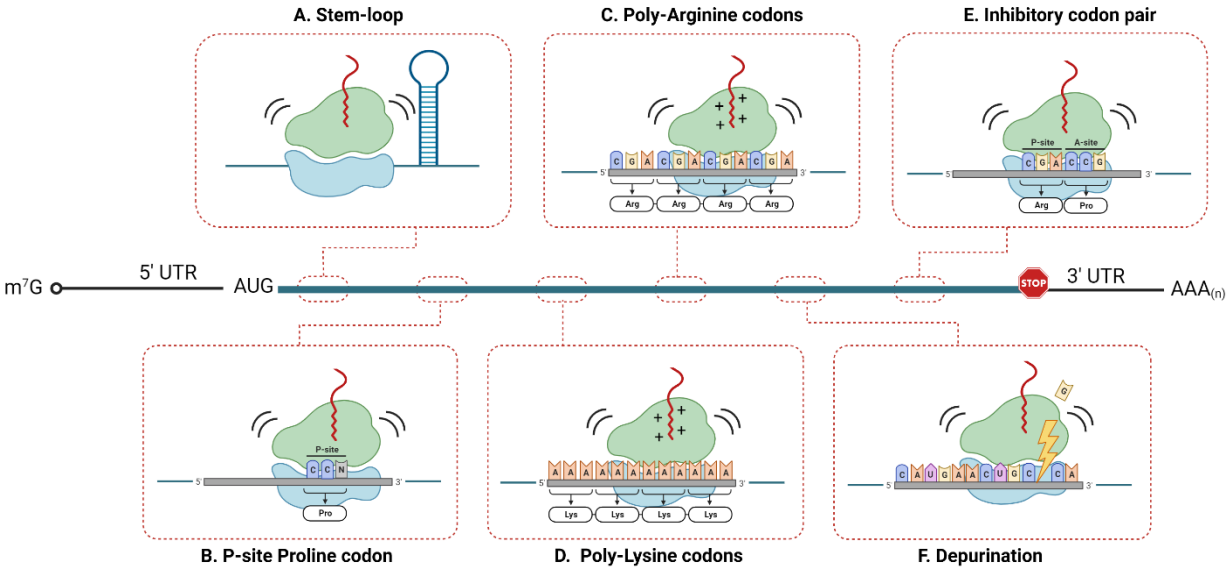

Figure 1.3.3. Schematic view of mRNA characteristics leading to ribosome stalling. (**A**) Large obstructive secondary structures, such as stem-loops, prevent the ribosome from proceeding. (**B**) Imino side chain of proline acts as a poor substrate in peptidyl transfer reaction, causing slow translation elongation and eventually stalling. (**C**) Poly-arginine tracts slow elongation and lead to stalling by electrostatic interactions in the peptide exit tunnel. (**D**) Similar to Poly-Arginine tracts, Poly-lysine codons reconfigure the decoding center, preventing new tRNA binding, and charge-specific interactions in the peptide exit channel led to stalling (**E**) Arg-Pro inhibitory codon pairs occupying ribosomal P- and A- sites respectively are decoded inefficiently, leading to stalling. (**F**) Chemical damage such as depurination slows elongation by disrupting tRNA binding.

What events and factors regulate RQC and NGD?

The ribosome load on the mRNA is also a critical factor for initiating NGD. Using reporters containing mutations that reduced ribosome density on the mRNA, the efficiency of NGD was also reduced (Park & Subramaniam, 2019; Simms et al., 2017). Using RNA probes against the 3' fragment in Ski2-defective yeast strains, the sites for endonucleolytic cleavage were mapped with

various reporters (Doma & Parker, 2006). Interestingly, most reads were found above the stall site and were at least 105 nt from the start codon, suggesting that multiple ribosomes are required for efficient NGD (Simms et al., 2017). In the case of CGA codons, the site of endonucleolytic cleavage occurred near them, further demonstrating ribosome stalling at these sites (Letzring et al., 2010). In 2006, only a few factors and their functions in NGD were known. Dom34 (Pelota in mammals) and Hbs1 (Hsb1L and GTP binding protein 2, (Gtpbp2) in mammals) were proposed to either mediate the endonucleolytic cleavage or have a role upstream of the cleavage (Doma & Parker, 2006). However, consequent studies demonstrated that they participate in ribosomal rescue, dissociation of the stalled ribosome, and quality control of non-stop mRNAs and are homologs of the eukaryotic termination factors eRF1 and eRF3, respectively, required for canonical translation termination (Graille et al., 2008; Ikeuchi et al., 2016; Ikeuchi & Inada, 2016; Kuroha et al., 2010). Moreover, in non-stop mRNAs, the endonucleolytic cleavage was independent of Dom34 but required the ribosomal protein Asc1 (RACK1 in mammals) (Ikeuchi et al., 2016; Kuroha et al., 2010). Additionally, a crucial function of Dom34 in the dissociation of stalled ribosomes and quality control for nonstop mRNAs was elucidated (Ikeuchi et al., 2016; Ikeuchi & Inada, 2016; Kuroha et al., 2010). Subsequently, reverse genetic screens and overexpression screens in diploid yeast using synthetic NGD reporters with either 12x CGA or 12x AAA stalling repeats inserted in the green fluorescent protein (GFP) CDS revealed that the endonuclease Cue2 is responsible for the mRNA cleavage (D'Orazio et al., 2019). The Cue2 homologs NONU1 and N4BP2 in *C. elegans* and mammalian cells, respectively, also possess endonucleolytic function suggesting that the mechanism of NGD is conserved (D'Orazio et al., 2019; Glover et al., 2020).

Another full genome screening with loss-of-function alleles using polybasic 12x Arg fluorescent reporter identified the ribosome stall recognition and resolving factors Ski2-like helicase, Slh1, Asc1, and Hel2 (ASCC3, RACK1, and ZNF598/ZFP598 in mammals) **(Table 1.3.1)** and the components of the RQC complex, Rqc1, Rqc2/Tae2, Ltn1, and Cdc48 (NEMF, Listerin/LTN1, and VCP in mammals), responsible for the degradation of nascent polypeptide chain stock in the stalled ribosomes (Bengtson & Joazeiro, 2010; Brandman et al., 2012; Kuroha et al., 2010; Letzring et al., 2013). In parallel to these discoveries, quantitative proteomic analysis of polysome fractionations identified the RQC-disome-specific factor Mbf1 (Multiprotein bridging factor 1, EDF1 in mammals) that prevents ribosome frameshifting in eukaryotes and represses translation initiation in mammals (Juszkiewicz et al., 2020; Sinha et al., 2020). Recently, the ribosomal proteins Rps28A and Rps19B interaction with Asc1-3xFlag were identified by liquid chromatography coupled to mass spectrometry (Alagar Boopathy et al., 2022). Both ribosomal proteins regulate the translation of the endogenous *HSP70* mRNA, SSA4 in yeast, by RQC without affecting its stability (Alagar Boopathy et al., 2022).

All these techniques and discoveries relied on the analysis of bulk mRNA populations obtained at a specific time-point, and so the fate of individual mRNAs undergoing surveillance and the temporal resolution of these events has been elusive. Recent advancements in fluorescence microscopy have enabled researchers to follow the real-time translation of single faulty mRNAs and their fate and provided the first insight into the dynamics of RQC events in mammalian cells. The use of polyA-containing fluorescent reporters to tag the mRNA with the MS2 system and the nascent peptide with the SunTag system demonstrated that faulty mRNAs accumulate queues of ribosomes (Goldman et al., 2021). Collisions are regulated by translation initiation, and ZNF598 accelerates ribosome splitting but is slow in general (8 s per ribosome), allowing mammalian cells

to 1) distinguish long-standing from transient collisions and 2) clear short queues of colliding ribosomes at a rate that is faster than translation elongation (Goldman et al., 2021). Although NGD did not degrade this specific reporter, this live imaging technique will provide insights into the temporal regulation of NGD.

1.3.5.2 Identifying endogenous RQC and NGD targets and how to study them at the single molecule resolution.

While initial work investigating the causes of ribosome stalling used reporter systems, recent efforts aim to identify endogenous stalling mRNAs and the specific physiological circumstances leading to their regulation by RQC and NGD. Ribosome footprinting has emerged as a useful tool for identifying stalling sites. This method involves the isolation of translating ribosomes, nuclease digestion, and deep sequencing of the protected regions (Ingolia et al., 2009; Joazeiro, 2017). The higher the frequency of a sequence detection, the more likely it is to be a stalling site. As such, endogenous Proline and polybasic residues were identified to cause stalling (Artieri & Fraser, 2014). Similarly, disome and trisome footprinting studies, in which yeast lysates and digested with RNAse I and fractionated on a sucrose gradient, effectively isolate collision-induced disomes and map them to consecutive Lys and Arg codons. These studies have confirmed that polybasic repeats and poly-CGA codons, the rarest Arg codon, induce stalling and collisions (Meydan & Guydosh, 2020). These studies also identified ribosome halt on mRNA sequences known to slow translation or inhibit translation without eliciting the RQC responses (Meydan & Guydosh, 2020). Therefore, a mechanism based on the structure of disomes allows the cell to distinguish functional stalling to prevent RQC and NGD actions on these mRNAs.

1.3.5.3 Structural characteristics of the RQC-disome unit.

Various stalling mRNA reporters have been used to identify the structure, components, and molecular interactions within RQC-disomes. They are first translated in cell-free systems to isolate mono-, di- or trisomes by sucrose gradient or affinity purification using the ribosome-nascent chain complex (RNC), and then subjected to cryo-electron microscopy. The reporters include the stall-inducing sequence of the SDD1-mRNA and CGA-CCG inhibitory codon pair reporter, both containing an N-terminal His-tag for affinity purification (Ikeuchi et al., 2019; Matsuo et al., 2020; Narita et al., 2022). Alternatively, stalls were induced on globin-translating ribosomes by a dominant negative mutation in the release factor eRF1AAQ and by affinity purification of Hel2-FTP (Flag-TEV-Protein A) from whole cell lysates (Juszkiewicz et al., 2018). These studies found that NGD follows ribosomal collisions for which the minimal unit is composed of two ribosomes (disome): the stalled leading ribosome and the following colliding ribosome.

The RQC-disome has specific structural characteristics that allow for the binding of Hel2 and subsequently trigger RQC and NGD (Ikeuchi et al., 2019; Matsuo et al., 2017). RQC-disomes are stalled at the rotated state with hybrid tRNAs and form a unique interface. The two ribosomes mainly interact through components of their small ribosomal subunits that are oriented towards each other and place the mRNA exit channel in the lead ribosome near the mRNA entry channel of the collided ribosome. The head-to-head interaction of both Asc1 proteins is essential for Hel2 binding to initiate RQC and NGD. In yeast, the Asc1-Asc1 interface is accompanied by the uS3-uS10 contact between the leading and colliding 40S, respectively. The intimate contact between the ribosome and the mRNA through Rps3 (uS3) near the mRNA entry channel is essential for NGD and is highly conserved from bacteria to metazoans (Simms et al., 2018). In addition, 40S body-to-body and platform-to-platform interactions occur through eS27 and eS7 with eS6c, and

eS17 with uS2 and eS21, respectively. Interactions of the 60S with 40S subunits also occur to a lesser extent. The RACK1-RACK1 interaction is conserved in human RQC-disomes, but certain 40S-40S and 40S-60S connections are distinct, making the structure of human RQC-disomes different from yeast and more stable (Narita et al., 2022). These interactions either do not exist or more flexible in disomes that normally form on mRNAs and transiently interrupt their translation (Zhao et al., 2021). In addition, there are structural differences between normal disomes and RQC-disomes. In normal disomes, the leading ribosome is in a rotated state with P/P and E/E tRNAs that suggest a temporary pause (Zhao et al., 2021). In RQC-disomes, the leading ribosome is in a post-translocation state, with P- and E-sites tRNAs and an empty A site, and the colliding ribosome in a hybrid state with A/P and P/E tRNAs and incomplete translocation, which forbids its translocation and translation elongation (Djumagulov et al., 2021; Matsuo et al., 2017, 2020; Pochopien et al., 2021; Zhao et al., 2021) (for further information on the transition state of tRNAs, we direct the readers to (Frank, 2017)). These structures and the Asc1-Asc1 interaction signal to RQC and NGD (Ikeuchi et al., 2019).

1.3.6 The RQC and NGD factors and their actions

The first step in activating RQC and NGD is the stabilization of the RQC-disome through the actions of Asc1 and Hel2. Stabilization of the RQC-disome is the signaling hub for quality control (Ikeuchi et al., 2019). Recent studies using mutants of Hel2 showed that NGD might also be independent of RQC or Hel2, and thus, the complete series of molecular events leading to NGD might be mRNA- and cell-state-dependent (Ikeuchi et al., 2019; Tomomatsu et al., 2023). We provide here an update on NGD factors and the sequence of events that ultimately direct the mRNA degradation, disassembly of the ribosomal subunits, and degradation of the truncated polypeptide chain **(Figure 1.3.4, Table 1.3.1)**.

Quality Control Factors (yeast)	Nomenclature mammals	Description	Localization/Target	Function
Asc1	RACK1	Beta-propellor protein bound to 40S ribosomal subunit	-40S in monosome -Asc1 on adjacent stalled ribosome in a disome	Stabilize disome and provide interface for E3 ubiquitin ligase recognition.
Hel2	ZNF598	E3 ubiquitin ligase	-eS10 and uS10 -Recruits GIGYF2-4EHP	-Ubiquitinates eS10 and uS10 to promote ribosomal splitting -Translation initiation repression
Dom34	Pelota	eRF1 homolog	A-site of stalled ribosome	Release 60S-bound peptidyl-tRNA
Hbs1	Hbs1L/Gtpbp2	eRF3 homolog	Dom34, A-site of stalled ribosome	Facilitate Dom34 loading onto A-site
Slh1	ASCC3	ATPse/Helicase	RQT complex	Disassembly the leading ribosome
Cue3	ASCC2	Ubiquitin-binding protein	RQT complex	Disassembly the leading ribosome
Rqt4	TRIP or ASC-1	Ubiquitin binding	RQT complex	Disassembly the leading ribosome
-	ASCC1	RNA ligase-like protein	hRQT complex	Disassembly the leading ribosome
Cue2	N4BP2 (NONU in *c. elegans*)	Endonuclease	-mRNA stalled at the A site of collided ribosomes -Ubiquitin	Cleavages mRNAs containing colliding ribosomes, binds Hel2-ubiqutylated ribosomal subunit for recruitment to stall sites
Xrn1	XRN1	5'-3' exonuclease	3' end fragment of cleavage mRNAs	Degrade NGD substrate from 5' to 3'
Ski	Exosome	3'-5' exonuclease	5' end fragment of cleavage mRNAs	Degrade NGD substrate from 3' to 5'
Syh1	GIGYF1/2	GYF domain protein	Collided ribosomes stabilized by Hel2	-Decapping and degradation of stalled mRNAs in yeast -Translational repression in mammals
Ltn1	LISTERINE	E3 ubiquitin ligase	60S ribosomal subunit	Peptide extraction for UPS degradation
Rqc1	TCF25	Ubiquitination	60S ribosomal subunit	Ubiquitination
Rqc2	NEMF	Recruitment of Ltn1	60S ribosomal subunit	-Stabilizes Ltn1 binding to ribosome -Mediates elongation of stalled peptide
Cdc48	P97	AAA ATPase	60S ribosomal subunit	Extraction of ubiquitinated nascent chain
Vms1	ANKZF	Hydrolase homologue of eRF1	60S ribosomal subunit	Hydrolyzes the peptide-tRNA linkage
Mbf1	EDI	Multiprotein bridging factor 1	40S ribosomal subunit binding site at the mRNA entry channel near collision	-Stabilize ZNF598-GIGYF2-4EHP In mammals to repress translation -Prevent leading ribosome from frameshifting

Table 1.3.1. **Factors involved in RQC and NGD.** Highlights of their targets and function.

1.3.6.1 Stabilization of RQC-Disomes and mRNA cleavage

Asc1 is a beta-propellor protein containing 7 repeats of WD40 motifs, allowing simultaneous interactions with different molecules (Gerbasi et al., 2004; Schmitt et al., 2017). Prior

studies demonstrated that Asc1 mediates the translation arrest induced by the consecutive stretch of polybasic amino acids (Kuroha et al., 2010). The Cryo-EM structure of the RQC-disome showed that the rotation of the colliding ribosome conveniently positions two Asc1 proteins in close proximity for interaction between the stalling and colliding ribosomes (Ikeuchi et al., 2019). The Asc1-Asc1 interaction provides an interface for recognition by E3 ubiquitin ligases such as Hel2 and Not4, as well as the RQC-trigger complex (RQT), composed of Slh1(Rqt2 (ASCC3)), Cue3 (Rqt3 (ASCC2)) and Rqt4 (yKR023 (TRIP4/ASC-1)) to promote the dissociation of the ribosomal subunits (Ikeuchi et al., 2019; Juszkiewicz & Hegde, 2017; Matsuo et al., 2017). Once bound to the RQC-disome, Hel2 interacts with the 18S RNA, mainly in the proximity of the mRNA entrance channel but also in the exit channel and the translated mRNA (Winz et al., 2019). Deletion of either Asc1 or Hel2 prevents RQC and NGD and allows for translation to continue (Sitron et al., 2017; Winz et al., 2019).

Hel2 ubiquitinates the ribosomal proteins in its proximity; uS10 (Rps20), uS3 (Rps3), and eS7 (Rps7) in yeast (Ikeuchi et al., 2019; Matsuo et al., 2017; T et al., 2019). In mammalian cells, ZNF598 ubiquitinates ribosomal proteins eS10 (Rps10) at K138/K139 and to a lesser extent uS10 at K4/K8 located in the mRNA entry channel of the 40S subunit (Ikeuchi et al., 2019; Juszkiewicz & Hegde, 2017; Matsuo et al., 2017; Winz et al., 2019). The ubiquitination of eS10 was not identified in this context in yeast (Matsuo et al., 2017; Tomomatsu et al., 2023). Hel2 was identified in a yeast genetic screen for factors mediating co-translational stalling under heat stress conditions along with Asc1 and factors involved in nascent chain release and degradation, Ltn1, Rqc1, Rqc2/Tae2, and Cdc48p (Brandman et al., 2012). Unlike Asc1, Hel2 is not pre-associated with the translating ribosome and is not required for stalling, which means it binds ribosomes once they collide (Sitron & Brandman, 2020). Hel2 and ZNF598 contain an N-terminal RING domain

exhibiting E3 ligase activity and multiple zinc-finger domains (Deshaies & Joazeiro, 2009). In NGD, Hel2 adds K63-linked polyubiquitin chains to the 40S ribosomal protein uS10 at K6/K8, which is essential for recognition by RQT to promote the splitting of stalled ribosomes (Ikeuchi et al., 2019; Matsuo et al., 2017; Narita et al., 2022; Saito et al., 2015). In the absence of Hel2, ribosomes do not respond to the stalling signals, and polybasic fluorescent reporters synthesize more proteins, potentially by preventing mRNA cleavage after stalling (Brandman et al., 2012). However, it was recently shown that Hel2-dependent polyubiquitylation of the 40S ribosome coordinates the endonucleolytic cleavage of mRNAs undergoing stalling by two independent mechanisms (Ikeuchi et al., 2019). The first mechanism encompasses the role of Hel2 in both NGD and RQC (referred to as NGD RQC+). Here, Hel2 is solely responsible for the initial monoubiquitination and further K63-linked polyubiquitination of uS10 at K6/K8. This ubiquitination event along with the helicase activity of Slh1/Rqt2 is required for the cleavage of the mRNA within the disome unit, indicating that ribosome splitting precedes the cleavage. Two cleavage events occur in the mRNA occupied by the collided (second) ribosome, while three are identified in the mRNA protected by the stalled (first) ribosome (Ikeuchi et al., 2019). The second mechanism (NGD RQC-) occurs when the C-terminal end of Hel2 is truncated and incapable of mediating RQC and uS10 monoubiquitination. In this case, Not4-catalyzes the initial monoubiquitination in eS7A at K4. Subsequently, the truncated Hel2 mediates eS7A K63-linked polyubiquitination (Ikeuchi et al., 2019). In the NGD RQC- pathway, cleavage occurs upstream of the first disome unit. In both pathways, the endonuclease Cue2 recognizes stalling ribosomes and cleaves the mRNA (Tomomatsu et al., 2023).

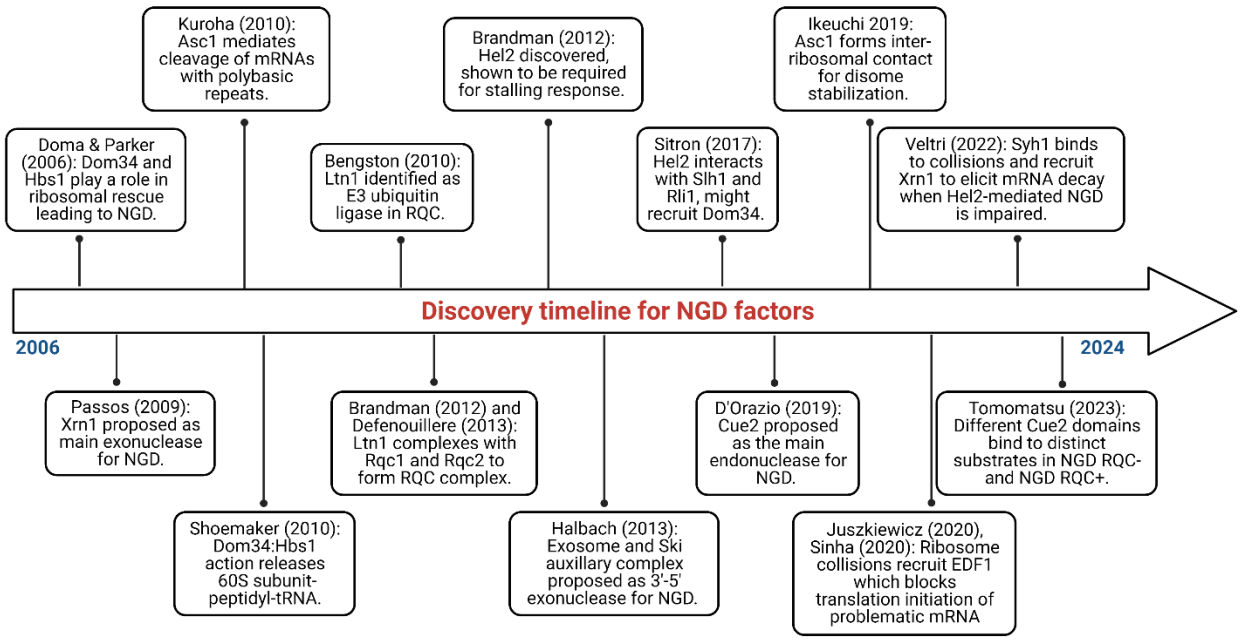

Figure 1.3.4. Timeline of discoveries of the main NGD factors and their interactions. The No-Go Decay mechanism was first described in 2006 together with the involvement of factors Dom34 and Hbs1 in ribosomal rescue. Since then, the list of factors involved in NGD has grown consistently. Ribosome-collision specific factors including Asc1 and Hel2 have been shown to stabilize the RQC-disome and mediate downstream RQC and NGD events. Subsequently, factors involved in ribosome dissociation such as Slh1, Rlil1 and nascent peptide release including Rqc1, Rqc2 and Ltn1 were also identified. Multiple studies have aimed to elucidate the mechanism of endonucleolytic cleavage and exonucleolytic decay of NGD substrates. While the involvement of exonucleases Xrn1 and Ski-exosome have been long accepted, the exact endonuclease responsible for mRNA cleavage is still debated. Most recent studies have proposed Cue2 as the main endonuclease for NGD. Additionally, cryo-EM studies of disome unit have shed some light on the structural arrangement required for the recognition of the collision interface and modification by Hel2. Further, in response to collisions, EDF1 recruits GIGYF2-4EHP to block translation initiation of the problematic mRNA. As an alternative mechanism, Syh1 has been proposed to elicit mRNA decay through recruitment of Xrn1 as a compensatory pathway when the Hel2-directed NGD is impaired. Most recently, different domains of Cue2 have been shown to recognize distinct ubiquitinated substrates (eS7 or uS10) and mediate RQC- dependent or RQC-independent NGD.

However, the ubiquitination of Rps3 at K212 does not play a role in inducing NGD or RQC (Ikeuchi et al., 2019; Matsuo et al., 2017; Simms et al., 2018). Instead, it is required to clear the 18S rRNA carrying defective mutations within the 40S ribosome decoding center. This mechanism

of defective rRNA elimination is referred to as 18S nonfunctional rRNA decay (NRD), which is functionally related to NGD and shares common factors including Asc1, Dom34, Hbs1, and uS3 (Limoncelli et al., 2017; Simms et al., 2018; T et al., 2019). In NRD, the ubiquitination of uS3 occurs in two steps, first Mag2 marks slow-moving ribosomes with mono-ubiquitination followed by Fap1 along with cofactor Yil161w (renamed as stalled monosome ubiquitination 2, SMU2) mediates the polyubiquitination which initiates the degradation of the defective ribosome (Li et al., 2022; T et al., 2019). CryoEM structures of the Fap1-bound ribosome complex revealed that Fap1 interacts with the mRNA at both entry and exit tunnels, precluding the ribosome collision through steric hindrance. Rare collision events in NRD prevent Fap1 binding; under such circumstances, Hel2 is speculated to ubiquitinate uS3 (Li et al., 2022; T et al., 2019).

Cue2 was first reported as a Hel2-dependent endonuclease involved in the NGD cleavage (D'Orazio et al., 2019). Cue2 contains two conserved CUE (coupling of ubiquitin to ER degradation) domains in the N-terminal, two putative ubiquitin associated domains (UBA), and a C-terminal SMR (small MutS-related) hydrolase domain (D'Orazio et al., 2019). It is speculated that CUE domains recognize multiple ubiquitinated sites within the same collided ribosome or adjacent collided ribosomes (D'Orazio et al., 2019). Once the ubiquitinated sites are recognized, the SMR domain is recruited to the A site of the collided-rotated ribosome, where the hydrolysis occurs (D'Orazio et al., 2019). Recently, domain analysis of Cue2 in NGD using a rare codon staller has elucidated 2 different modes of Cue2-mediated endonucleolytic mRNA cleavage. In NGD RQC-, the N-terminal CUE domains recognize the eS7 polyubiquitination and trigger the mRNA cleavage upstream of the collided ribosome. In the case of NGD RQC+, Cue2 acts after RQT-mediated dissociation of the stalled ribosome and the UBA domain, W122 of Cue2, along with the interaction between uS3 and Mbf1 is indispensable for the mRNA cleavage activity within

the RQC-disome (Tomomatsu et al., 2023). Single nucleotide resolution mapping of NGD fragments indicated that Cue2 cleavage occurs predominantly 45 nucleotides upstream of the stall-inducing sequence (Guydosh & Green, 2017; Simms et al., 2017, 2018). The cleavage results in a 5' NGD fragment lacking a poly-A tail and a 3' NGD fragment lacking a protective cap (m7GpppG) which are detected only when Ski2 or Xrn1 is deleted. The cleavage intermediates are highly unstable and quickly cleared up by the cell. Earlier studies have shown that Dom34-Hbs1-directed subunit dissociation precedes the degradation of 5' NGD fragment (Tsuboi et al., 2012). The 5' NGD fragment recruits SKI auxiliary complex, which is cleared by the 3' to 5' exosome complex formed by Ski2/3/8 and 7 (Figure 5) (Halbach et al., 2013). Specific mutations in ribosomal protein S3 (Rps3) located at the mRNA entry tunnel significantly reduce cleavage efficiency during NGD. This indicates that the mRNA entry tunnel of the 40S subunit plays a central role in mediating NGD (Simms et al., 2018).

Deletion of Cue2 abrogates the formation of NGD fragments, but destabilization of the reporter mRNA was still observed (D'Orazio et al., 2019; Yip & Shao, 2021). This suggests that ribosome collision-directed endonucleolytic fragmentation is only a pathway for removing problematic mRNAs (D'Orazio et al., 2019). Accordingly, the action of Cue2 is predominant in yeast strains depleted of the RNA helicase Slh1, where stalled ribosomes are accumulated on the problematic mRNA (D'Orazio et al., 2019). A redundant and compensatory pathway was recently proposed in wild-type yeast as the predominant mechanism to eliminate NGD transcripts. In this pathway, colliding ribosomes recruit Syh1 and signals to decapping and Xrn1-degradation of the problematic mRNA (Figure 5) (D'Orazio et al., 2019; Veltri et al., 2022). Yeast with a double deletion of SYH1 and HEL2 or CUE2 shows higher stability of stalling reporters, indicating that these pathways compensate for each other (Figure 5) (D'Orazio et al., 2019; Veltri et al., 2022).

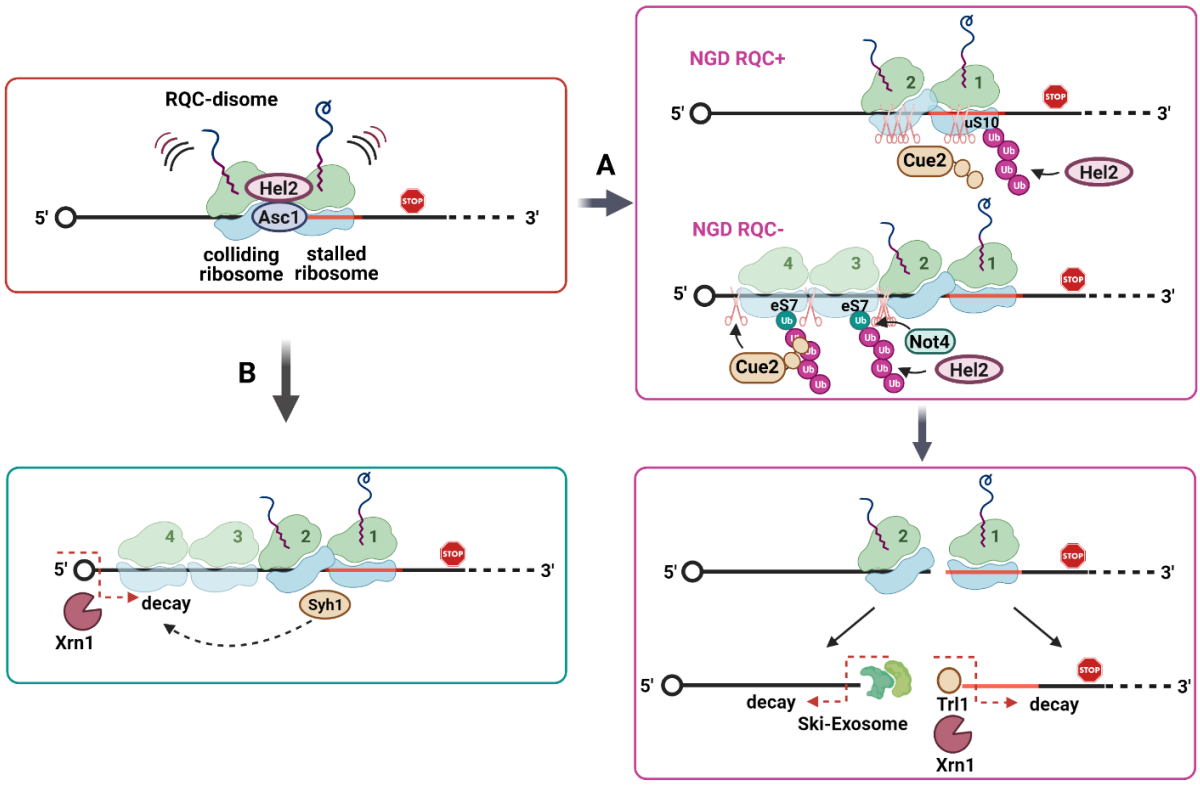

Figure 1.3.5. Schematic representation of the mechanism of No-Go Decay. Stall inducing codons often result in ribosome collisions (termed RQC-disome) which serve as a signal for No-Go Decay. Upon sensing the collisions, several factors are recruited to mediate the decay of the mRNA. **(A)** NGD has been reported to occur linked to RQC (NGD RQC+) as well as independently of RQC (NGD RQC-). In RQC competent NGD, a functional Hel2 ubiquitinates uS10, which is recognized by CUE domains of Cue2 and triggers multiple endonucleolytic cuts: 2 within the stalled ribosome (first ribosome, indicated as 1), and 3 within the collided ribosome (second ribosome, indicated as 2). In NGD RQC+ the mRNA cleavage occurs after the dissociation of ubiquitinated ribosome by RQT (not shown). RQC incompetent NGD occurs when Hel2 lacks a C-terminal domain which renders it incapable of mediating the first monoubiquitination on uS10. Instead, Not4 mediates the first ubiquitination on eS7 and the truncated Hel2 facilitates the polyubiquitination. Then the endonucleases cleave the transcript at the multiple sites not covered by ribosomes (2 cuts upstream of the RQC-disome and 1 cut upstream of the third and fourth ribosomes, respectively). The fragments generated by endonucleolytic cleavage are prone to degradation by Xrn1 and Ski-Exosome complex. While the Ski-Exosome complex can act directly on the 3' end of the 5' NGD intermediate, the conversion of the newly exposed 5' hydroxyl to a phosphate, by Trl1 kinase, is necessary for Xrn1 to function. **(B)** When Hel2-directed NGD is impaired, a less described compensatory pathway of NGD occurs by recruitment of Syh1 to the collided ribosomes which brings in Xrn1 to mediate the complete degradation of the transcript. The ribosomes are numbered 1 through 4 with the first ribosome that stalls as 1 and the consecutive ribosomes that the collide as 2, 3 and 4 in the order of collision.

A parallel study by Navickas and colleagues used a reporter mRNA with a region near the 3'UTR susceptible to cleavage by ribozyme that triggers NGD independently of Cue2 (Navickas et al., 2020). In this mRNA, the NGD cleavage occurred eight nucleotides upstream of the P-site of the third collided ribosome. The NGD cleavage also generates a 5' NGD fragment and a 3' NGD fragment. The ribosomes on the 5'NGD fragments can advance and stall on the new 3′-end with one nucleotide in the ribosomal A-site. The 3' NGD fragment needs the action of RNA kinase Trl1 (Rlg1) to phosphorylate the 5’-OH before the 5’-3' exonuclease Xrn1 can degrade the fragment (D'Orazio et al., 2019; Navickas et al., 2020; Passos et al., 2009). In the absence of the canonical 5’-3' exonuclease Xrn1, another enzyme, Dxo1, with exonuclease and decapping activity, functions to eliminate the 3' NGD intermediates. As Xrn1, Dxo1 requires a 5' phosphate and also depends on Trl1 activity (Chang et al., 2012; Navickas et al., 2020). Further, the 5' NGD fragment could be subjected to more than one cleavage depending on the number of collisions, the presence of multiple contiguous rare codons, and inefficient ribosome rescue **(Figure 1.3.5A)** (Navickas et al., 2020; Simms et al., 2017). Overall, more than one pathway is settled in a place to degrade the problematic mRNA. Future experiments using endogenous mRNA will elucidate whether the pathway affecting endogenous mRNAs depends on the type of stalling, the mRNA context, or the cell status (e.g., stress conditions, cell cycle progression).

1.3.6.2 Ribosome rescue and nascent peptide degradation

The leading and colliding ribosomes are rescued and returned to the pool of ribosomes. The Dom34-Hbs1 (Pelota-Hbs1L) rescues the colliding ribosome after the endonucleolytic cleavage event, whereas the leading ribosome is dissociated by the RQT complex (Simms et al., 2017; Sitron et al., 2017; Tsuboi et al., 2012; Young & Guydosh, 2022). The primary determinant of the route of ribosome disassembly is the presence of 3’-mRNA emerging from the lead ribosome

that a trailing of 80S can follow. In this case, ribosomes will be rescued by Slh1. However, the lack of mRNA in the A-site is a prerequisite for Dom34-Hbs1-mediated splitting (Best et al., 2023; Pisareva et al., 2011). In yeast, the ribosome rescue on mRNAs with stall sequences in the ORF predominantly occurs by RQT, whereas the action of Dom34-Hbs1 likely represents a minor pathway (D'Orazio et al., 2019; D'Orazio & Green, 2021; Matsuo et al., 2017, 2020).

Dissociation of the leading stalled ribosome

In yeast, the RQT complex consisting of Slh1, Cue3, and Rqt4 assembles onto the 3' mRNA exiting from the stalled ribosome (Best et al., 2023; Ikeuchi et al., 2019; Matsuo et al., 2017; Sitron et al., 2017). This complex is known as the ASC-1 complex (Activating signal cointegrator complex, ASCC) or hRQT in humans (Hashimoto et al., 2020). The first step in RQT is recognizing the Hel2-directed uS10 polyubiquitination site by the CUE domain of the Cue3 subunit. Then, the ATP-dependent RNA helicase Slh1 dissociates the ribosomal subunits at the expense of two ATP molecules (Best et al., 2023). Rqt4 is a zinc finger-containing protein, initially suggested to function as a cofactor to form a functional RQT complex along with Cue3 (Best et al., 2023; Matsuo et al., 2017). However, recent works with deletion of the CUE domain of Cue3 (ΔCUE), or N-terminal domain of Rqt4 (ΔN) reduced their interaction with ubiquitinated uS10 on the colliding ribosomes and decreased the RQT assembly. Additionally, double deletion (ΔCUE/ΔN) completely abolished the RQT assembly, indicating that Rqt4 compensates Cue3 for ubiquitin-binding defects. Overall, Rqt4 acts as a second arm of RQT in recognizing the K63-linked polyubiquitin to accelerate the RQT assembly and collided ribosome disassembly (Matsuo et al., 2022). Recent cryo-EM structures propose an initial model for the RQT-mediated subunit splitting mechanism by which the RQT complex exerts a pulling force on the 40S subunit of the leading stalled ribosome together with the colliding ribosome, which acts as a wedge to mediate

the separation between 40S and 60S subunits (Best et al., 2023). The ubiquitinated 40S subunit is released, and the peptidyl tRNA in the P-site remains bound to the liberated 60S subunit (Matsuo et al., 2020; Young & Guydosh, 2022). The RQT mechanism is conserved in multicellular organisms (Matsuo et al., 2022; Narita et al., 2022). In humans, the hRQT (ASCC) dissociates the leading ribosomes and liberates the nascent chain from the 60S. It comprises the ubiquitin-binding protein ASCC2, RNA helicase and ATPase ASCC3, zinc-finger type protein TRIP or ASC-1, and RNA ligase-like protein ASCC1 (no yeast homologs) (Hashimoto et al., 2020; Narita et al., 2022). The ASCC can form even without ASCC1, suggesting that ASCC1 is non-essential for RQT (D'Orazio & Green, 2021; Hashimoto et al., 2020; Juszkiewicz, Speldewinde, et al., 2020). The CUE domain of ASCC2 recognizes the ZNF598-mediated K63-polyubiquitination of uS10 and eS10 (polyubiquitinated to a minor extent) and induces the subunit dissociation through ASCC3 in an ATP-dependent manner (Brickner et al., 2017; Hashimoto et al., 2020; Juszkiewicz et al., 2020; Narita et al., 2022). The ASCC-mediated dissociation of the leading ribosome allows the trailing ribosome to resume translation (Juszkiewicz et al., 2020; Narita et al., 2022).

Dissociation of trailing or colliding ribosome

In ribosome rescue, Hbs1 is thought to load Dom34 onto the stalled ribosome's A-site in a codon-independent manner, unlike the stop-codon-dependent manner for canonical termination (Pisareva et al., 2011). The Dom34-Hbs1 complex acts on colliding ribosomes on the 5' NGD fragment generated after the endonucleolytic cleavage event (Hilal et al., 2016). The complex senses the mRNA vacancy at the A-site through Dom34 and the mRNA entry site through the Hbs1 N-terminal domain (Pisareva et al., 2011). Hbs1 holds Dom34 in an inactive state via Domain M of Dom34 to prevent association with translating ribosomes, thereby restricting its association to the naturally stalled ribosomes for co-translational protein folding (Pisareva et al., 2011).

Although the ribosome splitting activity of Dom34 is independent of Hbs1 in vitro, Hbs1 binding expediates the splitting event by 2.5-fold (Pisareva et al., 2011; Shoemaker & Green, 2011). Upon Dom34 binding to stalled ribosomes, the Hbs1- directed GTP hydrolysis separates itself from Dom34, rendering it in active conformation and allowing the Dom34 binding to Rlil1/ABCE1 (Becker et al., 2011; Kobayashi et al., 2010; Pisareva et al., 2011; Shoemaker & Green, 2011; Starosta & Wilson, 2014; van den Elzen et al., 2014). The Dom34-Rlil1 complex results in a 40S subunit bound to mRNA and a 60S subunit with the peptidyl tRNA. The 40S subunit can spontaneously separate from the cleaved mRNA or recruit 40S recycling factors: Tma20/MCT-1, Tma22/DENR, and Tma64/eIF2D (Young & Guydosh, 2022). Dom34 lacks the catalytically active GGQ motif required for peptide hydrolysis and the NIKS motif required for stop codon recognition (Shoemaker et al., 2010). As a result, the product released by the Dom34:Hbs1 complex is a peptidyl-tRNA bound to the 60S subunit, which is recognized by the RQC complex, ubiquitinated and degraded by the ubiquitin-proteasome system (UPS) (Shao et al., 2013, 2015; Shoemaker et al., 2010; Young et al., 2015; Young & Guydosh, 2022). Gtpbp2 mutants exhibit reduced stalling in mammals, but it was unclear if Pelota was binding Gtpbp2 at stall-inducing codons (Ishimura et al., 2014).

Nascent Peptide Release

Ribosome splitting provides the ubiquitination machinery access to the nascent peptide chain attached to the tRNA (Shao & Hegde, 2014). The truncated nascent peptide is likely to misfold and might become aggregation-prone and thus is ubiquitinylated to be degraded by the UPS via mRNA-independent elongation (Chiabudini et al., 2012; Defenouillère et al., 2013; Shao et al., 2013, 2015; Shao & Hegde, 2014; Simms et al., 2018; Yip & Shao, 2021). The factor Rqc2 (NEMF) binds to the 60S-tRNA complex and mediates the C-terminal addition of alanine and threonine residues, termed CAT tails, to the nascent polypeptide in a template-independent manner

(Kostova et al., 2017; Osuna et al., 2017; Sitron & Brandman, 2019). This action exposes the lysine residues buried in the peptide exit tunnel for K48-linked polyubiquitination by the E3 ligase Ltn1 (LISTERIN) while the peptide remains in complex with the 60S subunit (Bengtson & Joazeiro, 2010; Kostova et al., 2017; Osuna et al., 2017; Sitron & Brandman, 2019). Rqc2 also stabilizes the Ltn1 binding to the 60S subunit (Defenouillère et al., 2013; Shao et al., 2015). Rqc1 works with Ltn1-mediated peptide ubiquitination and the AAA ATPase Cdc48 (p97) with cofactors, Ufd1 and Npl4, extract the truncated nascent peptide from the 60S subunit. Vms1 (ANKZF1), a homolog of eRF1, hydrolyzes the peptide-tRNA linkage and cleavages the tRNA (Brandman et al., 2012; Defenouillère et al., 2013; Joazeiro, 2019; Verma et al., 2018; Yip & Shao, 2021; Zurita Rendón et al., 2018) (reviewed in (Inada, 2020)).

Deubiquitylating enzymes and small subunit recycling

After the dissociation of the ribosomal subunit, the fate of the ubiquitylated 40S subunit is determined by its ubiquitinylated status. Mammalian cells have several deubiquitylating enzymes (Dubs) that counteract the action of E3 ubiquitin ligases by acting on ubiquitin modified 40S ribosomal proteins in response to ribosome collision or stress (Garshott et al., 2020). In an overexpression screen for human Dubs using fluorescent poly A stall reporter (GFP-polyA-ChFP), three Dubs enhanced the poly A stall read-through. These Dubs include OTUD3, USP21, and USP10, which remove ubiquitin from ribosomal proteins (Garshott et al., 2020; Meyer et al., 2020). While OTUD3 specifically acts on eS10 and uS10 ubiquitinated by ZNF598 during RQC, USP21 reverses both RQC- and stress-induced ubiquitylation (Garshott et al., 2020).

A parallel study identified the deubiquitylating enzyme UBP10 which functions with the RNA-binding protein G3BP1 during its interaction with the 40S ribosome (Meyer et al., 2020). A proteome-wide search in USP10 knockout versus USP10 overexpressing cell lines identified- rps2,

rps3, and rps10 as potential targets of USP10. In UBP10 or G3BP1/2 knockout cells, a selective reduction of 40S ribosomal proteins was observed with respect to 60S ribosomal proteins (Meyer et al., 2020). This resulted from an increased autophagy flux and lysosomal degradation of ubiquitinated 40S subunit in USP10-KO compared to parental cells. USP10 deubiquitinates only on RQC-dissociated 40S, downstream of the RQC and does not impair functional RQC (Meyer et al., 2020). Both reports found that uS5 (Rps2) and uS10 (Rps20) ubiquitination occurs downstream of uS3 (Rps3) and eS10 (Rps10) ubiquitination, respectively (Garshott et al., 2020; Meyer et al., 2020). Overall, OTUD3 reverts the RQC-mediated ubiquitination while USP21 and USP10 act both RQC collision- and stress-induced- ubiquitylated 40S, otherwise degraded by lysosomal autophagy. Dubs restores the pool of ribosomes to return to the translation cycle (Garshott et al., 2020; Meyer et al., 2020).

1.3.6.3 Not all endings involve NGD; RQC and translation regulation.

Ribosome collisions and the formation of RQC-disomes do not always lead to the degradation of the problematic mRNA by NGD. An efficient mechanism to prevent the synthesis of aberrant proteins and a further collision is the inhibition of translation. Cryo-EM structures in mammals and yeast revealed conserved binding sites in collided ribosomes to the EDF1 (Mbf1 in yeast). The interaction of EDF1 extends along the mRNA entry channel near the A-site of colliding ribosomes, making a prominent interaction with conserved residues of uS3 and helices 16, 18, and 33 of 18s rRNA. The EDF1 serves to stabilize the mRNA with respect to the ribosome to prevent frameshifting (Hendrick et al., 2001; Wang et al., 2018). In mammalian cells, the early engagement of EDF1 to collided ribosomes has been shown to occur independent of ZNF598 but dependent on RACK1. Instead, ZNF598 recruits the factors GIGYF2-4EHP to the collided ribosomes (yeast homologs of GIGYF2 are Smy2p, Syh1p), and EDF1 functions to stabilize the ZNF598-GIGYF2-

4EHP complex (Juszkiewicz, Speldewinde, et al., 2020; Sinha et al., 2020). The factor 4EHP outcompetes eIF4E for mRNA cap-binding and represses translation initiation in cis as 4EHP cannot bind to eIF4G to form an eIF4F complex (Hickey et al., 2020; Morita et al., 2012; Rom et al., 1998; Zuberek et al., 2007). The GIGYF2-4EHP-mediated translation silencing of problematic mRNAs occurs in parallel with nascent peptide degradation to counter the accumulation of toxic peptides **(Figure 1.3.6)**. This indicates that ZNF598 has a dual function in RQC; Ubiquitination of the ribosome to mediate RQT and NGD and recruitment of GIGYF2-4EHP to the collided ribosomes to inhibit translation (Hickey et al., 2020).

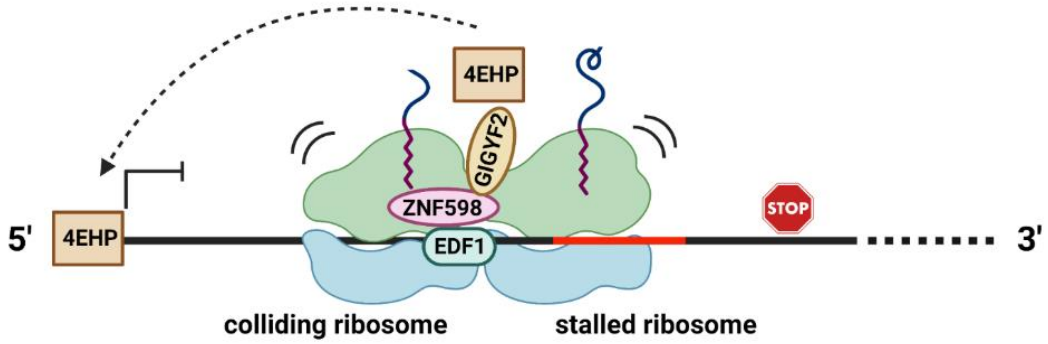

Figure 1.3.6. Ribosome-stalling feedbacks to inhibit translation initiation in mammalian cells. The collided ribosome binds EDF1, which is thought to stabilize the mRNA and prevent ribosome from frameshifting. Independent of EDF1 binding, ZNF598 of the colliding ribosome recruits the GIGYF2-4EHP complex, which is stabilized by EDF1. 4EHP competes with eIF4E to the 5' cap, thus inhibiting eIF4F formation which is required for translation initiation.

Yeasts lack the homolog of 4EHP, but their GIGYF2 homolog, Syh1, interacts with Eap1, an inhibitor of eIF4E function (Sezen et al., 2009). However, recent reports indicate that this feedback to inhibit translation initiation regulation through Syh1 might not be conserved in yeast. As mentioned in section 1.3.5.1 and **Figure1.3.5B**, Syh1 (and to a lesser extent its homolog

Smy2p) mediates the degradation of stalling mRNAs through Xrn1, and Syh1p absence resulted in an increased translational output of reporter mRNA containing non-optimal codons (Hickey et al., 2020; Veltri et al., 2022). Another mechanism that is not conserved in yeast is the recruitment of Syh1 through Mbf1, as deletion of Mbf1 did not affect mRNA decay mediated by Syh1 (Veltri et al., 2022). Therefore, although homolog RQC and NGD factors regulate the mRNA translation and decay of stall-inducing mRNAs, their functions might be different in yeast and multicellular eukaryotes. Our recent studies on the regulation of SSA4 mRNA translation in yeast indicated that the feedback from collisions to translation inhibition is conserved in yeast, at least under heat shock conditions, but it is not mediated by Syh1 (Alagar Boopathy et al., 2022). Future experiments will uncover the identity of factors involved in this repressive feedback. Likewise, we expect more factors, their organization on the collided ribosome, and their actions in RQC and NGD to be discovered by proteomic analysis, cryoEM, and in situ cryo electron tomography in the upcoming years, as well as the identification of the endogenous mRNAs being regulated by these mechanisms.

1.3.7 RQC and NGD are essential for cellular proteostasis

Diverse studies aimed to elucidate the role of critical components of RQC and NGD through their deletion found that these surveillance pathways are essential for proteostasis. As such, Dom34-mediated NGD is conserved from archaea to eukaryotes (Atkinson et al., 2008). Although most factors are conserved and only the name changes **(Table 1.2.1)**, a few others, such as Hbs1p and eRF3, are only found in eukaryotes. Bacteria has a different system to rescue stalled ribosomes, degrade the mRNA and nascent peptide. In *Escherichia coli*, a transcript lacking a stop codon or endonucleolytically cleaved mRNA due to an incurably stalled elongating ribosome, produces a non-stop complex that triggers mRNA surveillance (Keiler et al., 1996). The release of

the stalled ribosomes from an aberrant transcript (lack of stop codon) is mediated by a tRNA-mRNA (tmRNA) hybrid composed of a charged alanyl-tRNA and a short open reading frame (ORF) with a stop codon. The tmRNA is delivered by EF-tu to the A-site of halted ribosomes and adds its charged alanine to the still-bound polypeptide eventually triggering the movement of ribosomes (Himeno et al., 1997; Komine et al., 1994; Ushida et al., 1994; Williams et al., 1999). As the nascent chain is now transferred to tmRNA, the translation machinery also switches from the mRNA to the reading frame of tmRNA which encodes for a C-terminal degradation tag (Keiler et al., 1996; Tu et al., 1995). The translation terminates naturally upon encountering the stop codon. The non-stop mRNA is degraded by RNase R in 3'-5' direction immediately upon release from the ribosome (Hayes & Sauer, 2003; Pedersen et al., 2003). Whereas the polypeptide is degraded by proteases and the ribosomes are disassembled and recycled for new rounds of translation (Keiler et al., 1996; Tu et al., 1995).

Despite these variations among species, the RQC and NGD mechanisms are highly relevant at the molecular, cellular, and physiological levels to sustain proteostasis in eukaryotes. At the molecular level, RQC-dependent NGD prevents the synthesis of mutant proteins produced by ribosomes that frameshift at stalling sequences (Simms et al., 2019). The ability of the ribosome to accurately travel three nucleotides at a time during translation elongation preserves the reading frame to guarantee the correct interpretation of the genetic code. The positive correlation between ribosome density and frameshifting suggests that NGD has evolved to prevent detrimental frameshifting events resulting from unpredictable collisions **(Figure 1.3.7)** (Simms et al., 2019). In yeast, deletion of the RQC and NGD protein Asc1 results in significant frameshifting of ribosomes stalled in Arg CGA codon repeats, which hinges on codon dosage. Frameshifting depends on a slow translation rate as overexpression of tRNAArg (ICG) decreases its frequency.

Additionally, the length of the nascent peptide regulates Asc1-dependent frameshifting that mainly acts on CGA repeats located in at least 62 amino acids from the start methionine.Deletion of several RQC factors, Ltn1, Dom34, Hbs1, Hel2, and Rpl1B, did not induce frameshifting in the CGA reporter, suggesting that only some RQC components are needed to safeguard the translation frame (Wolf & Grayhack, 2015). Among them, the non-ribosomal factor Mbf1 interacts with uS3 and the mRNA entering the colliding ribosomes, to prevent the leading ribosome from a +1 frameshift when the CGA codon is in the P site (Hendrick et al., 2001; Wang et al., 2018).

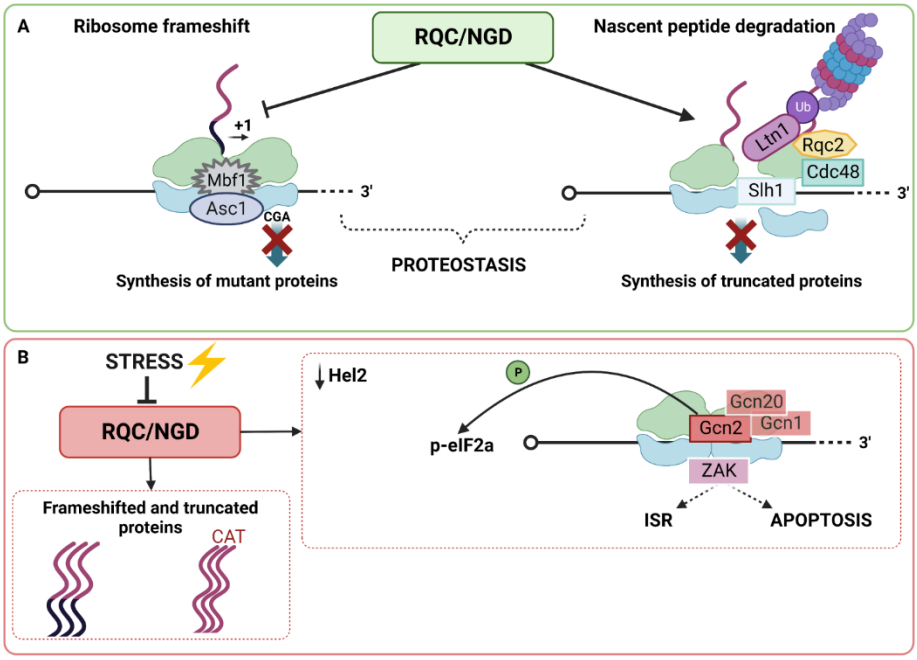

Figure 1.3.7. Loss of RQC/NGD disrupts proteostasis. A. RQC/NGD pathways prevent ribosome frameshifting in stalling sequences such as CGA repeats, avoiding the synthesis of mutant proteins due to the change in the reading frame. Furthermore, RQC solves ribosome collisions leading to ribosome splitting and to recycling and degradation of the nascent stalled peptide by the ubiquitin-proteasome system. **B**. The absence of RQC factors or if they are overloaded by stress conditions leads to the accumulation of frameshifted and truncated proteins, which upon CAT-tailed can aggregate and disrupt proteostasis. In addition, collided ribosomes are recognized by Gcn2 and Zakα, leading to the phosphorylation of eIF2α and the activation of the stress response and apoptosis. As a result, conditions that perturb the RQC/NGD pathways, such as aging, lead to proteostasis collapse and related diseases such as neurodegeneration.

Recent studies found that Mbf1 and uS3 yeast mutants suppress frameshifting when bearing mutations in the elongation factor EF3. On the contrary, yeast with mutations in the integrated stress response (ISR) regulator GCN1 underwent frameshifting even when Mbf1 was functional. Hel2, Gcn1, and Gcn20 act to preserve Mbf1 recruitment to colliding ribosomes, which opposes EF3 binding and prevents frameshifting (Houston et al., 2022). The proposed mechanism underlying the +1 frameshift is that the mRNA is entirely stretched when a ribosome collides with a stalled one. Under normal conditions, this triggers cleavage and downstream NGD events; however, if the cleavage is inhibited, the ribosome behind is free to pull on the mRNA since its A-site codon is competent, exerting force on the completely stretched RNA. This action results in slippage by the stalled ribosome, forcing it to frameshift (Simms et al., 2019). EF3 is not conserved in mammals, but the role of Mbf1 (EDF1) in constraining frameshifting is, although it occurs in the -1 direction and might have a different regulation (Juszkiewicz, Speldewinde, et al., 2020). Overall, certain quality control factors involved in RQC and NGD, such as Asc1 and Mbf1, prevent ribosome frameshifting **(Figure 1.3.7A)**. Degradation of the stalled mRNA by NGD endonucleolytic cleavage prevents new rounds of reading ribosomes from frameshift. This surveillance mechanism operates in mRNAs containing stalling sequences and preserves general proteostasis by degrading faulty mRNAs.

At the cellular level, NGD is associated with the RQC pathway and the stress response to maintain cell homeostasis. It is believed that RQC and NGD are coordinated via the ubiquitination activity of Hel2 (Ikeuchi et al., 2019). When Asc1 is deleted, or a functional Hel2 is absent from recognizing disomes, the phosphorylation level of eIF2α increases, suggesting an activated ISR (Alagar Boopathy et al., 2022; Alford et al., 2021; Brandman et al., 2012; Meydan & Guydosh, 2020; Sitron et al., 2017; Sitron & Brandman, 2020). Consistent with this notion, Gcn proteins are

capable of detecting ribosome collisions. For example, the kinase Gcn2, a regulator of eIF2α phosphorylation, can detect ribosome collision and become activated (Wu et al., 2020). With Hel2 deleted, more ribosome collisions are targeted by the Gcn pathway. Similarly, the deletion of Gcn2 and associated factors, Gcn1 and Gcn20, lead to hyper ubiquitination of stalled ribosomes by Hel2, suggesting that both RQC and ISR survey the transcriptome to detect ribosome collisions **(Figure 1.3.7B)** (Yan & Zaher, 2021). Under normal circumstances (absence of stress), Hel2 activation of RQC antagonizes the induction of the ISR. Conditions of stress, such as alkalization and oxidation, damage the mRNA prompting frequent ribosome stalling, which can overwhelm Hel2 leading to Gcn2 recognition of collision and activation of the ISR. Noticeably, Gcn2 preferentially recognizes stalled ribosomes with an empty A site, mainly occurring during stress (Yan & Zaher, 2021). In mammals, EDF1 binds to collided ribosomes to promote GIGYF2-4EHP-directed inhibition of translation initiation. In addition, ZAKα recognizes the extent of the ribosome stalling and signals either eIF2α -phosphorylation to repress translation or MAPK to promote cell apoptosis or prolong cell cycle arrest in G2 **(Figure 1.3.7B)** (De & Mühlemann, 2022; Stoneley et al., 2022; Wu et al., 2020). Gcn2 phosphorylation of eIF2α results in a general downregulation of translation and favors the synthesis of stress-regulated factors in both yeast and humans (Meydan & Guydosh, 2020; Pochopien et al., 2021; Wu et al., 2020; Yan & Zaher, 2021). The ISR is not the only stress response activated by colliding ribosomes. Accumulating truncated nascent peptides from stalled ribosomes activates the transcription factor - Heat Shock Factor 1 (HSF1) to transcribe molecular chaperones in charge of clearing misfolded and aggregated proteins. The signal for HSF1 activation relies on the RQC component Rqc2/Tae and, possibly, its role in adding C-terminal alanine-threonine (CAT) tails that promote protein aggregation (Brandman et al., 2012; Choe et al., 2016; Izawa et al., 2017; Kostova et al., 2017; Shen et al., 2015; Yonashiro et al., 2016). It is

thus logical to hypothesize that stress can overwhelm the RQC mechanism with faulty mRNAs promoting ribosome stalling and truncated nascent peptides in need of degradation. These events activate the ISR and HSF1 to sustain proteostasis by promoting the synthesis of molecular chaperones or inducible Heat Shock Proteins (HSPs). Surprisingly, the translation of the most inducible HSP70 mRNA in yeast, SSA4, is reduced by the RQC factors Asc1 and Hel2, suggesting that RQC regulates the extent of the heat shock response (Alagar Boopathy et al., 2022).

The loss of RQC and NGD threatens the fitness of the proteome with detrimental physiological consequences for higher eukaryotes. Proteostasis disruption by dysregulated mRNA surveillance and accumulation of misfolded proteins characterize diverse neurodegenerative diseases such as Alzheimer's, Parkinson's, or ALS (Labbadia & Morimoto, 2015; Tuck et al., 2020). The first evidence that defects in RQC lead to neurodegeneration was obtained in the LISTERIN mutant mouse model **(Figure 1.3.7A)** (Chu et al., 2009). Although all mouse cell types carried LISTERIN mutations, specific neurons were uniquely vulnerable to them, showing dendritic and axonal attrition, ALS-like hallmarks, and accumulation of soluble hyperphosphorylated TAU (Chu et al., 2009). The overproduction of nonstop nascent peptides added to the physiological significance of RQC and degradation of the stalled nascent peptide in neuronal proteostasis. The peptides aggregated after being CAT tailed by the RQC2/NEMF in neurons with a failed RQC system, leading to impaired neurite morphogenesis (Udagawa et al., 2021). Additional examples featuring the physiological relevance of RQC for neuronal functionality are pathogenic variants of RQC2/NEMF and mutations in the ASC-1 complex related to intellectual disability and ASM and ALS, respectively (Anazi et al., 2017; Chi et al., 2018) and excessive ribosome stalling causing neurodegeneration in mice (Ishimura et al., 2014). In Huntington's disease (HD), repeat expansions of the CGA trinucleotide encoding a polyglutamine

tract in the Huntingtin (HTT) gene caused this neuromuscular disorder. The CGA repeat promotes RNA-based toxicity by increasing the probability of ribosome collisions due to an elongation rate conflict betweenHuntington'slow translating portions of the mRNA. Moreover, mHTT protein also plays a role in translation failure since it sequesters translation factor eIF5A, promoting extensive ribosome stalling on hundreds of transcripts and causing widespread proteostasis breakdown (Aviner et al., 2022). Eventually, ribosome pausing and collisions occur across the transcriptome, altering the synthesis of essential proteostasis components such as ribosomes and proteasomes and deregulating stress responses. Potent protein and ribosome quality control likely resolve colliding ribosomes in young, healthy cells. However, aging cells with disrupted proteostasis become more susceptible to elongation stalls and protein aggregation, exacerbating their toxic consequences (Aviner et al., 2022; Maity & Iben, 2022). Accordingly, mRNAs in aging cells have increased ribosome occupancy and ribosome collisions at inhibitory codon pairs which are previously shown to delay translation elongation (Stein et al., 2022). Transcripts with age-dependent pausing, such as polybasic stretches, got enriched along with nascent ubiquitinated polypeptides that became part of protein aggregates (Stein et al., 2022). Thus, aging has pleiotropic effects on RQC, interfering with both the resolution of stalled ribosomes and the processing of stalled polypeptides. Interestingly, components of the proteostasis network were found among the age-dependent targets. In aged organisms, the decreased resolution of ribosome pausing increases the frequency of ribosome collisions, overpowering RQC and leading to proteostasis collapse (Stein et al., 2022). Taken together, these projects showed that the RQC and NGD pathways are especially relevant for neuronal proteostasis and prevent age-related neurodegeneration.

1.3.8 Future Perspectives

It is becoming apparent that RQC and NGD mechanisms are vital to preserving cellular protein homeostasis. As such, the molecular mechanisms that allow them to cooperate with the ISR and the proteostasis network machinery should be further explored with two goals. To improve our understanding of the dynamics of cellular proteostasis and also to open new venues to prevent the progression of untreatable neurodegenerative conditions. The exacerbated vulnerability of neurons to both proteotoxic stress conditions and the absence of RQC factors post essential questions for the field; Who are the endogenous RQC and NGD clients in the cell? And how do stress conditions and cell-specific factors regulate these pathways?

As highlighted in this review, the last fifteen years have greatly improved our knowledge of the structural and molecular events that act to solve colliding ribosomes and prevent the translation of problematic mRNAs. However, this knowledge relies on well-designed mRNA reporters. We recently found an endogenous mRNA, the inducible *HSP70* (*SSA4*), whose translation during heat shock conditions is regulated by the RQC components Asc1 and Hel2. Interestingly, RQC did not lead to NGD. Instead, Asc1 destabilized *SSA4* mRNA even when the ORF was optimized to abolish ribosomal collisions. Thus, endogenous mRNAs might be regulated by specific steps of the RQC and NGD pathways that are different from the descriptions obtained from stalling reporters. It is also essential to consider that these pathways might operate on specific mRNAs depending on the cell context. Likewise, stress-induced mRNA damage and an overwhelmed proteostasis network might module them. Continued progress in identifying mRNAs targeted by RQC and NGD and the spatiotemporal regulation of the events that regulate the mRNA fate will provide new insights into these mechanisms' physiological relevance and biomedical application.

CHAPTER 2: The ribosome quality control factor Asc1 determines the fate of *HSP70* mRNA on and off the ribosome.

Lokha R. Alagar Boopathy[1], Emma Beadle[1], Alan RuoChen Xiao[1], Aitana Garcia-Bueno Rico[1], Celia Alecki[1], Irene Garcia de-Andres[1], Kyla Edelmeier[1], Luca Lazzari[1], Mehdi Amiri[1], and Maria Vera[1*]

*To whom correspondence should be addressed: Tel: 514-398-2057; Email: maria.veraugalde@mcgill.ca

[1] Department of Biochemistry. McGill University, Montreal, Quebec, H3G 1Y6, Canada.
Present Address: Irene Garcia de-Andres, Technische Universität Dresden, Germany
Aitana Garcia-Bueno Rico, Department of Experimental and Health Sciences, Universidad Pompeu Fabra, Barcelona, 08003, Spain

2.1 Preface

This chapter is adapted from the manuscript entitled: The ribosome quality control factor Asc1 determines the fate of HSP70 mRNA on and off the ribosome. **Lokha R Alagar Boopathy**, Emma Beadle, Alan RuoChen Xiao, Aitana Garcia-Bueno Rico, Celia Alecki, Irene Garcia de-Andres, Kyla Edelmeier, Luca Lazzari, Mehdi Amiri, and Maria Vera. Nucleic Acids Res. 2023;51(12):6370-6388.

2.2 Abstract

Cells survive harsh environmental conditions by potently upregulating molecular chaperones such as heat shock proteins (HSPs), particularly the inducible members of the HSP70 family. The life cycle of *HSP70* mRNA in the cytoplasm is unique—it is translated during stress when most cellular mRNA translation is repressed and rapidly degraded upon recovery. Contrary

to its 5′ untranslated region's role in maximizing translation, we discovered that the HSP70 coding sequence (CDS) suppresses its translation via the ribosome quality control (RQC) mechanism. The CDS of the most inducible *Saccharomyces cerevisiae* HSP70 gene, *SSA4*, is uniquely enriched with low-frequency codons that promote ribosome stalling during heat stress. Stalled ribosomes are recognized by the RQC components Asc1p and Hel2p and two novel RQC components, the ribosomal proteins Rps28Ap and Rps19Bp. Surprisingly, RQC does not signal *SSA4* mRNA degradation via No-Go-Decay. Instead, Asc1p destabilizes *SSA4* mRNA during recovery from heat stress by a mechanism independent of ribosome binding and *SSA4* codon optimality. Therefore, Asc1p operates in two pathways that converge to regulate the *SSA4* mRNA life cycle during stress and recovery. Our research identifies Asc1p as a critical regulator of the stress response and RQC as the mechanism tuning HSP70 synthesis.

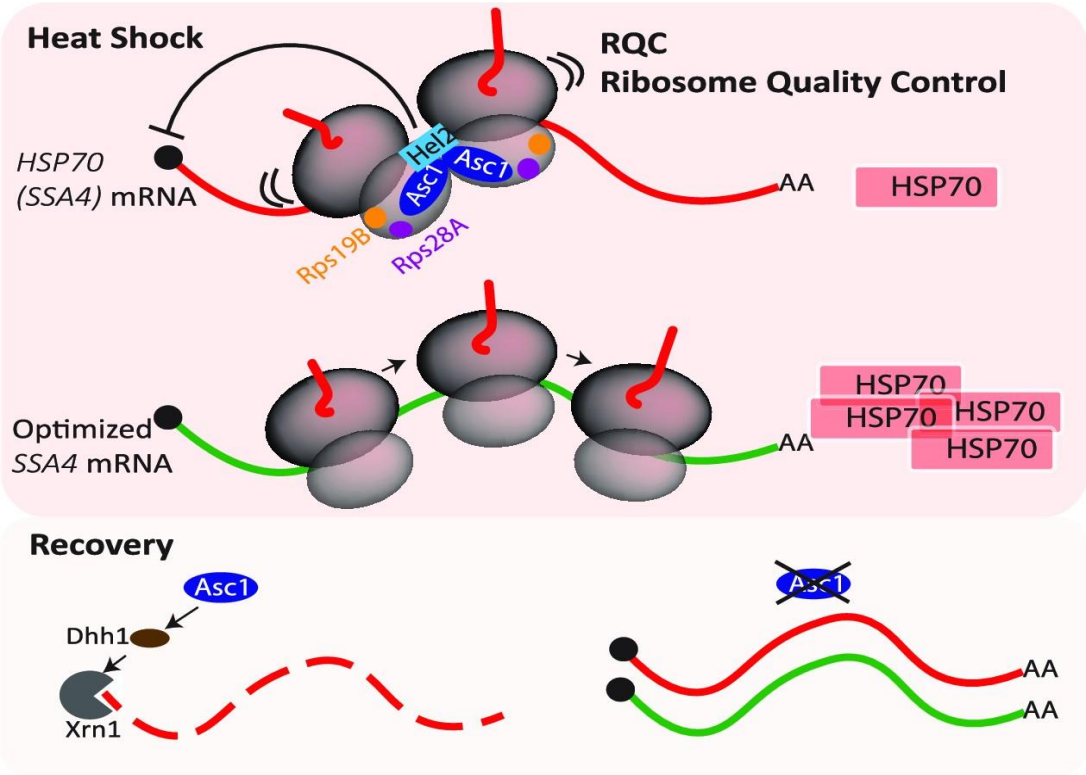

Figure 2.0. Graphical Abstract. Asc1 is a key regulator of the HSP70 mRNA life cycle during heat shock and recovery.

2.3 Introduction

Cells mitigate the detrimental effects of environmental stressors, such as heat, by rapidly inducing the expression of molecular chaperones known as heat shock proteins (HSPs) (1, 2). Cells tailor HSP levels to the burden of misfolded proteins by tuning the heat shock response (HSR). Its activation during stress leads to the potent upregulation of HSP transcription and preferential translation. Then, cells avoid unnecessary HSP accumulation during recovery by rapidly halting transcription and increasing HSP mRNA instability (3). This fast switch from induction to attenuation of the HSR is critical for cell function.

HSPs were initially classified into families based on their molecular weights and further categorized as constitutive or inducible based on their steady-state expression levels (4). Constitutive and inducible members of the HSP70 family play a key role in preserving protein homeostasis (proteostasis), preventing protein aggregation by assisting unfolded proteins back into their functional conformations, and clearing misfolded proteins in concert with the ubiquitin-proteasome system and autophagy (5). Fast resolution of their response is also crucial, as the persistent expression of inducible HSP70 under permissive conditions causes growth defects in *Drosophila* (6) and promotes transformation in mammalian cells (7).

In stress, activation of heat shock factor 1 (HSF1) induces robust HSP70 transcription (1, 3, 8–11). Newly synthesized *HSP70* mRNAs are translated despite the repression of cap-dependent translation initiation and elongation to prevent the accumulation of misfolded polypeptides (12–16). Translation initiation is further dampened by the phosphorylation of eIF2α, which inhibits GDP-GTP exchange (2, 3, 17–19). Co-transcriptional processing during stress favors HSP70 translation via a cap-independent pathway (20, 21). This mechanism involves the translation

elongation factor eEF1A1 and co-transcriptional modifications to the HSP70 5′ untranslated region (UTR) that are recognized by the translation initiation factor eIF3 (22–25). On-going translation promotes the mRNA's stability (26). During recovery, cells resume cap-dependent translation, and *de novo* synthesized HSP70 binds to the transactivation domain of HSF1 to repress its own expression and attenuate the HSR (2, 3, 10, 27). To rapidly shut down HSP70 expression, efficient degradation of its mRNA is critical, which requires its 3′ UTR (28, 29). Therefore, HSP70 transcripts go from highly stable during stress to highly unstable during recovery (28, 29). Although HSP70 translation is needed for its mRNA turnover, the factors tuning its fate in the cytoplasm in response to the cellular stress status remain unknown (3, 30).

The regulation of *HSP70* mRNA translation and stability relates to cellular changes in protein synthesis. The traditional mRNA surveillance model suggests that highly efficient translation increases mRNA stability because ribosomes protect the mRNA being translated from degradation (26, 31–36). Contrary to this model, recent findings showed that high translation initiation rates destabilize mRNAs containing pro-stalling codons in the budding yeast *Saccharomyces cerevisiae* (37–39). Increased ribosome loading favors collisions between stalled ribosomes, which result in the formation of di-ribosomes (disomes) consisting of the leading stalled ribosome and the subsequent colliding ribosome (40, 41). Colliding ribosomes signal to the ribosome quality control (RQC) mechanism to recycle stalled ribosomes and the mRNA surveillance mechanism No-Go Decay (NGD) to degrade the faulty mRNA (33, 42, 43).

The initiation of collision-associated RQC is mediated by Asc1p and Hel2p (the orthologs of RACK1 and ZNF598 in mammals, respectively), which stabilize the disomes (41, 43–47). Asc1p is a scaffold protein located at the head of the 40S subunit near the mRNA exit channel (48). In the context of the RQC, Asc1p-Asc1p interactions between disome's 40S subunits stabilize

the collision and provide an interface for recognition by the E3 ubiquitin ligase Hel2p (41, 46, 49). Hel2p ubiquitinates the 40S ribosomal protein Rps20p (uS10) in yeast and also Rps10p (eS10) in humans and promotes the splitting of the first stalled polyubiquitinated ribosome by the helicase Slh1p (44, 47, 50, 51). Alternatively, Not4 ubiquitinates Rps7p (eS7), which is a substrate for Hel2p polyubiquitination (41, 46, 52). The E3 ubiquitin ligase, Ltn1, ubiquitinates the aberrant peptide stocked in the 60S ribosomal subunit to be degraded by the ubiquitin proteosome system (UPS) and prevent its aggregation(53, 54). Disome stabilization by Asc1p and Hel2p is necessary to recruit endonucleases Cue2p or protein Syh1p that target the mRNA for degradation by NGD (42, 52, 55–59). To prevent the accumulation of partially synthesized peptides, ribosome collisions do not necessarily have to trigger NGD (55, 60–62). Instead, they can signal to repress translation initiation. In mammalian cells, ZNF598 recruits GIGYF2 and 4EHP to inhibit translation initiation by outcompeting eIF4E binding to the cap of the mRNA on a stalled ribosome (63).

Based on these studies, we hypothesized that by resuming cap-dependent translation during recovery, cells could link an increase in *HSP70* mRNA translation efficiency to its decay by NGD. To test this hypothesis, we studied the regulation of the four Stress Seventy sub-family A (Ssa) members, Ssa1-4, in *S. cerevisiae* (64). Ssa1p and Ssa2p are constitutively expressed, while Ssa3p and Ssa4p are inducible. The codon sequences of *SSA4* and *SSA3* mRNAs are biased toward low-frequency codons, which promote ribosome stalling and regulate their expression *via* the RQC and NGD. Accordingly, we found that the RQC factors Asc1p and Hel2p regulate the *SSA4* mRNA life cycle, but in unexpected ways. Firstly, the RQC mechanism downregulates Ssa4p synthesis during heat shock, which prevents its overproduction during stress. This regulation depends on the low codon optimality of the *SSA4* mRNA CDS and involves the ribosomal proteins Rps28Ap and Rps19Bp, which emerge as new RQC components. Secondly, the RQC mechanism does not lead

to NGD nor the degradation of *SSA4* mRNA during stress or recovery. Instead, Asc1p destabilizes *SSA4* mRNAs during recovery independently of its ribosome binding. This result points to two distinct functions for Asc1p that converge to control the fate of *SSA4* mRNA in the cytoplasm. Thus, we have identified Asc1p as a novel critical regulator of the yeast HSR.

2.4 Materials and methods

Yeast culture

All yeast strains are derived from the parental strain BY4741, and their genotypes are summarized in **Supplementary Table 2.1**. They were grown in yeast extract peptone dextrose (YPD) medium or the conditional medium appropriate for their genotype at 25°C with constant shaking at 250 rpm. Knock-in and deleted strains were created by homologous recombination of the parental strain after the transformation of a PCR fragment amplified from a plasmid carrying selection-specific markers. Gene deletions and knock-ins were verified by PCR analyses of genomic DNA extracted from individual colonies, as previously described (65). The primers and plasmids used are listed in **Supplementary Tables 2 and 3**, respectively.

Heat shock and recovery

For northern and western blot experiments, cells in the logarithmic growth phase (optical density at 600 nm (OD_{600}): 0.4–0.6) were heat shocked in a 42°C water bath with constant shaking at 150 rpm until the indicated time points. Immediately after heat shock, the heated medium was replaced with the same volume of room temperature (RT) medium. The culture flasks were then placed in a 25°C shaker incubator and rotated at 250 rpm until cultures were collected for downstream sample processing. For spot assays, cells at OD_{600} 1.0–1.5 were diluted in water to OD_{600} 0.5 and then serially diluted at a 1:5 ratio in water five times. Five µL of serially diluted cells were plated

on YPD-agar, then either incubated at 25°C or at 42°C for 16 h and then at 25°C. The preconditioning was performed by heat shock at 37°C for 1 h followed by 5 h of recovery at 25°C before moving the plates to 42°C. The plates were then checked for colonies every 24 h and images were acquired. For growth curves, cells at OD_{600} ~0.5 were heat shocked in a 42°C water bath with constant shaking at 150 rpm. Absorbance at 600nm was measured from the culture collected after heat shock and followed by 30, 60, 90, and 120 min of recovery.

Protein extraction, western blotting, and polysome profiling

Unstressed, heat-shocked, and recovered yeast (5 mL) were collected and centrifuged at 3,000 × *g* for 5 min. Cell pellets were first washed with 2 M LiOAc at RT and then with 0.4 M NaOH on ice. Cells were lysed with sodium dodecyl sulfate (SDS)-polyacrylamide gel electrophoresis (PAGE) buffer (60 mM Tris-HCl pH 6.8, 10% glycerol, 2% SDS, 5% 2-mercaptoethanol, and 0.0025% bromophenol blue). The lysates were heated for 10 min at 95°C, resolved by 10% SDS-PAGE, and transferred to nitrocellulose membranes. Ponceau S staining was used to confirm equal protein loading. Membranes were blocked with 5% skim milk in 1× phosphate-buffered saline with 0.05% Tween 20 (PBST) for 1 h at RT and then incubated with specific antibodies (eIF2α, phospho eIF2α (Ser51) (Cat# 9722, 9721S, Cell Signaling Technology, Danvers, MA, USA)), HA (Cat# 901501, BioLegend), tubulin (Developmental Studies Hybridoma Bank), and β-actin (Cat# A2228, EMD Millipore Corp) overnight at 4°C. Followed by three washes in PBST, membranes were incubated with horseradish peroxidase-conjugated goat-anti-mouse (Cat# 1706516, Bio-Rad) or goat-anti-rabbit antibody (Cat# 1706515, Bio-Rad) for 2 h at RT. Three washes with PBST were performed, followed by Clarity Western ECL treatment and imaging on a ChemiDoc Gel Imaging System (Bio-Rad). The intensity of the target protein signal was quantified using ImageJ version 2.1.0

(National Institutes of Health, Bethesda, MD, USA) and normalized to that of the loading control (β-actin or tubulin).

For protein isolation from polysomes, polysomes were prepared from heat shocked yeast extracts as previously described (66). Protein was extracted by adding 3 volumes of 100% cold ethanol to the monosome or polysome fractions. RNA-protein complexes were precipitated overnight at –20°C and centrifugated for 30 minutes at 13,000 rpm at 4°C. The pellets were washed once again with 70% ethanol, allowed to air-dry, and dissolved in the above-mentioned SDS-PAGE loading buffer.

RNA extraction, northern blotting, and RT-QPCR.

Unstressed, heat-shocked, and recovered yeast (5 mL) were collected and centrifuged at 3,000 × *g* for 5 min at 4°C. For the protocol below, all centrifugations were performed at 12,000 × *g*. The pellets were resuspended in 0.5 mL of RNA extraction lysis buffer (10 mM Tris-HCl pH 8.5, 5 mM EDTA, 2% SDS, 2% stock 2-mercaptoethanol), and transferred to 1.5 mL tubes. Cells were lysed by incubating the tubes in a heat block at 83°C for 20 min. After centrifugation for 5 min, the supernatant was transferred to a fresh tube containing 0.55 mL of pH 8 phenol. After vortexing for 30 s and centrifugation for 5 min, the top layer was transferred to a new tube labeled N. RNA extraction lysis buffer (0.25 mL) was added to the previous tube, which was vortexed briefly. An equal volume (0.25 mL) of chloroform was added, the tube was vortexed and centrifuged, and the top layer was transferred to tube N. Another 0.55 mL of pH 8 phenol was added to tube N, which was vortexed and spun as above, and the top layer was transferred to a new tube containing 0.55 mL of Acid Phenol-Chloroform, pH 4.5 (Cat# AM9720, Thermofisher Scientific, St. Austin, Texas, USA). The tubes were vortexed briefly, spun and 0.45 mL of the top layer was transferred to a new set of tubes containing 0.2 mL of 0.6 M sodium acetate, pH 4.5. The contents were mixed

by flicking followed by a quick spin. Once again, Acid Phenol-Chloroform, pH 4.5, 0.6 mL was added to the tubes accompanied by a vortex and spin. Approximately 0.35 mL of the top layer was once again transferred to new tubes containing 1.1 mL of 100% ethanol and 0.03 mL of 5 M ammonium acetate. After mixing, the samples were placed at -80°C overnight. The next day, the samples were spun at 4°C for 15 min and the supernatant was discarded. The pellet was washed twice with 80% ethanol and allowed to air dry, then dissolved in 0.04 mL of RNase-free water and the RNA was quantified. Equal amounts (1,000–2,000 ng) of RNA were aliquoted into fresh tubes and dried in a SpeedVac for 45 min at 45°C. Samples were resuspended in 5 µL of RNase-free water and mixed with 7 µL of homemade RNA loading dye. The RNA samples were run in a 1% denaturing gel in 1× MESA buffer. Transfer to zeta probe nylon membranes was set up using capillary electrophoresis overnight. The membrane was UV-crosslinked at 1200 mJ, stained for total RNA, prehybridized, hybridized, exposed to a phosphorscreen, and developed using a phosphorimager. Northern blotting and radiolabeling of probes were performed as in (67). Genomic BY4741 was used as a template to PCR amplify probes that target *SSA1*, *SSA2*, *SSA3*, *SSA4*, *SSA4*-Opt 3′ UTR (MS2V6) using primers listed in **Supplementary Table 2.2.**

For reverse transcription, 1 µg of total RNA was treated with 1 unit of DNaseI (Promega) for 30 min and 100 ng were reverse transcribed using 4 µL of iScript RT supermix (Biorad) in a 20 µL reaction following manufacturer instruction. For qPCR, cDNAs were diluted two-fold in water. PCR was performed in 5 µL reactions consisting of 1 µL of cDNA, 2.5 µL PowerUp SYBR Green master mix (ThermoFisher) and 0.25 µL of 1 µM of each primer. Standard curves were generated using a log titration of BY4741 WT or SSA4 optimized genomic DNA (50 to 0.05 ng). Data was collected using Viaa7 PCR system with 45 cycles. The standard curve was used to calculate RNA amounts.

mRNA half-life calculations

Northern blots were quantified using ImageJ and normalized to corresponding methylene blue staining. Considering the intensity of the heat shock sample (timepoint: 0 min) to be 100% induction, the relative intensity was calculated for recovery samples (timepoints: 15, 30, 60, 90 min). A polynomial curve was plotted for time *vs* the percentage of mRNA decayed. The polynomial equation was obtained for the curve and solved for X, given that Y is 50 using what-if analysis in Microsoft Excel.

Preferred codon percentage determination

A list of preferred codons in *S. cerevisiae* was procured from (68) and the CDSs of SSA mRNAs were obtained from the *Saccharomyces* Genome Database (https://www.yeastgenome.org/). A Python script was developed to count the occurrence of each preferred codon and divide it by the total number of codons to calculate the percentages of preferred codons (https://github.com/LR-MVU/YEAST-SSA.git).

Single-molecule in situ hybridization (smFISH) and imaging analysis

The smFISH procedure was performed as previously described (69). Briefly, yeast strains were grown in 25 mL YPD at 25°C to early log phase and heat shocked at 42°C. At the indicated time points, they were fixed in 4% paraformaldehyde, permeabilized in spheroplast buffer containing lyticase (as described in (69), (Cat# L2524, Sigma Aldrich, Oakville, ON, Canada)), and seeded onto poly-L-lysine-coated coverslips. After ethanol incubation, rehydration with 2× saline sodium citrate buffer, and prehybridization, the cells were hybridized with Stellaris smFISH probes to detect MS2V6 sequence in the tagged *SSA4* or *SSA2* mRNAs (LGC Biosearch Technologies) as previously described in (69). The coverslips were washed, dried, and mounted in Prolong Gold Antifade Mounting Medium (Invitrogen, Bulington, ON, Canada), then imaged using a wide-field

inverted Nikon Ti-2 wide-field microscope equipped with a Spectra X LED light engine (Lumencor), and an Orca-Fusion sCMOS camera (Hamamatsu) controlled by NIS-Elements Imaging Software. For yeast cells, a 100× 1.49 NA oil immersion objective lens (Nikon) was used with an xy pixel size of 67.5 nm and a z-step of 200 nm. Outlines were created using the CellProfiler pipeline, and single mRNAs were quantified using FISH-quant (70).

Ribosome profiling analysis

Ribosome profiling and RNA sequencing (RNA-Seq) data in yeast under heat shock conditions performed by Mühlhofer et al 2019 (71) were downloaded from the Gene Expression Omnibus (accession numbers: Riboseq data: SRR9265440 and SRR9265438; RNA-seq data: SRR9265437 and SRR9265428). Raw sequencing reads were processed first by trimming adapters using Cutadapt 3.4 and discarding the low-quality reads. The reads were next mapped to rRNAs and aligned reads were discarded. The remaining reads were then mapped to the yeast transcriptome and the resulting SAM files were further processed to SQLite files using a Python script from the Trips-Viz webserver (https://trips.ucc.ie/) for compatibility with PausePred (72), the built-in function of Trips-Viz (73). Default settings were used to detect ribosome stall sites on SSA4 mRNAs, which were visualized using Trips-Viz.

Protein immunoprecipitation and mass spectrometry

FLAG-tagged Asc1 (Asc1p-3×FLAG) yeast cultures were grown in 400 mL YPD at 25°C to early log phase and heat shocked for 1 h at 42°C. The cells were pelleted by centrifugation at 3,750 rpm for 3 min at 4°C. The pellets were washed with 10 mL water, transferred to Eppendorf tubes, snap-frozen with liquid nitrogen, thawed on ice, and resuspended in 2 mL of lysis buffer (100 mM HEPES pH 8.0, 20 mM magnesium acetate, 10% glycerol, 10 mM EGTA, 0.1 mM EDTA) containing Complete X protease inhibitor and phosphatase inhibitors (1M NaF, 0.2M NaAPi, and

Na2vO4). Glass beads (0.5 mm) were added, and tubes were vortexed 20 times with 30 s on-off cycles in a cold room. Lysates were separated from the beads by a quick centrifugation at 4°C and transferred to new tubes. About 100 µL of M2-anti-FLAG beads (Cat# M8823, Millipore sigma, Oakville, ON, Canada) were washed three times with 500 µL of lysis buffer, then incubated with the lysates for 2 h on a nutator in a cold room. The beads were magnetized, and the flowthrough was collected. The beads were then washed twice with 1 mL of lysis buffer and each wash was collected. Samples of the beads, lysate, flow-through, and washes were boiled in SDS-PAGE buffer, resolved by SDS-PAGE, and western blotted for FLAG. Immunoprecipitation samples were sent to Proteomics Services at the McGill University Health Centre Research Institute for mass spectrometry. For each sample, proteins on the beads were loaded onto a single stacking gel band to remove lipids, detergents, and salts. The single gel band containing all proteins was reduced with DTT, alkylated with iodoacetic acid, and digested with trypsin. Extracted peptides were re-solubilized in 0.1% aqueous formic acid and loaded onto a Thermo Acclaim Pepmap (Thermo, 75uM ID X 2cm C18 3uM beads) precolumn and then onto an Acclaim Pepmap Easyspray (Thermo, 75uM X 15cm with 2uM C18 beads) analytical column separation using a Dionex Ultimate 3000 uHPLC at 250 nl/min with a gradient of 2-35% organic (0.1% formic acid in acetonitrile) over 3 h. Peptides were analyzed using a Thermo Orbitrap Fusion mass spectrometer operating at 120,000 resolution (FWHM in MS1) with HCD sequencing (15,000 resolution) at top speed for all peptides with a charge of 2+ or greater. The raw data were converted into *.mgf format (Mascot generic format) for searching using the Mascot 2.6.2 search engine (Matrix Science) against yeast protein sequences (Uniprot 2022). The database search results were loaded onto Scaffold Q+ Scaffold_5.0 (Proteome Sciences) for statistical treatment and data

visualization. We only consider proteins as enriched or depleted upon HS if they exhibit a fold change >1.5 and have a p-value ≤ 0.05 (**Supplementary Table 2.4**).

For co-immunoprecipitation, Flag-tagged Asc1, Flag-tagged Asc1/TAP-tagged RPS28, and Flag-tagged Asc1/HA-tagged RPS19 strains were grown in 25 mL of YPD at 25°C to early log phase and heat shocked for 1 h at 42°C. The cells were pelleted by centrifugation at 3,750 rpm for 3 min at 4°C. The pellets were washed with 10 mL water, transferred to Eppendorf tubes, snap-frozen with liquid nitrogen, thawed on ice, and resuspended in 400 µL of lysis buffer (100 mM HEPES pH 8.0, 20 mM magnesium acetate, 10% glycerol, 10 mM EGTA, 0.1 mM EDTA) containing Complete X protease inhibitor. Glass beads (0.5 mm) were added, and tubes were vortexed 20 times with 30 s on-off cycles in a cold room. Lysates were separated from the beads by a quick centrifugation at 4°C and transferred to new tubes. About 10 µL of M2-anti-FLAG beads were washed three times with 200 µL of lysis buffer, then incubated with the lysates for 2 h on a nutator in a cold room. The beads were magnetized and washed thrice with 500 µL of lysis buffer and each wash was collected. Samples of the beads and lysate were boiled in SDS-PAGE buffer, resolved by SDS-PAGE, and immunoblotted for FLAG (Anit-FLAG_M2 antibody, F1804, Sigma, Saint Louis, MO, USA), HA (HA antibody, Cat#901501, Biolegend, San Diego, CA, USA) or TAP (Peroxidase Anti-Peroxidase Soluble Complex antibody (PAP) antibody, Cat#P1291 Sigma, Saint Louis, MO, USA).

2.5 Results

2.5.1 The RQC factors Asc1p and Hel2p repress Ssa4p expression during heat shock

In the SSA subfamily of yeast HSP70 genes, the CDSs of inducible *SSA3* and *SSA4* are biased towards low-frequency codons (50% optimal codons) compared to the constitutive *SSA1* and *SSA2*

CDSs (75% optimal codons; **Supplementary Figure 2.S1A**) (68). *SSA3* mRNA translation initiation is regulated by an upstream open reading frame (uORF), making *SSA4* the most inducible member of this subfamily (74). The presence of nonoptimal codons in highly translated mRNAs leads to slow decoding and ribosome stalling, favoring collisions (33). Therefore, we analyzed previously published ribosome profiling data (71) to identify the presence of stalled ribosomes over the *SSA4* mRNA CDS under heat shock (30 min at 42°C) (**Figure 2.1A and Supplementary Figure 2.S1B**). PausePred analysis identified stalled ribosomes (*i.e.*, peaks with 20-fold more ribosome occupancy than the following mRNA position) (72, 73) at position 400 (P1) on the *SSA4* mRNA in both experimental replicates and at position 1800 (P2) in one replicate. Although the *SSA4* mRNA codon sequence protected by the ribosome is identical to that of two other SSA mRNAs, the *SSA4* sequence contains three low-frequency codons following the stalled ribosome (**Figure 2.1A**). The presence of stalled ribosomes on *SSA4* transcripts and its enrichment in low-frequency codons led us to investigate the roles of the RQC mechanism and NGD in regulating *SSA4* mRNA translation and decay, respectively (75).

The RQC factors Asc1p and Hel2p stabilize ribosome collisions and repress the translation of the affected mRNA (40, 42). To investigate their roles in regulating Ssa4p synthesis during heat shock and subsequent recovery, we deleted *ASC1* or *HEL2* genes from haploid BY4741 wild-type (WT) *S. cerevisiae*. Given the high similarity between the four SSAs, we inserted 3×Hemagglutinin (HA) epitopes in the C-terminus and 12×MS2V6 RNA stem-loops in the 3'UTR of each of the endogenous SSA genes to distinguish their proteins and mRNAs by western blotting and smFISH, respectively. Compared to the WT strain, the *asc1Δ* and *hel2Δ* strains had significantly higher expression of Ssa4p during heat shock; however, no changes in Ssa1p, Ssa2p, Ssa3p, nor the non-heat shock protein Doa1p were observed between the basal (25°C), heat shock,

and recovery conditions (**Figure 2.1B-E, Supplementary Figure 2.S1C, and 2.S1D**). Increased Ssa4p expression in heat-shocked *asc1Δ* and *hel2Δ* yeast persisted during recovery, but the difference in expression compared to the WT strain did not increase further.

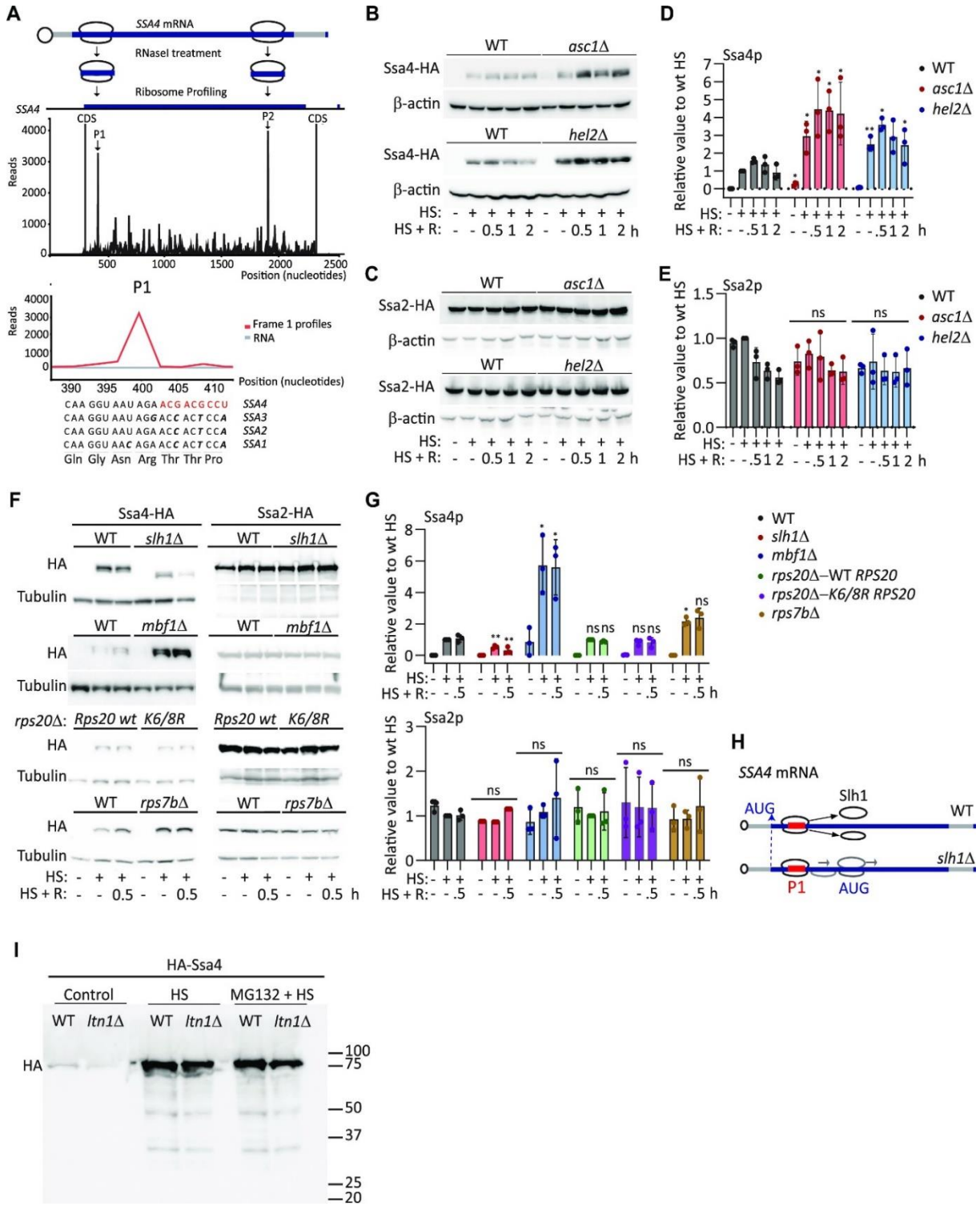
A
SSA4 mRNA
RNaseI treatment
Ribosome Profiling
SSA4
CDS
P1
P2
CDS
Reads
Position (nucleotides)
Frame 1 profiles
RNA
CAA GGU AAU AGA ACG ACG CCU SSA4
CAA GGU AAU AGG ACC ACT CCA SSA3
CAA GGU AAU AGA ACC ACT CCA SSA2
CAA GGU AAC AGA ACC ACT CCA SSA1
Gln Gly Asn Arg Thr Thr Pro
B
WT
asc1Δ
Ssa4-HA
β-actin
hel2Δ
HS:
HS + R:
C
Ssa2-HA
D
Ssa4p
Relative value to wt HS
E
Ssa2p
ns
F
Ssa4-HA
Ssa2-HA
slh1Δ
HA
Tubulin
mbf1Δ
rps20Δ:
Rps20 wt
K6/8R
rps7bΔ
G
Ssa4p
Ssa2p
slh1Δ
mbf1Δ
rps20Δ–WT RPS20
rps20Δ–K6/8R RPS20
rps7bΔ
H
SSA4 mRNA
Slh1
AUG
WT
slh1Δ
P1
I
HA-Ssa4
Control
HS
MG132 + HS
ltn1Δ
HA
100
75
50
37
25
20

Figure 2.1. Deletion of Asc1p or Hel2p increases *SSA4* mRNA translation during heat shock. **A**. Ribosome profiling analysis of *S. cerevisiae SSA4* mRNA after 30 min of heat shock at 42°C. Top: Schematic of *SSA4* mRNA with ribosomes stalled at two positions. Middle: A single transcript plot of the ribosome sequencing analysis aligned with RNA-Seq data (65). P1 and P2 indicate ribosome stall sites. Bottom: The *SSA4* nucleotide sequence protected by the ribosome at P1 and the corresponding nucleotide and amino acid sequences in *SSA1*, *SSA2*, and *SSA3*. **B-C.** Western blots of 3×-HA-tagged Ssa4p (**B**) and Ssa2p (**C**) in the WT, *asc1Δ*, and *hel2Δ* strains under basal conditions (25°C), after 30 min of heat shock at 42°C (HS), and at the indicated recovery (R) time points. β-actin was used as a loading control. **D-E**. Quantification of Ssa4p (**D**) and Ssa2p (**E**) expression. HA band intensities were first normalized to their corresponding β-actin band and are expressed relative to the normalized expression of heat-shocked WT yeast. Bars indicate the mean and standard deviation (SD) of three independent experiments, each represented by a dot. $*p < 0.05$, $**p < 0.001$, $***p < 0.0001$ (by unpaired *t*-test). **F**. Western blots of 3×-HA-tagged Ssa4p and Ssa2p in the WT, *slh1Δ*, *mbf1Δ*, and WT *Rps20* versus Lys6/8 Arg *Rps20* and *rps7BΔ* strains under basal conditions (25°C), after 30 min of heat shock at 42°C (HS), and after 30 min recovery (R). Tubulin was used as a loading control. **G**. Quantification of Ssa4p and Ssa2p expression. HA band intensities were first normalized to their corresponding Tubulin band and are expressed relative to the normalized expression of heat-shocked WT yeast. Bars indicate the mean and standard deviation (SD) of three independent experiments, each represented by a dot. $*p < 0.05$, $**p < 0.001$ (by unpaired *t*-test). **H**. Scheme of the SSA4 ORF where stalled ribosomes are disassembled by Slh1p in WT cells. In the absence of Slh1p, stalled ribosomes can be disassembled at a lower frequency and the 40S subunit will continue scanning the mRNA and initiate translation in the next AUG. **I.** Western blots of 3×-HA-N-terminal tagged Ssa4p under basal conditions (25°C) and after 30 min of heat shock at 42°C (HS) previously exposed or not to 0.25 M of MG132 for 6 hours. Right side numbers indicate the ladder molecular weight.

To exclude Ssa4p dilution by cell division during recovery, we measured yeast duplication after 30 min of heat shock (**Supplementary Figure 2.S1E**). None of the strains duplicated for the two hours that followed the heat shock, suggesting that *SSA4* mRNA is not translated during recovery. This indicates that the enrichment in low-frequency codons in the *SSA4* mRNA CDS downregulates Ssa4p expression *via* the RQC only during heat shock.

We modified other factors involved in RQC to confirm the regulation of Ssa4p synthesis by this mechanism. We deleted the RNA helicase Slh1p that splits the leading stalled ribosomes (50, 51) and the Multi-protein Bridging Factor 1 (Mbf1p) that prevents the leading ribosome from +1 frameshifting (76–79). Compared to WT, the *slh1Δ* strain had a significantly lower expression

of Ssa4p during heat shock and recovery (**Figure 2.1F and 2.1G**). Interestingly, the band corresponding to Ssa4-HA was slightly smaller (by ~5 KDa). This result was unexpected since *SLH1* deletion has the same effect as *HEL2* deletion in stalling mRNA reporters studied in yeast and mammalian cells (51, 80, 81). To explain both the lower expression and smaller Ssa4p band, we propose that in the absence of Slh1p, the leading stalled ribosome cannot be efficiently split and recycled and remains stabilized with the collided ribosomes by Asc1p and Hel2p. As a result, they could form a roadblock at P1 that prevents them from finishing translation, decreasing Ssa4p full-length expression. Interestingly, *SSA4* has a downstream AUG in-frame with the start codon at nucleotide 177 in the CDS, where translation could reinitiate and produce a polypeptide that is 53 amino acids shorter than the full length (**Figure 2.1H**). Thus, we suggest that from the few 80S ribosomes stalled in P1 that can disassemble without Slh1p, the 40S subunit remains bound to the mRNA and scans the CDS until the next AUG (nucleotide 177), where a new 80S is assembled reinitiating translation (similar to what happened in uORF containing mRNAs) (82, 83) (**Figure 2.1H**). This result fits with ribosomes stalled at P1, as detected by ribosome profiling (**Figure 2.1A**). Similarly to the *asc1Δ* and *hel2Δ* strains, the *mbf1Δ* strain expressed significantly more Ssa4p than WT. These results further support the regulation of *SSA4* mRNA translation by colliding ribosomes and RQC (**Figure 2.1F and 2.1G)**.

Two 40S ribosomal proteins, Rps7Bp and Rps20p, are involved in RQC. Monoubiquitination of Rps7Bp by Not4p followed by its polyubiquitination by Hel2p is required to resolve stalled ribosomes. Besides Rps7p ubiquitylation, a more canonical way to resolve stalling ribosomes implies ubiquitylation of Rps20p at Lys 6 and 8 by Hel2p (41, 46). To evaluate the role of these proteins in Ssa4p synthesis, we expressed the Rps20p (Lys 6/8 Arg) mutant or deleted Rps7Bp (**Figure 2.1F and 2.1G)**. Compared to WT, strains expressing the Rps20p (Lys

6/8 Arg) mutant or deletion of *RPS7B* had the same or only a two-fold increase Ssa4p expression (**Figure 2.1F and 2.1G).** Thus, during heat shock, an alternative mechanism probably mediates the ubiquitination of a different 40S ribosomal protein. The essential protein Rps3p is a good candidate because it regulates ribosome-associated quality control during the mammalian unfolded protein response in a Hel2- and Asc1-dependent manner (84).

The truncated Ssa4 nascent peptide should be excised from the 60S ribosomal subunit for degradation. Peptides are ubiquitinated by the E3 ligase Ltn1p and degraded by the UPS (53, 54). We HA-tagged Ssa4p in the N-terminus to identify an expected Ssa4 truncated peptide of ~3.5 KDa. Since small proteins are challenging to detect by western blotting, we aimed to find the larger polyubiquitinated form by inhibiting its UPS-mediated degradation with MG132. Under these conditions, we expected the polyubiquitinated 3xHA-Ssa4p to accumulate in WT cells and be absent in *ltn1Δ* yeast. However, we only identified the full-length 3xHA-Ssa4p and two smaller aberrant products that were the same in WT and *ltn1Δ* cells under mock- or MG132-treated conditions (**Figure 2.1I**). This result suggested that an alternative mechanism degraded the aberrant Ssa4 peptide. Since it only has one Lys in its sequence, it might not be a subject for Ltn1-directed ubiquitination, and it could be degraded instead by autophagy or proteases in the cytosol (85, 86).

2.5.2 Asc1p promotes SSA4 mRNA degradation during recovery from heat shock

We pondered two non-exclusive options to explain the regulation of Ssa4p synthesis during heat shock but not during recovery: Asc1p and Hel2p could only repress *SSA4* mRNA translation during heat shock, and/or rapid *SSA4* mRNA degradation at the permissive temperature could prevent its translation during recovery. To investigate the first option, we considered that heat

shock triggers the phosphorylation of eIF2α, favoring the translation of inducible HSP mRNAs, and that in *asc1Δ* and *hel2Δ* cells, Gcn2p recognizes the ribosome collision and phosphorylates eIF2α even under basal conditions to activate the integrated stress response (ISR) (61, 87). Accordingly, *asc1Δ* and *hel2Δ* strains had higher P-eIF2α levels than the WT strain under basal conditions, and all strains displayed P-eIF2α during heat shock. Interestingly, P-eIF2α decreased to WT basal levels within 15 min of recovery, even in the *asc1Δ* and *hel2Δ* cells, which could hinder *SSA4* mRNA translation during recovery and thus decrease the regulatory effects of Asc1p and Hel2p (**Figure 2.2A, 2.2B, and 2.1B**). These results point to specific repression of *SSA4* mRNA translation by Asc1p and Hel2p during heat shock.

To consider the role of mRNA stability in Ssa4p expression during recovery, we quantified *SSA* mRNA levels at the basal temperature, during heat shock, and after recovery for 15, 30, 60, and 90 min. Ribosome collisions can lead to endonucleolytic cleavage and the rapid degradation of problematic mRNAs by NGD (42, 52, 56, 58, 59). Thus, the stabilization of ribosome collisions by Asc1p and Hel2p could promote rapid *SSA4* mRNA decay during recovery. We detected full-length *SSA4, SSA3, SSA2,* and *SSA1* mRNAs by northern blot in the untagged strains using antisense probes against their 3′ UTRs, which contain the most distinct nucleotide sequences between them (**Figure 2.2C, 2.2D and Supplementary Figure 2.S2A and 2.S2B**). As expected, all SSA mRNAs were highly induced upon heat shock and rapidly returned to basal levels during recovery in the WT strain. The *asc1Δ* and *hel2Δ* strains only prolonged *SSA4* mRNA expression during recovery without affecting the decay of the rest of the SSA mRNAs. We plotted the intensities of the *SSA4* and *SSA2* mRNA bands to calculate their half-lives by non-linear regression, which best fitted the curves connecting mRNA intensities during heat shock and

recovery conditions. The effect was specific to *SSA4* mRNA, with 2.5- and 1.35-fold increases in its half-life upon deletion of *ASC1* and *HEL2*, respectively (**Figure 2.2D**).

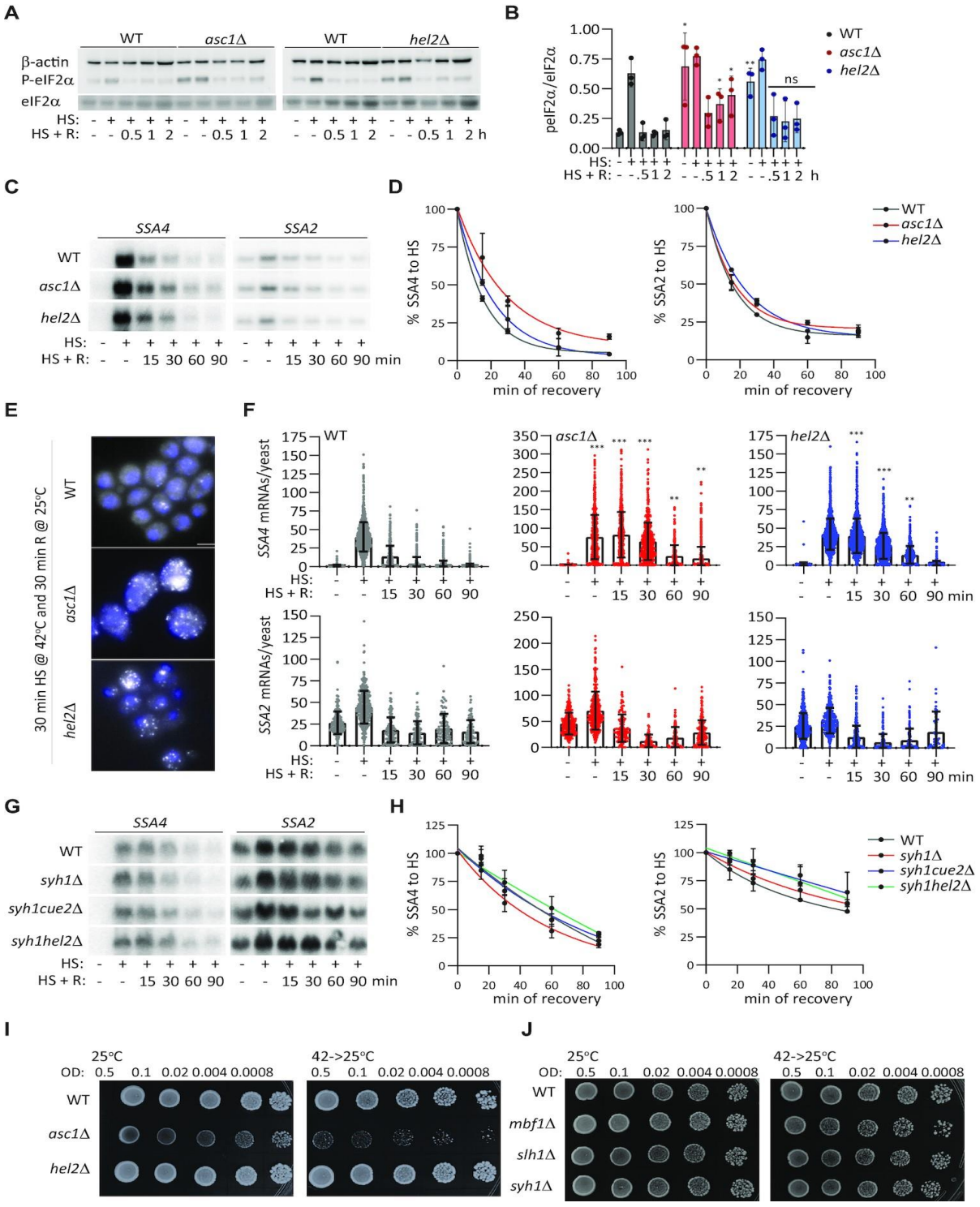

Figure 2.2. *SSA4* mRNA is stabilized in *asc1Δ* and *hel2Δ* cells during recovery from heat shock.

A. Western blots to detect eIF2α phosphorylation. P-eIF2α, total eIF2α, and β-actin were quantified in the WT, *asc1Δ,* and *hel2Δ* strains under basal, heat shock, and recovery conditions. **B**. Quantification of eIF2α phosphorylation. P-eIF2α band intensities were divided by their corresponding total eIF2α intensities. Bars indicate the mean and SD of three independent experiments, each represented by a dot. *$p < 0.05$, **$p < 0.001$ by unpaired *t*-test. **C**. Northern blots to detect the expression of *SSA4* and *SSA2* mRNAs in the WT, *asc1Δ,* and *hel2Δ* strains under basal conditions (25°C), after 30 min of heat shock at 42°C (H), and at the indicated recovery time points (R). **D**. Quantification of the half-lives of SSA mRNAs during recovery. Band intensities were normalized to the methylene blue staining and are expressed relative to the heat shock band for each strain (considered to be 100% induction) to obtain decay curves and calculate half-lives (t1/2 of *SSA4* mRNA: WT *16', asc1Δ 25'*, and *hel2Δ 19';* t1/2 of *SSA2* mRNA: WT *19', asc1Δ 22',* and *hel2Δ 27')*. Datapoints on the curves indicate the mean and SD of two independent experiments. **E**. Representative smFISH images of *SSA4-MS2V6* mRNA after 30 min recovery in the WT, *asc1Δ,* and *hel2Δ* yeast strains. Scale bar: 5 µm. **F**. Quantification of *SSA4* or *SSA2* mRNAs per yeast cell in each strain were detected by smFISH. Bars indicate the mean and SD of three experiments; dots represent individual cells (n=600–1,200). The unpaired *t*-test was used to compare each time point to the basal condition. **G**. Northern blots to detect the expression of *SSA4* and *SSA2* mRNAs in the WT, *syh1Δ, syh1/cue2Δ* and *syh1/hel2Δ* strains under basal conditions (25°C), after 30 min of heat shock at 42°C (H), and at the indicated recovery time points (R). **H**. Decay plot of *SSA* mRNAs during recovery. Band intensities were normalized to the methylene blue staining and are expressed relative to the heat shock band for each strain (considered to be 100% induction) to obtain decay curves and calculate half-lives **I-J**. Spot assays of the WT, *asc1Δ,* and *hel2Δ* strains and WT, *mbf1Δ, slh1Δ*, and *syh1Δ* strains grown at 25ºC and recovering at 25ºC after 16 h at 42ºC. OD, optical density at 600 nm.

We confirmed this prolonged *SSA4* mRNA stability and the lack of effects on *SSA2* mRNA stability during recovery by smFISH in the SSA4- and SSA2-3×HA-12MSV6 strains, respectively (**Figure 2.2E and 2.2F**), using a fluorescent probe against the MS2V6 sequence, and quantified them with FISH-quant (70). The average number of single *SSA4* mRNAs per cell was doubled in the *asc1Δ* strain compared to the WT and *hel2Δ* strains, probably because they are larger cells and produce more mRNAs to compensate for their volume, as *SSA2* mRNA was also more abundant. In the WT strain, most *SSA4* mRNAs were cleared within 30 min of recovery, while some *hel2Δ* cells and the majority of *asc1Δ* cells retained significantly higher numbers of *SSA4* mRNAs until after 90 min of recovery ($p < 0.05$, by unpaired *t*-test). Since only 5-10% of cells in all strains show

staining for transcription sites during recovery, this result indicated a prolonged *SSA4* mRNA half-live. All strains showed similar patterns of *SSA2* mRNA induction and decay during heat shock and recovery (**Figure 2.2F**). In the *asc1Δ* and *hel2Δ* strains, smFISH analyses revealed a delay in peak *SSA4* mRNA expression from heat shock to after 15 min of recovery. Since we could not quantify the contributions of nascent transcripts to the total mRNA pools by smFISH, we attribute this discrepancy with the northern blot results to turnover of the cytoplasmic mRNA population during the first 15 min of recovery. *SSA4* mRNA decay may occur faster than the export of nascent transcripts to the cytoplasm in WT cells but not in the *asc1Δ* and *hel2Δ* strains, shifting the timing of peak expression.

To analyze the role of colliding ribosomes and RQC in *SSA4* mRNA degradation by NGD, we quantified *SSA4* mRNA levels in yeast in which the main players of the two NGD pathways were deleted. The predominant pathway involves Syh1, and the secondary comprises Hel2 and the endonucleolytic cleavage by Cue2 (59). We detected full-length *SSA4* and *SSA2* mRNAs by northern blot in the untagged strains using antisense probes against their 3′ UTRs (**Figure 2.2G**). Compared to WT, *syh1Δ*, *syh1Δ* /*cue2Δ*, and *syh1Δ /hel2Δ* had the same *SSA4* and *SSA2* mRNA expression during heat shock and recovery and similar half-lives during recovery (**Figure 2.2H**). These results indicate that the degradation of *SSA4* mRNA is independent of NGD factors. We suggest that the prolonged *SSA4* mRNA half-lives detected in *asc1Δ* and *hel2Δ* cells might be due to elongating ribosomes protecting the mRNA from degradation or an NGD-independent role of these proteins in destabilizing *SSA4* mRNA during recovery.

Of all strains, *asc1Δ* has the highest Ssa4p expression and the longest *SSA4* mRNA half-live; thus, it should be better equipped to survive heat shock than the WT and strains deleted of other RQC and NGD factors. However, as previously reported (48), the *asc1Δ* strain grew the

slowest and was the most sensitive to heat shock, suggesting that its growth phenotype is independent of the expression of the cytoprotective Ssa4p (**Figure 2.2I**). Overall, our results indicate that *SSA4* mRNA degradation during recovery is independent of NGD and *asc1Δ* cells prolonged *SSA4* mRNA stability longer than *hel2Δ* cells, indicating that Asc1p plays an additional role in the *SSA4* mRNA decay during recovery from heat shock. Since prolonged *SSA4* mRNA stability during recovery did not further increase Ssa4p levels, Asc1p and Hel2p might regulate *SSA4* mRNA translation during heat shock and stability during recovery by independent mechanisms.

2.5.3 Optimizing the SSA4 coding sequence escapes the RQC, but its mRNA is still stabilized in asc1Δ cells.

To gain insight into the mechanisms by which Asc1p and Hel2p regulate *SSA4* mRNA translation and decay, we optimized the *SSA4* CDS to bypass ribosome stalling. We synonymized the CDS with a computational pipeline that considers the codon context of mRNA translate under specific conditions (88). Interestingly, the optimal *SSA4* CDS acquired the codons used in *SSA3*, *SSA2*, and *SSA1* for conserved amino acids, further supporting a role for *SSA4*'s specific enrichment in low-frequency codons (**Supplementary Figure 2.S3**). To generate an *SSA4* codon-optimized (Opt) strain, we substituted the endogenous *SSA4* CDS with the *SSA4*-Opt sequence, conserving the 5′- and 3′-UTR sequences. We tagged *SSA4*-Opt with 3×HA and 12MSV6 to study its effects on *SSA4* mRNA translation in WT cells (Opt-WT) and the roles of Asc1p and Hel2p in its translational regulation.

Opt-WT cells expressed Ssa4p even in basal conditions, indicating that the low-frequency codons in the WT CDS prevent the spurious accumulation of Ssa4p in the absence of stress. In addition, codon optimization dramatically increased Ssa4p upregulation during heat shock and

recovery by 20- and 40-fold, respectively (**Figure 2.3A and 2.3B**). Therefore, the WT *SSA4* CDS suppresses Ssa4p synthesis during heat shock. Remarkably, Ssa4p induction upon heat shock was similar in the Opt-WT and Opt-*hel2Δ* strains, further demonstrating that Hel2p's repression of Ssa4p synthesis depends on these low-frequency codons (**Figure 2.3C and 2.3D**). Likewise, *SSA4* codon optimization decreased Ssa4p induction during heat shock from 6-fold in the WT-*asc1Δ* strain to less than 2-fold in the Opt-*asc1Δ* strain (**Figure 2.1B, 2.1D, 2.3C, and 2.3D**). We concluded that the WT *SSA4* CDS is necessary for Asc1p and Hel2p to repress its translation during heat shock.

We next investigated whether the *SSA4*-Opt CDS stabilizes *SSA4* mRNA and prevents Asc1p and Hel2p from destabilizing it during recovery. We compared the expression and stability of *SSA4*-Opt mRNA (and *SSA2* mRNA as a control) in the Opt-WT, Opt-*asc1Δ*, and Opt-*hel2Δ* strains after 30 min heat shock at 42°C followed by 15, 30, 60, and 90 min of recovery at 25°C by northern blot. *SSA4*-Opt mRNA was 1.5 times more stable than *SSA4*-WT mRNA during recovery and completely abolished the effect of Hel2p on *SSA4* mRNA stability. Therefore, increasing the translational efficiency of Opt-*SSA4* mRNA slightly increased its mRNA stability. However, the rapid degradation of *SSA4*-Opt mRNA further supports that its main degradation pathways are independent of its codon optimality and NGD. Remarkably, the *SSA4*-Opt mRNA half-life was 2.5 times longer in the Opt-*asc1Δ* strain compared to Opt-WT, while the *SSA2* mRNA half-life was unaffected (**Figure 2.3E and 2.4E**). Optimizing *SSA4* CDS did not change the upregulation of *SSA4* mRNA induction at 30 min of heat shock. Likewise, the Opt-*asc1Δ* and Opt-*hel2Δ* strains had similar *SSA4* mRNA induction as the Opt-WT (**Figure 2.3G**). This result supports a role for Asc1p in promoting *SSA4* mRNA decay during recovery that it is independent of the *SSA4* CDS.

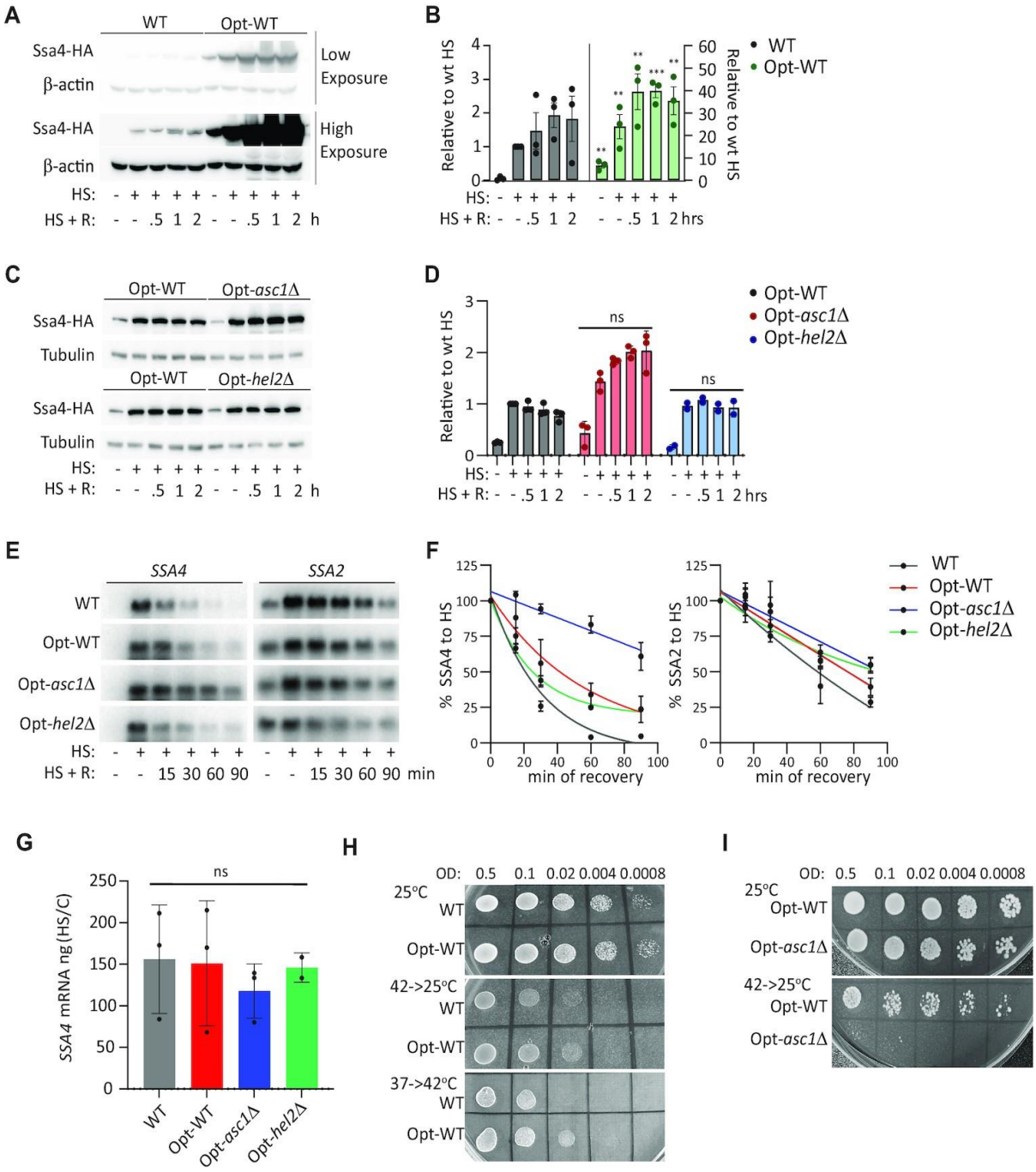
A
WT
Opt-WT
Ssa4-HA
β-actin
Low Exposure
High Exposure
HS:
HS + R:
B
Relative to wt HS
WT
Opt-WT
C
Opt-WT
Opt-asc1Δ
Opt-hel2Δ
Tubulin
D
Opt-asc1Δ
Opt-hel2Δ
ns
E
SSA4
SSA2
WT
Opt-WT
Opt-asc1Δ
Opt-hel2Δ
min
F
% SSA4 to HS
% SSA2 to HS
min of recovery
G
SSA4 mRNA ng (HS/C)
H
OD: 0.5 0.1 0.02 0.004 0.0008
25°C
42->25°C
37->42°C
I

Figure 2.3. A codon-optimized *SSA4* mRNA escapes the RQC mechanism, but it is still destabilized by Asc1p

A. Expression of the 3×HA-Ssa4p in the WT and Opt strains under basal conditions (25°C), after 30 min of heat shock at 42°C (HS), and at the indicated recovery time points (R). β-actin was used as a loading control**. B.** Quantification of 3×HA-Ssa4p expression. Band intensities were normalized to their corresponding β-actin band and are expressed relative to the normalized expression of *SSA4*-WT yeast under heat shock. Bars indicate the mean and SD of three independent experiments, each represented by a dot. **p* < 0.05, ***p* < 0.001, and ****p* < 0.0001 (by unpaired t-test). **C.** Expression of 3×HA-Ssa4p in the WT, Opt-WT, Opt-*asc1Δ*, and Opt-*hel2Δ* strains under basal conditions (25°C), after 30 min of heat shock at 42°C, and at the indicated recovery time points. Tubulin was used as a loading control**. D.** Quantification of Ssa4p expression. Band intensities were normalized to their corresponding tubulin band and are expressed relative to the normalized expression of WT yeast under heat shock. Bars indicate the mean and SD of three independent experiments, each represented by a dot. **p* < 0.05, ***p* < 0.001, ****p* < 0.0001, ns, not significant (by unpaired *t*-test). **E.** Northern blot detection of *SSA4* and *SSA2* mRNAs in the WT, Opt-WT, Opt-*asc1Δ*, and Opt-*hel2Δ* strains under basal conditions, after 30 min of heat shock at 42°C, and at the indicated recovery time points. **F.** Quantification of the half-lives of *SSA4* and *SSA2* mRNAs during recovery. Band intensities were normalized to the methylene blue staining and are expressed relative to the heat shock band for each strain (considered to be 100% induction) to obtain decay curves and calculate half-lives (t1/2 of *OPT* mRNA: in WT *22'*, Opt-WT *40'*, Opt-*asc1Δ 100'*, and Opt-*hel2Δ 27';* t1/2 of *SSA2* mRNA: in WT *57'*, Opt-WT *77'*, Opt-*asc1Δ 92'*, and Opt-*hel2Δ 118'*). **G.** Quantification of the fold induction of *SSA4* mRNA at 30 min of heat shock at 42°C. Induction was calculated by dividing the amount of cDNA in ng in heat shock to control. Bars indicate the mean and SD of three independent experiments, each represented by a dot (by unpaired *t*-test); ns, not significant. **H and I**. Spot assays of SSA4-WT and -Opt (**H**) and Opt-WT, Opt-*asc1Δ*, and Opt-*hel2Δ* (**I**) strains grown at 25ºC, recovering at 25ºC after 16 h at 42ºC, and preconditioned by mild stress (37ºC for 1 h, 6 h at 25ºC, and then heat shock at 42ºC). OD, optical density at 600 nm.

Given the existing notion that heat shock maximizes Ssa4p production to cope with protein misfolding, learning that the *SSA4* CDS attenuates its own translation via the RQC was unexpected. Thus, we investigated if Ssa4p overexpression is toxic. The WT and Opt-WT strains grew similarly at the permissive temperature and during recovery from stress, and Ssa4p overexpression enhanced the survival of Opt-WT cells to heat shock upon preconditioning (**Figure 2.3H**). However, Ssa4p overexpression did not overcome the increased vulnerability of *asc1Δ* cells to heat shock (**Figure 2.3I**). Thus, this strain's inability to survive heat shock is independent of Asc1p's role in regulating Ssa4p expression. Overall, our results support two separate functions of

Asc1p in controlling the life cycle of *SSA4* mRNA in the cytoplasm: translational repression during heat shock, a role which relies in the RQC mechanism (shared with Hel2p, Slh1p, and Mbf1p) and depends on the WT *SSA4* CDS, and mRNA decay during recovery, which is independent of the CDS and *SSA4* mRNA translation efficiency.

2.5.4 Asc1p regulates *SSA4* mRNA, not its intronic U24 small nucleolar (sno) RNA

The *ASC1* locus contains an intron that encodes the snoRNA *SNR24*, known as *U24* (89, 90). *U24* is a C/D box snoRNA that guides 2'-O-methylation of the 25S ribosomal RNA (rRNA). This role requires at least 10 nucleotides (nts) of perfect complementarity (91–94). Sequence analysis of the *SSA4* 3′ UTR revealed 10 nts of perfect complementarity with the *U24* sequence (TGAAGTAGCA; **Figure 2.4A**). Since the 3′ UTR is required to destabilize *SSA4* mRNA during recovery (29), we sought to determine whether the deletion of *U24* stabilizes *SSA4* mRNA in the *asc1Δ* strain, rather than Asc1p. Thus, we restored either the expression of Asc1p or *U24* by inserting centromeric plasmids into the *asc1Δ* strain (as described in (89)). We also mutated the 3′ UTR of the endogenous *SSA4* mRNA to prevent *U24* binding (TG*TTCAT*GCA; WT-3′ UTR mut) to determine whether this sequence destabilizes *SSA4* mRNA during recovery. Northern blot analysis of *SSA4* mRNA levels in basal, heat shock, and recovery conditions showed that Asc1p expression destabilized *SSA4* mRNA during recovery, while exogenous *U24* expression in the *Asc1Δ* strain increased *SSA4* mRNA stability by 3.4 times. Accordingly, mutating the 3′ UTR *U24* binding sequence did not affect *SSA4* mRNA stability during recovery (**Figure 2.4B and 2.4C**). To validate our results, we investigated the roles of Asc1p and *U24* in destabilizing the *SSA4*-Opt mRNA. As expected, Asc1p expression was sufficient to destabilize *SSA4*-Opt mRNA in the Opt-*asc1Δ* strain and revert its half-life to that observed in the Opt-WT strain. In contrast, *U24* did not change the *SSA4*-Opt mRNA half-life and neither Asc1p nor *U24* changed *SSA2* mRNA stability

in the Opt-*asc1Δ* (**Figure 2.4B, 2.4C, and Supplementary Figure 2.S4B and 2.S4C**). These results indicate that Asc1p regulates *SSA4* mRNA stability during recovery.

Although it is well known that Asc1p and Hel2p act together to regulate the translation of faulty mRNAs and trigger the RQC mechanism (47), we investigated whether *U24* also regulates *SSA4* mRNA translation. We quantified Ssa4p expression in *asc1Δ* cells expressing either Asc1p or *U24*. While Asc1p expression restored Ssa4p induction to the WT level, yeast expressing *U24* without Asc1p failed to rescue the high Ssa4p expression of the *asc1Δ* strain (**Figure 2.4D and 2.4E**). Restoring either Asc1p or *U24* in the Opt-*asc1Δ* strain did not change Ssa4p synthesis during heat shock and recovery. Altogether, these experiments indicate that *U24* does not regulate the *SSA4* mRNA life cycle, strongly supporting two independent roles for Asc1p in deciding the fate of cytoplasmic *SSA4* mRNA. First, Asc1p regulates *SSA4* mRNA translation during heat shock in response to its low-frequency codons and second, it regulates *SSA4* mRNA stability during recovery independently of its CDS or translation efficiency.

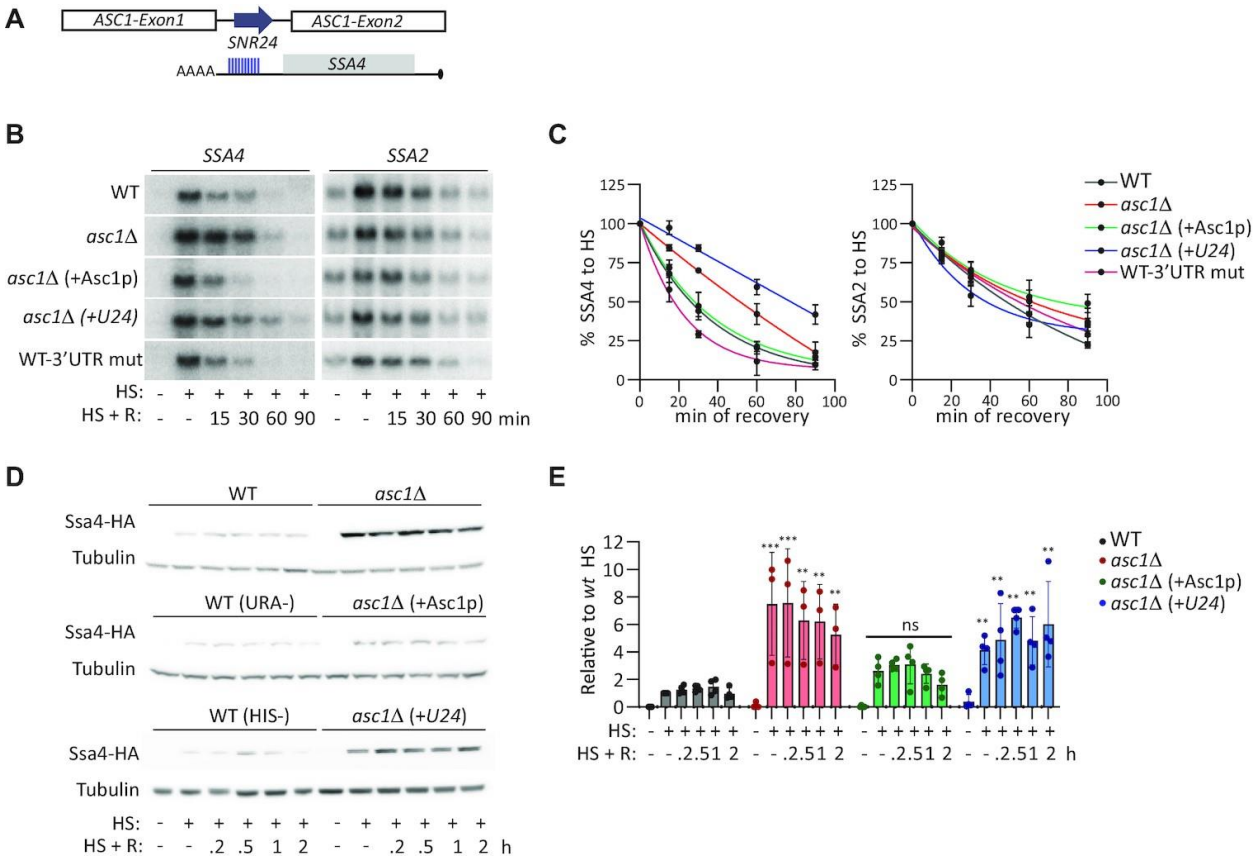

Figure 2.4. Asc1p, not *SNR24*, regulates *SSA4* mRNA translation and stability

A. Schematic of the *ASC1* locus. It contains two exons and an intron, which encodes the small nucleolar RNA *SNR24* (*U24*) upon splicing. The 10-nucleotide region in the 3′ UTR of *SSA4* mRNA that is complementary to *U24* is indicated by blue lines. **B.** Northern blots to detect the expression of *SSA4* and *SSA2* mRNAs in the WT, *asc1Δ*, *asc1Δ* expressing the CDS of Asc1p (*asc1Δ* +Asc1p), and *asc1Δ+U24* strains, and the WT strain with five 3′ UTR mutations in the U24 complementarity region (WT-3′ UTR mut) under basal conditions, after 30 min of heat shock at 42°C (HS), and at the indicated recovery time points (R). **C.** Quantification of the half-lives of *SSA4* and *SSA2* mRNAs during recovery. Band intensities were normalized to the methylene blue staining and are expressed relative to the heat shock band for each strain (considered to be 100% induction) to obtain decay curves and calculate half-lives (t1/2 of *SSA4* mRNA: in WT 28', *asc1Δ* 51*'*, *asc1Δ +Asc1p* 21*'*, *asc1Δ +U24* 78*'*, WT-*3′ UTR mut* 20*';* t1/2 of *SSA2* mRNA: WT 48*'*, *asc1Δ* 60*'*, *asc1Δ +Asc1* 68*'*, *asc1Δ +U24* 36*'*, WT-*3′ UTR mut* 55′). **D.** Expression of 3×HA-Ssa4p in the indicated strains under basal conditions (25°C), after 30 min of heat shock at 42°C, and at the indicated recovery time points. Tubulin was used as a loading control**. E** Quantification of Ssa4p expression. Band intensities were normalized to their corresponding tubulin band and are expressed relative to the normalized expression of WT yeast under heat shock. Bars indicate the mean and SD of three independent experiments, each represented by a dot. $^{**}p < 0.001$, $^{***}p < 0.0001$, ns, not significant (by unpaired *t*-test).

2.5.5 Asc1p binding to ribosomes is required for the RQC mechanism to regulate *SSA4* mRNA translation but not to destabilize it during recovery

Asc1p is a multifunctional protein with roles in and out of the ribosome (90). We examined whether Asc1p binding to the ribosome is needed to regulate *SSA4* mRNA translation during heat shock and destabilize *SSA4* mRNA during recovery. We obtained three *ASC1* mutants, *M1X, DE, and DY,* in the yeast sigma background described by Thompson et al (90). In the *M1X* mutant the start codon was substituted by a stop codon in the *ASC1* CDS that prevents Asc1p expression but maintains *ASC1* and *U24* RNA levels. The *DE* mutant holds two substitutions, R38D and K40E, in the N-terminus that decrease Asc1p's binding to ribosomes. The *DY* mutant, D109Y, has a lower ribosome binding capacity than the DE mutant and defects in NGD (90). Of these mutants, only *M1X* prolonged the half-life of *SSA4* mRNA during recovery, and none of the strains changed *SSA2* mRNA stability (**Figure 2.5A and 2.5B**). This result confirmed our previous findings in the BY4741 background, showing that Asc1p, but not *U24*, destabilizes *SSA4* mRNA during recovery from heat shock. They also show that *SSA4* mRNA decay is not mediated by NGD, because the *DY* mutant behaved like the WT strain. Finally, since the *SSA4* mRNA half-lives in the *DE* (24 min) and *D109Y* (27 min) strains were similar to the WT sigma strain (30 min), Asc1p's ability to regulate *SSA4* mRNA stability is unrelated to ribosome binding. These results were consistent with Asc1p destabilizing both *SSA4*-WT and *SSA4*-Opt mRNAs, and an additional role for Asc1p independent of the *SSA4* CDS (**Figure 2.2C-F, 2.3E, and 2.3F**).

We next investigated whether Asc1p needs to bind the ribosome to repress Ssa4p synthesis. We used centromeric plasmids to express the *WT*, *M1X,* or *DY ASC1* genes in the *asc1Δ* BY4741 strain, which had the *SSA4* locus tagged with 3×HA-12MS2V6. The *M1X* strain expressed ~7 times more Ssa4p than the WT strain upon heat shock, as we previously observed with the *asc1Δ*.

Interestingly, Ssa4p induction in the *DY* strain resembled that of the *M1X* strain upon heat shock, implying that low binding of Asc1p to the ribosome is not sufficient to repress *SSA4* mRNA translation (**Figure 2.5C and 2.5D**). We confirmed these results in the original sigma strains by tagging the *SSA4* locus with 3×HA-12MS2V6 in the *M1X*, *DE*, and *DY* strains. All three strains showed similar Ssa4p induction upon heat shock and recovery (**Figure 2.5E and 2.5F**). Therefore, Asc1p binding to the ribosome is needed for its translational control of *SSA4* mRNA during heat shock, further confirming the involvement of the RQC mechanism in regulating Ssa4p synthesis.

We also investigated whether Asc1p must bind to ribosomes to promote heat shock survival. The expression of the low ribosome-binding *DE* and *DY* mutants enabled *asc1Δ* yeast to survive heat shock. Thus, Asc1p's prosurvival role in heat shock is independent of ribosomal binding and the regulation of *SSA4* mRNA stability and translation (**Figure 2.5G**). Collectively, these results suggest that Asc1p repression of *SSA4* mRNA translation requires its binding to the ribosome, and Asc1p-mediated destabilization of *SSA4* mRNA is independent of ribosome binding. Thus, Asc1p probably uses two independent mechanisms, in and out of the ribosome, to regulate *SSA4* mRNA translation and decay.

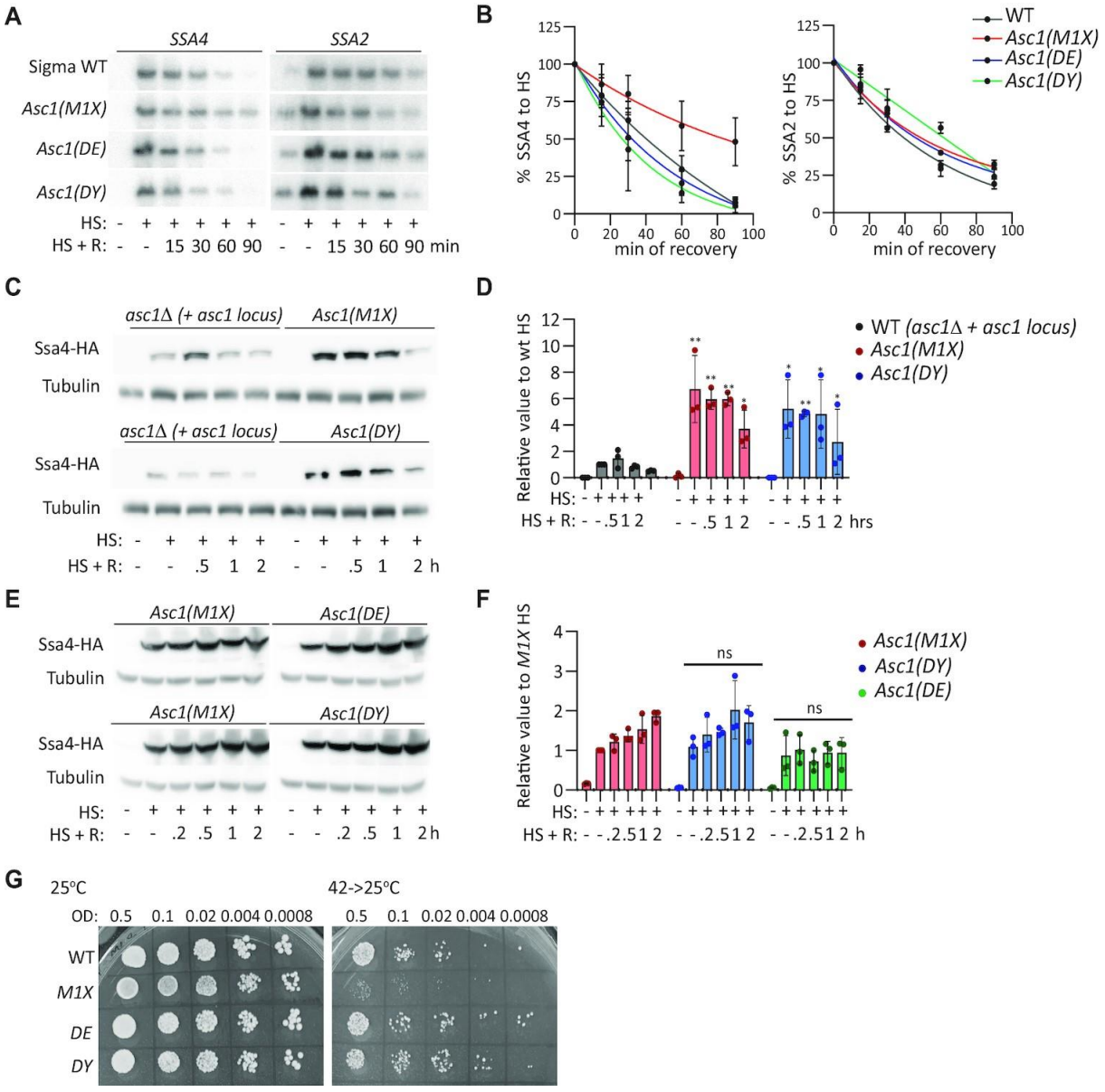
A
SSA4
SSA2
Sigma WT
Asc1(M1X)
Asc1(DE)
Asc1(DY)
HS: - + + + + + - + + + + +
HS + R: - - 15 30 60 90 - - 15 30 60 90 min
B
% SSA4 to HS
% SSA2 to HS
min of recovery
min of recovery
WT
Asc1(M1X)
Asc1(DE)
Asc1(DY)
C
asc1Δ (+ asc1 locus)
Asc1(M1X)
Ssa4-HA
Tubulin
asc1Δ (+ asc1 locus)
Asc1(DY)
Ssa4-HA
Tubulin
HS: - + + + + - + + + +
HS + R: - - .5 1 2 - - .5 1 2 h
D
Relative value to wt HS
WT (asc1Δ + asc1 locus)
Asc1(M1X)
Asc1(DY)
HS: - + + + + - + + + + - + + + +
HS + R: - - .5 1 2 - - .5 1 2 - - .5 1 2 hrs
E
Asc1(M1X)
Asc1(DE)
Ssa4-HA
Tubulin
Asc1(M1X)
Asc1(DY)
Ssa4-HA
Tubulin
HS: - + + + + + - + + + + +
HS + R: - - .2 .5 1 2 - - .2 .5 1 2 h
F
Relative value to M1X HS
ns
ns
Asc1(M1X)
Asc1(DY)
Asc1(DE)
HS: - + + + + + - + + + + + - + + + + +
HS + R: - - .2.5 1 2 - - .2.5 1 2 - - .2.5 1 2 h
G
25°C
42->25°C
OD: 0.5 0.1 0.02 0.004 0.0008 0.5 0.1 0.02 0.004 0.0008
WT
M1X
DE
DY

Figure 2.5. Roles of *ASC1* gene, Asc1p-null, and ribosome binding mutants on *SSA4* mRNA stability and translation and in heat shock survival

A. Northern blots to detect the expression of *SSA4* and *SSA2* mRNAs in the sigma WT, *Asc1_M1X*, *Asc1(DE),* and *Asc1(DY)* strains under basal conditions (25°C), after 30 min of heat shock at 42°C (HR), and at the indicated recovery time points (R). **B**. Quantification of the half-lives of *SSA4* and *SSA2* mRNAs during recovery. Band intensities were normalized to the methylene blue staining and are expressed relative to the heat shock band for each strain (considered to be 100% induction) to obtain decay curves and calculate half-lives (t1/2 of *SSA4* mRNA: in sigma WT *30'*, *Asc1_M1X 84'*, *Asc1 DE* 24'and *Asc1 DY 27';* t1/2 of *SSA2* mRNA: in sigma WT *39'*, *Asc1_M1X 47'*, *Asc1 DE* 43′ and *Asc1 DY 53′*). **C.** Expression of 3×HA-Ssa4p in *asc1Δ* BY4741 strains expressing the full *ASC1* locus or *ASC1 M1X* or *DY* mutants under basal conditions (25°C), after 30 min of heat shock at 42°C, and at the indicated recovery time points. Tubulin was used as a loading control**. D.** Quantification of Ssa4p expression. Band intensities were normalized to their corresponding tubulin band and are expressed relative to the normalized expression of WT yeast under heat shock. Bars indicate the mean and SD of three independent experiments, each represented by a dot. *p < 0.05, **p < 0.001 (by unpaired *t*-test). **E.** Expression of 3×HA-Ssa4p in sigma strains expressing Asc1p mutants under basal conditions (25°C), after 30 min of heat shock at 42°C, and at the indicated recovery time points. Tubulin was used as a loading control**. F.** Quantification of Ssa4p expression. Band intensities were normalized to their corresponding tubulin band and are expressed relative to the normalized expression of WT yeast under heat shock. Bars indicate the mean and SD of three independent experiments, each represented by a dot (by unpaired *t*-test); ns, not significant. **G.** Spot assays of sigma WT, *M1X*, *DE*, and *DY* strains plated on YPD under control (25ºC, left) and recovery (42ºC for 16 h then incubated at 25ºC, right) conditions. OD, optical density at 600 nm.

2.5.6 Heat shock enhances Asc1p binding to Rps28Bp and Rps19Ap, suppressing SSA4 mRNA translation

To identify the molecular partners sustaining the translational regulation and decay roles of Asc1p in *SSA4* mRNA fate in the cytoplasm, we FLAG-tagged endogenous Asc1p, immunoprecipitated it from yeast growing at 25°C or after 60 min of heat shock at 42°C, and performed liquid chromatography coupled to mass spectrometry (**Figures 2.6A, Supplementary Figure 2.5A, and Supplementary Table 2.S4**). Heat shock did not induce any posttranslational modifications of Asc1p, but significantly changed its interactome as detected in three independent replicas. Two main cluster of proteins were preferentially bound by Asc1p upon stress, stress-related proteins such as chaperones (proteins labeled in green circles), suggesting that Asc1p might partially unfold

during heat shock, and 40S ribosomal proteins (labeled in red circles), suggesting that heat changes the interaction between ribosomal proteins or their composition (**Figure 2.6A**). The four ribosomal proteins with a significantly tighter interaction with Asc1p during heat shock were Rps2, Rps7B, Rps19B (and paralog Rps19A), and Rps28A. Next, we investigated the contribution of these ribosomal proteins to Asc1p activity on SSA4 expression. We previously demonstrated that *RPS7B* deletion did not affect Ssa4p synthesis (**Figures 2.1E and 2.1F**). Since Rps2p is essential, we validated the interaction of Asc1p with Rps28Ap and Rps19Bp by immunoprecipitation followed by western blotting (**Supplementary Figure 2.S5)**. *RPS28A* or *RPS19B* genes were deleted to evaluate their role in *SSA4* mRNA stability and translation (**Figures 2.6B-E**). The ribosomal protein Rps28Ap was of particular interest because it functions outside the ribosome to degrade *YRA1* pre-mRNA and *RPS28B* mRNA by interacting with enhancer of mRNA decapping protein 3 (Edc3p) (95). Therefore, we also deleted *EDC3* to analyze their roles in *SSA4* mRNA decay and translation. *SSA4* and *SSA2* mRNAs had similar half-lives in the *rps19BΔ* and WT strains (**Figures 2.6B and 2.6C**). *SSA2* mRNA was also unaffected in the *rps28AΔ* and *edc3Δ* cells, while the half-life of *SSA4* mRNA was prolonged by 1.5 times (**Figures 2.6B and 2.6C**). This increase in *SSA4* mRNA stability was attenuated compared to *ASC1* deletion, which increased it by 2.5 times (**Figure 2.2B**). We concluded that Rps28Ap, Edc3p, and Rps19Bp do not function with Asc1p outside the ribosome to destabilize *SSA4* mRNA during recovery.

To define the mechanism by which *SSA4* mRNA is degraded during recovery, we investigated the role of well-known decapping and deadenylation factors. We found that *SSA4* mRNA degradation during recovery depends on the DEAD-box helicase and mRNA decapping enzyme Dhh1p and the exoribonuclease Xrn1p and is independent of deadenylase CCR4-Not complex component Not4p and the exosome component Ski7p (**Figures 2.6B and 2.6C**). These

results suggest a role for Asc1p in activating factors that decap the *SSA4* mRNA and favor its 5′ to 3′ degradation by the exonuclease Xrn1p independently of the Ccr4-Not complex, which has been implicated in the degradation of mRNAs with pro-stalling codons (55). *Not4Δ* yeast had similar Ssa4p induction that WT cells, further supporting that ubiquitination of Rps7p is not important for the regulation of *SSA4* mRNA translation by ribosomal collisions and RQC (**Figures 2.1F, 2.1G, Supplementary Figure 2.S5B and 2.S5C**). It is important to note that the prolonged half-life of *SSA4* mRNA in the *xrn1D* and *dhh1Δ* strains did not further increase Ssa4p during recovery, indicating that *SSA4* mRNA translation is suppressed during recovery (**Supplementary Figure 2.S5B and 2.S5C**).

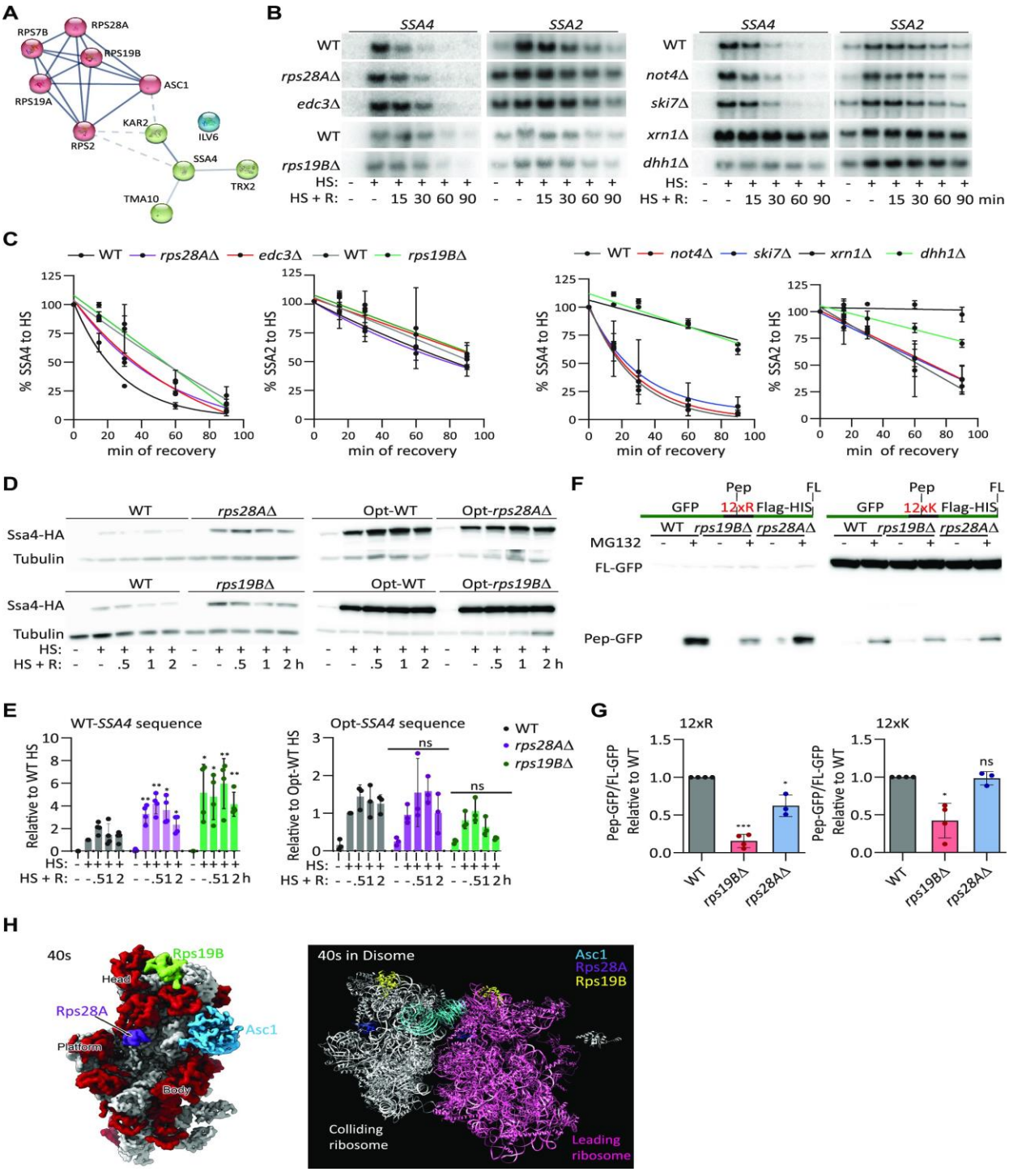
A
RPS7B
RPS28A
RPS19B
ASC1
RPS19A
KAR2
ILV6
RPS2
SSA4
TRX2
TMA10
B
SSA4
SSA2
WT
rps28AΔ
edc3Δ
rps19BΔ
not4Δ
ski7Δ
xrn1Δ
dhh1Δ
HS:
HS + R:
15 30 60 90 min
C
% SSA4 to HS
% SSA2 to HS
min of recovery
D
Ssa4-HA
Tubulin
Opt-WT
Opt-rps28AΔ
Opt-rps19BΔ
F
Pep
FL
GFP
12xR Flag-HIS
12xK Flag-HIS
MG132
FL-GFP
Pep-GFP
E
WT-SSA4 sequence
Opt-SSA4 sequence
Relative to WT HS
Relative to Opt-WT HS
ns
G
12xR
12xK
Pep-GFP/FL-GFP Relative to WT
H
40s
Rps19B
Head
Rps28A
Asc1
Platform
Body
40s in Disome
Asc1
Rps28A
Rps19B
Colliding ribosome
Leading ribosome

Figure 2.6. The ribosomal proteins Rps28Ap and Rps19Bp interact with Asc1p during heat shock to repress Ssa4p synthesis

(**A**) Asc1p interaction network showing proteins significantly enriched (p<0.05) more than 1.5 folds after 30 min of heat shock compared to basal conditions in three replicas ((plotted with STRING), (blue lines = known interactions), (dotted lines = edges between clusters)). (**B**) Northern blots to detect the expression of *SSA4* and *SSA2* mRNAs in WT, *rps28AΔ,* and *edc3Δ* and WT vs rp*s19BΔ* (left) and WT, *not4Δ, ski7Δ, xrn1Δ,* and *dhh1Δ* (right) under basal conditions (25°C), after 30 min of heat shock at 42°C, and at the indicated recovery time points. (**C**) Quantification of the half-lives of *SSA4* and *SSA2* mRNAs during recovery. Band intensities were normalized to the methylene blue staining and are expressed relative to the heat shock band for each strain (considered to be 100% induction) to obtain decay curves and calculate half-lives (t1/2 of *SSA4* mRNA: in WT 32', *rps28AΔ 34', edc3Δ 35',* WT 25′and *rps19BΔ 27';* t1/2 of *SSA2* mRNA: in WT *70', rps28AΔ 78, edc3Δ 92',* and WT 45', *rps19BΔ 48'*). **D**. Expression of 3×HA-Ssa4p expression in WT, *rps28AΔ* and *rps19BΔ* yeast and Opt-WT, Opt-*rps19BΔ,* and Opt-*rps28AΔ* strains under basal conditions (25°C), after 30 min of heat shock at 42°C, and at the indicated recovery time points. Tubulin was used as a loading control**. E.** Quantification of Ssa4p expression. Band intensities were normalized to their corresponding tubulin band and are expressed relative to the normalized expression of WT yeast under heat shock. Bars indicate the mean and SD of three independent experiments, each represented by a dot. *p < 0.05, **p < 0.001, ns, not significant (by unpaired *t*-test). **F**. Ectopic expression of GFP-R12-HIS or GFP-K12-HIS in WT, *rps19BΔ* and *rps28AΔ* strains treated with or without 0.25 M of MG132 treatment for 6 hours. **G**. Quantification of ratio of Pep-GFP (fragment) to Full length (FL)-GFP relative to WT expression in WT, *rps19BΔ* and *rps28AΔ* strains under MG132 exposure. Bars indicate the mean and SD of three independent experiments, each represented by a dot. *p < 0.05, **p < 0.001 (by unpaired *t*-test). **H**. Structure of the *S. cerevisiae* 40S subunit as a monomer (left, surface representation, ribosomal proteins in red and ribosomal RNA in gray) and as a disome (right, ribbon representation) with Asc1p, Rps28Ap, and Rps19Bp indicated.

Given the increased interaction of Rps28Ap and Rps19Bp with Asc1p during heat shock, we next investigated their roles in regulating *SSA4* mRNA translation. Remarkably, *rps28aΔ* and *rps19bΔ* cells induced significantly more Ssa4p than WT cells during heat shock, supporting a role for Rps28Ap and Rps19Bp in the regulation of *SSA4* mRNA translation, probably through the RQC mechanism (**Figure 2.6D and 2.6E**). This induction is comparable to that exhibited by *asc1Δ* cells (**Figure 2.1B, 2.1D, 2.4D, and 2.4E**). To determine if this novel role for Rps28Ap and Rps19Bp as translational regulators of *SSA4* expressiondepends on its binding to the ribosome and the presence of low-frequency codons, we deleted *RPS28A* or *Rps19B* in the *SSA4*-Opt strain. In this case, the absence of either Rps28Ap or Rps19Bp did not affect Ssa4p expression during heat

shock, pointing to Rps28Ap and Rps19Bp as new ribosomal components of the RQC mechanism, at least under heat shock conditions (**Figure 2.6D and 2.6E**). To rule out the possibility that these factors play an indirect role in RQC by recruiting Asc1p to the polysomes during heat shock, we analyze the distribution of Asc1p in monosome and polysomes obtained from heat shocked WT, *rps28AΔ*, and *rps19BΔ* cells (**Supplementary Figure 2.S5D**). Heat shocked yeast had a wide 80S peak and flat polysomes because heat shock represses global translation (96). We pooled together the polysome fractions to enrich their proteins and detected Asc1-3xFlag in the monosome and polysome by western-blotting. In all strains, Asc1p is almost exclusively localized with polysomes (**Supplementary Figure 2.S5D**). Therefore, Rps28Ap and Rps19Bp directly affect RQC and *SSA4* mRNA translation regulation by ribosome collisions during heat shock.

Since we proposed a novel role of Rps28Ap and Rps19Bp in quality controls induced by ribosome collisions, we clarified their broader RQC activity using two standard stalling reporters: GFP-R12-FlagHIS3 and GFP-K12-FlagHIS3 (97). We detected truncated GFP peptides (Pep-GFP) in MG132-treated WT yeast that were more prominent in the R12 than the K12 construct (**Figures 2.6E and 2.6F**). Compared to the WT, the fraction of truncated GFP peptides was significantly lower in the *rps19BΔ* strain. We observed the deletion of *RPS19B* to have a higher effect on R12 than K12 stretches. Deletion of RPS28A only reduced the formation of truncated peptides in the R12 construct, but the effect of Rps28A was much lower than the effect of Rps19Ap. These results indicate that Rps19Bp is a bona fide RQC factor. However, Rps28Ap might only affect certain stalling mRNAs under certain conditions. We identified the positions of Asc1p, Rps28Ap, and Rps19Bp in both the 40S subunit ((4V7R) PDB data bank) and the published structure of the yeast disome (41); however, direct interactions between these three ribosomal proteins were not detected (**Figure 2.6H**). Since these structures were obtained from yeast growing

under permissive temperatures, we speculate that the increased interactions between these ribosomal proteins upon heat shock could be due to either temperature-mediated changes in the 40S ribosome structure and/or the positions or amounts of additional factors linking them.

2.6 Discussion

Cells rapidly adapt to survive harsh environmental conditions through the potent upregulation of HSPs. Regulatory elements controlling this quick and transient activation have been identified in the *HSP70* promoter, which contains heat shock elements that direct transcription, and the 5′ and 3′ UTRs of *HSP70* mRNA, which regulate translation and mRNA stability, respectively (3). Our work demonstrates that the CDS of *SSA4*, the most induced HSP70 gene in yeast, also regulates its expression. Surprisingly, its enrichment in low-frequency codons dampens Ssa4p synthesis during heat shock by activating the RQC mechanism, which feeds back to repress its own translation. Hence, our data argue that not all stress-induced gene expression pathways act to increase HSP70 expression during stress. Recently, a mechanism to attenuate HSP70 synthesis was found in mammalian cells undergoing heat shock. In this case, the regulation was independent of the *HSP70* mRNA sequence and relied on the heat-induced non-coding RNA Heat, which reduces HSP70 transcriptional induction (98). In addition to the role of the *SSA4* CDS during heat shock, we discovered that it also prevents the spurious accumulation of Ssa4p under optimal growth conditions. This observation suggests that the *SSA4* CDS lessens the synthesis of Ssa4p at permissive temperatures and provides an extra checkpoint to tailor HSP70 levels to the burden of misfolded proteins both with and without stress.

As the four Ssa proteins have more than 80% amino acid identity, the use of nonoptimal codons provides the means to specifically regulate translation through ribosome decoding kinetics.

In our study, we fully reverted the *SSA4* CDS to the optimal codons used by *SSA1* and *SSA2* (88), revealing that for SSA4, codon low-optimality causes ribosome stalling instead of stretches of polybasic amino acids (which are shared by all *SSA* genes) (33, 42, 99, 100). RQC and NGD components have primarily been studied under permissive conditions either by inserting a stretch of polybasic or rare amino acids in an endogenous or reporter gene or by deleting a stop codon so the polyA tail is translated into a stretch of basic arginine residues (60, 97, 101, 102). Hence, we have revealed *SSA4* as one of the few known endogenous mRNAs whose translation is controlled by ribosome stalling and the RQC mechanism (103).

Interestingly, RQC regulation of Ssa4p synthesis is restricted to heat shock, as indicated by experiments done in yeast deleted of *ASC1* or *HEL2*. First, *asc1Δ* and *hel2Δ* cells did not augment the translation of *SSA4*-WT mRNA during recovery (**Figures 2.1B and 2.1D**). Secondly, expressing *SSA4*-Opt in the *ASC1* and *HEL2* deletion strains did not further augment the spurious accumulation of Ssa4p under non-stress conditions (**Figures 2.3C and 2.3D**). These results imply a mechanism boosting *SSA4* mRNA translation under heat shock, which probably depends on eIF2α phosphorylation, as *asc1Δ* and *hel2Δ* cells only exhibited basal eIF2α phosphorylation at early recovery time points. Identifying these factors will also help define the pathway used by the ribosomes stalled in *SSA4* mRNAs to repress translation. In mammalian cells, the RQC mechanism signals to inhibit translation initiation via ZNF598's recruitment of GIGYF2 and 4EHP. 4EHP outcompetes eIF4E binding to the cap of the mRNA holding the stalled ribosomes (63). Yeast does not have a 4EHP orthologue, but *SSA4* mRNA translation is unaffected by the deletion of *SYH1*, which has a GYF domain, suggesting an alternative mechanism in yeast (**Supplementary Figure 2.2C and 2.2D**).

Besides Asc1p and Hel2p, we found the canonical downstream RQC factors, Slh1p and Mbf1p, to regulate Ssa4p expression indicating that ribosomes stalled in *SSA4* mRNA are disassembled by Slh1p and prevented from frameshifting by Mbf1 (76–79). However, not all RQC steps described for stalling mRNAs applied to *SSA4*. In the case of *SLH1* deletion, the *SSA4* mRNA translation is down- instead of up-regulated, as previously described for stalling mRNA reporters (51, 80, 81). In *slh1Δ* cells, reporters have an increased readthrough over the stalling sequence despite higher stalling peaks in the mRNA (51). We propose that most of the leading 80S ribosomes stalled in *SSA4* mRNA do not disassemble. However, if they do, collided ribosomes will not be able to continue translation due to their stabilization in collisions by Asc1p and Hel2p, forming a roadblock (61). Since we observe a smaller Ssa4-HAp, we propose that a few 80S disassemble, allowing the 40S to scan the downstream CDS and reinitiate translation at an appropriate AUG. Future experiment will determine the factors mediating ribosome splitting in the absence of Slh1p and whether they are specific of heat shock or certain stalling sequences.

Likewise, future experiments will identify the ubiquitinated ribosomal proteins acting in the *SSA4* ribosome quality controls as neither Rps20p nor Rps7 does so. It might be possible that a stress dependent-E3 ligase cooperates with Hel2 to solve ribosome collisions induced under non-permissive conditions (84, 104). The analysis of Asc1 interactome upon heat stress helped us to define the ribosomal proteins Rps28Ap and Rps19Bp as new RQC components. Beyond *SSA4* mRNA, the Rps19B regulates well-known stalling RNA at permissive conditions. However, Rps28A had a lower than Rps19B or no effect in the formation of truncated peptides produced from stalled ribosomes. Thus, their tighter interaction with Asc1 upon heat stress might point to changes in the conformation of components of disomes that are either mRNA or temperature specific.

In yeast, the RQC mechanism and NGD are intimately connected (42, 56). Further, recent work has shown that stalled ribosomes signal to the CCR4-NOT complex via Not5p to deadenylate the mRNA and trigger its decay (55). However, NGD did not trigger *SSA4* mRNA decay, as shown by its high stability during heat shock and the discrete increase in the half-life of the optimized over the WT *SSA4* mRNA during recovery. None of the factors involved in NGD pathways, Syh1p and Cue2p, destabilized *SSA4* mRNA, further suggesting a decay mechanism independent of the stalled ribosomes (42, 52, 55–59). Therefore, it was unexpected to discover Asc1p's involvement in destabilizing *SSA4* mRNA during recovery, independently of the *SSA4* CDS or ribosome binding affinity. Asc1p is a multifunctional protein with diverse roles in and out of the ribosome (90). It is possible that the mechanism used by Asc1p to destabilize *SSA4* mRNA is independent of direct interactions with regulatory factors. Instead, Asc1p's capacity to regulate the assembly of processing bodies might facilitate the release of decay enzymes that degrade *SSA4* mRNA (105). Since condensate formation is critical for cells to survive stress (74, 106), it is tempting to speculate that this role of Asc1p explains the inability of *asc1Δ* cells to recover from heat stress while strains expressing Asc1p mutants DE and DY survive to heat stress.

Previously Asc1 was identified as a factor communicating the stress signal from RQC to HSF1 and regulating the heat shock response independently of its control by HSP70/HSP40 (107, 108). Our work establishes a new role for the RQC mechanism in regulating the expression of the inducible HSP Ssa4p. Interestingly, the RQC factor Asc1p also mediated *SSA4* mRNA decay during recovery and regulated heat shock survival independently of Ssa4p expression. Overall, Asc1p emerges as a critical prosurvival factor that operates in independent pathways, on and off the ribosome, to regulate the fate of *SSA4* mRNA in the cytoplasm, the strength, and duration of the heat shock response, and whether the cell survives heat stress. If these roles are conserved in

mammalian cells, its ortholog RACK1 could be targeted therapeutically to recover proteostasis under pathological conditions like cancer and neurodegeneration.

2.7 Data availability

Proteomics data is accessible through ProteomeXchange via the PRIDE Archive (Project accession: PXD037545), and the program to calculate codon optimality is available at https://github.com/LR-MVU/YEAST-SSA.git

2.8 Supplementary data

Supplementary Data are available at NAR online.

2.9 Conflict of interest

The authors declare no conflict of interest.

2.10 Acknowledgments

We would like to thank Drs. Wendy Gilbert (Yale School of Medicine), Roy Parker (University of Boulder, Colorado), Daniel Klionsky (University of Michigan), Arlen Johnson (The University of Texas at Austin), Rachel Green (John Hopkins University), and Toshifumi Inada (The University of Tokyo) for providing yeast strains and plasmids, Delina Efrem, Kevin Munoz Portocarrero, Jessamine Mattson, Ryan Huang, Suleima Jacob-Tomas, Sonya Madan, and Maanasa Koripalli from Vera's lab for technical help, and Dr. Joaquin Ortega (McGill University) for help localizing proteins in the structures of the 40S monosome and disomes (Figure 6H). We

also thank Dr. Rafael Cuesta Sanchez for technical help and critical reading and High-Fidelity Science Communications for manuscript editing.

2.11 Funding

This work is supported by the Natural Sciences and Engineering Research Council of Canada [grant number RGPIN-2019-04767] and Fonds de recherche du Québec (FRQS) [grant number NC-2999446]. Lokha R. Alagar Boopathy is funded by the FRQS scholarship program (315076) and the Centre de Recherche en Biologie Structurale at McGill University, and Dr. Celia Alecki is funded by an FRQS postdoctoral fellowship (300232).

2.12 REFERENCES

1. Morimoto,R.I. (1993) Cells in stress: transcriptional activation of heat shock genes. *Science*, **259**, 1409–1410.
2. Silver,J.T. and Noble,E.G. (2012) Regulation of survival gene hsp70. *Cell Stress Chaperones*, **17**, 1–9.
3. Boopathy,L.R.A., Jacob-Tomas,S., Alecki,C. and Vera,M. (2022) Mechanisms tailoring the expression of heat shock proteins to proteostasis challenges. *J. Biol. Chem.*, **298**.
4. Kampinga,H.H., Hageman,J., Vos,M.J., Kubota,H., Tanguay,R.M., Bruford,E.A., Cheetham,M.E., Chen,B. and Hightower,L.E. (2009) Guidelines for the nomenclature of the human heat shock proteins. *Cell Stress Chaperones*, **14**, 105–111.
5. Rosenzweig,R., Nillegoda,N.B., Mayer,M.P. and Bukau,B. (2019) The Hsp70 chaperone network. *Nat. Rev. Mol. Cell Biol.*, **20**, 665–680.
6. Feder,J.H., Rossi,J.M., Solomon,J., Solomon,N. and Lindquist,S. (1992) The consequences of expressing hsp70 in Drosophila cells at normal temperatures. *Genes Dev.*, **6**, 1402–1413.
7. Kumar,S., Stokes,J., Singh,U.P., Gunn,K.S., Acharya,A., Manne,U. and Mishra,M. (2016) Targeting Hsp70: A possible therapy for cancer. *Cancer Lett.*, **374**, 156–166.
8. Anckar,J. and Sistonen,L. (2011) Regulation of HSF1 function in the heat stress response: implications in aging and disease. *Annu. Rev. Biochem.*, **80**, 1089–1115.
9. Baler,R., Dahl,G. and Voellmy,R. (1993) Activation of human heat shock genes is accompanied by oligomerization, modification, and rapid translocation of heat shock transcription factor HSF1. *Mol. Cell. Biol.*, **13**, 2486–2496.
10. Dayalan Naidu,S. and Dinkova-Kostova,A.T. (2017) Regulation of the mammalian heat shock factor 1. *FEBS J.*, **284**, 1606–1627.
11. Hentze,N., Le Breton,L., Wiesner,J., Kempf,G. and Mayer,M.P. (2016) Molecular mechanism of thermosensory function of human heat shock transcription factor Hsf1. *eLife*, **5**, e11576.
12. Alain,T., Morita,M., Fonseca,B.D., Yanagiya,A., Siddiqui,N., Bhat,M., Zammit,D., Marcus,V., Metrakos,P., Voyer,L.-A., *et al.* (2012) eIF4E/4E-BP Ratio Predicts the Efficacy of mTOR Targeted Therapies. *Cancer Res.*, **72**, 6468–6476.
13. Andrei,M.A., Ingelfinger,D., Heintzmann,R., Achsel,T., Rivera-Pomar,R. and Lührmann,R. (2005) A role for eIF4E and eIF4E-transporter in targeting mRNPs to mammalian processing bodies. *RNA N. Y. N*, **11**, 717–727.
14. Vries,R.G.J., Flynn,A., Patel,J.C., Wang,X., Denton,R.M. and Proud,C.G. (1997) Heat Shock Increases the Association of Binding Protein-1 with Initiation Factor 4E *. *J. Biol. Chem.*, **272**, 32779–32784.
15. Liu,B., Han,Y. and Qian,S.-B. (2013) Cotranslational response to proteotoxic stress by elongation pausing of ribosomes. *Mol. Cell*, **49**, 453–463.
16. Shalgi,R., Hurt,J.A., Krykbaeva,I., Taipale,M., Lindquist,S. and Burge,C.B. (2013) Widespread Regulation of Translation by Elongation Pausing in Heat Shock. *Mol. Cell*, **49**, 439–452.
17. Kimball,S.R., Fabian,J.R., Pavitt,G.D., Hinnebusch,A.G. and Jefferson,L.S. (1998) Regulation of Guanine Nucleotide Exchange through Phosphorylation of Eukaryotic Initiation Factor eIF2α: ROLE OF THE α- AND δ-SUBUNITS OF eIF2B *. *J. Biol. Chem.*, **273**, 12841–12845.

18. Liu,B. and Qian,S.-B. (2014) Translational reprogramming in stress response. *Wiley Interdiscip. Rev. RNA*, **5**, 301–305.
19. Yoshizawa,F., Kimball,S.R. and Jefferson,L.S. (1997) Modulation of translation initiation in rat skeletal muscle and liver in response to food intake. *Biochem. Biophys. Res. Commun.*, **240**, 825–831.
20. Guzikowski,A.R., Chen,Y.S. and Zid,B.M. (2019) Stress-induced mRNP granules: Form and function of processing bodies and stress granules. *Wiley Interdiscip. Rev. RNA*, **10**, e1524.
21. Zid,B.M. and O'Shea,E.K. (2014) Promoter sequences direct cytoplasmic localization and translation of mRNAs during starvation in yeast. *Nature*, **514**, 117–121.
22. Coots,R.A., Liu,X.-M., Mao,Y., Dong,L., Zhou,J., Wan,J., Zhang,X. and Qian,S.-B. (2017) m6A Facilitates eIF4F-Independent mRNA Translation. *Mol. Cell*, **68**, 504-514.e7.
23. Meyer,K.D., Patil,D.P., Zhou,J., Zinoviev,A., Skabkin,M.A., Elemento,O., Pestova,T.V., Qian,S.-B. and Jaffrey,S.R. (2015) 5′ UTR m6A Promotes Cap-Independent Translation. *Cell*, **163**, 999–1010.
24. Vera,M., Pani,B., Griffiths,L.A., Muchardt,C., Abbott,C.M., Singer,R.H. and Nudler,E. (2014) The translation elongation factor eEF1A1 couples transcription to translation during heat shock response. *eLife*, **3**.
25. Zhou,J., Wan,J., Gao,X., Zhang,X., Jaffrey,S.R. and Qian,S.-B. (2015) Dynamic m6A mRNA methylation directs translational control of heat shock response. *Nature*, **526**, 591–594.
26. Parker,R. (2012) RNA Degradation in Saccharomyces cerevisae. *Genetics*, **191**, 671–702.
27. Krakowiak,J., Zheng,X., Patel,N., Feder,Z.A., Anandhakumar,J., Valerius,K., Gross,D.S., Khalil,A.S. and Pincus,D. (2018) Hsf1 and Hsp70 constitute a two-component feedback loop that regulates the yeast heat shock response. *eLife*, **7**, e31668.
28. Bönisch,C., Temme,C., Moritz,B. and Wahle,E. (2007) Degradation of hsp70 and Other mRNAs in Drosophila via the 5′–3′ Pathway and Its Regulation by Heat Shock *. *J. Biol. Chem.*, **282**, 21818–21828.
29. Petersen,R.B. and Lindquist,S. (1989) Regulation of HSP70 synthesis by messenger RNA degradation. *Cell Regul.*, **1**, 135–149.
30. Didomenico,B.J., Bugaisky,G.E. and Lindquist,S. (1982) The heat shock response is self-regulated at both the transcriptional and posttranscriptional levels. *Cell*, **31**, 593–603.
31. Chan,L.Y., Mugler,C.F., Heinrich,S., Vallotton,P. and Weis,K. (2018) Non-invasive measurement of mRNA decay reveals translation initiation as the major determinant of mRNA stability. *eLife*, **7**, e32536.
32. Heck,A.M. and Wilusz,J. (2018) The Interplay between the RNA Decay and Translation Machinery in Eukaryotes. *Cold Spring Harb. Perspect. Biol.*, **10**, a032839.
33. Park,H. and Subramaniam,A.R. (2019) Inverted translational control of eukaryotic gene expression by ribosome collisions. *PLOS Biol.*, **17**, e3000396.
34. Roy,B. and Jacobson,A. (2013) The intimate relationships of mRNA decay and translation. *Trends Genet.*, **29**, 691–699.
35. Schwartz,D.C. and Parker,R. (1999) Mutations in Translation Initiation Factors Lead to Increased Rates of Deadenylation and Decapping of mRNAs inSaccharomyces cerevisiae. *Mol. Cell. Biol.*, **19**, 5247–5256.
36. Schwartz,D.C. and Parker,R. (2000) mRNA Decapping in Yeast Requires Dissociation of the Cap Binding Protein, Eukaryotic Translation Initiation Factor 4E. *Mol. Cell. Biol.*, **20**, 7933–7942.

37. Presnyak,V., Alhusaini,N., Chen,Y.-H., Martin,S., Morris,N., Kline,N., Olson,S., Weinberg,D., Baker,K.E., Graveley,B.R., *et al.* (2015) Codon Optimality Is a Major Determinant of mRNA Stability. *Cell*, **160**, 1111–1124.
38. Radhakrishnan,A., Chen,Y.-H., Martin,S., Alhusaini,N., Green,R. and Coller,J. (2016) The DEAD-Box Protein Dhh1p Couples mRNA Decay and Translation by Monitoring Codon Optimality. *Cell*, **167**, 122-132.e9.
39. Webster,M.W., Chen,Y.-H., Stowell,J.A.W., Alhusaini,N., Sweet,T., Graveley,B.R., Coller,J. and Passmore,L.A. (2018) mRNA Deadenylation Is Coupled to Translation Rates by the Differential Activities of Ccr4-Not Nucleases. *Mol. Cell*, **70**, 1089-1100.e8.
40. Ikeuchi,K., Izawa,T. and Inada,T. (2019) Recent Progress on the Molecular Mechanism of Quality Controls Induced by Ribosome Stalling. *Front. Genet.*, **9**, 743.
41. Ikeuchi,K., Tesina,P., Matsuo,Y., Sugiyama,T., Cheng,J., Saeki,Y., Tanaka,K., Becker,T., Beckmann,R. and Inada,T. (2019) Collided ribosomes form a unique structural interface to induce Hel2-driven quality control pathways. *EMBO J.*, **38**, e100276.
42. Doma,M.K. and Parker,R. (2006) Endonucleolytic cleavage of eukaryotic mRNAs with stalls in translation elongation. *Nature*, **440**, 561–564.
43. Simms,C.L., Yan,L.L. and Zaher,H.S. (2017) Ribosome Collision Is Critical for Quality Control during No-Go Decay. *Mol. Cell*, **68**, 361-373.e5.
44. Brandman,O., Stewart-Ornstein,J., Wong,D., Larson,A., Williams,C.C., Li,G.-W., Zhou,S., King,D., Shen,P.S., Weibezahn,J., *et al.* (2012) A ribosome-bound quality control complex triggers degradation of nascent peptides and signals translation stress. *Cell*, **151**, 1042–1054.
45. Juszkiewicz,S. and Hegde,R.S. (2017) Initiation of Quality Control during Poly(A) Translation Requires Site-Specific Ribosome Ubiquitination. *Mol. Cell*, **65**, 743-750.e4.
46. Matsuo,Y., Ikeuchi,K., Saeki,Y., Iwasaki,S., Schmidt,C., Udagawa,T., Sato,F., Tsuchiya,H., Becker,T., Tanaka,K., *et al.* (2017) Ubiquitination of stalled ribosome triggers ribosome-associated quality control. *Nat. Commun.*, **8**, 159.
47. Sitron,C.S. and Brandman,O. (2020) Detection and Degradation of Stalled Nascent Chains via Ribosome-Associated Quality Control. *Annu. Rev. Biochem.*, **89**, 417–442.
48. Gerbasi,V.R., Weaver,C.M., Hill,S., Friedman,D.B. and Link,A.J. (2004) Yeast Asc1p and mammalian RACK1 are functionally orthologous core 40S ribosomal proteins that repress gene expression. *Mol. Cell. Biol.*, **24**, 8276–8287.
49. Winz,M.-L., Peil,L., Turowski,T.W., Rappsilber,J. and Tollervey,D. (2019) Molecular interactions between Hel2 and RNA supporting ribosome-associated quality control. *Nat. Commun.*, **10**, 563.
50. Best,K., Ikeuchi,K., Kater,L., Best,D., Musial,J., Matsuo,Y., Berninghausen,O., Becker,T., Inada,T. and Beckmann,R. (2023) Structural basis for clearing of ribosome collisions by the RQT complex. *Nat. Commun.*, **14**, 921.
51. Sitron,C.S., Park,J.H. and Brandman,O. (2017) Asc1, Hel2, and Slh1 couple translation arrest to nascent chain degradation. *RNA*, **23**, 798–810.
52. Tomomatsu,S., Watanabe,A., Tesina,P., Hashimoto,S., Ikeuchi,K., Li,S., Matsuo,Y., Beckmann,R. and Inada,T. (2023) Two modes of Cue2-mediated mRNA cleavage with distinct substrate recognition initiate no-go decay. *Nucleic Acids Res.*, **51**, 253–270.
53. Joazeiro,C.A.P. (2019) Mechanisms and functions of ribosome-associated protein quality control. *Nat. Rev. Mol. Cell Biol.*, **20**, 368–383.

54. Doamekpor,S.K., Lee,J.-W., Hepowit,N.L., Wu,C., Charenton,C., Leonard,M., Bengtson,M.H., Rajashankar,K.R., Sachs,M.S., Lima,C.D., *et al.* (2016) Structure and function of the yeast listerin (Ltn1) conserved N-terminal domain in binding to stalled 60S ribosomal subunits. *Proc. Natl. Acad. Sci.*, **113**.
55. Buschauer,R., Matsuo,Y., Sugiyama,T., Chen,Y.-H., Alhusaini,N., Sweet,T., Ikeuchi,K., Cheng,J., Matsuki,Y., Nobuta,R., *et al.* (2020) The Ccr4-Not complex monitors the translating ribosome for codon optimality. *Science*, **368**, eaay6912.
56. D'Orazio,K.N., Wu,C.C.-C., Sinha,N., Loll-Krippleber,R., Brown,G.W. and Green,R. (2019) The endonuclease Cue2 cleaves mRNAs at stalled ribosomes during No Go Decay. *eLife*, **8**, e49117.
57. Shoemaker,C.J. and Green,R. (2012) Translation drives mRNA quality control. *Nat. Struct. Mol. Biol.*, **19**, 594–601.
58. Navickas,A., Chamois,S., Saint-Fort,R., Henri,J., Torchet,C. and Benard,L. (2020) No-Go Decay mRNA cleavage in the ribosome exit tunnel produces 5′-OH ends phosphorylated by Trl1. *Nat. Commun.*, **11**, 122.
59. Veltri,A.J., D'Orazio,K.N., Lessen,L.N., Loll-Krippleber,R., Brown,G.W. and Green,R. (2022) Distinct elongation stalls during translation are linked with distinct pathways for mRNA degradation. *eLife*, **11**, e76038.
60. Goldman,D.H., Livingston,N.M., Movsik,J., Wu,B. and Green,R. (2021) Live-cell imaging reveals kinetic determinants of quality control triggered by ribosome stalling. *Mol. Cell*, **81**, 1830-1840.e8.
61. Meydan,S. and Guydosh,N.R. (2020) Disome and Trisome Profiling Reveal Genome-wide Targets of Ribosome Quality Control. *Mol. Cell*, **79**, 588-602.e6.
62. Meydan,S. and Guydosh,N.R. (2021) A cellular handbook for collided ribosomes: surveillance pathways and collision types. *Curr. Genet.*, **67**, 19–26.
63. Hickey,K.L., Dickson,K., Cogan,J.Z., Replogle,J.M., Schoof,M., D'Orazio,K.N., Sinha,N.K., Hussmann,J.A., Jost,M., Frost,A., *et al.* (2020) GIGYF2 and 4EHP Inhibit Translation Initiation of Defective Messenger RNAs to Assist Ribosome-Associated Quality Control. *Mol. Cell*, **79**, 950-962.e6.
64. Andersson,R., Eisele-Bürger,A.M., Hanzén,S., Vielfort,K., Öling,D., Eisele,F., Johansson,G., Gustafsson,T., Kvint,K. and Nyström,T. (2021) Differential role of cytosolic Hsp70s in longevity assurance and protein quality control. *PLoS Genet.*, **17**, e1008951.
65. Hocine,S., Vera,M., Zenklusen,D. and Singer,R.H. (2015) Promoter-Autonomous Functioning in a Controlled Environment using Single Molecule FISH. *Sci. Rep.*, **5**, 9934.
66. Coudert,L., Adjibade,P. and Mazroui,R. (2014) Analysis of Translation Initiation During Stress Conditions by Polysome Profiling. *J. Vis. Exp.*, 10.3791/51164.
67. Amador-Cañizares,Y., Bernier,A., Wilson,J.A. and Sagan,S.M. (2018) miR-122 does not impact recognition of the HCV genome by innate sensors of RNA but rather protects the 5′ end from the cellular pyrophosphatases, DOM3Z and DUSP11. *Nucleic Acids Res.*, **46**, 5139–5158.
68. Bennetzen,J.L. and Hall,B.D. (1982) Codon selection in yeast. *J. Biol. Chem.*, **257**, 3026–3031.
69. Tutucci,E., Vera,M., Biswas,J., Garcia,J., Parker,R. and Singer,R.H. (2018) An improved MS2 system for accurate reporting of the mRNA life cycle. *Nat. Methods*, **15**, 81–89.
70. Mueller,F., Senecal,A., Tantale,K., Marie-Nelly,H., Ly,N., Collin,O., Basyuk,E., Bertrand,E., Darzacq,X. and Zimmer,C. (2013) FISH-quant: automatic counting of transcripts in 3D FISH images. *Nat. Methods*, **10**, 277–278.

71. Mühlhofer,M., Berchtold,E., Stratil,C.G., Csaba,G., Kunold,E., Bach,N.C., Sieber,S.A., Haslbeck,M., Zimmer,R. and Buchner,J. (2019) The Heat Shock Response in Yeast Maintains Protein Homeostasis by Chaperoning and Replenishing Proteins. *Cell Rep.*, **29**, 4593-4607.e8.
72. Kumari,R., Michel,A.M. and Baranov,P.V. (2018) PausePred and Rfeet: webtools for inferring ribosome pauses and visualizing footprint density from ribosome profiling data. *RNA*, **24**, 1297–1304.
73. Kiniry,S.J., Judge,C.E., Michel,A.M. and Baranov,P.V. (2021) Trips-Viz: an environment for the analysis of public and user-generated ribosome profiling data. *Nucleic Acids Res.*, **49**, W662–W670.
74. Iserman,C., Desroches Altamirano,C., Jegers,C., Friedrich,U., Zarin,T., Fritsch,A.W., Mittasch,M., Domingues,A., Hersemann,L., Jahnel,M., *et al.* (2020) Condensation of Ded1p Promotes a Translational Switch from Housekeeping to Stress Protein Production. *Cell*, **181**, 818-831.e19.
75. Brandman,O. and Hegde,R.S. (2016) Ribosome-associated protein quality control. *Nat. Struct. Mol. Biol.*, **23**, 7–15.
76. Juszkiewicz,S., Slodkowicz,G., Lin,Z., Freire-Pritchett,P., Peak-Chew,S.-Y. and Hegde,R.S. (2020) Ribosome collisions trigger cis-acting feedback inhibition of translation initiation. *eLife*, **9**, e60038.
77. Houston,L., Platten,E.M., Connelly,S.M., Wang,J. and Grayhack,E.J. (2022) Frameshifting at collided ribosomes is modulated by elongation factor eEF3 and by integrated stress response regulators Gcn1 and Gcn20. *RNA*, **28**, 320–339.
78. Hendrick,J.L., Wilson,P.G., Edelman,I.I., Sandbaken,M.G., Ursic,D. and Culbertson,M.R. (2001) Yeast Frameshift Suppressor Mutations in the Genes Coding for Transcription Factor Mbf1p and Ribosomal Protein S3: Evidence for Autoregulation of S3 Synthesis. *Genetics*, **157**, 1141–1158.
79. Wang,J., Zhou,J., Yang,Q. and Grayhack,E.J. (2018) Multi-protein bridging factor 1(Mbf1), Rps3 and Asc1 prevent stalled ribosomes from frameshifting. *eLife*, **7**, e39637.
80. Matsuo,Y., Ikeuchi,K., Saeki,Y., Iwasaki,S., Schmidt,C., Udagawa,T., Sato,F., Tsuchiya,H., Becker,T., Tanaka,K., *et al.* (2017) Ubiquitination of stalled ribosome triggers ribosome-associated quality control. *Nat. Commun.*, **8**, 159.
81. Juszkiewicz,S., Speldewinde,S.H., Wan,L., Svejstrup,J.Q. and Hegde,R.S. (2020) The ASC-1 Complex Disassembles Collided Ribosomes. *Mol. Cell*, **79**, 603-614.e8.
82. Zhang,H., Wang,Y. and Lu,J. (2019) Function and Evolution of Upstream ORFs in Eukaryotes. *Trends Biochem. Sci.*, **44**, 782–794.
83. Munzarová,V., Pánek,J., Gunišová,S., Dányi,I., Szamecz,B. and Valášek,L.S. (2011) Translation Reinitiation Relies on the Interaction between eIF3a/TIF32 and Progressively Folded cis-Acting mRNA Elements Preceding Short uORFs. *PLoS Genet.*, **7**, e1002137.
84. Sundaramoorthy,E., Leonard,M., Mak,R., Liao,J., Fulzele,A. and Bennett,E.J. (2017) ZNF598 and RACK1 Regulate Mammalian Ribosome-Associated Quality Control Function by Mediating Regulatory 40S Ribosomal Ubiquitylation. *Mol. Cell*, **65**, 751-760.e4.
85. Sitron,C.S. and Brandman,O. (2019) CAT tails drive degradation of stalled polypeptides on and off the ribosome. *Nat. Struct. Mol. Biol.*, **26**, 450–459.
86. Thrun,A., Garzia,A., Kigoshi-Tansho,Y., Patil,P.R., Umbaugh,C.S., Dallinger,T., Liu,J., Kreger,S., Patrizi,A., Cox,G.A., *et al.* (2021) Convergence of mammalian RQC and C-end rule proteolytic pathways via alanine tailing. *Mol. Cell*, **81**, 2112-2122.e7.

87. Wu,C.C.-C., Peterson,A., Zinshteyn,B., Regot,S. and Green,R. (2020) Ribosome Collisions Trigger General Stress Responses to Regulate Cell Fate. *Cell*, **182**, 404-416.e14.
88. Lanza,A.M., Curran,K.A., Rey,L.G. and Alper,H.S. (2014) A condition-specific codon optimization approach for improved heterologous gene expression in Saccharomyces cerevisiae. *BMC Syst. Biol.*, **8**, 33.
89. Li,Z., Lee,I., Moradi,E., Hung,N.-J., Johnson,A.W. and Marcotte,E.M. (2009) Rational Extension of the Ribosome Biogenesis Pathway Using Network-Guided Genetics. *PLOS Biol.*, **7**, e1000213.
90. Thompson,M.K., Rojas-Duran,M.F., Gangaramani,P. and Gilbert,W.V. (2016) The ribosomal protein Asc1/RACK1 is required for efficient translation of short mRNAs. *eLife*, **5**, e11154.
91. Galardi,S., Fatica,A., Bachi,A., Scaloni,A., Presutti,C. and Bozzoni,I. (2002) Purified Box C/D snoRNPs Are Able To Reproduce Site-Specific 2′-O-Methylation of Target RNA In Vitro. *Mol. Cell. Biol.*, **22**, 6663–6668.
92. Kiss-László,Z., Henry,Y., Bachellerie,J.P., Caizergues-Ferrer,M. and Kiss,T. (1996) Site-specific ribose methylation of preribosomal RNA: a novel function for small nucleolar RNAs. *Cell*, **85**, 1077–1088.
93. Qu,L.H., Henry,Y., Nicoloso,M., Michot,B., Azum,M.C., Renalier,M.H., Caizergues-Ferrer,M. and Bachellerie,J.P. (1995) U24, a novel intron-encoded small nucleolar RNA with two 12 nt long, phylogenetically conserved complementarities to 28S rRNA. *Nucleic Acids Res.*, **23**, 2669–2676.
94. Reichow,S.L., Hamma,T., Ferré-D'Amaré,A.R. and Varani,G. (2007) The structure and function of small nucleolar ribonucleoproteins. *Nucleic Acids Res.*, **35**, 1452–1464.
95. He,F., Li,C., Roy,B. and Jacobson,A. (2014) Yeast Edc3 Targets RPS28B mRNA for Decapping by Binding to a 3′ Untranslated Region Decay-Inducing Regulatory Element. *Mol. Cell. Biol.*, **34**, 1438–1451.
96. Kramer,S., Queiroz,R., Ellis,L., Webb,H., Hoheisel,J.D., Clayton,C. and Carrington,M. (2008) Heat shock causes a decrease in polysomes and the appearance of stress granules in trypanosomes independently of eIF2α phosphorylation at Thr169. *J. Cell Sci.*, **121**, 3002–3014.
97. Dimitrova,L.N., Kuroha,K., Tatematsu,T. and Inada,T. (2009) Nascent Peptide-dependent Translation Arrest Leads to Not4p-mediated Protein Degradation by the Proteasome*. *J. Biol. Chem.*, **284**, 10343–10352.
98. Ji,Q., Zong,X., Mao,Y. and Qian,S.-B. (2021) A heat shock–responsive lncRNA Heat acts as a HSF1-directed transcriptional brake via m6A modification. *Proc. Natl. Acad. Sci.*, **118**, e2102175118.
99. Chen,L., Muhlrad,D., Hauryliuk,V., Cheng,Z., Lim,M.K., Shyp,V., Parker,R. and Song,H. (2010) Structure of the Dom34-Hbs1 complex and implications for no-go decay. *Nat. Struct. Mol. Biol.*, **17**, 1233–1240.
100. Letzring,D.P., Dean,K.M. and Grayhack,E.J. (2010) Control of translation efficiency in yeast by codon–anticodon interactions. *RNA*, **16**, 2516–2528.
101. Ito-Harashima,S., Kuroha,K., Tatematsu,T. and Inada,T. (2007) Translation of the poly(A) tail plays crucial roles in nonstop mRNA surveillance via translation repression and protein destabilization by proteasome in yeast. *Genes Dev.*, **21**, 519–524.
102. Wilson,M.A., Meaux,S. and van Hoof,A. (2007) A Genomic Screen in Yeast Reveals Novel Aspects of Nonstop mRNA Metabolism. *Genetics*, **177**, 773–784.

103. Matsuo,Y., Uchihashi,T. and Inada,T. (2023) Decoding of the ubiquitin code for clearance of colliding ribosomes by the RQT complex. *Nat. Commun.*, **14**, 79.
104. Sugiyama,T., Li,S., Kato,M., Ikeuchi,K., Ichimura,A., Matsuo,Y. and Inada,T. (2019) Sequential Ubiquitination of Ribosomal Protein uS3 Triggers the Degradation of Non-functional 18S rRNA. *Cell Rep.*, **26**, 3400-3415.e7.
105. Tkach,J.M., Yimit,A., Lee,A.Y., Riffle,M., Costanzo,M., Jaschob,D., Hendry,J.A., Ou,J., Moffat,J., Boone,C., *et al.* (2012) Dissecting DNA damage response pathways by analysing protein localization and abundance changes during DNA replication stress. *Nat. Cell Biol.*, **14**, 966–976.
106. Franzmann,T.M. and Alberti,S. (2019) Protein Phase Separation as a Stress Survival Strategy. *Cold Spring Harb. Perspect. Biol.*, 10.1101/cshperspect.a034058.
107. Brandman,O., Stewart-Ornstein,J., Wong,D., Larson,A., Williams,C.C., Li,G.-W., Zhou,S., King,D., Shen,P.S., Weibezahn,J., *et al.* (2012) A Ribosome-Bound Quality Control Complex Triggers Degradation of Nascent Peptides and Signals Translation Stress. *Cell*, **151**, 1042–1054.
108. Alford,B.D., Tassoni-Tsuchida,E., Khan,D., Work,J.J., Valiant,G. and Brandman,O. (2021) ReporterSeq reveals genome-wide dynamic modulators of the heat shock response across diverse stressors. *eLife*, **10**, e57376.

2.13 SUPPLEMENTARY INFORMATION

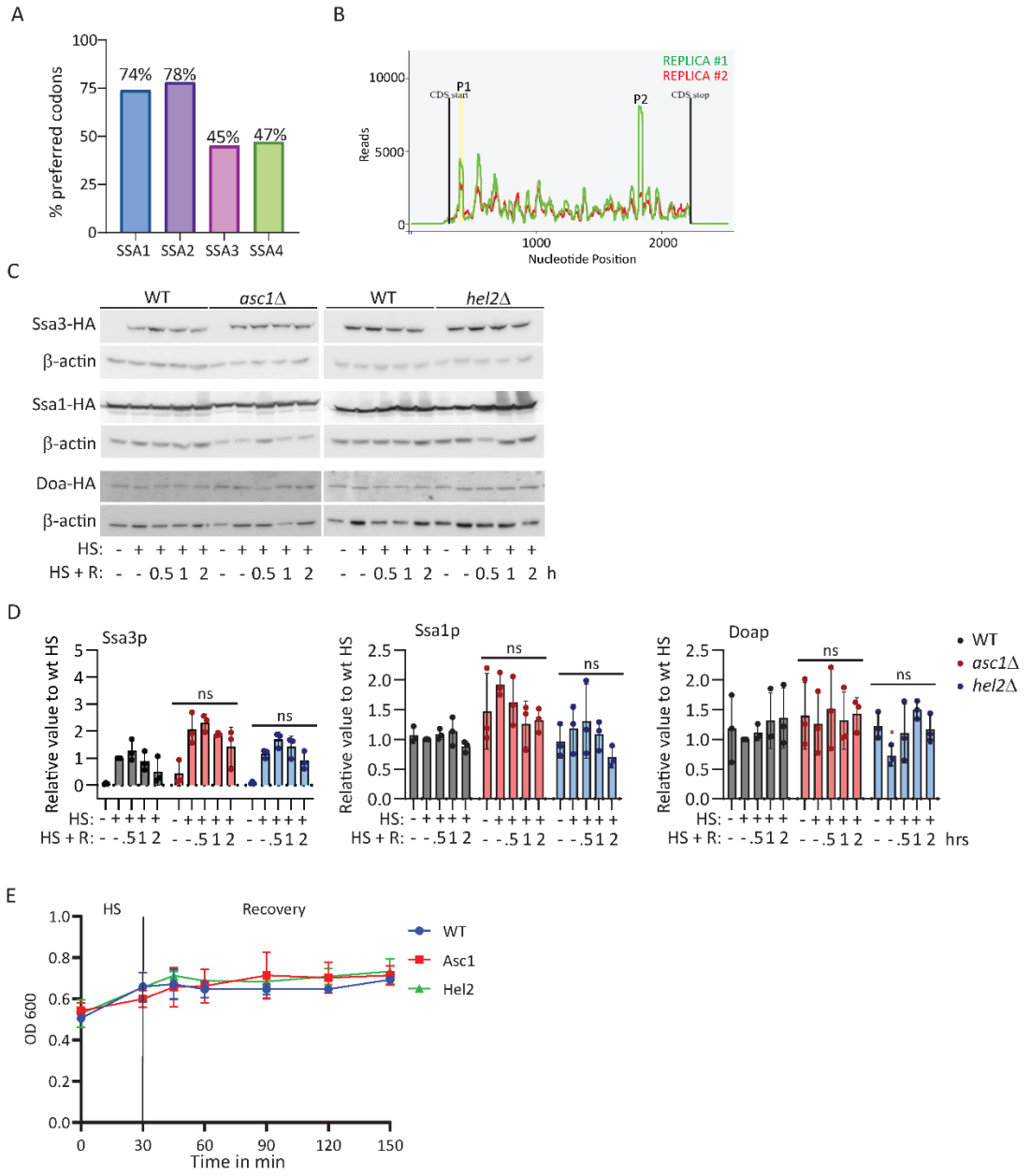

Supplementary Figure 2.1. Asc1p and Hel2p do not regulate the translation of *SSA3* and *SSA1* mRNAs

A. Percentage of preferred codons in individual *SSA* mRNAs in *S.cerevisiae*: *SSA1* 74%, *SSA2* 78%, *SSA3* 45%, *SSA4* 47%. List of preferred codons in *S.cerevisiae* is procured from Bennetzen & Hall, 1982. Number indicates times a preferred codon is substitute to a low-frequent codon in *SSA4* mRNA **B.** Ribosome profiling analysis of *SSA4* mRNA in *S. cerevisiae* upon 30 min of HS from Mühlhofer et al. 2019. Two independent replicates of ribosome density reads on the *SSA4* mRNA obtained from pausepred analysis (indicated in green and red) found 2 major ribosome

pause sites P1 and P2 within the CDS to position 400 and 1831 in replica 1 and only P1 in replica 2. **C.** Immunoblots to detect the expression of Ssa3p (top), Ssa1p (middle) and Doap (bottom) tagged with 3 tandem HA epitopes and b-actin as the loading control in *wt, asc1Δ,* and *hel2Δ* strains under basal under basal, 30 min of HS at 42ºC HS, and indicated recovery time points. **D.** Quantification of the expression of Ssa3p, Ssa1p and Doap. The HA band intensity in Ssa3p, Ssa1p, and Doap (right) was first normalized to the b-actin band intensity for each condition and then related to the normalized expression of HS *wt* yeast. The bars indicate the mean and SD of 3 independent experiments, each of them represented by a dot. Unpaired t-test (ns = non-significant differences, * = $p<0.05$). **E**. The growth of *wt, asc1Δ,* and *hel2Δ* strains during the 30 min of heat shock (HS) and subsequent recovery time points plotted as OD600 vs time. The dots indicate the mean and SD of 2 independent experiments.

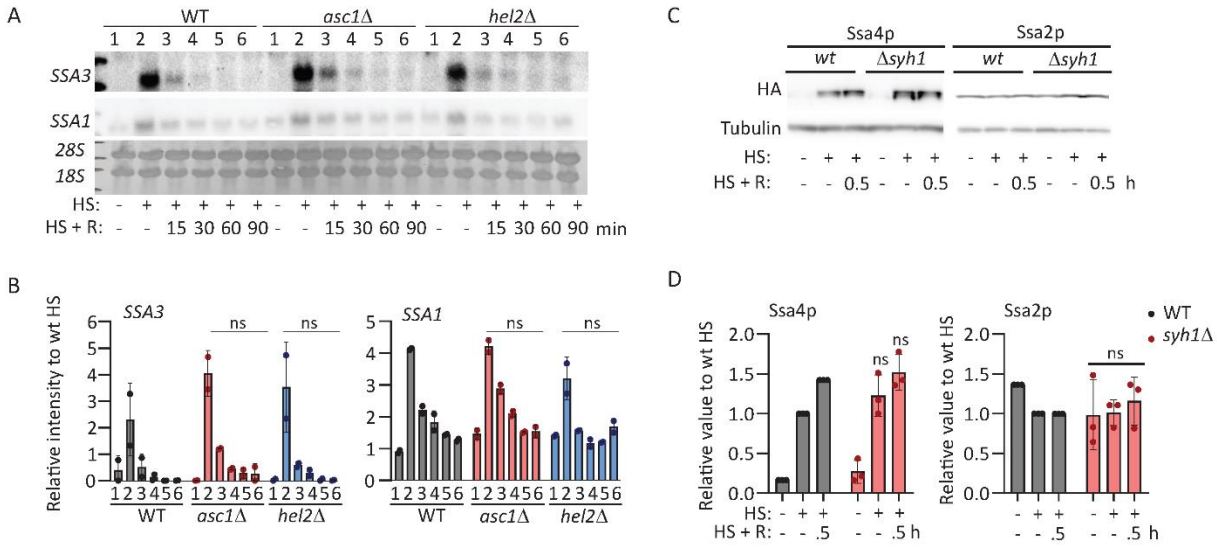

Supplementary Figure 2.2. Asc1p and Hel2p do not stabilize *SSA3* and *SSA1* mRNAs during recovery and Syh1 does not regulate *SSA4* mRNA translation

A. Northern blots to detect the expression of *SSA3* and *SSA1* mRNAs in *wt*, *asc1Δ,* and *hel2Δ* strains under basal, 30 min of HS at 42°C HS, and indicated recovery time points and corresponding methylene blue staining (bottom). **B**. Quantification of the expression of *SSA* mRNAs. The band intensity of *SSA3* and *SSA1* mRNAs was normalized to the RNA loading by the methylene blue staining. Bars indicate the average and SD of 2 independent experiments. No significant differences were found between *wt* and the *asc1Δ*, and *hel2Δ* strains. **C**. Western blots of 3×-HA-tagged Ssa4p and Ssa2p in the WT and *syh1Δ* strains under basal conditions (25°C), after 30 min of heat shock at 42°C (HS), and after 30 min recovery (R). Tubulin was used as a loading control. **D**. Quantification of Ssa4p and Ssa2p expression. HA band intensities were first normalized to their corresponding Tubulin band and are expressed relative to the normalized expression of heat-shocked WT yeast. Bars indicate the mean and standard deviation (SD) of three independent experiments, each represented by a dot (ns by unpaired *t*-test).

Supplementary Figure 2.3. Codon optimization of *SSA4* mRNA

Aligned of SSA4-wt (query) and SSA4 optimized (subject) coding sequences both containing 1926 nucleotides and sharing 77% identity (1487/1926).

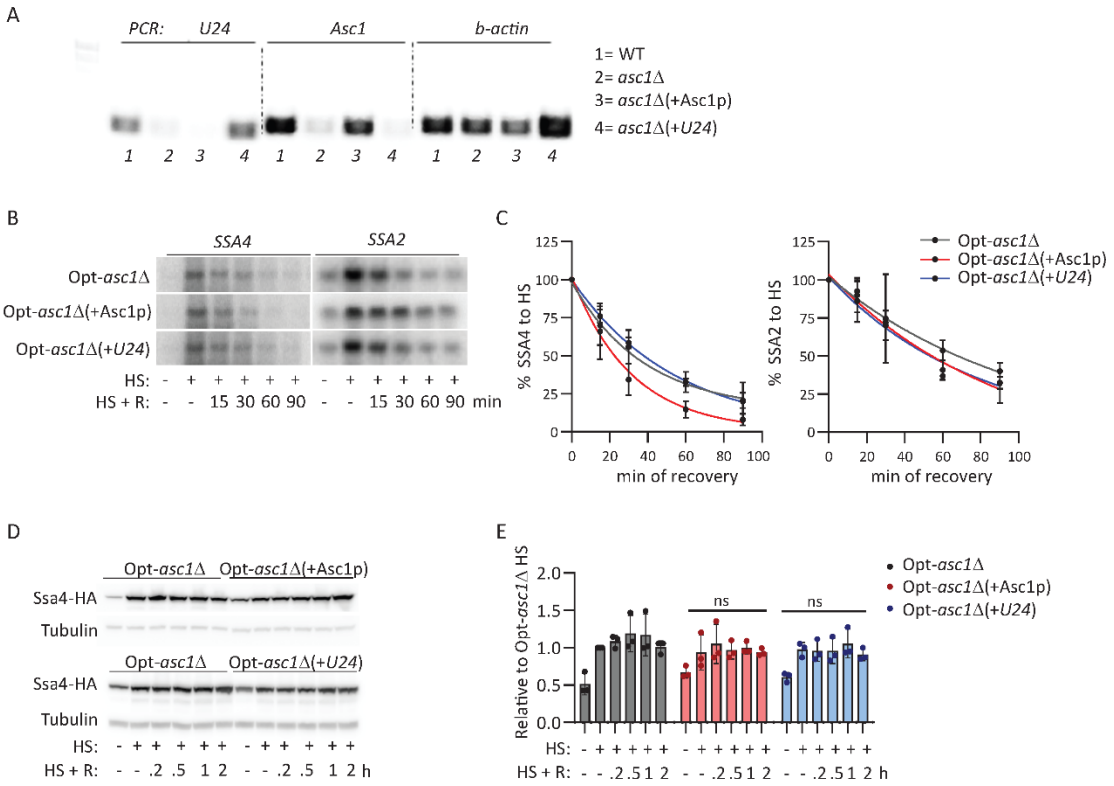

Supplementary Figure 2.4. Asc1p regulates the Opt-*SSA4* mRNA stability not *SNR24* and has no effect on Opt-*SSA4* mRNA translation

A. RT-PCR to confirm the expression of *U24* (left), b-*actin* (middle), and Asc1 (right) in *wt*, *asc1Δ*, *asc1Δ* transform with a centromeric plasmid to express the CDS of Asc1p (*asc1Δ* + Asc1p), or *U24* from the intron of the *b-ACTIN* gene *(asc1Δ* + *U24*). **B.** Northern blots to detect the expression of *SSA4* Opt (left) and *SSA2* (right) mRNAs in Opt, Opt-*asc1Δ*, Opt-*asc1Δ* with exogenous expression Asc1p (Opt-*asc1Δ* + Asc1p), Opt-*asc1Δ* with exogenous expression of U24 *(*Opt-*asc1Δ* +*U24*) under basal, 30 min of HS at 42ºC HS, and indicated recovery time points. (**C**) Quantification of the half-life of *SSA4* Opt (left) and *SSA2* (right) mRNAs during recovery. The band intensity of *SSA4* Opt and *SSA2* mRNA was normalized to the RNA loading by the methylene blue staining. Then, each recovery time was related to the intensity of the HS (considered as 100% of induction) band for each strain to obtain the decay curve and calculate the half-life. **D.** Immunoblots to detect the expression of Ssa4p tagged with three tandem HA epitopes and Tubulin as the loading control Opt, Opt-*asc1Δ* with exogenous expression Asc1p (Opt-*asc1Δ*+Asc1p), Opt-*asc1Δ*, Opt-*asc1Δ* with exogenous expression of U24 *(*Opt-*asc1Δ+U24*) yeast strains under basal, 30 min of HS at 42ºC HS, and indicated recovery time points. **E.** Quantification of the expression of Ssa4p. The HA band intensity in ssa4 tagged strains was first normalized to the tubulin band intensity for each condition and then related to the normalized expression of Opt-*asc1Δ* yeast under HS. The bars indicate the mean and standard deviation (SD) of three independent experiments, each of them represented by a dot. Unpaired t-test (ns = non-significant).

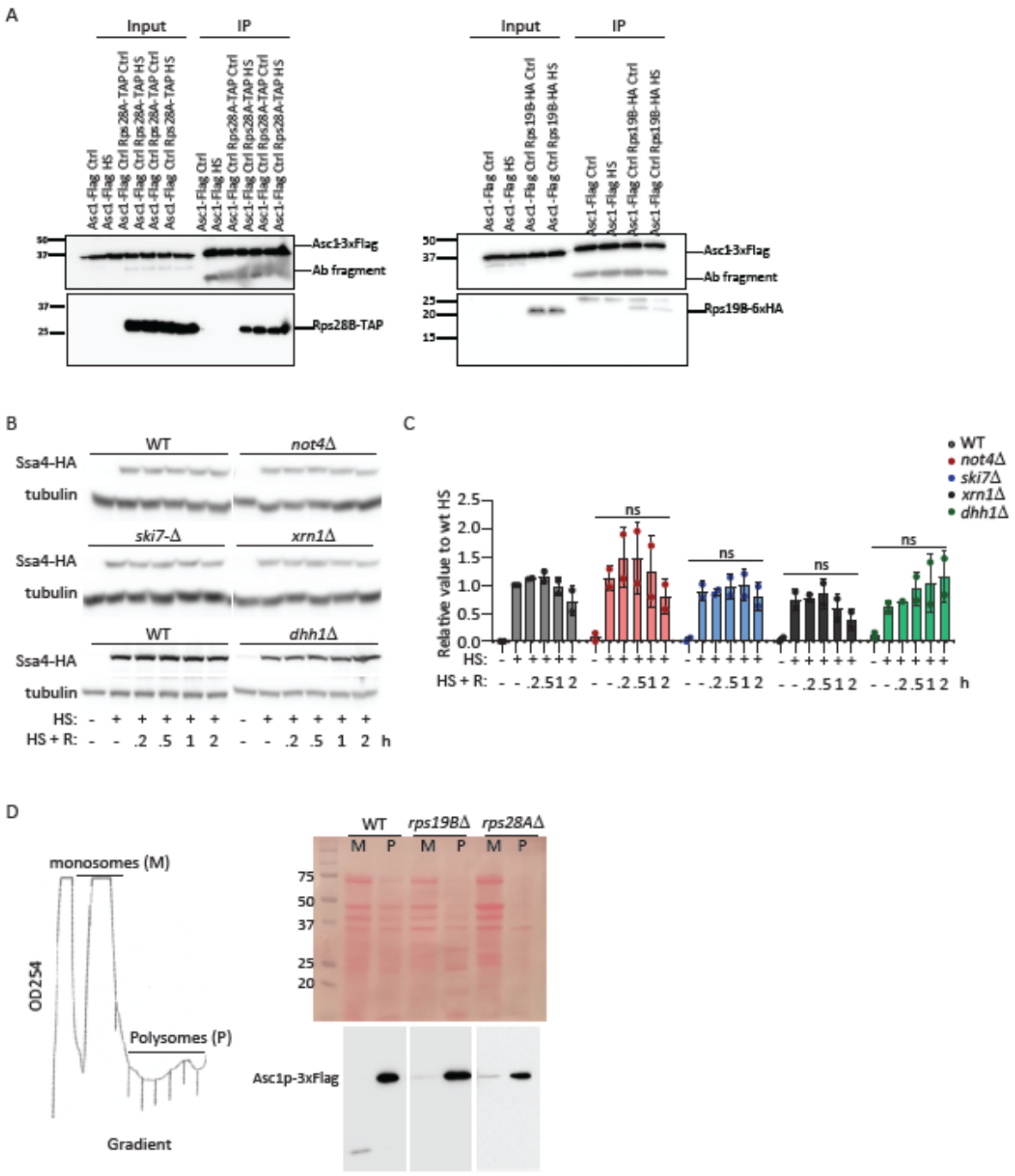

Supplementary Figure 2.5. Asc1 interaction with Rps28Ap and Rps19Bp and translation of Ssa4p

A. Immunoprecipitation to validate the interaction of Asc1p with Rps28Ap (left) and Rps19Bp (right). The control and heat shock crude extracts or Asc1-3x flag immunoreacted proteins were blotted to identify Asc1p using an antibody that recognizes Flag, Rps28Ap using an antibody that recognizes TAP, and Rps19Bp using antibody that recognizes HA. **B.** Quantification of the half-life of *SSA4* (left) and *SSA2* (right) mRNAs during recovery. The band intensity of *SSA4* and *SSA2*

mRNA was normalized to the RNA loading by the methylene blue staining and then, each recovery time was related to the intensity of the HS (considered as 100% of induction) band for each strain to obtain the decay curve and calculate the half-life. **C**. Immunoblots to detect the expression of Ssa4p tagged with three tandem HA epitopes and Tubulin as the loading control in *wt*, *not4Δ*, *ski7Δ*, *xrn1Δ*, and *dhh1Δ* strains under basal, 30 min of HS at 42ºC HS, and indicated recovery time points. **C**. Quantification of the expression of Ssa4p. The HA band intensity in Ssa4 tagged strains was first normalized to the tubulin band intensity for each condition and then related to the normalized expression of *wt* yeast under HS. The bars indicate the mean and standard deviation (SD) of three independent experiments, each of them represented by a dot. Unpaired t-test (ns = non-significant). **D**. Polysome profile of yeast strains subjected to 30 minutes of heat shock (left). Monosome (M) and polysome (P) fractions. Ponceau for total protein staining of extracted proteins run in an SDS-page as a control for loading (top right). Immunoblots to detect the expression of Asc1-3xFlag in WT, *rps19BΔ* and *rps28AΔ* strains in monosome and polysome fractions.

Transition to Chapter 3

The process of transcriptional induction, selective translation upon stress and degradation of *Hspa1a* mRNA upon recovery is highly conserved. Investigations conducted over the past decades have identified the significance of the 5'UTR in selective translation and 3'UTR in selective degradation (119,120). However, the length and composition of 5'UTR varies among organisms. For example, in *S. cerevisiae*, the 5'UTR is 28% GC rich whereas human and mouse 5'UTR are 63-65% GC rich, respectively (116–118). The GC content of 5'UTR and codon optimality of inducible *HSP70* mRNA shows an inverse relationship across species **(Table 2.2**). This suggests that the GC content and codon optimality have been influenced by evolutionary pressures corresponding to the organismal growth conditions and their gene expression requirements. The lesser GC content on the 5'UTR of *SSA4* mRNAs is unlikely to favor a stable secondary structure formation (116–118). Conversely, the mammalian *Hspa1a* mRNA contains higher GC content that promotes the formation of stable secondary structures on the mRNA for cap-independent translation initiation (PMID: 34991611, 23262490). While the GC content increases over the evolution, the codon optimality of *SSA4* mRNA drops by 30% in mouse *Hspa1a* mRNA. This implies that the translation regulatory mechanism has become intricate and reliant on RNA folding into a thermosensor in mammalian cells during evolution. Thus, the goal of my thesis was to discover the mechanisms of translation regulation in mammalian cells, especially in mouse embryonic fibroblasts as they are non-cancerous, non-transformed cells with no basal HSPA1A expression. In my next chapter, we investigated the role of RNA structural components, sequence elements and initiation factors in mediating the induction and regulation of *Hspa1a* mRNA translation during heat shock and recovery conditions.

	Escherichia coli (DNAK)	*Saccharomyces cerevisiae* (*SSA4*)	*Caenorhabditis elegans* (hsp-1)	*Drosophila melanogaster* (*Hsp70Aa*)	*Mus musculus* (*Hspa1a*)	*Homosapiens* (*HSPA1A*)
5'UTR	-	130bp 28% GC	5 bp 0% GC	255bp 35% GC	231bp 65% GC	213bp 63% GC
CDS	1917bp 51% GC	1926bp 43% GC	1923bp 51% GC	1926bp 58% GC	1926bp 65% GC	1926bp 63% GC
3'UTR	-	138bp 29% GC	145bp 36% GC	198bp 25% GC	641bp 43% GC	260bp 33% GC
Codon optimality	51% non-optimal	53% non-optimal	57% non-optimal	38% non-optimal	21% non-optimal	20% non-optimal

Table 2.1. Comparison of the inducible *HSP70* mRNA across species. Table comparing the length and GC content of 5'UTR, CDS, 3'UTR and the codon optimality of the CDS across *S.cerevisiae, D. melanogaster, M. musculus, and Homosapiens,* respectively.

CHAPTER 3: Characterization of *cis*- and *trans*-regulatory factors required for the translation HSP70 mRNA during heat shock and recovery.

Lokha R. Alagar Boopathy[1], Shruti Iyer[1], and Maria Vera[1*]

[1] Department of Biochemistry. McGill University, Montreal, Quebec, H3G 1Y6, Canada.

* Correspondence: maria.veraugalde@mcgill.ca

3.1 Abstract

Heat Shock Protein 70 (HSP70) family consists of constitutive and inducible molecular chaperones of 70 kDa essential to maintain proteins in their functional folding. Due to its significance in protein homeostasis (proteostasis), eukaryotic cells highly upregulate the expression of the inducible HSP70 when experiencing stress conditions harmful to protein folding, such as heat shock. The upregulation of the inducible HSP70 expression is selective and opposite to the general turn-off of ubiquitous transcription and translation. In mammalian cells, translation of the inducible HSP70, *Hspa1a* mRNA, occurs during heat shock and expands into the recovery period upon return to permissive temperature. The 5'UTR of *Hspa1a* mRNA plays a critical role in its translation regulation during heat shock and recovery. However, the precise regulatory elements on the 5' UTR sequence, the factors regulating *Hspa1a* mRNA translation, and whether they are active during both heat shock and recovery remain undefined. Based on the need for translation initiation factors eIF4A and eIF2α, we found that the *Hspa1a* mRNA switches from eIF4A and eIF2α independent translation upon heat shock to eIF4A and eIF2α -dependent translation during recovery. Additionally, the first 102 nucleotides of the coding sequence act with the 5' UTR to regulate *Hspa1a* translation. Using single-nucleotide editing and modifications of stem-loops defined in an *in-vitro* model, we found that both specific nucleotides and secondary structure of the 5'UTR region regulate *Hspa1a* mRNA translation, inducing it upon heat shock and repressing during homeostatic conditions, respectively. Our data suggest the presence of a temperature

induced internal ribosome entry (IRES) in the 5’ end region of *Hspa1a* mRNA that might act as a thermosensor.

3.2 Introduction

Certain environmental stressors, such as increased temperature, lead to the loss of native conformation of proteins, posing a significant threat to cell function and survival. To preserve the protein folding, cells upregulate the synthesis of molecular chaperones known as heat shock proteins (HSPs) (1). This cellular adaptation mechanism to survive stress conditions is known as the heat shock response (HSR) because the first ever characterized proteotoxic stressor was an increase in temperature (1–8). The heat-induced proteins were originally categorized in families based on the molecular weight and then adopted the HUGO Gene Nomenclature Committee (HGNC) nomenclature (9). During stress, members of the HSP70 family are the fastest and most inducible (10–14). Although the synthesis of HSPs was initially thought to be only stress-inducible, their constitutive expression and family members, as well as their function, were later identified (15–21).

The stimulation of the HSR is mainly ascribed to the induction of HSP transcription by the transcription factor heat shock factor 1, HSF1 (22). In the case of the HSP70 family, the expression of stress-inducible member *HSPA1A* mRNA is transient with very low expression levels (less than ten mRNA molecules per cell) under physiological homeostatic conditions in healthy fibroblast (23). Whereas the constitutive HSP70, Hspa8 mRNA, is expressed under permissive conditions and further transcriptionally induced upon heat shock. The critical difference between HSPA1A and HSPA8 regulation is their mRNA translation efficiencies upon heat shock and during recovery; while a significant increase in HSPA1A levels are detected, only a slight upregulation

can be quantified for HSPA8 upon heat shock and recovery (23,24). As such, a unique hallmark of HSPA1A is its preferential synthesis during stress.

Hspa1a mRNA translation overcomes the general translational attenuation of stressed cells that prevents newly synthesized peptides from misfolding and contributes to the burden of misfolded proteins. First, heat-shocked cells downregulate cap-dependent translation initiation by inhibiting the assembly of the cap-binding translation initiation complex, eIF4F, composed of eIF4E, eIF4A, and eIF4G (25–29). Second, stress prevents the formation of the ternary complex consisting of eIF2α, GTP, and Met-tRNAi, that binds to the start codon AUG. Exposure to high temperature, activates the Integrated Stress Response (ISR) through Heme Regulated Kinase (HRI) predominantly in mammals and General aminoacid Control Nonderepressible 2 (GCN2) in yeast (to a weaker extent in mammals) which phosphorylates the eIF2α at Ser51 (30–36). The resultant phosphorylation sterically hinders the GTP loading by eIF2B, thus decreasing the abundance of ternary complex for translation initiation (32,37). Furthermore, stress limits the availability of translation initiation factors such as eIF4G, eIF4A/B, eIF3, RACK1, and 40S subunit by sequestering them in stress granules (SGs) (25,38–41). Besides, in stressed cells the abundance of unfolded proteins dilutes the ribosome-associated chaperones involved in cotranslational protein folding. Consequently, ribosome stalling has been observed on ubiquitously expressed mRNAs at nucleotide 189-195 as the nascent peptide chain protruding out of the ribosome exit tunnel is not assisted by chaperones (42,43). In spite of the limited availability of translation factors, Hspa1a mRNA gets preferentially translated under conditions of heat stress (44).

The escape of Hspa1a mRNA from the shutoff of global protein synthesis was explained by the existence of specialized stress ribosomes. They carry a mitochondrial protein, MRPL18, that might facilitate the recruitment of factors involved in translation elongation (45). However, another study

contradicted these findings as the results were not reproducible in the human cell lines HeLa and U87 (46). Thus, it has been declared that MRPL18 is not essential for Hspa1a mRNA translation in all cellular systems on HS (47). Recent efforts aimed to define the Hspa1a cis- and trans-regulators of translation found that upon heat stress, the 5' UTR of Hspa1a mRNAs are co-transcriptionally imprinted by N6-methylation (m6A) at Adenosine 103 (48,49). This m6A modification supports non-canonical translation initiation by binding to the initiation complex eIF3, that recruits the ribosome to the mRNA, and to the factor ABCF1, that serves as an alternative recruiter for the ternary complex to the *Hspa1a* mRNA (50). These studies raised the possibility that dynamic posttranscriptional modifications determine the fate of the mRNA in response to stress. However, a recent work has confronted that m6A modification upstream of start codon does not increase the translation efficiency if an RNA during stress or permissive conditions (51). Additionally, the O-linked β-N-acetylglucosamination of the initiation factor eIF4G favored translation of *Hspa1a* mRNA during recovery from stress and facilitates SGs disassembly, suggesting that these events could be coordinated at the cellular level (29).

Despite the dispute on the factor the *cis*- and *trans*- regulatory factors, most of these studies were done in mammalian cells during the four-hour recovery period that follows heat stress. At this timepoint, cap-dependent translation has recovered and SGs have dissolved (25,52). Hence, they provide evidence on the mechanisms supporting *Hspa1a* mRNA translated during recovery but leaves an open question on how *Hspa1a* mRNAs get translated during heat stress and whether it requires different translation factors than during recovery. Another caveat of these studies is that the experiments were conducted using cancer cell lines such as HeLa, which exhibit high HSPA1A levels even under permissive conditions. Thus, the use of cancer cell lines defeats the purpose of studying the mechanism of induction of HSPA1A under stress conditions. Similarly, using

truncation of segments in 5'UTR of human *HSPA1A* mRNA in 293 cells and TE671 medulloblastoma cells, studies have shown IRES-like activity. Once again, the study used cell lines with high basal expression of HSPA1A (53). Therefore, it remains unknown how the newly transcribed *Hspa1a* mRNAs bypass the general repression of translation.

To explain HSPA1A synthesis during heat stress, we hypothesized the 5' end of *Hspa1a* mRNA sequence to form an RNA structure in response to an increase in temperature and for this structure to mediate cap-independent translation. Such RNA thermosensors are known to melt or undergo conformational changes upon sensing changes in temperature and modulate the translational output (54). As such, a functional thermosensor would make *Hspa1a* mRNA behave similar to an internal ribosomal entry (IRES) capable of directing translation independently of eIF4F and/or the ternary complex, as previously described for RNA viruses such as Type III HCV IRES and Type IV CrPV IRES, respectively (55). The sequence of these IRESs include the intergenic region (IGR), however, while HCV IRES recruits the ternary complex and eIF3 to initiate translation (56), the CrPV IRES does not require any initiation factors because forms the pseudoknot 1 (PK-I) that mimics the tRNA-mRNA interactions in the A-site and it is capable of recruiting a functional 80S or 40S ribosome (57,58). After eEF2 mediated the ribosome translocation, the PK-I occupies the ribosomal Peptidyl (P-site and eEF1A1 brings the first tRNA to commence protein synthesis (57,58). Thus, the induction of an CrPV like IRES in the Hspa1a mRNA by heat would also provide the means for the cell to precisely recognize this mRNA as the one to be translated during heat stress.

Our previous data support our hypothesis. First, we found that eEF1A1 links *Hspa1a* mRNA transcription to translation during heat shock (23). Secondly, in a recent collaboration with Ana Marie Pyle, we have characterized that the 5'UTR and the first 102 nts of the coding sequence

(CDS) of the *Hspa1a* mRNA forms a stable tertiary structure in vitro only when incubated at 42oC (59). The inclusion of 102 nts of CDS could resemble the IGR IRES as in HCV or CrPV (59). Using unzip and complementary mutations of stem loops and visualizing their electrophoretic mobility, three stem loops were identified as critical for the formation of a compact structure in vitro. Nonetheless, this work lacks in-vivo evidence to support the role for this heat triggered tertiary structure and the identified stem loops in *Hspa1a* mRNA cap-independent translation during heat shock.

Our work aims to identify the dependency of HSPA1A synthesis on translation initiation factors and to validate the regulatory role of the first 102 nts of the CDS and each of the identified stem loops involved in the formation of the heat-induced compact structure. To achieve our goals, we have assessed HSPA1A synthesis in mouse fibroblast treated to modify the availability of translation initiation factors and express *Hspa1a* mRNA mutants. We found that the translation of *Hspa1a* mRNA during heat shock and recovery requires different translation initiation factors. Interestingly, the synthesis of HSPA1A during heat shock is independent of eIF4A and eIF2α and it is enhanced by the first 102 nts of the CDS, suggesting the presence of a type IV IRES. However, unzipping the stem-loops relevant for a structure formation in vitro did not affect the translation competency of *Hspa1a* mRNA upon heat shock in cells. To identify potential regions in the 5' end of *Hspa1a* mRNA relevant for its translation, we undertook an unbiassed approach based on the editing capacity of Clustered Regularly Interspaced Short Palindromic Repeats-Cas9 fused to deaminase (CRISPR)-Cas9 (60). This experimental set-up points to the role of specific nucleotides in the 5'UTR and CDS in upregulating Hspa1a translation in response to heat stress.

3.3 Results

3.3.1 The translation efficiency of *Hspa1a* mRNA is higher during recovery than during heat shock

Previous literature has shown that *Hspa1a* mRNA is translated under both heat shock and recovery conditions (49,61–63). To compare the efficiency of *Hspa1a* mRNA translation under both conditions we used polysome profiling following by northern blot because it provides quantitative data on the occupancy of *HSPA1A* mRNAs by ribosomes. We used immortalized Mouse Embryonic Fibroblasts (MEFs) as they are non-transformed cells with no HSPA1A expression under permissive conditions. MEFs responded to heat stress by shifting their polysome profile from active translation (presence of light and heavy monosomes) during permissive conditions (control) to minimal translation (high monosome) during heat stress. At five hours of recovery, we identified a decreased in the monosome peaks comparing to heat shock and a corresponding slight increase in polysome peaks relative to heat stress **(Fig 3.1A)**. These results confirmed that heat shock downregulated the general translation and the cells slowly resumed general translation during recovery.

To determine the ribosome occupancy on *Hspa1a* mRNA, we extracted the RNA from polysome fractions and performed northern blotting **(Figs 3.1B-D)**. The quality and quantity of the RNA was evaluated by methylene blue staining before probing the blots for *Hspa1a* or *Actb* mRNAs **(Fig 3.1B)**. The methylene blue staining showed sharp bands for the 28S and 18S ribosomal RNAs, supporting the integrity of the RNA. The ribosomal RNA staining also indicated a shift of ribosomes from high polysome fractions to monosomes and low polysomes upon heat shock and shift back to high polysomes at five hours of recovery, further supporting changes in the translation efficiency in these conditions (**Fig 3.1B**).

As expected, under permissive conditions, there were no *Hspa1a* mRNAs, and a significant upregulation was detected upon heat shock, which lasted at 5 h of recovery **(Fig 3.1C)**. The *Hspa1a* mRNAs were predominantly occupied in monosome to light polysome during HS and a slight increase towards heavy polysomes was observed during recovery **(Figs 3.1C, 3.1E)**. As a control, we quantified the ribosome occupancy of the housekeeping *Actb* mRNA which was detected under permissive, HS, and recovery conditions **(Fig 3.1D)**. Under permissive conditions, the *Actb* mRNAs were predominantly occupied by heavy polysomes. As expected, heat stress shifted its ribosome occupancy towards monosomes, that was pushed back to heavy polysomes at 5 h of recovery **(Fig 3.1D, 3.1F)**. The results indicate that the efficiency of *Hspa1a* mRNA translation is moderate under heat shock and recovery as the mRNAs is rarely found in the high polysome fraction. In addition, recovery conditions are more favorable than heat shock for the translation of *Hspa1a* mRNA.

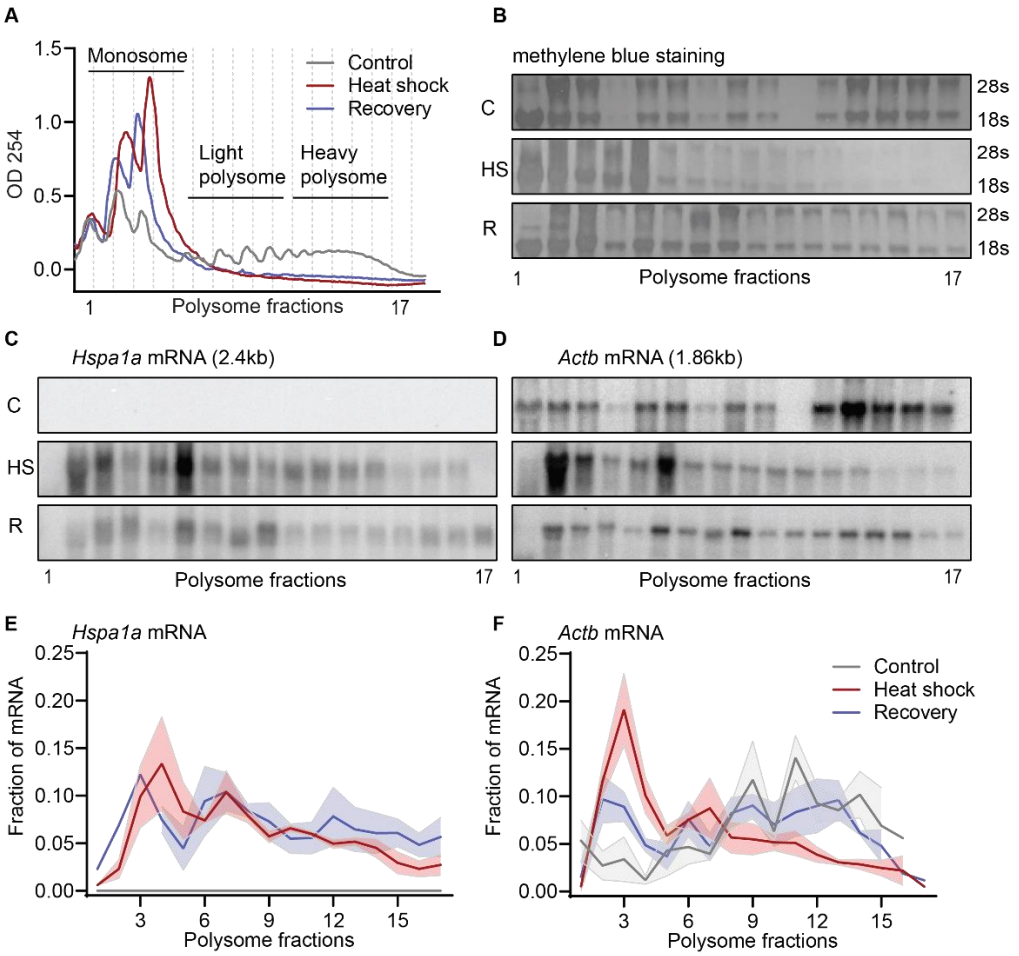

Figure 3.1: Translation efficiency of *Hspa1a* mRNA increases during recovery from stress

A. Polysome profiles of mouse embryonic fibroblasts (MEFs) under control (C, grey line), after heat shock (HS, 42^{o}C for 2 h, red line), or recovery after heat shock (R, 37^{o}C for 5 h, blue line). **B-D.** Northern blotting of polysome fractions in A subjected to methylene blue staining for total RNA (B) or hybridized with radioactive probe specific for *Hspa1a* mRNA (C) or *Actb* mRNA (D) under C, HS, and R respectively. **E-F**. Quantifications of northern blot expressed as percent of either *Hspa1a* mRNA (E) or *Actb* mRNA (F) in each fraction collected under C, HS, and R indicated in grey, red and blue, respectively. The solid lines represent mean value of three replicates and the hue represents Standard Error of Mean (SEM).

3.3.2 *Hspa1a* mRNA translation depends on different translation initiation factors during heat shock and recovery

The higher accumulation of *Hspa1a* mRNA in monosomes and light polysomes in heat shock than during recovery suggests a lower translation efficiency. However, it might be that ribosomes are stalled and not translating *Hspa1a* mRNAs during recovery. To differentiate these two options, we quantified the amount of HSPA1A synthesized under both conditions by western blot **(Figs 3.2A-3.2D, mock treated cells)**. We observed a three- to four- fold increase in the amount of HSPA1A protein during recovery than heat shock, which supports a lower efficiency of *Hspa1a* mRNA translation during heat shock than recovery since recovery cells had only doubled the number of cytoplasmic mRNAs, as quantified by single-molecule in situ hybridization (smFISH) (**Figs 3.1E and 3.1D, mock treated cells**). However, the occupancy of *Actb mRNA*s by ribosomes is likely reflecting stalled ribosomes at the elongation step (42,43), as we do not observe an increase in the ACTB expression upon heat shock and during recovery **(Fig 3.2C, mock treated cells)**.

It is well established that heat shock inhibits cap-dependent translation and has been suggested that *Hspa1a* mRNA translation occurs by a cap-independent mechanism (48,49,53,61,64,65). However, the factors involved are not yet depicted. Since some viral IRES still required translation initiation factors (56), we first investigated how inhibition of the eIF4F complex factors, eIF4E and eIF4A, alters the synthesis of HSPA1A during heat shock and recovery. eIF4E was indirectly inhibited by treatment cells with Torin1, which inhibits mTOR and promotes the dephosphorylation of 4E-BP and their binding to eIF4E (66). Cells treated with 1 μM of Torin1 for 30 min had a decrease in HSPA1A protein expression during heat stress and recovery (**Fig 3.2A and 3.2B**). With torin1 treatment, the levels of cytoplasmic *Hspa1a* mRNA were comparable to the mock translation under heat shock and recovery (67) **(Fig 3.2E)**.

Interestingly, the inhibition of eIF4A binding to mRNA by treatment with 200 nM of hippuristanol for 3 hours before initiating heat shock, enabled the same induction of HSPA1A protein as mock treatment (68). Nonetheless, hippuristanol treated cells were unable to increase the synthesis HSPA1A during recovery (**Fig 3.2A and 3.2B**). Additionally, treatment of cells with hippuristanol did not preclude the transcriptional induction of HSPA1A neither it affected the localization of *Hspa1a* mRNAs in the cytoplasm during recovery **(Fig 3.2E)**. Although, the results obtained with Torin1 are inconclusive as of the dependency of *Hspa1a* mRNA translation on eIF4E, the treatment with hippuristanol support previous work indicating that translation of *Hspa1a* mRNA during heat shock is independent of eIF4F (53,61,65). Our data further indicates that there is a change in the dependency of *Hspa1a* mRNA on eIF4A, which is not required during heat shock but becomes essential for its translation during recovery. Therefore, the translation independency of *Hspa1a* mRNA from eIF4A is similar to that of the CrPV IRES, as previously described by the Pelletier group (69).

An additional characteristic of the CrPV IRES is that it does not need the ternary complex to initiate translation (70). Since heat shock induces the phosphorylation of eIF2α at Serine 51, that inhibits the formation of the ternary complex and translation initiation (71), we next assess whether the ternary complex participates in *Hspa1a* mRNA translation during heat shock and recovery. We treated MEFs with 100 μM of salubrinal for 24 h to retain eIF2α in an inactive phosphorylated state (72,73). As such, the cells treated with salubrinal showed slightly higher *Hspa1a* mRNA levels than mock treated cells under heat but no difference during recovery **(Figs 3.2D and 3.2E)**. Since the differences in the expression of cytoplasmic *Hspa1a* mRNA did not account for the differences in protein **(Fig 3.2E)**, these results indicate that *Hspa1a* mRNA

translation only requires the ternary complex during recovery form heat shock. Therefore, *Hspa1a* mRNA mimics the dependency of a type IV IRES on translation initiation factors.

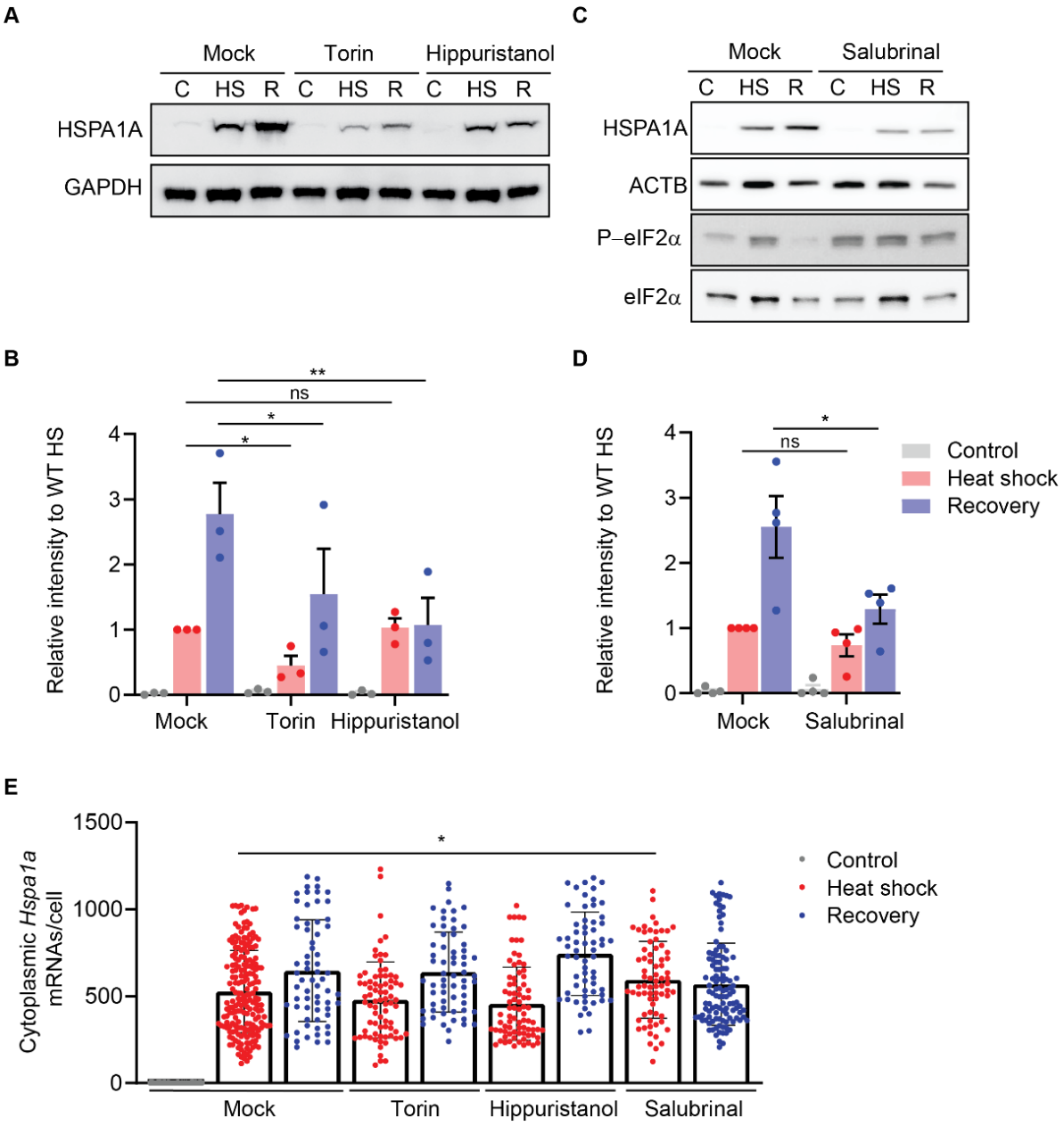

Figure 3.2. Translation of *Hspa1a* mRNA occurs in two different modes during heat shock and recovery.
A. Western blot of HSPA1A and GAPDH protein levels in untreated MEFs or treated with 1 μM torin or 200 nM hippuristanol under C, HS, and R respectively. **B**. Quantification of HSPA1A protein levels normalized to loading control (GAPDH) and related to the value obtained for WT HS cells. All plots are mean and SEM with each dot representing values from individual experiments, n=3. Unpaired t-test was used for statistical analysis. **C**. Western blot of HSPA1A and ACTB untreated MEFs or MEFs treated with 100 μM salubrinal under C, HS, and R respectively. **D**. Quantification of HSPA1A protein levels normalized to loading control (ACTB) and related to the value obtained for WT HS cells. All plots are mean and SEM with each dot representing values from individual experiments, n=4. Unpaired t-test was used for statistical analysis. SmFISH quantification of *Hspa1a* mRNA levels in MEFs treated with torin1 (n=77, 64), hippuristanol (n= 80, 62), or salubrinal (n= 72, 114) compared to mock cells (102, 196, 65) under C, HS, and R depicted as grey, red and blue dots, respectively. Each dot denotes number of cytoplasmic mRNAs in an individual cell. Dunnett's test was used for statistical analysis.

3.3.3 Translation of *Hspa1a* mRNA does not require RACK1 or eIF3D during stress and recovery

We next aimed to identify translation factors that could mediate the translation initiation of *Hspa1a* mRNA. Although cap-dependent translation initiation is the most common mode of translation initiation, certain mRNAs use cap-independent factors to initiate translation, especially in conditions that limit the formation of the eIF4F complex. Recent work have described that a negative charge on the loop of RACK1, a ribosomal protein located on the head of 40S subunit, mediates the rotation of the 40S head domain similar to IRES and promotes non-canonical translation initiation (74). Another study has shown that eIF3d can bind to conserved structures on 5' end of the *c-Jun* mRNA to mediate eIF4F- independent translation (75–77).

To investigate the requirement of RACK1 or eIF3d for *Hspa1a* mRNA translation, we knock them down by infecting MEFs with lentivirus expressing two specific small-hairpin RNAs (shRNAs). After 72 h of transfection, when the levels of RACK1 and eIF3d proteins were decreased by 63% and 70%, respectively, MEFs were subjected to heat shock or heat shock followed by recovery or left them under homeostatic conditions, and we analyzed the induction of

HSPA1A expression by western blot (**Figs 3.3A-C**). Cells depleted of RACK1 and eIF3d expressed similar HSPA1A protein levels than mock transfected cells upon heat shock and recovery **(Figs 3.3B-E)**. Likewise, the quantification of cytoplasmic *Hspa1a* mRNA levels by smFISH indicated no differences among the three experimental groups **(Fig 3.3F-G)**. Therefore, the expression of HSPA1A is independent of RACK1 or eIF3d. Based on previous reports we were expecting to identify a role for eIF3d on the regulation of *Hspa1a* mRNA translation since the eIF3 complex has been shown to favor translation of *Hspa1a* mRNA by binding to m6A modification 4-6 h post-stress (49). Since the experiments conducted by the authors did not specify a particular eIF3 subunit in the study, it might be that other mRNA binding subunits of the eIF3 complex could participate in translation regulation of *Hspa1a* mRNA. Based on our results, we can exclude the involvement of eIF3d and RACK1 in promoting the *Hspa1a* mRNA translation during HS as well as recovery from stress.

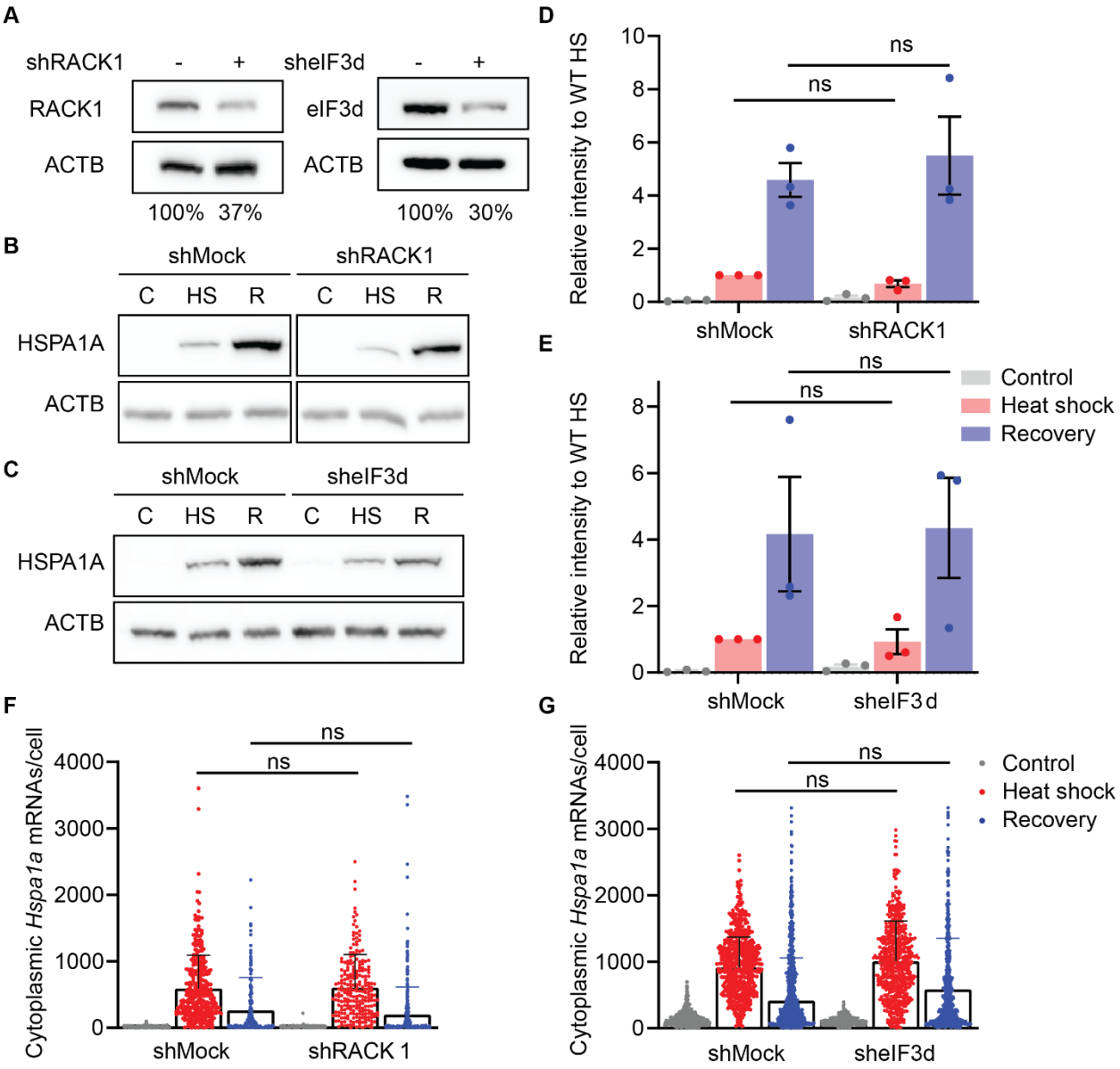

Figure 3.3: Translation of *Hspa1a* mRNA is independent of RACK1 and eIF3d

A. Western blot showing the knock down efficiency RACK1 and eIF3d shRNAs. **B-C**. Western blot of HSPA1A and ACTB in MEFs subjected to scrambled shRNAs (shMock) or shRNAs targeting RACK1 or eIF3d under C, HS, and R. **D-E**. Quantification of HSPA1A protein levels normalized to loading control (ACTB) and related to the value obtained for WT HS cells. All plots are mean and SEM with each dot representing values from individual experiments, n=3. Unpaired t-test was used for statistical analysis. **F-G**. SmFISH quantification of *Hspa1a* mRNA levels in shMock (n=185, 342, 240) vs shRACK1 (n=302, 238, 347) (F) or shMock (n=539, 531, 710) vs sheIF3d (n=521, 580, 620) (G) cells under C, HS, and R depicted as grey, red and blue dots, respectively. Each dot denotes number of cytoplasmic mRNAs in an individual cell. Dunnett's test was used for statistical analysis.

3.3.4 The 5' UTR and the first 102 nts of *Hspa1a* mRNA CDS participate in translation regulation upon stress.

Since *Hspa1a* mRNA translation is independent of non-canonical initiation factors, RACK1 and eIF3d, and also of eIF4A and eIF2α, we propose that it might may harbor an IRES akin to CrPV IRES with a PK-I, enabling internal ribosome recruitment for translation (58,78). Recent work from Ana Marie Pyle's laboratory supports this hypothesis and suggest that heat induces a conformational change in the structure of the RNA (59). They expected the presence of a PK-I to compact the RNA structure (59). Thus, they tested whether the addition of nucleotides of the coding sequence (CDS) to the 5'UTR region of *Hsap1a* mRNA compacts the structure *in vitro* upon an increased in the incubation temperature from 37°C to 42°C. Their findings indicated that the first 102 nts of the CDS plus the entire 5'UTR region are required to form a temperature-induced compact structure. They resolved the secondary structure by *in vitro* SHAPE analysis CDS (**Fig 3.4A** is an adaptation of the Pyle's lab paper, (59)).

To identify the functional relevance of these sequence and structure for translation upregulation in live MEFs undergoing heat shock, we fused the *Hspa1a* 5'UTR sequence and the 102 first coding nucleotides in frame with the luciferase sequence lacking the AUG (**Fig 3.4B**, UTR7). We compare the capacity of this construct to drive luciferase expression with constructs that lack a 5'UTR region (**Fig 3.4B,** No_UTR, (Promega pControl plasmid)) or contain the *Hspa1a* 5'UTR region (**Fig 3.4B,** UTR1) or the 5'UTR region with the first 30 nts of the coding sequence (**Fig 3.4B,** UTR2). It is important to indicate that the transcription of all these cDNAs was under the control of the endogenous *Hspa1a* gene promoter and all contain the *Hspa1a* 3' UTR sequence and polyadenylation signals **(Fig 3.4B)**.

The UTR1, UTR2, and UTR7 functionality was tested *in vivo* by co-transfecting MEFs with a Renilla-luciferase reporter, which we used to normalize the luciferase activity to the efficiency of transfection. Unlike the endogenous *Hspa1a* gene, luciferase activity was detected in control conditions probably because the expression from plasmids is leaky as it does not have the same transcriptional regulation as chromatin (79,80). This was an advantage because it enabled us to study the translation regulation of these constructs under homeostatic conditions. Under homeostatic conditions, the 5'UTR sequence enhanced translation as it augmented the firefly-luciferase activity by 20-fold when compared with the No_UTR construct. Interestingly, adding the first 102 nts of the CDS but not 30 nts, damped down luciferase activity to the No_UTR levels **(Fig 3.4C)**. Upon two hours at 42^{o}C, we detected a 10-fold increase in the luciferase levels activity from No UTR, UTR1, and UTR2 constructs that increased to 25-fold in the UTR7 containing construct **(Fig 3.4D)**. Based on the results, we propose that the 5'UTR region and 102 nts act together to tune the translation during homeostatic conditions and heat stress. They might form an RNA structure that behaves as an RNA thermosensor to regulate its own translation initiation, repressing it under homeostatic conditions and activating it upon heat stress.

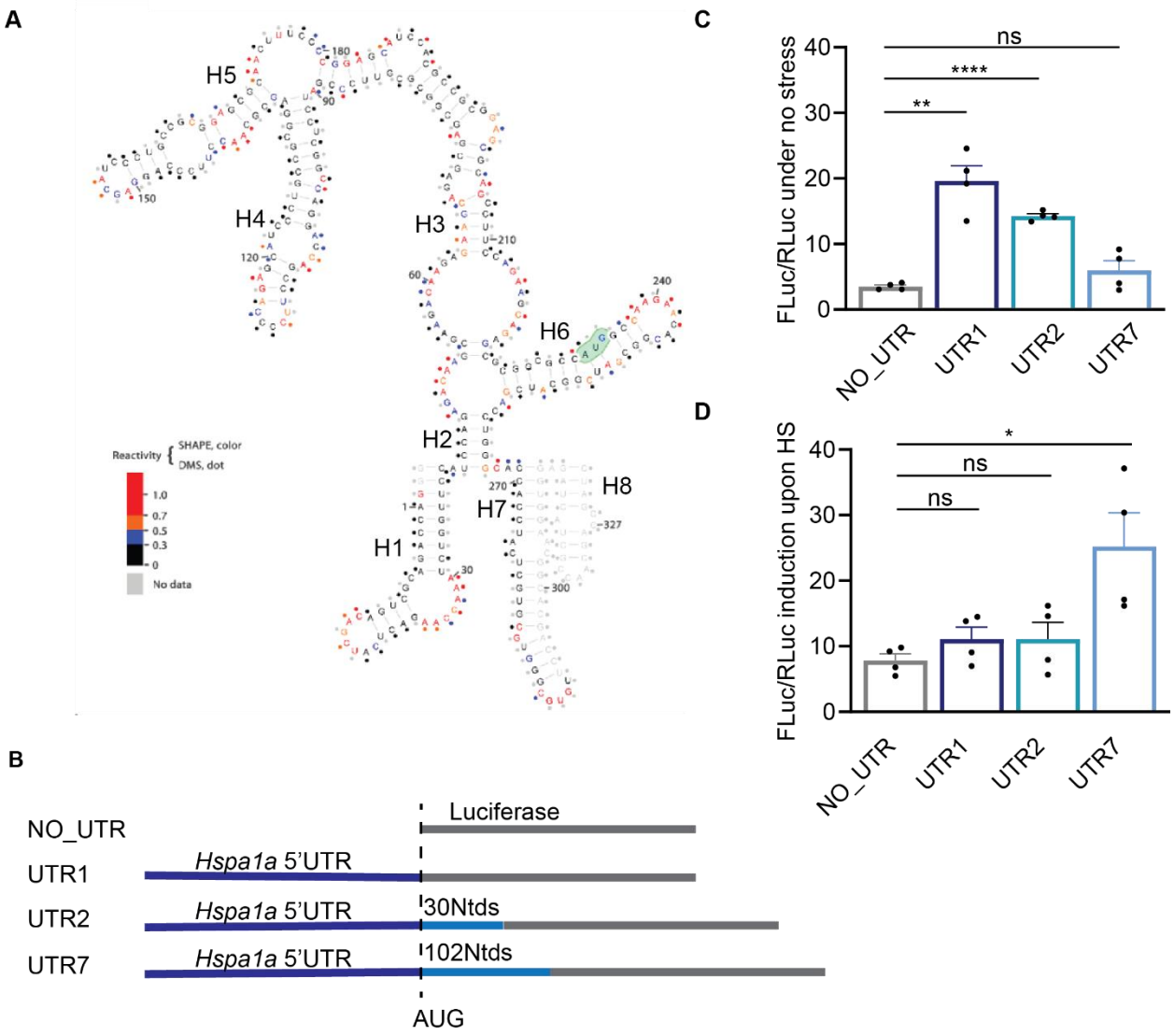

Figure 3.4. *Hspa1a* mRNA 5'UTR with 102 nts of CDS regulate its translation

A. Predicted secondary structure of 5' UTR and 102 nts of *Hspa1a* mRNA by *in vitro* SHAPE analysis with DMS (59). Reactivity of nucleotides were shown in color scale with red being highly reactive and black being less reactive and DMS reactivity represented as dots. The stem loops are numbered from H1 to H8; canonical start codon AUG in H6 is highlighted in green. **B**. Schematic representation of luciferase reporter construct with different regions of 5' end of *Hspa1a* mRNA used for cotransfection with Renilla luciferase in MEFs. **C**. Firefly-luciferase activity normalized to Renilla under no stress conditions in MEFs transfected with constructs No_UTR, UTR1, UTR2, and UTR7. **D**. Firefly-luciferase activity normalized to Renilla after 2 h of HS in MEFs transfected with constructs No_UTR, UTR1, UTR2, and UTR7. All plots are mean and SEM with each dot representing values from individual experiments, n=4. Unpaired t-test was used for statistical analysis in all graphs.

3.3.5 The stem loops H1, H4 and H6 in the 5'UTR of *Hspa1a* mRNA do not regulate its translational induction upon heat shock

By inserting unzipped and complementary mutations in each of the stem-loops of UTR7 (5'UTR and 102 nts of CDS), the Pyle's lab found that disrupting the structure but not the sequence of three stem loops H1, H4 and H6 impaired the UTR7 RNA folding during HS (**Fig 3.4**). To test the role of these stem-loops in recruiting the ribosome and initiating translation, we inserted the same unzipped mutation in a plasmid expressing the *Hspa1a* gene (containing the promoter, 5'UTR sequence, CDS, and 3' UTR and poly A sequences) to keep the endogenous sequence context and induction upon heat shock **(Fig 3.5A)**. Thus, our experiments preserve the codon optimality of most part of the CDS, except mutations M1 and M5 that are inserted in H6 after the AUG, and any sequence bound by RBPs and microRNAs regulating HSPA1A expression **(Fig 3.5B)**. To distinguish the plasmid expression from the endogenous *Hspa1a* gene, we transfected the MEFs$^{HSP70-/-}$ which lack the expression of HSPA1A (81). Each of the HSPA1A expressing plasmids, WT and mutants, was co-transfected with a GFP expression plasmid into MEFs$^{HSP70-/-}$, to normalized for the efficiency of translation by the western blot signal obtained with an antibody recognizing GFP. Twenty-four hours after transfection, cells were kept under homeostatic conditions or subjected to 2 h of heat shock at 42^{o}C and the expression of HSPA1A and GFP were detected by western blot and subsequently quantified (**Fig 3.5C**).

As expected, we did not detect expression of HSPA1A protein in the cells transfected only with the GFP plasmid, thus confirming the efficient knockout **(Fig 3.5C)**. Although the transfection of HSPA1A expressing plasmids led to a leaky expression of HSPA1A protein and mRNA under control conditions that is not usually observed with the endogenous HSPA1A, heat shock significantly increased the expression of the WT HSPA1A expression, resembling the

regulation of the endogenous gene **(Figs 3.5C and 3.5D)**. The unzip mutations M1 and M5 in H6, harboring the start codon AUG, behaved differently. While expression from M1 was equal to the expression of HSPA1A WT under control conditions and upon heat shock, the expression from M5 was significantly lower than WT **(Figs 3.5E and 3.5F)**. The differences in protein expression were not due to changes in mRNA levels as these were similar among the three plasmids WT, M1, and M5 **(Figs 3.5G and 3.5H)**. To explain this result, we identified in M5 two changes in the amino acid sequence, I9R and D10R, in addition to the A6R that is common with M1 **(Fig 3.5B)**. The addition of three basic residues in the coding sequence might slow-down ribosome in M5 leading to a decrease in HSPA1A expression (82). Hence, and solely based on the results from the M1 mutant, the H6 stem-loop does not change the regulation of *Hspa1a* mRNA translation even though it prevented the formation of a compact structure upon heat shock in vitro (59).

The unzipped mutation M7 in stem-loop H4 has double the expression of HSPA1A than the WT sequence under control conditions and upon heat shock (**Figs 3.5C-5H**). However, this increase was probably caused by an elevated *Hspa1a* mRNA levels (5-fold under control and 3-fold under HS) as detected by RT-qPCR (**Figs 3.5D and 3.5G**). Therefore, unzipping stem-loop H4 does not affect the translation regulation of *Hspa1a* mRNA. On the contrary, the unzipped mutation M9 in stem-loop H1 has a significantly higher expression of HSPA1A protein (average of ~8-fold, n = 4 replicas) and mRNA (average of ~4-fold, n = 6 replicas) than the WT sequence under control conditions (**Figs 3.5C, 3.5D, 3.5E, and 3.5G**). Overall M9 exhibited a significantly higher protein to mRNA fold change under control **(Fig 3.5I)**. Since H1 stem-loop encompasses the first nucleotides after the cap, we propose that it is also formed under control conditions and inhibits cap-dependent translation, as it has been previously demonstrated to other stem-loops located by the 5’ end of an mRNA (83). When heat shocked, the expression of HSPA1A protein

and mRNA was also higher in cells transfected with the M9 mutant than with the WT expressing plasmids (**Figs 3.5C, 3.5D, 3.5F and 3.5H**). However, the induction of protein relative to mRNA did not show any significant difference for M9 and any of the other unzipped mutations, which indicates that these stem-loops do not regulate *Hspa1a* mRNA translation even though they are essential to form a compact structure induced by heat shock *in vitro* **(Fig 3.5J)** (59).

Together, the three stem loops (H1, H4 and H6) characterized as significant by the Pyle's group did not have influence the translation induction of *Hspa1a* mRNA during HS. The only discernable impact we observed was that under permissive condition, M9 (in H1) exhibited significantly higher protein expression than WT. This indicates that H1, located near the 5' cap, represses translation in the absence of stress. It has been described that the presence of any stable stem loops or structures close to the 5' end would impede the binding of cap-recognition factors that promote translation initiation (83).

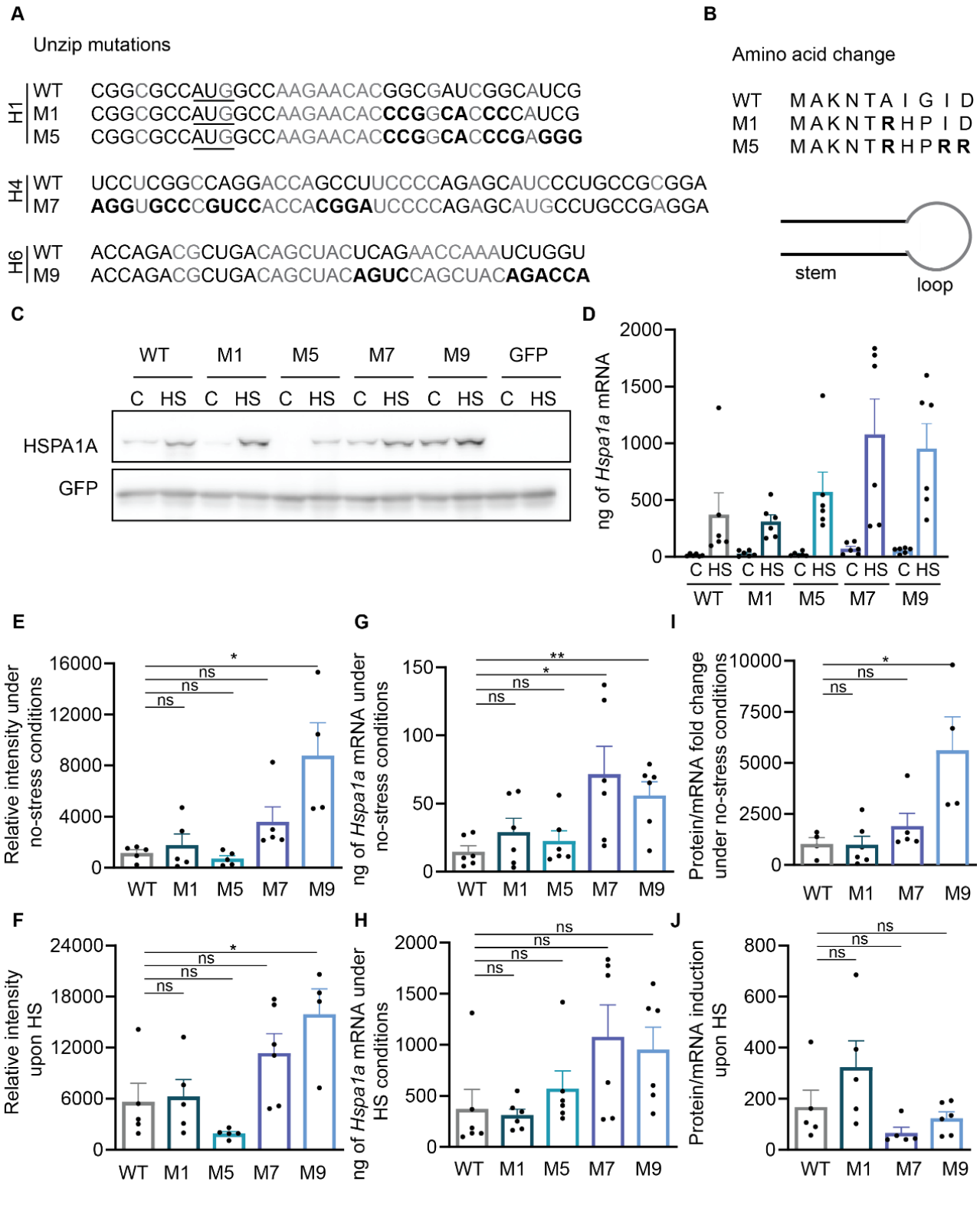
A
Unzip mutations
H1
WT CGGCGCCAUGGCCAAGAACACGGCGAUCGGCAUCG
M1 CGGCGCCAUGGCCAAGAACACCCGGCACCCCAUCG
M5 CGGCGCCAUGGCCAAGAACACCCGGCACCGAGGG
H4
WT UCCUCGGCCAGGACCAGCCUUCCCCAGAGCAUCCCUGCCGCGGA
M7 AGGUGCCCGUCCACCACGGAUCCCCAGAGCAUGCCUGCCGAGGA
H6
WT ACCAGACGCUGACAGCUACUCAGAACCAAAUCUGGU
M9 ACCAGACGCUGACAGCUACAGUCCAGCUACAGACCA
B
Amino acid change
WT M A K N T A I G I D
M1 M A K N T R H P I D
M5 M A K N T R H P R R
stem
loop
C
WT M1 M5 M7 M9 GFP
C HS C HS C HS C HS C HS C HS
HSPA1A
GFP
D
ng of Hspa1a mRNA
2000
1500
1000
500
0
C HS C HS C HS C HS C HS
WT M1 M5 M7 M9
E
Relative intensity under no-stress conditions
16000
12000
8000
4000
0
* ns ns ns
WT M1 M5 M7 M9
G
ng of Hspa1a mRNA under no-stress conditions
150
100
50
0
** * ns ns
WT M1 M5 M7 M9
I
Protein/mRNA fold change under no-stress conditions
10000
7500
5000
2500
0
* ns ns
WT M1 M7 M9
F
Relative intensity upon HS
24000
18000
12000
6000
0
* ns ns ns
WT M1 M5 M7 M9
H
ng of Hspa1a mRNA under HS conditions
2000
1500
1000
500
0
ns ns ns ns
WT M1 M5 M7 M9
J
Protein/mRNA induction upon HS
800
600
400
200
0
ns ns ns
WT M1 M7 M9

Figure 3.5. The unzip mutation M9 activates *Hspa1a* mRNA translation under permissive conditions

A. Scheme depicting the sequence of stem loop H1, H4 and H6 versus the respective unzip mutations M9, M7, M1, and M5. The nucleotides forming stem, loop and unzip mutations are in black, grey and bold letters, respectively. The start codon AUG is underlined. **B**. Changes in amino acid sequence (in bold) caused by the M1 and M5 mutation. **C**. Western blot of HSPA1A and GFP in *Hspa1a* null MEFs transiently cotransfected with plasmid carrying WT or indicated unzip mutants of HSPA1A minigene and GFP plasmid are then subjected to C and HS treatment. **D**. Absolute quantification of *Hspa1a* mRNA levels by RT-qPCR expressed in of nanograms. **E-F**. Quantification of HSPA1A protein levels under C (E) and HS (F), respectively. **G-H**. Absolute quantification of *Hspa1a* mRNA levels by RT-qPCR under C (G) and HS (H), respectively. **I.** Ratio of protein to mRNA fold change under control condition. **J.** Ratio of protein to mRNA fold change under HS normalized to expression under C. All plots are mean and SEM with each dot representing values from individual experiments, n=4-6. Unpaired t-test was used for statistical analysis in all graphs.

3.3.6 The stem loop near the 5'end of *Hspa1a* mRNA mediates translation regulation under permissive conditions.

The M9 unzipped mutation in H1 encompasses two small stem-loops H1a and H1b **(Fig 3.6A)**. To identify which stem-loops represses *Hspa1a* mRNA translation under control conditions, we start by unzipping H1a (H1a unzip) because it is the closest to the cap. In this case, we also created the complementary mutation (H1a rezip), which recovers the structure changing the sequence **(Fig 3.6A)**. We transfected the H1a unzip and rezip with GFP into MEFs$^{HSP70-/-}$ and compared their expression with the WT or the M9 plasmids by western blot. Remarkably, the H1a unzip and M9 have the same HSPA1A upregulated expression under control conditions while the H1a rezipped mutant expressed the same HSPA1A levels than the WT plasmid **(Fig 3.6A)**. We observed that under permissive conditions, similar to longer unzip mutation of M9, unzipping H1a showed a 5-fold increase in HSPA1A protein levels relative to the WT **(Figs 3.6B-E)**. Nonetheless, the induction upon heat stress was the same as the WT in both H1a unzip and rezip mutations further supporting our findings that H1 does not play a role in the induction of HSPA1A synthesis

upon heat stress **(Figs 3.6B-C)**. This further confirms the function of a stem loop close to the 5' cap in repressing the translation under permissible conditions.

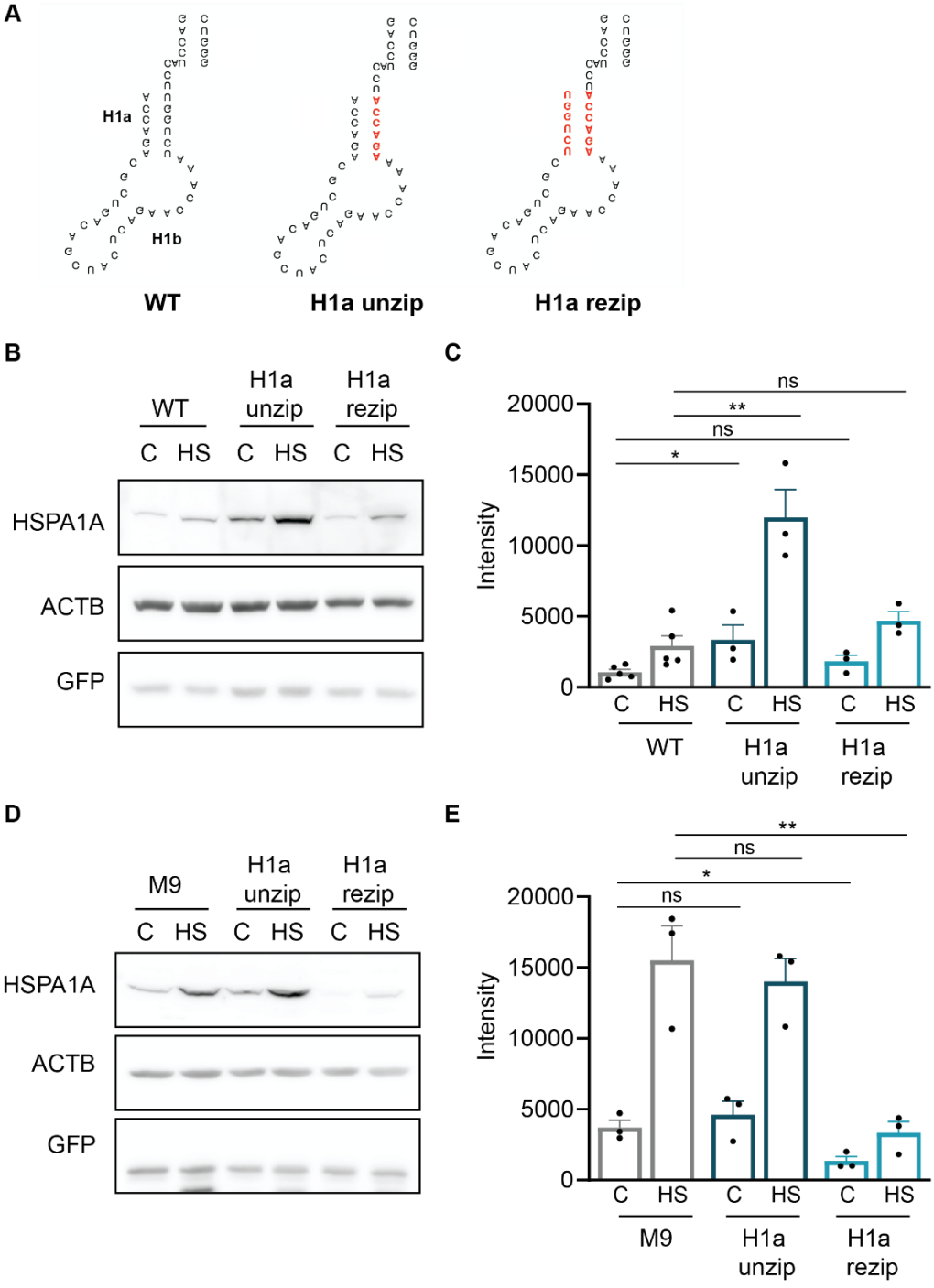

Figure 3.6. The stem-loop H1 represses *Hspa1a* mRNA translation under control conditions

A. Representation of stem loop H1 in wildtype, H1a unzip and H1a rezip mutations shown in red. **B.** Western blot of HSPA1A, ACTB (loading control) and GFP in (transfection control) *Hspa1a* null MEFs transiently cotransfected with plasmid carrying WT or indicated unzip and rezip mutants of H1a with GFP plasmid are then subjected to C and HS treatment. **C.** Quantification of HSPA1A levels in B expressed as intensity. All plots are mean and SEM with each dot representing values from individual experiments, n=3-5. Unpaired t-test was used for statistical analysis. **D.** Immunoblot of HSPA1A, ACTB (loading control) and GFP (Transfection control) in *Hspa1a* null MEFs transiently transfected with plasmid carrying M9 or H1a unzip or rezip mutants with GFP plasmids and then subjected to C and HS treatment. **E.** Quantification of HSPA1A levels in D expressed as intensity. All plots are mean and SEM with each dot representing values from individual experiments, n=3. Unpaired t-test was used for statistical analysis.

3.3.7 Single base editing revealed essential nucleotides on the 5'UTR sequence of the *Hspa1a* mRNA for its translational induction during heat shock

We next set up an unbiased approach in cells to identify nucleotides in the 5'UTR region and first 102 nts of the *Hspa1a* CDS involved in its translational activation upon heat shock. We leveraged a recently developed CRISPR-Cas9 based single nucleotide editing technique to insert C to T mutations (**Fig 3.7A**). We created a library of 41 guide RNAs (gRNAs) with an ability to modify one, two or three nts as listed in the **Table 3.1** (60). In order to edit *Hspa1a* gene in MEFs, we first generated an stable MEF line expressing the base editor nCas9 fused with the cytosine deaminase APOBEC1 that recognizes the NGG PAM sequence (60). This cell line had an editing efficiency of 90%, as established with a control base editor using a single guide (sgRNA) targeting *Rosa26* gene and was used to create 36 stable cell lines (we are still in the process of making stable cell lines with gRNAs 14, 37-41), each expressing one of the gRNAs (**Table 3.1**). The editing efficiency was confirmed by PCR amplification of the genome followed by Sanger sequencing and calculation of the editing efficiency (**Table 3.1)** (https://ice.synthego.com/#/). We were surprised to identify high editing efficiencies since MEFs are tetraploids. Changes in the amino

acid sequences were annotated and the sg4, which introduces a stop codon (Q22X) in frame with the AUG was used as a positive control (**Table 3.2**).

To quantify the role of the editing nucleotides on the translation of *Hspa1a* mRNA during heat shock, the expression of HSPA1A in each edited clone was compered to the NGG parental cell line. Clones were analyzed in five batches **(Figs 3.7B-C)**. MEFs expressing sg4 have inserted a stop codon in 80% of the locus, which led to almost undetectable expression of HSPA1A, supporting the efficiency of our system to detect nucleotides relevant for HSPA1A synthesis.

Among all tested clones, 58% (1, 3, 7-11, 13, 15-17, 18, 22-31) had similar HSPA1A expression than the parental NGG line and 9% (21, 35, 36) had a slightly higher expression (1.5-fold) than the NGG parental cell line (**Figs 3.7B-C**). Interestingly, MEFs edited by sg5, sg6, sg12, sg14, sg16, sg19, sg23, sg24, sg32 and sg40 had a significant lower induction of HSPA1A than the NGG parental cell at 2 hours of heat stress **(Figs 3.7B-C)**. It is important to note that none of the stem loops where these mutations are located were altered by the Pyle's lab (59).

sg	reference	edited	site	Nt#	Guide Sequence (5'-coding strand-3')	% editing efficiency
Rosa 26	GTGCCT	GTGCTT	C1		AAGTGCTTGTCAGTCTTAGG	90
sg1	ATGATC	ATAATC	C1	315	GAGATTATCGCCAACGACCA	81
sg2	TGATCT	TAATCT		315	GGAGATTATCGCCAACGAC	failed
sg3	GGGGTC	GGGGTT	C1	342	GGGCAACCGCACAACCCCCA	99
sg4	GGAACA	AAAACA	C1	295	CGTGTTCTAGCACGGCAAGG	76
			C2	294	CGTGTTTCAGCACGGCAAGG	80
sg5	ATCTCC	ATTTTT	C1	312	GCACGGCAAGGTGGAAATCA	84
			C2	310	GCACGGCAAGGTGAAGATCA	79
			C3	309	GCACGGCAAGGTAGAGATCA	48
sg6	GTGGTG	ATAATG	C1	272	GGCACCATCTACTCGTGCGT	23
			C2	270	GGCACTACCTACTCGTGCGT	88
			C3	269	GGCATCACCTACTCGTGCGT	94
sg7	TGGTGC	TAATGC	C1	270	GGGCACTACCTACTCGTGCG	74
			C2	269	GGGCATCACCTACTCGTGCG	88
sg8	ACACGC	ATATGC	C1	291	ACTCGTGCGTGGGCGTATTC	93
			C2	289	ACTCGTGCGTGGGCATGTTC	96
sg9	CGCCCA	TGCTTA	C1	289	CCTACTCGTGCGTGGGCATG	35
sg9			C2	286	CCTACTCGTGCGTGAGCGTG	91
sg9			C3	285	CCTACTCGTGCGTAGGCGTG	96
sg10	TCGCCG	TCGCCA	C1	245	CATGGCGATCGGCATCGACC	68
sg11	CACGAG	CATGAG	C1	279	GGGCACCACCTACTCATGCG	98
sg12	TTGGCC	TTAGCC	C1	237	ATGGCTAAGAACACGGCGAT	78
sg13	TGGCGC	TAGCGC	C1	231	CGGCGCTATGGCCAAGAACA	94
sg14	TGCCGA	TGCTGA		253	AGAACACGGCGATCAGCATC	56
sg15	TCGCCG	TTGCTG	C1	249	TGGCCAAGAACACGGCAATC	49
			C2	246	TGGCCAAGAACACAGCGATC	75
sg16	GGAAGG	AAAAAG	C1	212	AGCCTTCTAGAAGCAGAGCG	95
			C2	211	AGCCTTTCAGAAGCAGAGCG	92
			C3	208	AGCTTTCCAGAAGCAGAGCG	21
sg17	GGCGCC	GGCGCT	C1	226	GAAGCAGAGCGCAGCGCCAT	8
sg18	CCGCGC	CTGCGC	C1	226	TCCAGAAGCAGAGCGCAGCG	41
sg19	TCCGGG	TCCAAA	C1	181	TCCCTGGAGCATCCACGCCG	97
			C2	180	TCCTCGGAGCATCCACGCCG	95
			C3	179	TCTCCGGAGCATCCACGCCG	66
sg20	CTGGAA	TTGGAA		214	CGGAGCGCAGCCTTCCAAAA	failed
sg21	TCCGCG	TTTGCG	C1	199	GAGCATCCACGCCGCGAAGC	99
			C2	198	GAGCATCCACGCCGCAGAGC	99
sg22	CCGCGG	TTGCGG	C1	199	GGAGCATCCACGCCGCGAAG	50
			C2	198	GGAGCATCCACGCCGCAGAG	75
sg23	CGCGGC	TGCGGC	C1	198	CGGAGCATCCACGCCGCAGA	50
sg24	TCCTGG	TCCTAA	C1	147	TCCTAGGAGCATCCCTGCCG	94
			C2	146	TCTCAGGAGCATCCCTGCCG	90
sg25	CCGCGG	TTGCGG	C1	166	GGAGCATCCCTGCCGCGAAG	50
			C2	165	GGAGCATCCCTGCCGCAGAG	70
sg26	CGCGGC	TGCGGC	C1	165	AGGAGCATCCCTGCCGCAGA	0
sg27	TCTGGG	TCTAAA	C1	115	TCCCTAGAGCATCCCTGCCG	96
			C2	114	TCCTCAGAGCATCCCTGCCG	96
			C3	113	TCTCCAGAGCATCCCTGCCG	77
sg28	TCCGCG	TTTGCG	C1	133	GAGCATCCCTGCCGCGAAGC	0
			C2	132	GAGCATCCCTGCCGCAGAGC	10
sg29	CCGCGG	TTGCGG	C1	133	AGAGCATCCCTGCCGCGAAG	89
			C2	132	AGAGCATCCCTGCCGCAGAG	91
sg30	CGCGGC	TGCGGC	C1	132	CAGAGCATCCCTGCCGCAGA	42
sg31	GGAACG	AAAACG	C1	87	CGCGTTCTCGATCCTCGGCC	65
			C2	86	CGCGTTTCCGATCCTCGGCC	63
sg32	TCTGGG	TTTGGG	C1	117	GGACCAGCCTTCCCCAAAGC	95
sg35	CTGGTC	CTGGTT	C1	102	ATCCTCGGCCAGAACCAGCC	99
sg36	TGGTCC	TGGTTT	C1	102	GATCCTCGGCCAGAACCAGC	89
			C2	101	GATCCTCGGCCAAGACCAGC	73
sg37	CTCTTG	CTCTTA	C1	59	GATAAGAGAAGCAGAGCGAG	pending
sg38	CTTGTC	TTTGTT	C1	52	GAGACAAACGAAGACAAGAGA	failed
			C2	47	GAAACAAGCGAAGACAAGAGA	failed
sg39	TCTTCG	TTTTTG	C1	57	TCCAGAGACAAGCGAAAACA	pending
			C2	54	TCCAGAGACAAGCAAAGACA	pending
sg40	AGTAGC	AATAGC	C1	19	CAGCTATTCAGAACCAAATC	96
sg41	TCTGGA	TTTGGA	C1	45	GCACGGCAAGGTGGAAATCA	pending

Table 3.1: List of the guide RNAs targeting the *Hspa1a* mRNA and their knock in efficiency. The sgRNAs are 20 nts long and they target the sequence between position 3-8 known as the "reference" located proximal to the NGG PAM site (not shown). The guide sequence is represented in 5' to 3' direction on the mRNA. The base editor, nCas9, causes C to T or G to A mutation depending on the targeting strand of the guide RNAs on the *Hspa1a* gene. The expected mutation, the site of mutation (C1, C2 or C3), nucleotide position on the mRNA were listed along with the editing efficiency. The guide sequence is represented in 5' to 3' direction on the mRNA.

sg#	unedited	edited
sg1	GAG ATA ATC GCC	GAG ATt ATC GCC
	E I I A	E I I A
sg2	GAG ATA ATC GCC	GAG ATt ATC GCC
	E I I A	E I I A
sg3	CGC ACG ACC CCC	CGC ACa ACC CCC
	R T T P	R T T P
sg4	GTG TTC CAG CAC	GTG TTT tAG CAC
	V F Q H	V F X H
sg5	GTG GAG ATC ATC	GTa aAa ATC ATC
	V E I I	V K I I
sg6	GGC ACC ACC TAC	GGt Att ACC TAC
	G T T Y	G I T Y
sg7	GGC ACC ACC TAC	GGC Att ACC TAC
	G T T Y	G I T Y
sg8	GGC GTG TTC CAG	GGC aTa TTC CAG
	G V F Q	G I F Q
sg9	GTG GGC GTG TTC	GTa aGC aTG TTC
	V G V F	V S M F
sg10	ACG GCG ATC GGC	AtG GCG ATC GGC
	T A I G	M A I G
sg11	TAC TCG TGC GTG	TAC TCa TGC GTG
	Y S C V	Y S C V
sg12	ATG GCC AAG AAC	ATG GCa AAG AAC
	M A K N	M A K N
sg13	GGC GCC ATG GCC	GGC GCt ATG GCC
	- - M A	- - M A
sg14	GCG ATC GGC ATC	GCG ATC aGC ATC
	A I G I	A I S I
sg15	ACG GCG ATC GGC	ACa GCa ATC GGC
	T A I G	T A I G

Table 3.2: List of guide RNAs that target the CDS of *Hspa1a* mRNA. The nucleotide changes for each guide RNA (top row) are indicated in small letters and amino acid (bottom row) changes are indicated in red as single letter code.

While we are yet to analyze further our latest clones sg14, sg23 and sg40. The editing in sg19 clone changed 3 nts (179-181, 2 in a loop and 1 in a stem), sg24 edited 2 nts (146-147, loop) whereas sg32 changed 1 nt (1177) in the 5' UTR region of *Hspa1a* mRNA. There are four sgRNAs that land on the CDS sg5, sg6 and sg12. The editing in sg5 and sg6 changes 3 nts (309, 310, and 312 in sg5; 269, 271, 272 in sg6) introduces an amino acid change (E27K in sg5, T13I in sg6). The editing in sg12 led to a 1 nts (237) but no changes in aminoacid sequence. (**Tables 3.1 and**

3.2 and Fig 3.4). *Hspa1a* mRNA levels in sg5, sg12, sg19 and sg32 edited cells were similar compared to the unedited NGG MEFs. While we are yet to analyse the sg24, clone sg6 showed 1.5- fold lower *Hspa1a* mRNA compared to unedited NGG MEF which could account for the decrease in HSPA1A levels (**Fig 3.7D**). Interestingly, we found 24 nts sequence (GAGCATCCCTGCCGCGGAGCGCAAC) occurring twice (117-141 and 150-174) in the 5'UTR of *Hspa1a* mRNA in H4 and H5 stem loop (**Fig 3.7E**). Each of the 24 nts repetition is followed by a highly conserved 8 nt C/U region rich making a loop. Interestingly, sg24 and sg19 edited the highly C/U rich region of the first and second repeat, respectively. Such conservancy within a sequence is rare and it was striking that both editing reduced HSPA1A expression upon heat shock. Thus, we postulated that this region could be a target for cellular microRNAs. Using a screen for potential miRNAs with miRWalk, we identified Mir-30c-1-3p harboring two binding site 132-150 and 165-185 overlapping with the 24 nt repeat sequence (84). This resembles the HCV 5'UTR which holds two binding sites for miR122 and recruits Ago2 to stimulate a translation competent IRES formation (85). To support this theory, the guide RNAs in clones sg19 and sg24 lands in the Mir-30c-1-3p binding site on the 5'UTR that significantly reduced the HSPA1A expression. Altogether, single-base editing underscores the impact of specific base alterations on HSPA1A expression under HS, implying the essential role of these sites in HSPA1A induction during stress.

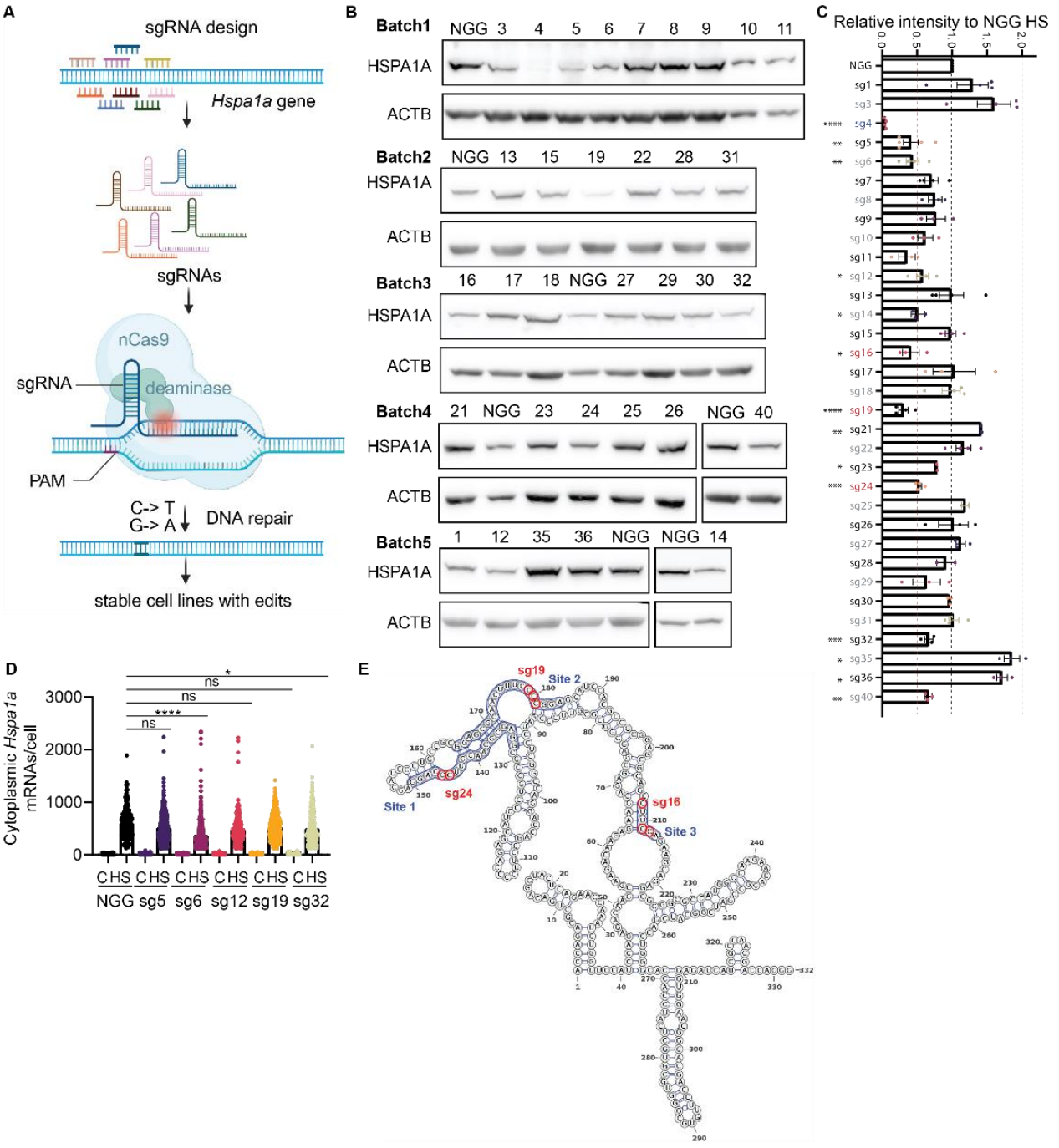
A
sgRNA design
Hspa1a gene
sgRNAs
nCas9
sgRNA
deaminase
PAM
C-> T
G-> A
DNA repair
stable cell lines with edits
B
Batch1
NGG 3 4 5 6 7 8 9 10 11
HSPA1A
ACTB
Batch2
NGG 13 15 19 22 28 31
HSPA1A
ACTB
Batch3
16 17 18 NGG 27 29 30 32
HSPA1A
ACTB
Batch4
21 NGG 23 24 25 26 NGG 40
HSPA1A
ACTB
Batch5
1 12 35 36 NGG NGG 14
HSPA1A
ACTB
C
Relative intensity to NGG HS
0.0 0.5 1.0 1.5 2.0
NGG
sg1
sg3
**** sg4
** sg5
** sg6
sg7
sg8
sg9
sg10
sg11
* sg12
sg13
* sg14
sg15
* sg16
sg17
sg18
**** sg19
** sg21
sg22
* sg23
*** sg24
sg25
sg26
sg27
sg28
sg29
sg30
sg31
*** sg32
* sg35
* sg36
** sg40
D
Cytoplasmic Hspa1a mRNAs/cell
3000
2000
1000
0
*
ns
ns
****
ns
CHS CHS CHS CHS CHS CHS
NGG sg5 sg6 sg12 sg19 sg32
E
sg19
Site 2
sg24
Site 1
sg16
Site 3

Figure 3.7: Single base editing revealed essential nucleotides on 5'end of *Hspa1a* mRNA for translation induction upon stress.

A. Outline of the CRISPR-Cas9 based single nucleotide editing from designing sgRNAs against *Hspa1a* gene, generation of sgRNAs, Cas9-mediated C to T editing and generation of stable cell lines. **B**. Western blot performed in batches to compare the HSPA1A and ACTB (loading control) levels upon HS in unedited NGG MEFs vs NGG MEFs edited by sgRNAs (indicated as numbers). **C.** Quantification of HSPA1A protein levels during HS normalized to ACTB relative to WT (unedited NGG). All plots are mean and SEM with each dot representing values from individual experiments, n=2-4. Unpaired t-test was used for statistical analysis. **D**. SmFISH quantification of *Hspa1a* mRNA levels in NGG MEFs (n= 95, 173) vs NGG MEFs edited by sgRNAs 5 (n=222, 350), 6 (n=143, 377), 12 (n=169, 196), 19 (n=146, 383) and 32 (n= 112, 312) cells under C and HS, respectively. Dunnett's test was used for statistical analysis. **E**. Structural representation of 333 nts of *Hspa1a* mRNA highlighting repeated sequences of 24 nts in green and red. The two binding site for Mir-30c-1-3p on the 5' UTR are marked in blue.

3.4 Discussion

We observed that *Hspa1a* mRNA is translated more efficiently during the recovery than heat shock, suggesting that *Hspa1a* mRNA translation is regulated differently under these two conditions. This increased translation efficiency correlates with elevated levels of the HSPA1A protein and a transition in the mode of translation during recovery. Interestingly, *Actb* mRNA exhibits comparable ribosome occupancy during both heat shock and recovery, similar to *Hspa1a* mRNA (Fig 1). Given that polysome profiling cannot discern between active and stalled translation, it suggests the possibility that *Actb* mRNA may not undergo translation during the heat shock. This is supported by no increase in the ACTB level during the heat shock (**Fig 3.2B**). Alternative it is possible that the anti-beta-actin antibody is not in the dynamic range to detect the changes in ACTB level, if any. Hence, a metabolic labeling experiment would elucidate the translation state of *Actb* mRNA. We have identified that during heat shock, *Hspa1a* mRNA translation is independent of the translation initiation factors eIF4A and eIF2α, suggesting a cap-independent translation mechanism that skips the repression imposed by the phosphorylation of

eIF2α. Conversely, eIF4A and eIF2α are required to translate during recovery, pointing to a cap-dependent translation initiation mechanism similar to ubiquitously expressed genes (**Fig 3.2** This conclusion is supported by the lack of dependency of non-canonical translation initiation factors such as eIF3d and RACK1 (**Fig 3.3**) (262). The switch from eIF4A and eIF2α-independent to cap-dependent translation increases the efficiency of HSPA1A synthesis during recovery, probably tailoring the amount of chaperone to the load of misfolded proteins. In order to determine the ribosomal occupancy of *Hspa1a* in cells treated with translation initiation factor inhibitors (Torin1, Hippuristanol, Salubrinal, shRACK1 or sheIF3d) versus mock treated cells, RNA fractionation followed RT-qPCR experiments could be performed. The experiments could provide us insights on whether fewer *Hspa1a* mRNA are translated at higher efficiency or many *Hspa1a* mRNAs are translated at lower efficiency to directly assess changes in *Hspa1a* mRNA translation efficiency upon heat shock and recovery.

The requirements of *Hspa1a* mRNA translation during heat shock suggest the presence of an IRES. Certain IRES, such as the HCV and CrPV, translate independently of eIF4F but differ on the reliability on ternary complex and eIF3. As CrPV IRES can translate in the absence of eIF3 and ternary complex, HCV has a type III IRES that needs eIF3 and ternary complex to translate. In particular, HCV IRES is bound by eIF3a and eIF3c that brings the 40S ribosome subunit and mediates the start codon recognition by eIF2α and eventual recruitment of 60S subunit (56). We originally expected the eIF3 complex to regulate HSPA1A synthesis because Zhou *et al.,* 2015 showed that the post-transcriptional N6-methylation of Adenosine 103 on the 5'UTR region of *Hspa1a* mRNA recruited the eIF3 complex upon heat shock to initiate translation (49). However these findings have been confronted by studies demonstrating that a single m6A modification upstream of start codon does not affect the translational output of the mRNA or the assembly of

initiation complex which supports our findings (51). We still have to investigate whether other eIF3 subunits with RNA binding activity, 3a, 3b, 3e and 3g, regulate HSPA1A synthesis during heat shock or recovery (77,86,87).

Hspa1a mRNA translation regulation during heat shock resembles the type IV CrPV IRES based on the lack of requirement from eIF4A and eIF2α. The type IV CrPV IRES forms a PK-I in the intergenic regions, which brings the 80S ribosome and mimics the tRNA structure, allowing to initiate translation upon the translocation of the ribosome (57,58,70,78). Therefore, the increased in temperature might induce a conformational change in the structure of *Hspa1a* mRNA that behaves as a type IV IRES and allows it to translate during heat shock. Recent findings by our collaborators support the temperature-mediated induction of an RNA compact structure encompassing the 5'UTR sequence and the first 102 nts of the *Hspa1a* mRNA CDS (59). Since their experiments were done *in vitro* and the translation capabilities of such structure were not analyzed, we investigated its translation activity in cells.

We first found that first 102 nts, but not the 30 first nts of *Hspa1a* mRNA CDS regulate the actions of the 5' UTR sequence when fused to luciferase, supressing it expression under control conditions and boosting it upon heat shock **(Figs 3.4C-3.4D)**. Thus, the CDS sequence of the *Hspa1a* mRNA needed to form a compact structure at 42 ^{o}C *in vitro* regulates translation *in vivo*. We next investigated the role of the stem-loops H1, H4, and H6 essential for *in vitro* compacting the *Hspa1a* mRNA in translation under control and heat shock conditions (59). Only unzipping stem-loop H1, which is adjacent to the cap structure, lead to an increased in the expression of HSPA1A during control conditions. Probably, the H1 loop represses HSPA1A synthesis of those mRNAs that escape the translational silencing of its encoded gene and prevents its spurious accumulation from having detrimental effects for the cell (86,87). In the future, we will investigate

the role of H1 during recovery from stress. Noticeably, none of the stem-loops was required for the upregulation of HSPA1A synthesis *in vivo*. It might that these loops are not formed in heat shocked cells due to interactions of the mRNA with proteins, or that they do not control heat-induced translation.

Because eIF4A is not necessary to unwind RNA structures in *Hspa1a* mRNA for its translation during heat shock and the 102 nts of the CDS were needed to regulate its translation *in-vivo*, we took an unbiased approach to edit nucleotides (C to T) in the 5'UTR region and 102 nts of the CDS and identify their role in *Hspa1a* mRNA translation. We found that changes to the bases positioned in nts 146-147, 179-181, 237 on 5'UTR, 309-312 on CDS compromised the translation of *Hspa1a* mRNA during heat shock. We identified the position 132-150 and 165-185 harbors binding site for Mir-30c-1-3p. We think the sgRNA mediated edits in 146-147 and 179-181 is impairing the binding of Mir-30c-1-3p and so compromising the *Hspa1a* mRNA translation during heat shock. We are yet to evaluate the presence of Mir-30c-1-3p in MEFs and assess the structure formation similar to HCV IRES which holds two binding sites for miR122 and recruits Ago2 to stimulate a translation competent IRES formation (85).

Our current experiments, done in collaboration with the Lecuyer's lab at the IRCM, aim to identify how changes in these nucleotides affect the heat-induced structure of *Hspa1a* mRNA by *in vitro* SHAPE analysis, as these specific stem-loops were not analyzed by the Pyle's group. Importantly, these experiments are being conducted with the full sequence of *Hspa1a* mRNA to analyze the influence of the whole *Hspa1a* mRNA sequence on the formation of this structure. It is important to remark that the same heat-induced structure as the described by the Pyle's group has been found. In addition, nanopore RNA sequencing showed that the highly purine regions from nts 43 to 78 in the 5'UTR region are highly reactive at 42 °C compared to 37 °C. Although

they have four target sgRNA disrupting the stem in our CRISPR-Cas9 editing experiment and we are currently making these cell lines.

The IRES of HCV and CrPV exist in the intergenic region comprising some parts of the CDS and forms a PK-I capable of recruiting the ribosome and starting translation in the 2072 codon (70). Since the translation of *Hspa1a* mRNA is independent of eIF4A mediated unwinding and scanning during stress and requires the CDS, we hypothesize that *Hspa1a* mRNA folds into a PK-I upon heat shock acting as an RNA thermosensor. Given the position of nts 178-181 on 5'UTR, our next model to test if this stem-loop could act as a hinge region for RNA folding to form a PK formation in *Hspa1a* mRNA. Additionally, H4 has unpaired CAU sequence complementary to the start codon AUG in the stemloop H6, providing a possible region involved in folding and translation induction during heat shock.-We will test the hypothesis of the presence of an IRES forming a PK with the following experiments: 1) Using a bicistronic vector to express GFP followed by *Hspa1a* and 2) deciphering the tertiary structure of the *Hspa1a* mRNA by full length RNA nanopore sequencing (90). From this experiment, we could determine if the *Hspa1a* mRNA possess an IRES that is formed during heat shock *in vivo* by acting as an RNA thermosensor just as seen *in vitro*.

Notably, RNA thermosensor has been previously described to function in bacterial HSPs as a part of host defense mechanism (54,91). When bacterial cells enter the host, the stem loops of pre-existing HSP mRNAs melt to expose the Shine-Dalgarno sequence allowing instant translation while slowly turning on transcription (92,93). Upon return to normal growth temperature, the structures fold back to immediately cease the synthesis of HSPs. This suggests that the concept of RNA thermosensor HSP mRNA could be evolutionarily conserved from prokaryotes to eukaryotes but act differently. While bacterial RNA thermosensors melt upon increase in temperature, the

mouse *Hspa1a* mRNA does the opposite i.e., forming a compact tertiary structure to allow translation. In order to bring more relevance to human disease, it is important to identify if the RNA thermosensors are conserved in humans. The *HSPA1A* mRNA in humans possess similar GC composition and 18 nts shorter 5'UTR than the mouse *Hspa1a* ortholog. Hence it is very likely for the RNA thermosensor to function in the regulation of HSR in humans.

3.5 Materials and methods

Cell lines and treatments.

Immortalized MEFs from wildtype mice (94) and *HSPA1A/1B*-null MEFs (81) were grown at 37 ^{o}C, 5% CO_2 in DMEM supplemented with 5% of FBS and Penicillin/Streptomycin. Heat shock treatment was induced by parafilm wrapping the plates and submerging it in a water bath at 42 ^{o}C. Recovery is achieved by transferring the heat shocked plate back to the cell culture incubator at 37 ^{o}C. Cells were treated with 200 nM of hippuristanol (a gentle donation of Dr. Jerry Pelletier at McGill University) 3 h, 100 μM of salubrinal (Cat# SML0951, Sigma) for 24 h, 1 μM torin1 (Cat# 4247, Tocris) for 30 min before being heat shocked for 2 h.

Plasmids.

Firefly-luciferase expression plasmids have pGL3-Control vector (Promega) as a backbone. The SV40 promoter was replaced by the *Mus musculus Hspa1a* promoter using enzymes MluI and HindIII. HSPA1A promoter was amplified from mouse genomic DNA (NIH 3T3 New England Biolabs) using primers HSPA1APMluIF and HSPA1APHIndIIIR. Luciferase was re-cloned to create an EcoRI site for cloning of the different 5'UTR sequences by PCR amplification using

primers: The 3'UTR of *Hspa1a* was PCR from genomic DNA with primers: RLucFseI and FLUCEcoRI and cloned in the XbaI site after the stop codon of firefly-luciferase. Each of the UTRs was amplified by PCR from genomic DNA and cloned into the HindIII and EcoRI. All constructs have the same forward primer: 5UTRFFHIndIII and different reverse primer. UTR1REcoRI, UTR2EcoRI, UTR7REcoRI, and UTR26REcoRI. The plasmids with UTRs containing the AUG of *Hspa1a* were depleted of the AUG of luciferase by recloning luciferase after PCR with primers: LucFEcoRI and LucRBamHI. Direct mutagenesis was inserted using the (QuickChange Mutagenesis Multi-site directed Mutagenesis kit, Agilent technologies) and performed by NorClone Biotech. The primer sequences are listed in **Table 3.5.**

ShRNA knockdown

ShRNAs targeting Eif3d and RACK1 in mus musculus (gene ID 55944 and 14694) are listed in table below. All shRNAs were expressed in pLKO.1 vector backbone, obtained from GPP portal (https://portals.broadinstitute.org/gpp/public/) purchased from McGill University shRNA library (McGill Platform for Cellular Perturbation Services). The TNRC number and shRNA sequences are provided in **Table 3.3**. For knock down experiments, MEFs were infected with lentivirus expressing shRNAs targeting eIF3d or RACK1. Stable cells were selected using puromycin and the efficiency of knock down was verified by western blot.

Transient transfection

Transfection of luciferase plasmids was done in 12- well plates. At 50% confluence, each well was transfected with 0.2 μg of the Renilla-lucifeasere plasmid (pRL-SV40 vector, Promega) and 0.8 μg of the Firefly-luciferase plasmid using 12 μl of the jetPRIME transfection reagent (Polyplus). The cells were subjected to heat stress 36 hours after transfection. The cells were then collected and lysed using lysis buffer (Promega). About 5 μl of 1:10 diluted samples were then taken for

measuring the firefly and Renilla luciferase expression by luminometry. For transfection of unzip mutant plasmids, *Hspa1a/a1b* null MEFs were plated (approximately 150,000 cells per well of a 6 well plate). At 50-60% confluence, 1.8 μg of WT HSPA1A, unzip, and/or rezip mutation plasmids transiently co-transfected with a carrier GFP plasmid using 15 μl of the jetPRIME transfection reagent (Polyplus) and 200 μl of the jetPRIME transfection buffer (Polyplus). The media was changed 4-6 h post transfection and GFP expression was verified using fluorescence microscope. After 24 h, the cells were subjected to heat shock at 42 ^{o}C for 2 h and collected with PBS for western blot analysis or directly lysed with TRIzol (Cat# 15596026, Invitrogen) for RNA extraction and qPCR.

CRISPR-Cas9 editing and genotyping

MEFs stably expressing base editor FNLS-NGG-BLAST under Blasticidin (Cat# A1113903, Gibco) expression was generated by sequential lentiviral infection facilitated by 10 μg/ml polybrene (259). Two days after the infection, cells were selected by treatment with 5 μg/ml of Blasticidin for 10 days (259). The designing of guide RNA for sgRNAs for the coordinates chr17:35190782:35191150 region of interest +/- 18nt was done using in house pipeline. The guides listed below (**Table 3.4**) are purchased from iDT as forward and reverse oligos, annealed, and PNK treated. The guide RNAs are then cloned into pLenti-Guide-Puro backbone as described in (274). Lentivirus carrying the plasmids were produced by transfection of 293T cells using 4-vector system (TAT, REV, GAG/Pol, and VSVG). NGG MEFs stably expressing Flag tagged Cas9 was then infected with lentivirus expressing individual guide RNAs and the cells were selected using 6 μg/ml of Puromycin (Cat# A1113803, Gibco; Cat# P8833, Sigma) and 5 μg/ml of Blasticidin for 5 days, 48 h post infection. Then maintained at 6 μg/ml of puromycin and 2.5 μg/ml of Blasticidin

for another 3 days. On day 10 post infection, a portion of the cells were collected to check for target modification by PCR and sanger sequencing.

Protein extraction and western blotting

Cells from dug treatment and knock down experiments were lysed with modified RIPA buffer (50 mM Tris-HCl pH 8.0, 150 mM NaCl, and 1% ND40) and then subjected to ultrasonication followed by mixing with 4X lamelli buffer (Bio-Rad) for SDS-PAGE. Cells from transient transfection experiments were lysed directly in SDS-PAGE buffer (60 mM Tris–HCl pH 6.8, 10% glycerol, 2% SDS, 5% 2-mercaptoethanol and 0.0025% bromophenol blue) for SDS-PAGE. Immunoblotting was performed as mentioned in (99). The blots were incubated with specific antibodies HSPA1A (1:2000), ACTB (1:10000), RACK1 (1:2000), eIF3d (1:1000), GAPDH (1:10000), JL8 GFP (1:5000), goat-anti-mouse (1:5000) and goat-anti-rabbit antibody (1:5000). The product details of antibodies are provided in **Table 3.6.**

Single-molecule in situ hybridization (smFISH)

SmFISH probes were designed using the LGC Biosearch Technologies probe designer (masking level 5, oligo length 20, minimum spacing 2). Fluorescently labelled *HSPA1A* or SunTag probes were purchased from Stellaris™. Detailed protocol for smFISH, imaging and analysis has been previously described (275). In brief, MEFs were plated on cover slips. After treatment (if any), the cells were washed thrice with PBS supplemented with 5 mM Magnesium Chloride (PBSM) and fixed using 4% PFA (Thermo Scientific). Quenching is achieved using 0.1 M Glycine in PBSM. Following 2 washes with PBSM, the cells were permeabilized using 0.1% Triton X-100 (Invitrogen™) 2 mM Ribonuclease Vanadyl Complex (VRC, Sigma-Aldrich). The cells were washed once again and incubated with prehybridization solution, 10% Formamide, 2X SSC at 37

ºC for 30 min. Cells were placed on top of 50 µl of Hybridization solution containing 2X SSC, 10% Formamide, 1 mg/ml E. coli tRNA (Sigma-Aldrich), 10% Dextran Sulfate, 0.2 mg/ml UltraPure™ BSA (Invitrogen™), 2 mM VRC, 10 U/ml RNaseOUT™ Recombinant Ribonuclease Inhibitor (Invitrogen™), and 125 nM smFISH (Stellaris™) probes on a humidified chamber. Hybridization was performed for 3 h at 37 ºC. The coverslips were then returned to well plates where they are washed twice with prewarmed prehybridization solution followed by washing with 2X SSC twice. The coverslips were then dried and mounted on slides using ProLong™ Gold or ProLong™ Diamond Antifade Mountant with DAPI (Invitrogen™). The coverslips were allowed to cure at least overnight before imaging.

Imaging and smFISH analysis

The slides were imaged using custom wide-field Inverted Nikon Ti-2 wide-field microscope with 1.4 NA oil immersion 60X objective lens, Spectra X LED light engine with a Cy7+ bandpass filter (Lumencor), and Orca-Fusion sCMOS camera (Hamamatsu). The outlines were created using Cell profiler version 2.2. The acquired images were analyzed using free analysis software developed by Mathworks using Matlab (version greater than 2017) programming language, FISH-quant (http://code.google.com/p/fish-quant/) (98). The detailed protocol for analysis has been described in (97).

DNA extraction and PCR amplification

DNA extraction was performed using 0.1 ml DNA extraction buffer (10 mM Tris HCl pH 8.0, 20 mM EDTA, 200 mM NaCl, 0.2% Triton-X 100) supplemented with 100 µg/ml of proteinase K (Cat# P2308, Sigma-Aldrich) followed by incubation at 37 ºC for 1.5 h. The lysate was then precipitated by 2.5 µl of 2.5 M NaCl and 0.1 ml of isopropanol. The samples were then centrifuged

at 14000 rpm for 15 min. The pellet was air dried and resuspended in water and 1µl of RNase for 1.5 h to overnight at 37 ^{o}C. Ultrasonication was performed 30 s ON and OFF cycle at 30% amplitude for 3 min. PCR was performed using 100 ng of genomic DNA and the samples sent for sanger sequencing with primer UpHSPA1ApromF and pSEQR.

RNA isolation and RT-qPCR

The cells were lysed with 0.5 ml of TRIzol and RNA extraction was performed by adding 100µl of chloroform and collecting the top aqueous layer. Then, RNA was precipitated by adding 0.25 ml of isopropanol with 1 µl of glycogen (Invitrogen). RNA pellet was obtained by cold centrifugation at 13000 x g for 15 min, then washed twice with 75% ethanol. The pellet was dried in a heat block at 65 ^{o}C for 5-10 min and then resuspended in 50 µl of RNase free water. For DNase treatment, 500ng or 1 µg of RNA was taken in a 10 µl reaction (Promega) for 20-30 min at 37 ^{o}C. The treatment was quenched by adding 1 µl of stop buffer and incubation at 65 ^{o}C for 10 min. Dnase treated RNA (about 100 ng) was taken for reverse transcription reaction with iSCRIPT (Bio-Rad). The cDNAs were diluted in 1:2 ratio from which 1 µl of cDNA was taken for qPCR reaction with 2X PowerUp™ SYBR™ Green Master Mix (Applied Biosystems) for a final reaction volume of 5 µl. QPCR was performed for HSPA1Agene1 mouse and ACTIN mouse primers (Table) using QuantStudio™ qPCR Systems (Applied Biosystems), and absolute RNA levels (in ng) was quantified using desktop version of QuantStudio Design & Analysis 2.7.0 software (Applied Biosystems).

Polysome profiling and Northern blotting

MEFs were seeded on 150 mm plates and once they reach 80-90% confluency, they were subjected to heat shock and recovery. The cells were placed on ice after the treatment and washed with ice

cold PBS supplemented with 100 µg/ml of Cycloheximide (BioShop). The cells were then scraped and lysed using 5 mM Tris-HCl pH 7.5, 2.5 mM Magnesium chloride, 1.5 mM KCl. The sample extraction was performed as described in (99). The clarified extract was then carefully loaded onto sucrose gradient prepared with 10-50% sucrose. The polysome profiling experiment was conducted on fractionator Teledyne ISCO as described in (99). RNA extraction from the polysome fractions were performed as described in (100). In brief, the RNA from sucrose was precipitated using 2-3 volumes of 100% ethanol overnight at -20 ^{o}C and subjected to cold centrifugation at 13000 rpm for 30 min. The excess sucrose was removed by a wash with 70% ethanol and the pellet obtained was subjected to TRIzol- chloroform as mentioned earlier. RNA pellets were resuspended in RNase free water and mixed using home-made RNA loading dye for denaturing gel and transferred on to a nylon membrane (Cytiva) by capillary action overnight. The northern blotting was performed as mentioned in (96). HSPA1A template was amplified using HSPA1AF and HSPA1AR for qpcr primers. Actin template was a generous donation from Sophie Cousineau from Dr. Selena Sagan laboratory (University of British Columbia, Canada). The templates were radiolabeled with ^{32}P prepared using RadPrime DNA Labeling System (Invitrogen™) as described in (101). Northern blots were developed using Typhoon biomolecular imager (Cytiva).

Table 3.3: Tabulation of shRNAs based on the target, its TRC number and the sequence.

Target	TRC number	shRNA sequence
sheIF3d-1	TRCN0000196233	5'-CCGG-GCTGATGAAGATGCGCTACTT-CTCGAG-AAGTAGCGCATCTTCATCAGC-TTTTTTG-3'
sheIF3d-2	TRCN0000179496	5'-CCGG-GCAGTTTAAGCCCAATGAGTT-CTCGAG-AACTCATTGGGCTTAAACTGC-TTTTTTG-3'
shRACK1-1	TRCN0000012698	5'-CCGG-GCTTTCTGAAACTGGCTTCTA-CTCGAG-TAGAAGCCAGTTTCAGAAAGC-TTTTT-3'
shRACK1-2	TRCN0000054378	5'-CCGG-GTCTTAGAAATAAACTGGCTT-CTCGAG-AAGCCAGTTTATTTCTAAGAC-TTTTTG-3’

Table 3.4: Tabulation of forward and reverse oligos used for making sgRNAs.

sgRNA#	Foward Oligo	Reverse Oligo
sg1	CACCGGAGATCATCGCCAACGACCA	AAACTGGTCGTTGGCGATGATCTCC
sg2	CACCGGGAGATCATCGCCAACGACC	AAACGGTCGTTGGCGATGATCTCCC
sg3	CACCGTGGGGGTCGTGCGGTTGCCC	AAACGGGCAACCGCACGACCCCCAC
sg4	CACCGCGTGTTCCAGCACGGCAAGG	AAACCCTTGCCGTGCTGGAACACGC
sg5	CACCGTGATCTCCACCTTGCCGTGC	AAACGCACGGCAAGGTGGAGATCAC
sg6	CACCGGGCACCACCTACTCGTGCGT	AAACACGCACGAGTAGGTGGTGCCC
sg7	CACCGGGGCACCACCTACTCGTGCG	AAACCGCACGAGTAGGTGGTGCCCC
sg8	CACCGGAACACGCCCACGCACGAGT	AAACACTCGTGCGTGGGCGTGTTCC
sg9	CACCGCACGCCCACGCACGAGTAGG	AAACCCTACTCGTGCGTGGGCGTGC
sg10	CACCGCACGGCGATCGGCATCGACC	AAACGGTCGATGCCGATCGCCGTGC
sg11	CACCGCGCACGAGTAGGTGGTGCCC	AAACGGGCACCACCTACTCGTGCGC
sg12	CACCGATGGCCAAGAACACGGCGAT	AAACATCGCCGTGTTCTTGGCCATC
sg13	CACCGCGGCGCCATGGCCAAGAACA	AAACTGTTCTTGGCCATGGCGCCGC
sg14	CACCGGATGCCGATCGCCGTGTTCT	AAACAGAACACGGCGATCGGCATCC
sg15	CACCGGATCGCCGTGTTCTTGGCCA	AAACTGGCCAAGAACACGGCGATCC
sg16	CACCGAGCCTTCCAGAAGCAGAGCG	AAACCGCTCTGCTTCTGGAAGGCTC
sg17	CACCGATGGCGCCGCGCTCTGCTTC	AAACGAAGCAGAGCGCGGCGCCATC
sg18	CACCGCGCCGCGCTCTGCTTCTGGA	AAACTCCAGAAGCAGAGCGCGGCGC
sg19	CACCGTCCCCGGAGCATCCACGCCG	AAACCGGCGTGGATGCTCCGGGGAC
sg20	CACCGTTCTGGAAGGCTGCGCTCCG	AAACCGGAGCGCAGCCTTCCAGAAC
sg21	CACCGGCTCCGCGGCGTGGATGCTC	AAACGAGCATCCACGCCGCGGAGCC
sg22	CACCGCTCCGCGGCGTGGATGCTCC	AAACGGAGCATCCACGCCGCGGAGC
sg23	CACCGTCCGCGGCGTGGATGCTCCG	AAACCGGAGCATCCACGCCGCGGAC
sg24	CACCGTCCCAGGAGCATCCCTGCCG	AAACCGGCAGGGATGCTCCTGGGAC
sg25	CACCGCTCCGCGGCAGGGATGCTCC	AAACGGAGCATCCCTGCCGCGGAGC
sg26	CACCGTCCGCGGCAGGGATGCTCCT	AAACAGGAGCATCCCTGCCGCGGAC
sg27	CACCGTCCCCAGAGCATCCCTGCCG	AAACCGGCAGGGATGCTCTGGGGAC
sg28	CACCGGCTCCGCGGCAGGGATGCTC	AAACGAGCATCCCTGCCGCGGAGCC
sg29	CACCGCTCCGCGGCAGGGATGCTCT	AAACAGAGCATCCCTGCCGCGGAGC
sg30	CACCGTCCGCGGCAGGGATGCTCTG	AAACCAGAGCATCCCTGCCGCGGAC
sg31	CACCGCGCGTTCCCGATCCTCGGCC	AAACGGCCGAGGATCGGGAACGCGC
sg32	CACCGGCTCTGGGGAAGGCTGGTCC	AAACGGACCAGCCTTCCCCAGAGCC
sg35	CACCGGGCTGGTCCTGGCCGAGGAT	AAACATCCTCGGCCAGGACCAGCCC
sg36	CACCGGCTGGTCCTGGCCGAGGATC	AAACGATCCTCGGCCAGGACCAGCC
sg37	CACCGGACAAGAGAAGCAGAGCGAG	AAACCTCGCTCTGCTTCTCTTGTCC
sg38	CACCGCTCTTGTCTTCGCTTGTCTC	AAACGAGACAAGCGAAGACAAGAGC
sg39	CACCGTGTCTTCGCTTGTCTCTGGA	AAACTCCAGAGACAAGCGAAGACAC
sg40	CACCGCAGCTACTCAGAACCAAATC	AAACGATTTGGTTCTGAGTAGCTGC
sg41	CACCGTCTCTGGATGGAACCAGATT	AAACAATCTGGTTCCATCCAGAGAC
Rosa26	CACCGAAGTGCCTGTCAGTCTTAGG	AAACCCTAAGACTGACAGGCACTTC

Table 3.5: Tabulation of primers and their sequences.

Primer name	Primer sequence
HSPA1APMluIF	CTCTTACGCGTAAACTAGTAACGCGATTGGAGAGG
HSPA1APHIndIIIR	ATATATAAGCTTGACCTGCTCGCCGCCCTGCGCCTTTAAG
RLucFseI	GAAGCGGCCGGCCGCCCGACTCTAGAATTACACGGCGATCTTTC
FLUCEcoRI	ATATATGAATTCATGGAAGACGCCAAAAACATAAAG
5UTRFFHIndIII	CAGGTCAAGCTTACCAGACGCTGACAGCTAC
UTR1REcoRI	TTCCATGAATTCGGCGCCGCGCTCTGCTTCTGGAA
UTR2EcoRI	TTCCATGAATTGGTCGATGCCGATCGCCG
UTR7REcoRI	TTCCATGAATTCCGCCTGGTCGTTGGCGATGATCTCCACC
UTR26REcoRI	TTCCATGAATTCGTCGTTGGCGATGATCTCCACC
LucFEcorI	TTCCATGAATTCGAAGACGCCAAAAACATAAAGA
LucRBamHI	GTCGACGGATCCGCTGTGGAATGTGTGTC
pSEQFHSP70	ACCAGACGCTGACAGCTACTCAG
pSEQR	GATCGCCGTGTTCTTGGCCATG
UpHSPA1ApromF	GCTGGGACAGAGCCTCTAGTTCC
U6	GAGGGCCTATTTCCCATGATTCCT
HSPA1Agene1mouseF	GAGATCGACTCTCTGTTCGA
HSPA1Agene1mouseR	ATCTGCGCCTTGTCCATCTT
ACTIN Mouse F	TGCTCCCCGGGCTGTATT
ACTIN Mouse R	ACATAGGAGTCCTTCTGACCCATT
HSPA1AF for qpcr	TCAGGACCCACCATCGAGGA
HSPA1AR for qpcr	AAGCCCACGTGCAATACACA

Table 3.6: Tabulation of antibodies, company name and the corresponding catalog number.

Target	Vendor	Catalog number
HSPA1A	R&D systems	AF1663
ACTB	Millipore Sigma	MAB1501
RACK1	Novus Biotechne	NBP2-76864
eIF3d	Novus Biotechne	NBP2-39069
GAPDH	ProteinTech	60004-1-Ig
JL8 GFP	Takara	632381
goat-anti-mouse	Bio-Rad	1706516
goat-anti-rabbit	Bio-Rad	1706515

3.6 References

1. Lindquist S. The heat-shock response. Annu Rev Biochem. 1986;55:1151–91.
2. Morimoto RI. Cells in stress: transcriptional activation of heat shock genes. Science. 1993 Mar 5;259(5100):1409–10.
3. Morimoto RI. Regulation of the heat shock transcriptional response: cross talk between a family of heat shock factors, molecular chaperones, and negative regulators. Genes Dev. 1998 Dec 15;12(24):3788–96.
4. Lis J, Wu C. Protein traffic on the heat shock promoter: Parking, stalling, and trucking along. Cell. 1993 Jul 16;74(1):1–4.
5. Wu C. Heat shock transcription factors: structure and regulation. Annu Rev Cell Dev Biol. 1995;11:441–69.
6. Ritossa F. A new puffing pattern induced by temperature shock and DNP in drosophila. Experientia. 1962 Dec 1;18(12):571–3.
7. Parsell DA, Lindquist S. The function of heat-shock proteins in stress tolerance: degradation and reactivation of damaged proteins. Annu Rev Genet. 1993;27:437–96.
8. Lindquist S, Craig EA. The heat-shock proteins. Annu Rev Genet. 1988;22:631–77.
9. Kampinga HH, Hageman J, Vos MJ, Kubota H, Tanguay RM, Bruford EA, et al. Guidelines for the nomenclature of the human heat shock proteins. Cell Stress Chaperones. 2009 Jan;14(1):105–11.
10. Ashburner M. Patterns of puffing activity in the salivary gland chromosomes of Drosophila. Chromosoma. 1970 Sep 1;31(3):356–76.
11. Lindquist S. Varying patterns of protein synthesis in Drosophila during heat shock: Implications for regulation. Dev Biol. 1980 Jun 15;77(2):463–79.
12. Lindquist S. Translational efficiency of heat-induced messages in Drosophila melanogaster cells. J Mol Biol. 1980 Feb;137(2):151–8.
13. Welch WJ, Feramisco JR. Nuclear and nucleolar localization of the 72,000-dalton heat shock protein in heat-shocked mammalian cells. J Biol Chem. 1984 Apr 10;259(7):4501–13.
14. Velazquez JM, Lindquist S. hsp70: Nuclear concentration during environmental stress and cytoplasmic storage during recovery. Cell. 1984 Mar 1;36(3):655–62.
15. Borkovich KA, Farrelly FW, Finkelstein DB, Taulien J, Lindquist S. hsp82 is an essential protein that is required in higher concentrations for growth of cells at higher temperatures. Mol Cell Biol. 1989 Sep;9(9):3919–30.
16. Zimmerman JL, Petri W, Meselson M. Accumulation of a specific subset of D. melanogaster heat shock mRNAs in normal development without heat shock. Cell. 1983 Apr;32(4):1161–70.
17. Yahara I, Iida H, Koyasu S. A heat shock-resistant variant of Chinese hamster cell line constitutively expressing heat shock protein of Mr 90,000 at high level. Cell Struct Funct. 1986 Mar;11(1):65–73.
18. Dworniczak B, Mirault ME. Structure and expression of a human gene coding for a 71 kd heat shock “cognate” protein. Nucleic Acids Res. 1987 Jul 10;15(13):5181–97.
19. O’Malley K, Mauron A, Barchas JD, Kedes L. Constitutively expressed rat mRNA encoding a 70-kilodalton heat-shock-like protein. Mol Cell Biol. 1985 Dec;5(12):3476–83.

20. Ingolia TD, Craig EA. Drosophila Gene Related to the Major Heat Shock-Induced Gene is Transcribed at Normal Temperatures and not Induced by Heat Shock. Proc Natl Acad Sci U S A. 1982;79(2):525–9.
21. Schiaffonati L, Bardella L, Cairo G, Rappocciolo E, Tacchini L, Bernelli-Zazzera A. Constitutive and Induced Synthesis of Heat Shock Proteins in Transplantable Hepatomas. Tumori J. 1987 Dec 1;73(6):559–65.
22. Vihervaara A, Sistonen L. HSF1 at a glance. J Cell Sci. 2014 Jan 15;127(Pt 2):261–6.
23. Vera M, Pani B, Griffiths LA, Muchardt C, Abbott CM, Singer RH, et al. The translation elongation factor eEF1A1 couples transcription to translation during heat shock response. Green MR, editor. eLife. 2014 Sep 16;3:e03164.
24. Dean DO, Kent CR, Tytell M. Constitutive and Inducible Heat Shock Protein 70 Immunoreactivity in the Normal Rat Eye. Invest Ophthalmol Vis Sci. 1999 Nov 1;40(12):2952–62.
25. Alagar Boopathy LR, Jacob-Tomas S, Alecki C, Vera M. Mechanisms tailoring the expression of heat shock proteins to proteostasis challenges. J Biol Chem. 2022 Mar 3;298(5):101796.
26. Vries RGJ, Flynn A, Patel JC, Wang X, Denton RM, Proud CG. Heat Shock Increases the Association of Binding Protein-1 with Initiation Factor 4E *. J Biol Chem. 1997 Dec 26;272(52):32779–84.
27. Cuesta R, Laroia G, Schneider RJ. Chaperone Hsp27 inhibits translation during heat shock by binding eIF4G and facilitating dissociation of cap-initiation complexes. Genes Dev. 2000 Jun 15;14(12):1460–70.
28. Kedersha NL, Gupta M, Li W, Miller I, Anderson P. RNA-Binding Proteins Tia-1 and Tiar Link the Phosphorylation of Eif-2α to the Assembly of Mammalian Stress Granules. J Cell Biol. 1999 Dec 27;147(7):1431–42.
29. Zhang X, Shu XE, Qian SB. O-GlcNAc modification of eIF4GI acts as a translational switch in heat shock response. Nat Chem Biol. 2018 Oct;14(10):909–16.
30. Wek SA, Zhu S, Wek RC. The histidyl-tRNA synthetase-related sequence in the eIF-2 alpha protein kinase GCN2 interacts with tRNA and is required for activation in response to starvation for different amino acids. Mol Cell Biol. 1995 Aug;15(8):4497–506.
31. Dong J, Qiu H, Garcia-Barrio M, Anderson J, Hinnebusch AG. Uncharged tRNA activates GCN2 by displacing the protein kinase moiety from a bipartite tRNA-binding domain. Mol Cell. 2000 Aug;6(2):269–79.
32. McEwen E, Kedersha N, Song B, Scheuner D, Gilks N, Han A, et al. Heme-regulated inhibitor kinase-mediated phosphorylation of eukaryotic translation initiation factor 2 inhibits translation, induces stress granule formation, and mediates survival upon arsenite exposure. J Biol Chem. 2005 Apr 29;280(17):16925–33.
33. Suragani RNVS, Zachariah RS, Velazquez JG, Liu S, Sun CW, Townes TM, et al. Heme-regulated eIF2α kinase activated Atf4 signaling pathway in oxidative stress and erythropoiesis. Blood. 2012 May 31;119(22):5276–84.
34. Harding HP, Zhang Y, Zeng H, Novoa I, Lu PD, Calfon M, et al. An integrated stress response regulates amino acid metabolism and resistance to oxidative stress. Mol Cell. 2003 Mar;11(3):619–33.
35. Martín R, Berlanga JJ, de Haro C. New roles of the fission yeast eIF2α kinases Hri1 and Gcn2 in response to nutritional stress. J Cell Sci. 2013 Jul 15;126(14):3010–20.

36. Taniuchi S, Miyake M, Tsugawa K, Oyadomari M, Oyadomari S. Integrated stress response of vertebrates is regulated by four eIF2α kinases. Sci Rep. 2016 Sep 16;6(1):32886.
37. Kimball SR, Fabian JR, Pavitt GD, Hinnebusch AG, Jefferson LS. Regulation of Guanine Nucleotide Exchange through Phosphorylation of Eukaryotic Initiation Factor eIF2α: ROLE OF THE α- AND δ-SUBUNITS OF eIF2B *. J Biol Chem. 1998 May 22;273(21):12841–5.
38. Khong A, Matheny T, Jain S, Mitchell SF, Wheeler JR, Parker R. The Stress Granule Transcriptome Reveals Principles of mRNA Accumulation in Stress Granules. Mol Cell. 2017 Nov 16;68(4):808-820.e5.
39. Ivanov P, Kedersha N, Anderson P. Stress Granules and Processing Bodies in Translational Control. Cold Spring Harb Perspect Biol. 2019 May;11(5):a032813.
40. Markmiller S, Soltanieh S, Server KL, Mak R, Jin W, Fang MY, et al. Context-Dependent and Disease-Specific Diversity in Protein Interactions within Stress Granules. Cell. 2018 Jan 25;172(3):590-604.e13.
41. Bordeleau ME, Cencic R, Lindqvist L, Oberer M, Northcote P, Wagner G, et al. RNA-Mediated Sequestration of the RNA Helicase eIF4A by Pateamine A Inhibits Translation Initiation. Chem Biol. 2006 Dec 1;13(12):1287–95.
42. Liu B, Han Y, Qian SB. Cotranslational response to proteotoxic stress by elongation pausing of ribosomes. Mol Cell. 2013 Feb 7;49(3):453–63.
43. Shalgi R, Hurt JA, Krykbaeva I, Taipale M, Lindquist S, Burge CB. Widespread Regulation of Translation by Elongation Pausing in Heat Shock. Mol Cell. 2013 Feb;49(3):439–52.
44. Liu B, Qian SB. Translational reprogramming in stress response. Wiley Interdiscip Rev RNA. 2014 May;5(3):301–5.
45. Zhang X, Gao X, Coots RA, Conn CS, Liu B, Qian SB. Translational control of the cytosolic stress response by mitochondrial ribosomal protein L18. Nat Struct Mol Biol. 2015 May;22(5):404–10.
46. Choi A, Barrientos A. Reevaluating the role of human mitochondrial uL18m in the cytosolic stress response. Nat Struct Mol Biol. 2021 Jun;28(6):474–5.
47. Zhang X, Ji Q, Qian SB. Reply to: Reevaluating the role of human mitochondrial uL18m in the cytosolic stress response. Nat Struct Mol Biol. 2021 Jun;28(6):476–7.
48. Meyer KD, Patil DP, Zhou J, Zinoviev A, Skabkin MA, Elemento O, et al. 5′ UTR m6A Promotes Cap-Independent Translation. Cell. 2015 Nov;163(4):999–1010.
49. Zhou J, Wan J, Gao X, Zhang X, Jaffrey SR, Qian SB. Dynamic m6A mRNA methylation directs translational control of heat shock response. Nature. 2015 Oct;526(7574):591–4.
50. Coots RA, Liu XM, Mao Y, Dong L, Zhou J, Wan J, et al. m6A Facilitates eIF4F-Independent mRNA Translation. Mol Cell. 2017 Nov 2;68(3):504-514.e7.
51. Guca E, Alarcon R, Palo MZ, Santos L, Alonso-Gil S, Davyt M, et al. N6-methyladenosine in 5' UTR does not promote translation initiation. Mol Cell. 2024 Jan 15;S1097-2765(23)01074-2.
52. Mateju D, Franzmann TM, Patel A, Kopach A, Boczek EE, Maharana S, et al. An aberrant phase transition of stress granules triggered by misfolded protein and prevented by chaperone function. EMBO J. 2017 Jun 14;36(12):1669–87.
53. Rubtsova MP, Sizova DV, Dmitriev SE, Ivanov DS, Prassolov VS, Shatsky IN. Distinctive Properties of the 5′-Untranslated Region of Human Hsp70 mRNA*. J Biol Chem. 2003 Jun 20;278(25):22350–6.

54. Somero GN. RNA thermosensors: how might animals exploit their regulatory potential? J Exp Biol. 2018 Feb 22;221(4):jeb162842.
55. Svitkin YV, Siddiqui N, Sonenberg N. Protein Synthesis Initiation in Eukaryotes: IRES-mediated Internal Initiation. In: Encyclopedia of Life Sciences [Internet]. John Wiley & Sons, Ltd; 2015 [cited 2024 Jan 25]. p. 1–11. Available from: https://onlinelibrary.wiley.com/doi/abs/10.1002/9780470015902.a0000544.pub3
56. Sun C, Querol-Audí J, Mortimer SA, Arias-Palomo E, Doudna JA, Nogales E, et al. Two RNA-binding motifs in eIF3 direct HCV IRES-dependent translation. Nucleic Acids Res. 2013 Aug;41(15):7512–21.
57. Fernández IS, Bai XC, Murshudov G, Scheres SHW, Ramakrishnan V. Initiation of translation by cricket paralysis virus IRES requires its translocation in the ribosome. Cell. 2014 May 8;157(4):823–31.
58. Jan E, Sarnow P. Factorless ribosome assembly on the internal ribosome entry site of cricket paralysis virus. J Mol Biol. 2002 Dec 13;324(5):889–902.
59. Wang W, Liu F, Ugalde MV, Pyle AM. A compact regulatory RNA element in mouse Hsp70 mRNA. BioRxiv Prepr Serv Biol. 2023 Aug 9;2023.02.22.529618.
60. Cuella-Martin R, Hayward SB, Fan X, Chen X, Huang JW, Taglialatela A, et al. Functional interrogation of DNA damage response variants with base editing screens. Cell. 2021 Feb 18;184(4):1081-1097.e19.
61. Sun J, Conn CS, Han Y, Yeung V, Qian SB. PI3K-mTORC1 Attenuates Stress Response by Inhibiting Cap-independent Hsp70 Translation. J Biol Chem. 2011 Feb 25;286(8):6791–800.
62. Balakrishnan K, De Maio A. Heat shock protein 70 binds its own messenger ribonucleic acid as part of a gene expression self-limiting mechanism. Cell Stress Chaperones. 2006 Mar;11(1):44–50.
63. Van Nieuwenhoven FA, Martin X, Heijnen VVT, Cornelussen RN, Snoeckx LHEH. HSP70-mediated acceleration of translational recovery after stress is independent of ribosomal RNA synthesis. Eur J Cell Biol. 2001 Sep 1;80(9):586–92.
64. McGarry TJ, Lindquist S. The preferential translation of Drosophila hsp70 mRNA requires sequences in the untranslated leader. Cell. 1985 Oct 1;42(3):903–11.
65. Joshi-Barve S, Benedetti AD, Rhoads RE. Preferential translation of heat shock mRNAs in HeLa cells deficient in protein synthesis initiation factors eIF-4E and eIF-4 gamma. J Biol Chem. 1992 Oct 15;267(29):21038–43.
66. Thoreen CC, Kang SA, Chang JW, Liu Q, Zhang J, Gao Y, et al. An ATP-competitive Mammalian Target of Rapamycin Inhibitor Reveals Rapamycin-resistant Functions of mTORC1. J Biol Chem. 2009 Mar 20;284(12):8023–32.
67. Quaresma AJC, Sievert R, Nickerson JA. Regulation of mRNA export by the PI3 kinase/AKT signal transduction pathway. Mol Biol Cell. 2013 Apr 15;24(8):1208–21.
68. Cencic R, Pelletier J. Hippuristanol - A potent steroid inhibitor of eukaryotic initiation factor 4A. Transl Austin Tex. 2016 Jun;4(1):e1137381.
69. Bordeleau ME, Mori A, Oberer M, Lindqvist L, Chard LS, Higa T, et al. Functional characterization of IRESes by an inhibitor of the RNA helicase eIF4A. Nat Chem Biol. 2006 Apr;2(4):213–20.
70. Wilson JE, Pestova TV, Hellen CUT, Sarnow P. Initiation of Protein Synthesis from the A Site of the Ribosome. Cell. 2000 Aug 18;102(4):511–20.

71. Wek RC, Jiang HY, Anthony TG. Coping with stress: eIF2 kinases and translational control. Biochem Soc Trans. 2006 Feb;34(Pt 1):7–11.
72. Jousse C, Oyadomari S, Novoa I, Lu P, Zhang Y, Harding HP, et al. Inhibition of a constitutive translation initiation factor 2alpha phosphatase, CReP, promotes survival of stressed cells. J Cell Biol. 2003 Nov 24;163(4):767–75.
73. Boyce M, Bryant KF, Jousse C, Long K, Harding HP, Scheuner D, et al. A Selective Inhibitor of eIF2α Dephosphorylation Protects Cells from ER Stress. Science. 2005 Feb 11;307(5711):935–9.
74. Rollins MG, Shasmal M, Meade N, Astar H, Shen PS, Walsh D. Negative charge in the RACK1 loop broadens the translational capacity of the human ribosome. Cell Rep. 2021 Sep 7;36(10):109663.
75. Jia L, Qian SB. A Versatile eIF3d in Translational Control of Stress Adaptation. Mol Cell. 2021 Jan 7;81(1):10–2.
76. Lee AS, Kranzusch PJ, Doudna JA, Cate JHD. eIF3d is an mRNA cap-binding protein that is required for specialized translation initiation. Nature. 2016 Aug 4;536(7614):96–9.
77. Lamper AM, Fleming RH, Ladd KM, Lee ASY. A phosphorylation-regulated eIF3d translation switch mediates cellular adaptation to metabolic stress. Science. 2020 Nov 13;370(6518):853–6.
78. Costantino DA, Pfingsten JS, Rambo RP, Kieft JS. tRNA–mRNA mimicry drives translation initiation from a viral IRES. Nat Struct Mol Biol. 2008 Jan;15(1):57–64.
79. Reeves R, Gorman CM, Howard B. Minichromosome assembly of non-integrated plasmid DNA transfected into mammalian cells. Nucleic Acids Res. 1985 May 24;13(10):3599–615.
80. Recillas-Targa F. Multiple strategies for gene transfer, expression, knockdown, and chromatin influence in mammalian cell lines and transgenic animals. Mol Biotechnol. 2006 Nov 1;34(3):337–54.
81. Hunt CR, Dix DJ, Sharma GG, Pandita RK, Gupta A, Funk M, et al. Genomic Instability and Enhanced Radiosensitivity in Hsp70.1- and Hsp70.3-Deficient Mice. Mol Cell Biol. 2004 Jan 15;24(2):899–911.
82. Lu J, Deutsch C. Electrostatics in the ribosomal tunnel modulate chain elongation rates. J Mol Biol. 2008 Dec 1;384(1):73–86.
83. Babendure JR, Babendure JL, Ding JH, Tsien RY. Control of mammalian translation by mRNA structure near caps. RNA N Y N. 2006 May;12(5):851–61.
84. Sticht C, Torre CDL, Parveen A, Gretz N. miRWalk: An online resource for prediction of microRNA binding sites. PLOS ONE. 2018 Oct 18;13(10):e0206239.
85. Chahal J, Gebert LFR, Gan HH, Camacho E, Gunsalus KC, MacRae IJ, et al. miR-122 and Ago interactions with the HCV genome alter the structure of the viral 5' terminus. Nucleic Acids Res. 2019 Jun 4;47(10):5307–24.
86. Ma S, Liu JY, Zhang JT. eIF3d: A driver of noncanonical cap–dependent translation of specific mRNAs and a trigger of biological/pathological processes. J Biol Chem. 2023 May 1;299(5):104658.
87. Wagner S, Herrmannová A, Malík R, Peclinovská L, Valášek LS. Functional and biochemical characterization of human eukaryotic translation initiation factor 3 in living cells. Mol Cell Biol. 2014 Aug;34(16):3041–52.
88. Feder JH, Rossi JM, Solomon J, Solomon N, Lindquist S. The consequences of expressing hsp70 in Drosophila cells at normal temperatures. Genes Dev. 1992 Aug 1;6(8):1402–13.

89. Kumar S, Stokes J, Singh UP, Gunn KS, Acharya A, Manne U, et al. Targeting Hsp70: A possible therapy for cancer. Cancer Lett. 2016 Apr 28;374(1):156–66.
90. Stephenson W, Razaghi R, Busan S, Weeks KM, Timp W, Smibert P. Direct detection of RNA modifications and structure using single-molecule nanopore sequencing. Cell Genomics. 2022 Feb 9;2(2):100097.
91. Kortmann J, Narberhaus F. Bacterial RNA thermometers: molecular zippers and switches. Nat Rev Microbiol. 2012 Apr;10(4):255–65.
92. Waldminghaus T, Gaubig LC, Klinkert B, Narberhaus F. The Escherichia coli ibpA thermometer is comprised of stable and unstable structural elements. RNA Biol. 2009;6(4):455–63.
93. Chowdhury S, Ragaz C, Kreuger E, Narberhaus F. Temperature-controlled structural alterations of an RNA thermometer. J Biol Chem. 2003 Nov 28;278(48):47915–21.
94. Lionnet T, Czaplinski K, Darzacq X, Shav-Tal Y, Wells AL, Chao JA, et al. A transgenic mouse for in vivo detection of endogenous labeled mRNA. Nat Methods. 2011 Feb;8(2):165–70.
95. Sanjana NE, Shalem O, Zhang F. Improved vectors and genome-wide libraries for CRISPR screening. Nat Methods. 2014 Aug;11(8):783–4.
96. Alagar Boopathy LR, Beadle E, Xiao AR, Garcia-Bueno Rico A, Alecki C, Garcia de-Andres I, et al. The ribosome quality control factor Asc1 determines the fate of HSP70 mRNA on and off the ribosome. Nucleic Acids Res. 2023 Jul 7;51(12):6370–88.
97. Jacob-Tomas S, Alagar Boopathy LR, Vera M. Using Single-Molecule Fluorescence Microscopy to Uncover Neuronal Vulnerability to Protein Damage. Methods Mol Biol Clifton NJ. 2022;2515:237–54.
98. Mueller F, Senecal A, Tantale K, Marie-Nelly H, Ly N, Collin O, et al. FISH-quant: automatic counting of transcripts in 3D FISH images. Nat Methods. 2013 Apr;10(4):277–8.
99. Gandin V, Sikström K, Alain T, Morita M, McLaughlan S, Larsson O, et al. Polysome fractionation and analysis of mammalian translatomes on a genome-wide scale. J Vis Exp JoVE. 2014 May 17;(87):51455.
100. Coudert L, Adjibade P, Mazroui R. Analysis of Translation Initiation During Stress Conditions by Polysome Profiling. J Vis Exp JoVE. 2014 May 19;(87):51164.
101. Amador-Cañizares Y, Bernier A, Wilson JA, Sagan SM. miR-122 does not impact recognition of the HCV genome by innate sensors of RNA but rather protects the 5′ end from the cellular pyrophosphatases, DOM3Z and DUSP11. Nucleic Acids Res. 2018 Jun 1;46(10):5139–58.

CHAPTER 4: GENERAL DISCUSSION

Since the discovery of the transcription factor HSF1, it has been well-accepted that the induction of the heat shock response is mainly regulated at the transcription levels and that HSF1 is its master regulator in eukaryotic cells (121). Our work in yeast and mammalian cells demonstrates that the posttranscriptional regulation of the inducible *Hsp70* mRNAs plays an essential role in fine-tuning the production of the inducible HSP70 protein. This posttranscriptional regulation of the inducible HSP70 expression is encoded in its genetic material and plays a dual role: repressing the inducible *Hsp70* mRNA translation under homeostatic conditions and activating it upon heat shock (99). Remarkably, the coding sequence emerges as an important cis-regulatory element in the regulation of the inducible *Hsp70* mRNA translation. However, the regulatory mechanisms governing the output of *Hsp70* mRNA translation in yeast and mammalian cells are different, probably reflecting the increased complexity of mammalian systems when compared to yeast.

In this section, I will mainly discuss the three key conclusions from my work and what are the relevant open questions that we have to address. First, I will discuss the regulatory elements that are embedded in the CDS of inducible HSP70 controlling its expression through RQC during heat shock. Second, the structural and sequence elements that are responsible for mammalian inducible HSP70 synthesis during heat shock. Third, the fate of inducible *Hsp70* mRNA during recovery by comparing the differences in the translation profile and degradation in yeast and mammalian cells. As I discuss these points, I will highlight the novel roles of factors that appear as cytosolic master regulators of the HSR and probably balance the extremely high transcriptional induction of HSP70 during heat shock to navigate a cytosolic environment that is not optimal for translation.

4.1 Role of coding sequence on HSP70 expression through RQC

In Chapter 2, we explored the function of the inducible *Hsp70* mRNA coding sequence in regulating its expression upon heat shock in yeast. We identified that the CDS of the inducible *Hsp70* mRNA, *SSA4,* is rich in non-optimal codons. The non-optimal codons cause ribosome stalling during heat shock as the ribosome has to wait longer for cognate-tRNA to arrive at the site of protein synthesis. The ribosomal stalling results in a collision with subsequent ribosomes, which are then resolved by an mRNA surveillance pathway, RQC. Despite the cellular efforts to increase *SSA4* mRNA levels, we discovered an unexpected inhibition of Ssa4p expression by the CDS, which initiates the RQC mechanism. This observation suggests that cells exhibit a regulatory mechanism aimed at conserving energy resources by limiting the synthesis of excessive Ssa4p beyond what is necessary to restore proteostasis. Since translation is a metabolically demanding process, prioritization of energy conservation gains significance, especially under conditions of cellular stress (122,123).

RQC regulation of Ssa4p is mediated by the following key factors in yeast: Asc1p, Hel2p, Mbf1p, and Slh1p. These factors recognize and stabilize the ribosome collision and trigger a series of downstream events to inhibit translation, prevent frameshifting, disassemble ribosome subunits mRNA decay and degrade the nascent polypeptide chain (99,124–130).

4.1.1 The emerging role of Asc1 as a master regulator of HSR

We have uncovered a novel role for Asc1p in yeast as a pivotal regulator of the HSR, complementing the well-established function of HSF1 as a master transcription factor. Asc1p exerts its regulatory influence on the HSR through three distinct mechanisms. Firstly, it suppresses the translation of *SSA4* mRNA during heat shock via the RQC mechanism. Secondly, Asc1p

facilitates the attenuation of HSR by destabilizing *SSA4* mRNA during recovery, a process independent of RQC or Asc1p ribosome binding activity. Lastly, Asc1p demonstrates a pro-survival function during heat shock, which operates independently of ribosome association or Ssa4p expression levels.

Prior investigations have highlighted the heightened sensitivity of *ASC1-deleted* yeast strains to heat shock (131). Beyond its ribosomal functions, cytoplasmic-free Asc1p contributes to PB formation under stress conditions and aids in maintaining cell wall integrity during budding in yeast (131). These non-ribosomal functions of Asc1p could facilitate cell survival which we plan to understand in the future. Through physical interaction analysis from the Saccharomyces Genome Database, Asc1p associates with various factors in cell wall biogenesis, remodeling and integrity such as Nab6p, Fks1p, Slt2p, and Kin2p as well as chaperones, and cytoskeleton proteins (132). Thus, Asc1p emerges as a pivotal mediator in aligning cellular status with growth by orchestrating cytoskeletal reorganization and facilitating cell wall synthesis. We plan to perform growth assay in the yeast strains depleted of cell wall remodelling factors to evaluate their function on cell survival under normal and heat shock conditions.

Notably, Asc1p deleted strains overexpressed Ssa4p levels. However, the excessive Ssa4p did not help the cells overcome the dependency on Asc1p for repairing the cell wall damage created by stress. Thus, in the absence of Asc1p the yeast strains show poor survival to stress conditions.

4.1.2 Discovery of novel RQC factors Rps19b and Rps28a

Asc1p plays a central role in the RQC mechanism by binding to the 40S ribosomal subunits of collided ribosomes which is essential to recruit the downstream components of this quality control mechanism. In our Asc1p IP experiment, we discovered two additional RQC factors that operate during heat shock, Rps19 and Rps28. The precise functions of these ribosomal proteins are not

fully understood, but their interaction with Asc1p is significantly enriched during heat shock. We speculate that these ribosomal proteins may contribute to collision stabilization in conjunction with Asc1p. It is likely that the structure of the disome or the interaction among the ribosomal components may vary during heat shock to favor the interaction of Asc1p with Rps19b and Rps28a and deliver their function in RQC. Through experimentation in yeast, we tested the RQC function of Rps19b and Rps28a using stalling reporters containing GFP-K12-HIS or GFP-R12-HIS under permissive conditions (99).

While stalling reporter mRNAs are being translated, the presence of polybasic stretches can induce ribosome stalling, thereby hindering the synthesis of full-length proteins. In the absence of stress, we observed that the deletion of Rps19b resulted in the production of more full-length proteins with both polybasic reporters compared to wild-type strains. This observation underscores the involvement of Rps19b in the RQC mechanism under permissive conditions as well as heat shock. However, Rps28a promoted stalling of the only R12 reporter but not the K12 reporter in the absence of stress. This discrepancy suggests that Rps28a may demonstrate substrate preference or respond differently based on the cellular state, such as heat shock (99). In future investigations, we aim to elucidate whether the mammalian orthologs of ribosomal proteins eS19 and eS28 retain their RQC function in mammalian systems during normal conditions and heat shock. Single particle Cryo-EM studies performed in mammalian cells of ribosome collisions identified two primary interfaces where the stalled and collided 40S ribosomes interact (133). The first interface includes RACK1 (Asc1 ortholog) of stalled ribosome and interactions with ribosomal proteins eS3, eS10 and uS10 (Rps3, Rps10, and Rps20 in yeast) of collided ribosome. The second interface is where the ribosomal protein eS28 (as well eS1, uS11, eS26) of stalled ribosome interacts with 18S rRNA and uS4 of the collided ribosome. This direct physical interaction between eS28 of

stalled ribosome and 18S rRNA of collided ribosome signifies a promising role for eS28 in RQC perhaps in collision stabilization (133). It is likely that eS28 might function in RQC both in the absence and presence of stress which is different from its yeast ortholog Rps28a.

4.1.3 Ubiquitination by E3 ubiquitin ligase, Hel2

Ribosome biogenesis encompasses numerous stages, including transcription, post-transcriptional modifications, and translational events, all of which contribute to its intricate assembly. Clearly, ribosome biogenesis is an energy-intensive process (134–136). Therefore, the primary role of RQC is to release ribosomal subunits from aberrant mRNAs with collided ribosomes. This event is initiated by Hel2p-mediated ubiquitination of ribosomal proteins on the collided ribosomes (125). The E3 ligase Hel2p binds to the platform provided by the binding of two Asc1p at the collided ribosomes and ubiquitinates ribosomal proteins in the vicinity such as Rps20, Rps7, and Rps3 in yeast (137–141). Interestingly, neither mutation of ubiquitination sites on Rps20 (K6/8R) nor knockdown of Rps7b affected Ssa4p expression (99). Furthermore, in experiments conducted by our postdoctoral researcher, Dr. Celia Alecki, we did not detect ubiquitination marks on Rps3 via western blot analysis (data not shown). Consequently, the specific ribosomal proteins undergoing ubiquitination under heat shock conditions in the *SSA4* mRNA remain unidentified.

To identify the ubiquitinated ribosomal proteins, we will look into ribosomal proteins proximal to the Hel2p binding site on the ribosomes by performing structural analysis on isolated disomes during heat shock would provide valuable insights to identify the novel ubiquitination sites. We will also investigate the lysine residues of newly identified RQC factors such as Rps19b and Rps28a by mutating potential lysine residues for ubiquitination. Further, we could refer to our Asc1p-IP data and screen for more ribosomal proteins. These experiments will help us to discern the targets of Hel2p during heat shock.

4.1.4 Dual role of Mbf1p in yeast

The ribosome collisions send a feedback signal to inhibit the translation initiation of the *SSA4* mRNA through a mechanism in yeast that we still do not understand (124,142). Studies conducted in mammalian cells revealed that during ribosome collisions, the mammalian ortholog of Hel2p, ZNF598 recruits GIGYF2 that binds to 4EHP, which competitively inhibits eIF4E binding to the mRNA 5'cap (143). This complex is bound by the collision sensor Mbf1p, EDF1 in mammals, to prevent ribosome frameshifting and feedback to translation initiation repression (130,142). However, yeasts lack the 4EHP ortholog and we demonstrated that the GIGYF2 orthologs in yeast (Smy2 and Syh1p) do not function in feedback inhibition of translation initiation. Although Mbf1p has been proposed to serve only on mRNA frameshifting, we speculate that Mbf1p might interact with other proteins to repress translation initiation (129,144). For example, the protein Whi3p is among the physical interactors of Mbf1p and has been shown to modulate the translation efficiency of other mRNAs, such as *CLN3*. The *CLN3* mRNA encodes a G1 to S phase cyclin, whose expression must be tightly regulated in yeast to advance to the next phase of the cell cycle. The transient expression pattern of *CLN3* mRNA resembles that of *SSA4* mRNA, suggesting that Whi3p is a promising candidate for investigating feedback inhibition of translation (145). As such, the feedback from the RQC to translation initiation might also operate in yeast but with different players. It is also possible that the Mbf1p interactome changes upon heat stress and binds to factors that have not been considered before. By performing a pulldown of Mbf1p during heat shock, we could identify the factors involved in the feedback regulation of *SSA4* mRNA translation initiation.

4.1.5 Mechanism of translation induction of *SSA4* mRNA during heat shock

Despite the global translation repression during heat shock, a question arises: How do cells discern *SSA4* mRNA and selectively initiate its translation? In yeast, the 5' UTR of *SSA4* mRNA is notably 72% AU rich (118). Moreover, in yeast, an unstructured A-rich region within the 5' UTR has been demonstrated to facilitate cap-independent translation by recruiting the PolyA binding protein Pab1p to the poly-A region in the 5' UTR (146). Since we found that the 5' UTR of *SSA4* mRNA possesses A-rich region but not in *SSA2* mRNA (constitutive HSP70 in yeast), we are currently investigating if the functions of A-rich region function prompt a preferential translation of *SSA4* mRNA during heat shock, this investigation includes truncation mutations in the 5' UTR of *SSA4* mRNA to further elucidate the role of the A-rich region in facilitating selective translation during heat shock. Then, we will use the Auxin-Degron system to deplete temporally Pab1p and determine its role in the initiation of *SSA4* mRNA translation (147–149).

4.1.6 Mechanism of translation repression of *SSA4* mRNA during physiological conditions

By optimizing the CDS of SSA4, we have discovered that its translation is also regulated under homeostatic conditions. In this case, translation is repressed by the non-optimal *SSA4* codon sequence. An ongoing project in the lab is to define the mechanism by which the CDS feedback inhibits translation and the repressors involved in such mechanism. It appears that the inherent property of *SSA4* mRNA CDS is designated to counteract the spurious expression of Ssa4p in the event of leaky transcription under permissive conditions. This signifies the presence of another mechanism in action to control the Ssa4p synthesis and is independent of RQC because deletion of RQC factors does not lead to Ssa4p induction under homeostatic conditions. Interestingly, the CDS of optimized *SSA4* mRNA resembles that of *SSA2* mRNA which is 78% optimal. This might

imply that an unknown factor is regulating the spurious expression of Ssa4p by binding to the CDS and coordinating with the 5'UTR in the absence of stress. We are in the process of identifying these factors by performing a pull down of factors interacting with *SSA4* and *SSA2* (as a control) 5'UTR sequences followed by mass spectrometry analysis. From the factors that we will identify, we plan to validate their effect by performing gene deletion or temporal depletion with the auxin degron system by looking at the Ssa4p expression in the absence of stress. The experimental outcomes we expect to identify the mechanism that controls the undesired expression of Ssa4p under physiological conditions. Yeast cells are not as sensitive to unwanted Ssa4p expression in the absence of stress as seen from our growth assay in codon-optimized *SSA4* mRNA (99). However, the undesired expression of inducible HSP70 is cytotoxic in mammalian cells and causes growth defects in *D. melanogaster* (114,150,151). We intend to investigate whether this regulatory mechanism is conserved in mammalian cells and to elucidate how cancer cells evade this regulation for their own benefit.

4.2 Role of the 5' UTR and CDS on HSPA1A expression in MEFs

Unlike yeast, *Hspa1a* mRNA CDS in mouse is highly optimal (78%). Since the non-optimality was not conserved over the evolution, the function of RACK1 (Asc1 ortholog) in HSR was not conserved. Through the knockdown of RACK1 in MEFs, we have demonstrated that RACK1 failed to mediate the stability or translation of *Hspa1a* mRNA (**Figure 3.3**).

In higher eukaryotes, the degree of complexity in the regulation of HSP70 expression increases. The 5' UTR of *Hspa1a* mRNAs in mice are inherently biased towards higher GC content (72%) suggesting a likelihood of forming secondary structure (152). Highly structured regions (termed IRES) are typically a secondary structure or a tertiary structure on mRNA. The translation initiation of the highly structured mRNAs is poor under physiological conditions due

to inefficient ribosome scanning (153,154). However, these structures provide an advantage of direct ribosome recruitment at the start codon without the need for ribosome scanning in conditions when translation initiation factors are deficient in cells such as during stress (155–157). For instance, viral mRNAs are known to have IRESs for their translation in the host cell without initiation factors (156,157). Similar to viral RNAs, initial studies conducted in HeLa cells identified that the *Hspa1a* mRNA could translate with no requirement of eIF4G and eIF4E cap recognition factors (158).

Despite a decade-long effort, studies have failed to determine the IRES on 5'UTR of *Hsp70* mRNA. Those studies have limited themselves by looking only at the 5'UTR region and under non-stress conditions. As there are IRESs formed in the intergenic region (such as HCV and CrPV), we considered a portion of the CDS (102 nts) along with 5'UTR of *Hspa1a* mRNA in our approach to characterize the structure formed during heat shock. Through *in vitro* SHAPE analysis, Pyle's group described that the 5'UTR with 102 nts of CDS could form a heat-inducible stable structure. Using luciferase constructs, we elucidated that 102 nts of the CDS is participating in the induction of translation along with the 5'UTR. The results suggest a role for the CDS in translation induction, however, there is not enough evidence to conclude the presence of an IRES. We can achieve this in several ways (1) using traditional bicistronic vector replacing luciferase reporter with GFP which is compatible with heat shock followed by the *Hspa1a* mRNA (2) doing live-cell SHAPE analysis of *Hspa1a* mRNA during heat shock (3) determining its structure using nanopore sequencing of the mRNA and (4) performing UV crosslinking followed by CryoEM to analyze the three-dimensional folding of the mRNA during heat shock. From these experiments, we can conclude if there is an IRES on the *Hspa1a* mRNA formed during heat shock.

In addition to that, we performed cellular validation of the stem-loops H1, H4, and H6 described to trigger the formation of a compact structure by Pyle's group. However, unzipping these stem loops did not influence the *Hspa1a* mRNA translation during HS. These discrepancies between *in vitro* and *in vivo* data could happen because cellular regulatory factors such as RBPs and miRNAs are absent in in vitro setup.

Nonetheless, we identified that the stem loop H1 proximal to the 5' cap inhibits the cap-dependent translation under permissive conditions. This suggests that mammalian cells possess a mechanism to control the undesirable expression of HSPA1A in the absence of stress similar to yeast. However, we do not know the structure of human *Hspa1a* mRNA. Given that the GC content and the length are relatively similar to the mouse *Hspa1a* mRNA, we expect a similar behavior that we will analyze using human cell lines and doing in-vitro SHPAE analysis with the human *Hspa1a* mRNA sequence (**Fig 3.7**).

Our *in vivo* validation of the in *vitro* data did not yield a candidate stem loop or region associated with HSPA1A expression during heat shock. Hence, we used the CRISPR-Cas9 single base editing approach to identify critical regions for the *Hspa1a* mRNA translation that do not essentially land on the structure. Interestingly, we identified several regions targeted by sgRNAs (179-181, 146-147, 231, and 309-312) within the 5'UTR and 102 nts of CDS that significantly decreased the HSP70 expression (**Fig 4.1**). The editing in the CDS by sg5 introduces an amino acid change E27K. Notably, C237T modification by sg12 affects the CDS but does not introduce any change in amino acid also influences translation of *Hspa1a* mRNA during heat shock. Thus, we plan to detect the structure of the *Hspa1a* mRNAs with the modification in positions 146-147, 179-181 and 309-312 using mRNA nanopore sequencing. We expect to determine whether the above-mentioned regions are vital for the formation of a tertiary structure.

Interestingly, sg19 and sg24 landing on a region of 24 nts repeats regions surrounded by C/U rich motifs sequence (117-141 and 150-174) also reduced the HSPA1A expression. This region could regulate translation in two possible means. First, this region spans two binding sites for a Mir-30c-1-3p and both sgRNAs mutated 3 and 2 nts, respectively, on the target sequence of Mir-30c-1-3p. The binding of miRNA could promote translation in through the recruitment of Ago2-mediated conformation change on the RNA to an IRES as described on HCV viral RNA (159). Alternatively or additionally, the 24 repeat regions possess site for poly(rC)-binding protein1 and 2 (PCBP1 and PCBP2) which is a translation activator in Type I PV IRES (160,161). We are yet to explore both the possibilities of miRNA and PCBPs binding. We plan to start by checking for the expression level of Mir-30c-1-3p in MEFs. We will also create a Mir-30c-1-3p binding mutant by changing its binding sequence on the *Hspa1a* mRNA. We will transiently transfect the mutant plasmid in *HSPA1A/1B*-null MEFs followed by assessing the HSPA1A expression by western blot during no stress and heat shock conditions. We expect reduced HSPA1A expression to validate the miRNA function on translation. To explore our second possibility, we will do an RNA-immunoprecipitation (RIP) followed by mass spectrometry. We expect to see a significantly enriched interaction with PCBP1 and PCBP2 during heat shock. In addition, we will knock down PCBP1 and PCBP2 expression using shRNAs, which should decrease the induction of HSPA1A upon heat shock.

Together, our work has revealed the participation of CDS in the HSPA1A induction and critical sequence elements on the 5'UTR mediating the formation of functional structure for HSPA1A expression during heat shock although further experimental validation is required.

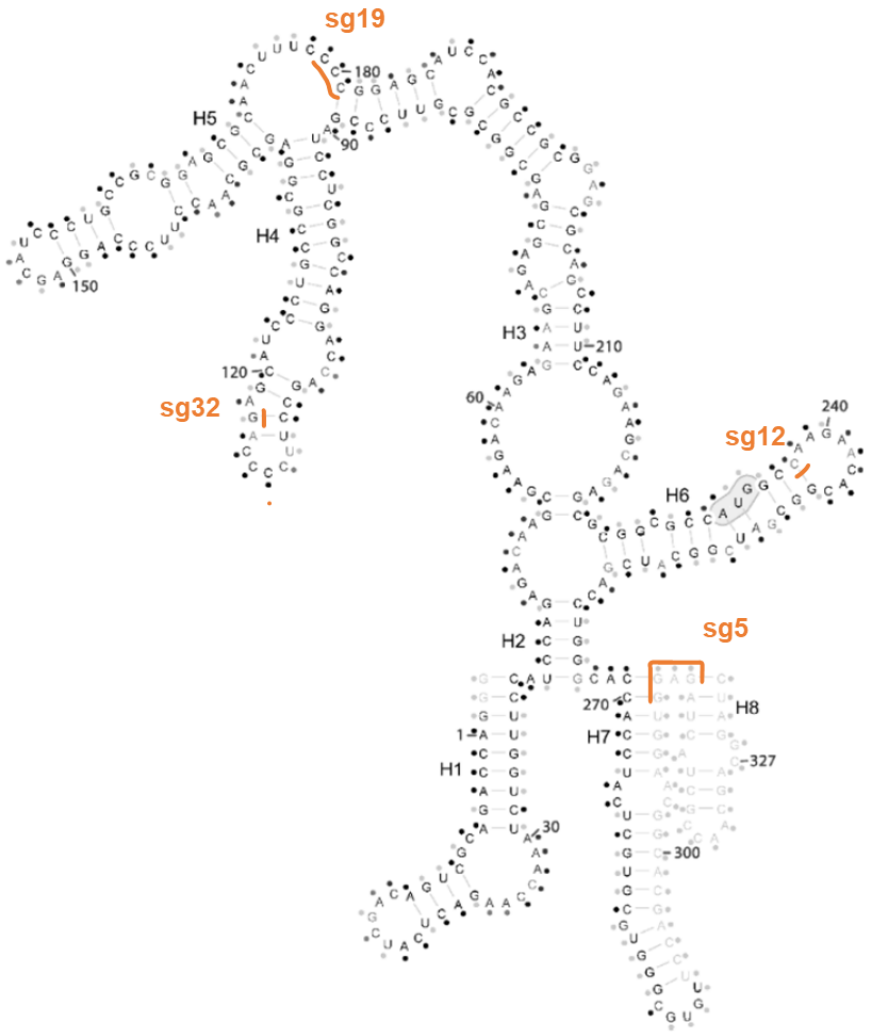

Figure 4.1. Representation of base editing by sgRNAs on the *In vitro* SHAPE structure of *Hsp70* mRNA from Pyle's group. Shown here are the sequences edited by sg5, 6, 12, 19 and 32 which decreases the HSP70 expression. The sg5 makes three G to A mutations in 309-312, sg6 makes three C to T mutations in 269-272, sg12 edits C to T at position 237, sg19 edits three bases from C to T in 179-181 and sg32 makes one G to A edit at position 117.

4.2.1 How does *Hspa1a* mRNA differ from other known IRESs?

Viral IRESs were first identified in 1988 picornaviral family of RNAs by two different groups in Encephalomyelitis virus (EMCV) and Polio Virus (PV), respectively (156,157). These viral mRNAs are known for undergoing translation without a 5' m7G cap or certain initiation factors. The viral IRESs are of several classes, the one that is of interest to us is Type IV IRES of Cricket

paralysis virus (CrPV) located in between coding sequences i.e., intergenic and can recruit ribosome for translation devoid of translation initiation factors and ribosome scanning.

A decade after the discovery of viral IRESs, cellular IRESs were identified and are shown to translate during the conditions of stress. The first cellular IRES described was human *BiP* (immunoglobulin heavy chain-binding protein) mRNA also known as GRP78 (glucose-regulated protein 78), an ER-localized HSP70 (162). BiP is responsible for the folding of secretory proteins and misfolded proteins in the ER (163). Similar to HSPA1A, the expression of BiP is tightly regulated at the level of both transcription and translation. Apart from the inherent levels of *BiP* mRNA within the cell, the onset of ER stress induces *BiP* mRNA synthesis as well its selective translation (164–167). Following the discovery of the *BiP* IRES, several cellular IRESs were reported with the use of bicistronic vectors and observing the translational output of the cistron located downstream of presumed IRES elements. Although no common structure or sequence has been identified among cellular IRESs, they undergo a low rate of translation during physiological conditions and the translation efficiency is greatly increased during mitosis and stress conditions (109,110). Some of the examples of cellular IRESs include factors involved in various cellular processes including vascular endothelial growth factor (VEGF), proto-oncogene and transcription factor c-myc, and X-linked inhibitor of apoptosis (XIAP) (170–174). The cellular IRES element have been reported to form in the 5'UTR and they have different requirements of translation initiation factors and/or IRES *trans*- acting factors (ITAFs) (162,175,176). Some cellular IRESs during stress conditions deplete the initiation factors, and so they require only ITAFs. For example, *BiP* and *XIAP* mRNA translation is enhanced in the presence of La antigen (176,177). On the other hand, the *c-myc* IRES-mediated translation do require both initiation factors - eIF4A, eIF3 and mRNA binding protein, hnRNP as ITAF to stimulate the translation (173).

The 5'UTR of these mRNA has been described to hold IRES activity influencing cell survival, proliferation and apoptosis (178). However, the existence of cellular IRESs remains a subject of debate, largely due to discrepancies in the bicistronic reporter system employed to investigate the cellular IRES. First, unlike Viral IRES elements, cellular IRESs lack structural evidence demonstrating their interaction with ribosomes (179,180). Second, the lack of ITAFs *in vitro* systems which are typically required for cellular IRES activity, poses a challenge. Third, the expression of reporters may possess an alternative transcription site or splicing site which is not accounted for in the experimental setup, especially in *Hoxa9* IRES (181). Finally, distinguishing between ribosome readthrough after translation of the first ORF (cap-dependent) and re-initiation at the second ORF (IRES-dependent) can be difficult (182). Thus, in our experimental setup to study the *Hspa1a* mRNA in Chapter 3, we considered the limitations of methods used to study the cellular IRES. We conducted our experiments in vivo using MEFs, which provide regulatory factors such as miRNA and ITAFs. We utilized the endogenous *HSPA1A* promoter and retained the endogenous UTRs and CDS intact to avoid discrepancies. With proper controls and experimental design, we will continue to investigate the induction of *Hspa1a* mRNA by a possible IRES encompassing the 5' UTR and first 102 nts of the CDS. Certain plant viruses and cellular mRNAs has been reported to undergo a translation mechanism that is neither cap- nor IRES-dependent instead possess translation inducing tertiary structures called cap-independent translation enhancers (CITEs). The mRNAs harboring CITES often circularize and interact with the cap-binding complex and favor ribosome recruitment. The presence of CITE on *Hspa1a* mRNA could be assessed in the future (PMID: 18031280, 23268449, 22733589).

Unlike cellular mRNA, *Hspa1a* mRNA differs in several ways. First, *Hspa1a* mRNAs are not present under physiological growth conditions, and they do not possess introns (183). The

Hspa1a mRNA synthesis is robustly upregulated during stress. Second, we think the IRES of *Hspa1a* mRNA lies in the 5'UTR and the CDS similar to IGR IRES (184). The CDS involvement in the formation of an IRES structure has never been considered in the previous investigations in the context of *Hspa1a* mRNA or other cellular mRNAs. Another striking difference lies in the possibility of the increase in temperature inducing the formation of an IRES. As such, it might be possible that the *Hspa1a* mRNA structure behaves as a thermosensor and possibly folds into tertiary structures upon heat shock. Typical RNA thermosensors were reported in *E. coli HSP* mRNAs for rapid translational induction during heat shock (185,186). In a bacterial system, the increase in temperature melts the structure of the *HSP* mRNA (186). Conversely, the mouse *Hspa1a* mRNA compactly folds with an increase in temperature. This underscores how evolutionarily conserved *HSP* mRNA can sense temperature changes and adapt by either unfolding or folding in different systems.

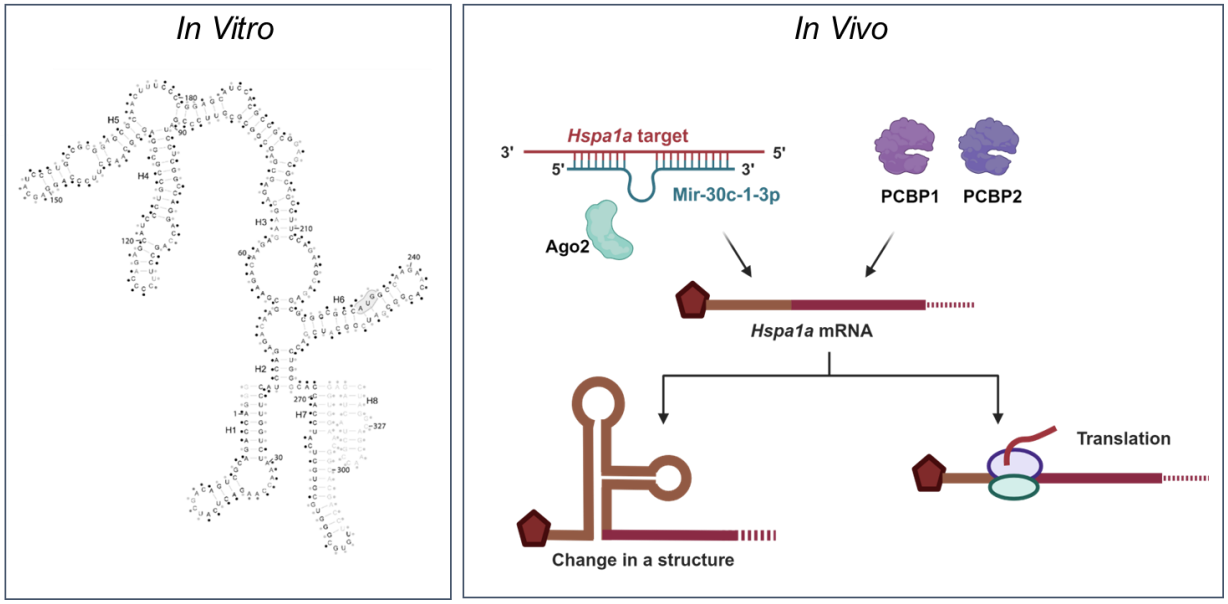

Figure 4.2. Differences in structure formation *in vitro* and *in vivo* on *Hspa1a* mRNAs. Left: *In vitro* SHAPE structure of 5'UTR of *Hspa1a* mRNA from Pyle's group. **Right**: Our current model showing the Mir-30c-1-3p or PCBPs binding to 5'UTR of *Hspa1a* mRNA may promote the IRES-like structure formation and/or translation.

The question is, does stressors other than heat, can activate the translation? If the structure is formed upon sensing an increase in temperature, then how does the structure form in response to stressors such as arsenite or viral infection? It is possible that cellular factors, possibly ITAFs, microRNAs, and RBPs (such as PCBP) might be involved in the structure stabilization, and translation induction. For instance, the HCV IRES formation is mediated by the binding of miR122-Ago2 that triggers a conformational change exposing another site for miR122-Ago2 binding (159). This induces the final conformational change resembling a structure that is translation-competent. Similar to HCV IRES, we have found two binding sites for Mir-30c-1-3p on the 5'UTR of *Hspa1a* mRNA. We are currently exploring the possibility that miRNA-mediated IRES formation on *Hspa1a* mRNA (**Fig 4.3**).

4.2.2 HSPA1A and HSPA8 expression regulation during heat shock

It is known that the expression of HSPA1A, stress-inducible isoform, occurs during stress whereas the expression of HSPA8 occurs under permissive conditions. Although the *Hspa8* mRNA expression is transcriptionally induced, unlike *Hspa1a*, *Hspa8* mRNA contains introns which need to be spliced before the mRNA can enter the cytoplasm for translation. During stress, the mRNA processing and splicing are downregulated, thus newly transcribed *Hspa8* mRNAs do not enter the translation pool. In addition to that cytoplasmic pre-existing *Hspa8* mRNAs are sequestered in SGs therefore it is unlikely to get translated. Further, checking for codon optimality of CDS revealed that *Hspa8* carries 58% non-optimal codons whereas *Hspa1a* exhibits only 21% of non-optimal codons (**Fig 4.3**). These variations in the codon optimality could account for the poor translation of *Hspa8* mRNAs over *Hspa1a* mRNAs during stress conditions. The non-optimal codons would greatly contribute to translation regulation of mRNAs. It has been described that during stress, the abundance of the tRNA pool changes to favor translation of stress-related

transcripts thereby resulting in the synthesis of survival proteins (187). Thus the stress-related transcripts have a different composition of codons than the constitutive transcripts so the cells can preferentially translate stress-related genes for survival (188).

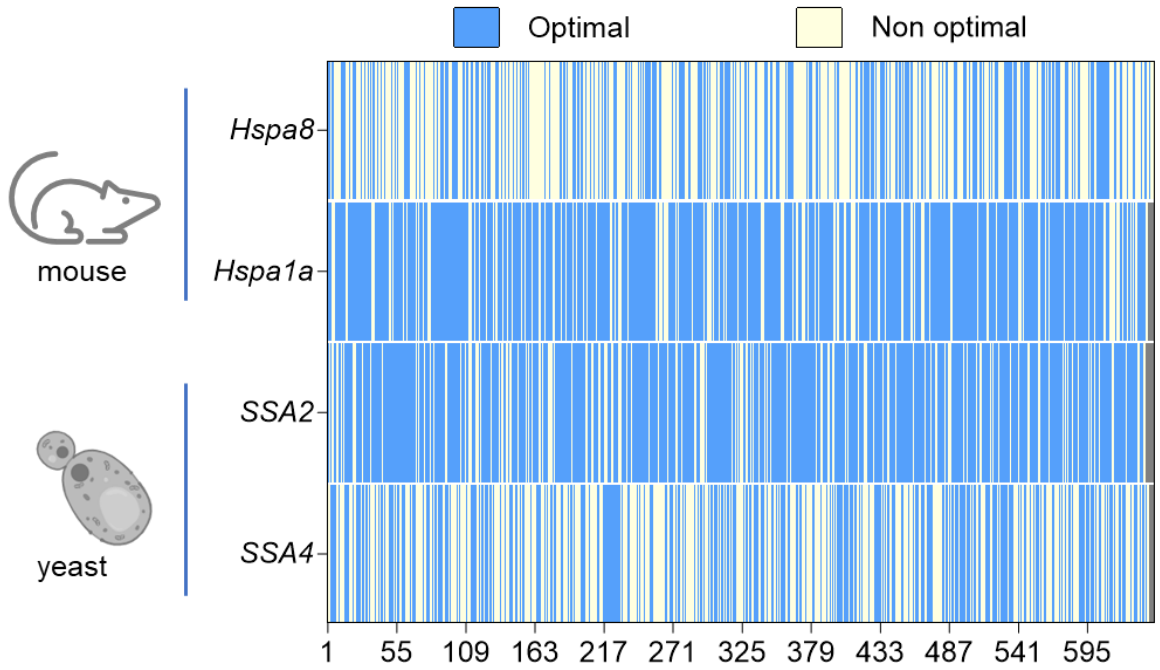

Figure 4.3. Codon optimality of mouse and yeast constitutive and stress-inducible *Hsp70* mRNAs. Heat map showing the optimal codons in blue and non-optimal codons in pale yellow across the codons of *Hspa8* and *Hspa1a* mRNAs in mice versus *SSA2* and *SSA4* mRNAs in yeast. The mouse CDS of *Hspa8* and *Hspa1a* mRNA have 58% and 21% non-optimality, respectively. The yeast CDS of *SSA2* and *SSA4* mRNA have 22% and 53% non-optimality, respectively.

4.3 The change of the *Hsp70* mRNA fate during recovery from stress

4.3.1 Translation profile of inducible Hsp70 mRNA during recovery in yeasts and mammalian cells

In yeast, the inducible *Hsp70* mRNA is translated only upon heat shock not during the recovery (99). From the results in Chapter 2, we have also shown that the inducible *SSA4* mRNA rapidly disappears during the recovery from stress and there is no further induction of its translation during recovery. In MEFs however, we show that the translation efficiency of *Hspa1a* mRNA is higher

during recovery than the heat shock. This is confirmed by increased ribosome occupancy on inducible *Hsp70* mRNA in polysome fraction as well as western blotting (**Chapter 3, Fig. 3.1**). This indicates that mammalian cells have a higher demand for HSP70 proteins to recover from the stress than the yeasts. We believe the inducible *Hsp70* mRNA codon has evolved to be more optimal in mammalian cells for its efficient translation during recovery just to meet cellular requirements (**Fig 4.2**). This optimization is due to the fact that yeasts have a simpler proteome and a faster cell cycle (~90 min), resulting in rapid turnover of gene expression. Consequently, yeasts synthesize sufficient inducible HSP70 proteins during stress to swiftly progress into the cell cycle upon recovery. Conversely, mammalian cells possess a more complex proteome and slower cell cycle (~12-24 h). Hence, they take advantage of the cap-dependent translation machinery (especially eIF4A) and maximize the inducible HSP70 synthesis during recovery and subsequently degrade the mRNA.

4.3.2 Inducible *Hsp70* mRNA clearance during recovery

When the cells recover from stress, the inducible *HSP70* transcripts are rapidly cleared by the cells. In yeast, we found that Asc1p clears the *SSA4* transcripts through the recruitment of Dhh1p and Xrn1p in a pathway that is not yet understood. From the Asc1p physical interactome analysis, we proposed that the LSM heteroheptameric complex could degrade the mRNA by binding to its 3'UTR in the cytoplasm (189–191). LSM complex functions exclusively in pre-mRNA splicing by interaction with U6 small nuclear RNA and is conserved from yeasts to humans. In the cytoplasm, the LSM complex has been shown to function with 5'-3' degradation factors including Xrn1p, Dhh1p, and Dcp1p to degrade the *SSA4* mRNA (189–191). Another possibility is that the promoter of the *SSA4* gene recruits co-translationally decay factors, as has been shown for cell cycle-regulated genes and stress-regulated genes upon glucose starvation (192,193) We have

assessed whether the Asc1 binds to the 3' UTR, 5' UTR, or promoter of *SSA4* to mediate its decay by replacing these regions with those of constitutive *SSA2 gene* (see appendix). However, none of these regions played a role in the clearance of inducible *Hsp70* mRNA during recovery mediated by Asc1p. This leaves us with two possibilities: The first possibility is the presence of a conserved region in both the WT and Optimized *SSA4* CDS for an RBP that binds Asc1, thereby facilitating its specific action in degrading *SSA4* mRNA. The second possibility is that Asc1p could indirectly influence the decay of *SSA4* mRNA by regulating the assembly and disassembly of PBs (194,195). Accordingly, we found that mammalian cells localize *SSA4* mRNAs at 3 hrs of recovery from stress before they completely degrade all *HSPA1A* mRNAs (data not shown). Destabilization of inducible *Hsp70* mRNA is highly critical. This marks the attenuation of HSR, and prevents the cells from cytotoxic effects of inducible HSP70 in healthy cells (114,196,197). Failure to attenuate HSP70 synthesis is clinically associated with tumorigenesis (38).

4.3.3 Biomedical implications of our study on HSP70 expression:

Healthy cells present at relatively low levels of HSPA1A and its expression is rapidly induced upon stress at mRNA and protein level. During stress, the HSPA1A aids in coping with cellular proteostasis by refolding misfolded protein, preventing aggregation, promoting degradation of damaged protein, and regulating apoptosis. Upon return to growth conditions, HSPA1A returns to the normal threshold by controlling its translation and mRNA stability (114,115,197). Thus, healthy cells maintain a tight regulation of HSPA1A induction and downregulation. Due to constant proliferation, the cancer cells are always in a state of stress. HSPA1A promotes the survival of the cancer cells against various apoptotic signals (198). Thus, not surprisingly, in certain tumors such as breast cancer, acute leukemia, and endometrial cancer, HSPA1A is ubiquitously expressed to protect tumor cells from both intrinsic replicative stress and extrinsic

environmental challenges (38,199). Notably, nuclear localization and activation of HSF1 has been related to malignancy by blocking pro-apoptotic signals, promoting translation, protein folding, and rapid cell proliferation (PMID: 23869022).

Clearly, the HSPA1A expression is misregulated in cancer cells (151). To understand if the misregulation is coming from the mRNA or protein level, we established a collaboration with Dr. Peter Siegel working on leptomeningeal metastases (LM). Dr. Seigel's laboratory has generated patient-derived xenograft models of both primary breast tumors and secondary LM (200–202). By RNA-seq analysis, they have found that *Hspa1a* mRNA levels were significantly downregulated in LM compared to primary tumor lesions. However, the HSPA1A protein expression remained the same in breast tumor and LM. This suggests a differential regulation of *Hspa1a* mRNA translation and degradation. In order to check the *Hspa1a* mRNA levels and localization, we performed a tissue-smFISH. We found that very few cancer cells in LM have a transcriptional induction while the rest of the cancer cells contain mature *Hspa1a* mRNA in the cytoplasm. This indicates an increase in the stability of the *Hspa1a* mRNAs and contributing to the lower yet constant synthesis of HSPA1A. The constant expression of HSPA1A is associated with therapeutic resistance and poor patient prognosis (151).

This renders HSPA1A an optimal target for anticancer therapy. Numerous small molecule inhibitors of HSP70 have been developed to target ATPase activity, prevent interaction with co-chaperones, or inhibit binding to client proteins (203). However, the use of direct inhibitors HSP70 is often associated with therapeutic resistance thereby limiting their long-term efficacy. Consequently, there is an urgent need to explore effective alternatives for targeting HSP70 expression in cancer cells, either by modulating the translation or stability of *Hspa1a* mRNA. In our research, we have identified key regions that play a significant role in promoting *Hspa1a*

mRNA translation although in mice. Checking the conservation in humans and targeting these sites using RNA interference (RNAi) presents a promising alternative for controlling HSPA1A dysregulation in cancer treatment.

4.4 Concluding remarks

From Chapter 2 and Chapter 3, we found that the CDS of the inducible HSP70 plays different roles in the activation of HSPA1A expression in mammalian and yeast cells undergoing heat stress. In yeast, the CDS dampens down RQC and mediates its regulation. Although not completely elucidated, in mammalian cells the CDS favor translation induction probably through an IRES-like structure formation upon heat shock. This implies that the regulatory mechanisms governing the posttranscriptional regulation of the inducible HSP70 expression are not conserved during evolution.

5. REFERENCES

1. Lindquist S. The heat-shock response. Annu Rev Biochem. 1986;55:1151–91.
2. Kültz D. Molecular and evolutionary basis of the cellular stress response. Annu Rev Physiol. 2005;67:225–57.
3. Poljšak B, Milisav I. Clinical implications of cellular stress responses. Bosn J Basic Med Sci. 2012 May;12(2):122–6.
4. Richter K, Haslbeck M, Buchner J. The heat shock response: life on the verge of death. Mol Cell. 2010 Oct 22;40(2):253–66.
5. Zeuthen E. Synchrony in Tetrahymena by heat shocks spaced a normal cell generation apart. Exp Cell Res. 1971 Sep 1;68(1):49–60.
6. Lindquist S. Varying patterns of protein synthesis in Drosophila during heat shock: Implications for regulation. Dev Biol. 1980 Jun 15;77(2):463–79.
7. Yost HJ, Lindquist S. RNA splicing is interrupted by heat shock and is rescued by heat shock protein synthesis. Cell. 1986 Apr 25;45(2):185–93.
8. Kedersha N, Chen S, Gilks N, Li W, Miller IJ, Stahl J, et al. Evidence that ternary complex (eIF2-GTP-tRNA(i)(Met))-deficient preinitiation complexes are core constituents of mammalian stress granules. Mol Biol Cell. 2002 Jan;13(1):195–210.
9. Anderson P, Kedersha N. Visibly stressed: the role of eIF2, TIA-1, and stress granules in protein translation. Cell Stress Chaperones. 2002 Apr;7(2):213–21.
10. Mazroui R, Sukarieh R, Bordeleau ME, Kaufman RJ, Northcote P, Tanaka J, et al. Inhibition of Ribosome Recruitment Induces Stress Granule Formation Independently of Eukaryotic Initiation Factor 2α Phosphorylation. Mol Biol Cell. 2006 Oct 1;17(10):4212–9.
11. Kedersha NL, Gupta M, Li W, Miller I, Anderson P. RNA-binding proteins TIA-1 and TIAR link the phosphorylation of eIF-2 alpha to the assembly of mammalian stress granules. J Cell Biol. 1999 Dec 27;147(7):1431–42.
12. Parker R, Sheth U. P bodies and the control of mRNA translation and degradation. Mol Cell. 2007 Mar 9;25(5):635–46.
13. Bley N, Lederer M, Pfalz B, Reinke C, Fuchs T, Glaß M, et al. Stress granules are dispensable for mRNA stabilization during cellular stress. Nucleic Acids Res. 2015 Feb 27;43(4):e26–e26.
14. Alluri RK, Li Z, McCrae KR. Stress Granule-Mediated Oxidized RNA Decay in P-Body: Hypothetical Role of ADAR1, Tudor-SN, and STAU1. Front Mol Biosci. 2021;8:480.
15. Ivanov P, Kedersha N, Anderson P. Stress Granules and Processing Bodies in Translational Control. Cold Spring Harb Perspect Biol. 2019 May;11(5):a032813.
16. Walters RW, Muhlrad D, Garcia J, Parker R. Differential effects of Ydj1 and Sis1 on Hsp70-mediated clearance of stress granules in Saccharomyces cerevisiae. RNA. 2015 Sep;21(9):1660–71.
17. Ritossa F. Discovery of the heat shock response. Cell Stress Chaperones. 1996 Jun;1(2):97–8.
18. Cox JS, Walter P. A novel mechanism for regulating activity of a transcription factor that controls the unfolded protein response. Cell. 1996 Nov 1;87(3):391–404.
19. Bertolotti A, Zhang Y, Hendershot LM, Harding HP, Ron D. Dynamic interaction of BiP and ER stress transducers in the unfolded-protein response. Nat Cell Biol. 2000 Jun;2(6):326–32.

20. Harding HP, Zhang Y, Bertolotti A, Zeng H, Ron D. Perk is essential for translational regulation and cell survival during the unfolded protein response. Mol Cell. 2000 May;5(5):897–904.
21. Michels AA, Kanon B, Konings AW, Ohtsuka K, Bensaude O, Kampinga HH. Hsp70 and Hsp40 chaperone activities in the cytoplasm and the nucleus of mammalian cells. J Biol Chem. 1997 Dec 26;272(52):33283–9.
22. Benjamin IJ, McMillan DR. Stress (Heat Shock) Proteins. Circ Res. 1998 Jul 27;83(2):117–32.
23. Lindquist S, Craig EA. The Heat-Shock Proteins. Annu Rev Genet. 1988;22(1):631–77.
24. Gething MJ, Sambrook J. Protein folding in the cell. Nature. 1992 Jan;355(6355):33–45.
25. Ingolia TD, Slater MR, Craig EA. Saccharomyces cerevisiae contains a complex multigene family related to the major heat shock-inducible gene of Drosophila. Mol Cell Biol. 1982 Nov;2(11):1388–98.
26. Bienz M. Developmental control of the heat shock response in Xenopus. Proc Natl Acad Sci. 1984 May;81(10):3138–42.
27. Hunt C, Morimoto RI. Conserved features of eukaryotic hsp70 genes revealed by comparison with the nucleotide sequence of human hsp70. Proc Natl Acad Sci U S A. 1985 Oct;82(19):6455–9.
28. Morimoto RI, Hunt C, Huang SY, Berg KL, Banerji SS. Organization, nucleotide sequence, and transcription of the chicken HSP70 gene. J Biol Chem. 1986 Sep 25;261(27):12692–9.
29. Bardwell JC, Craig EA. Major heat shock gene of Drosophila and the Escherichia coli heat-inducible dnaK gene are homologous. Proc Natl Acad Sci U S A. 1984 Feb;81(3):848–52.
30. Corces V, Pellicer A, Axel R, Meselson M. Integration, transcription, and control of a Drosophila heat shock gene in mouse cells. Proc Natl Acad Sci U S A. 1981 Nov;78(11):7038–42.
31. Ritossa F. A new puffing pattern induced by temperature shock and DNP in drosophila. Experientia. 1962 Dec 1;18(12):571–3.
32. Moran L, Mirault ME, Arrigo AP, Goldschmidt-Clermont M, Tissieres A. Heat Shock of Drosophila melanogaster Induces the Synthesis of New Messenger RNAs and Proteins. Philos Trans R Soc Lond B Biol Sci. 1978;283(997):391–406.
33. Tissières A, Mitchell HK, Tracy UM. Protein synthesis in salivary glands of Drosophila melanogaster: relation to chromosome puffs. J Mol Biol. 1974 Apr 15;84(3):389–98.
34. Hartl FU. Molecular chaperones in cellular protein folding. Nature. 1996 Jun;381(6583):571–80.
35. McEwen E, Kedersha N, Song B, Scheuner D, Gilks N, Han A, et al. Heme-regulated inhibitor kinase-mediated phosphorylation of eukaryotic translation initiation factor 2 inhibits translation, induces stress granule formation, and mediates survival upon arsenite exposure. J Biol Chem. 2005 Apr 29;280(17):16925–33.
36. Nevins JR. Induction of the synthesis of a 70,000 dalton mammalian heat shock protein by the adenovirus E1A gene product. Cell. 1982 Jul;29(3):913–9.
37. Li GC. Induction of thermotolerance and enhanced heat shock protein synthesis in Chinese hamster fibroblasts by sodium arsenite and by ethanol. J Cell Physiol. 1983 May;115(2):116–22.

38. Daugaard M, Rohde M, Jäättelä M. The heat shock protein 70 family: Highly homologous proteins with overlapping and distinct functions. FEBS Lett. 2007 Jul 31;581(19):3702–10.
39. Hu C, Yang J, Qi Z, Wu H, Wang B, Zou F, et al. Heat shock proteins: Biological functions, pathological roles, and therapeutic opportunities. MedComm. 2022 Aug 2;3(3):e161.
40. Kaimal JM, Kandasamy G, Gasser F, Andréasson C. Coordinated Hsp110 and Hsp104 Activities Power Protein Disaggregation in Saccharomyces cerevisiae. Mol Cell Biol. 2017 May 16;37(11):e00027-17.
41. Glover JR, Lindquist S. Hsp104, Hsp70, and Hsp40: a novel chaperone system that rescues previously aggregated proteins. Cell. 1998 Jul 10;94(1):73–82.
42. Gupta RS. Evolution of the chaperonin families (Hsp60, Hsp10 and Tcp-1) of proteins and the origin of eukaryotic cells. Mol Microbiol. 1995 Jan;15(1):1–11.
43. Ostermann J, Horwich AL, Neupert W, Hartl FU. Protein folding in mitochondria requires complex formation with hsp60 and ATP hydrolysis. Nature. 1989 Sep;341(6238):125–30.
44. Cheng MY, Hartl FU, Martin J, Pollock RA, Kalousek F, Neupert W, et al. Mitochondrial heat-shock protein hsp60 is essential for assembly of proteins imported into yeast mitochondria. Nature. 1989 Feb 16;337(6208):620–5.
45. Hemmingsen SM, Woolford C, van der Vies SM, Tilly K, Dennis DT, Georgopoulos CP, et al. Homologous plant and bacterial proteins chaperone oligomeric protein assembly. Nature. 1988 May;333(6171):330–4.
46. Georgopoulos CP, Hendrix RW, Casjens SR, Kaiser AD. Host participation in bacteriophage lambda head assembly. J Mol Biol. 1973 May 5;76(1):45–60.
47. Hartl FU, Ostermann J, Guiard B, Neupert W. Successive translocation into and out of the mitochondrial matrix: targeting of proteins to the intermembrane space by a bipartite signal peptide. Cell. 1987 Dec 24;51(6):1027–37.
48. Frydman J, Nimmesgern E, Ohtsuka K, Hartl FU. Folding of nascent polypeptide chains in a high molecular mass assembly with molecular chaperones. Nature. 1994 Jul;370(6485):111–7.
49. Horwich AL, Low KB, Fenton WA, Hirshfield IN, Furtak K. Folding in vivo of bacterial cytoplasmic proteins: Role of GroEL. Cell. 1993 Sep 10;74(5):909–17.
50. Horwich AL, Willison KR, Cowan NJ, Viitanen P, Micklethwaite P, Gething M -j., et al. Protein folding in the cell: functions of two families of molecular chaperone, hsp 60 and TF55-TCP1. Philos Trans R Soc Lond B Biol Sci. 1997 Jan;339(1289):313–26.
51. Lewis VA, Hynes GM, Zheng D, Saibil H, Willison K. T-complex polypeptide-1 is a subunit of a heteromeric particle in the eukaryotic cytosol. Nature. 1992 Jul 16;358(6383):249–52.
52. Odunuga OO, Hornby JA, Bies C, Zimmermann R, Pugh DJ, Blatch GL. Tetratricopeptide repeat motif-mediated Hsc70-mSTI1 interaction. Molecular characterization of the critical contacts for successful binding and specificity. J Biol Chem. 2003 Feb 28;278(9):6896–904.
53. Chen S, Sullivan WP, Toft DO, Smith DF. Differential interactions of p23 and the TPR-containing proteins Hop, Cyp40, FKBP52 and FKBP51 with Hsp90 mutants. Cell Stress Chaperones. 1998 Jun;3(2):118–29.
54. Connell P, Ballinger CA, Jiang J, Wu Y, Thompson LJ, Höhfeld J, et al. The co-chaperone CHIP regulates protein triage decisions mediated by heat-shock proteins. Nat Cell Biol. 2001 Jan;3(1):93–6.

55. Basso AD, Solit DB, Chiosis G, Giri B, Tsichlis P, Rosen N. Akt forms an intracellular complex with heat shock protein 90 (Hsp90) and Cdc37 and is destabilized by inhibitors of Hsp90 function. J Biol Chem. 2002 Oct 18;277(42):39858–66.
56. Doong H, Rizzo K, Fang S, Kulpa V, Weissman AM, Kohn EC. CAIR-1/BAG-3 abrogates heat shock protein-70 chaperone complex-mediated protein degradation: accumulation of poly-ubiquitinated Hsp90 client proteins. J Biol Chem. 2003 Aug 1;278(31):28490–500.
57. Hunt C, Calderwood S. Characterization and sequence of a mouse hsp70 gene and its expression in mouse cell lines. Gene. 1990 Mar 15;87(2):199–204.
58. Brocchieri L, Conway de Macario E, Macario AJL. hsp70 genes in the human genome: Conservation and differentiation patterns predict a wide array of overlapping and specialized functions. BMC Evol Biol. 2008 Jan 23;8:19.
59. Ingolia TD, Craig EA. Drosophila Gene Related to the Major Heat Shock-Induced Gene is Transcribed at Normal Temperatures and not Induced by Heat Shock. Proc Natl Acad Sci U S A. 1982;79(2):525–9.
60. Schiaffonati L, Bardella L, Cairo G, Rappocciolo E, Tacchini L, Bernelli-Zazzera A. Constitutive and Induced Synthesis of Heat Shock Proteins in Transplantable Hepatomas. Tumori J. 1987 Dec 1;73(6):559–65.
61. Morimoto RI. Heat shock: the role of transient inducible responses in cell damage, transformation, and differentiation. Cancer Cells Cold Spring Harb N 1989. 1991 Aug;3(8):295–301.
62. Mckay D, Wilbanks S, Flaherty K, Ha J, O'Brien MC, Shirvanee L. 7 Stress-70 Proteins and Their Interaction with Nucleotides. Cold Spring Harb Monogr Arch [Internet]. 1994 [cited 2023 Dec 28]; Available from: https://www.semanticscholar.org/paper/7-Stress-70-Proteins-and-Their-Interaction-with-Mckay-Wilbanks/4616ef1f731bb3c4ac9f7788d44b621836fed0d8
63. De Maio A. HEAT SHOCK PROTEINS: FACTS, THOUGHTS, AND DREAMS. Shock. 1999 Jan;11(1):1–12.
64. Cintron NS, Toft D. Defining the requirements for Hsp40 and Hsp70 in the Hsp90 chaperone pathway. J Biol Chem. 2006 Sep 8;281(36):26235–44.
65. Misselwitz B, Staeck O, Rapoport TA. J proteins catalytically activate Hsp70 molecules to trap a wide range of peptide sequences. Mol Cell. 1998 Nov;2(5):593–603.
66. Tzankov S, Wong MJH, Shi K, Nassif C, Young JC. Functional divergence between co-chaperones of Hsc70. J Biol Chem. 2008 Oct 3;283(40):27100–9.
67. Kityk R, Kopp J, Mayer MP. Molecular Mechanism of J-Domain-Triggered ATP Hydrolysis by Hsp70 Chaperones. Mol Cell. 2018 Jan 18;69(2):227-237.e4.
68. Gragerov A, Zeng L, Zhao X, Burkholder W, Gottesman ME. Specificity of DnaK-peptide binding. J Mol Biol. 1994 Jan 21;235(3):848–54.
69. Rüdiger S, Germeroth L, Schneider-Mergener J, Bukau B. Substrate specificity of the DnaK chaperone determined by screening cellulose-bound peptide libraries. EMBO J. 1997 Apr 1;16(7):1501–7.
70. Richarme G, Kohiyama M. Specificity of the Escherichia coli chaperone DnaK (70-kDa heat shock protein) for hydrophobic amino acids. J Biol Chem. 1993 Nov 15;268(32):24074–7.
71. Blond-Elguindi S, Cwirla SE, Dower WJ, Lipshutz RJ, Sprang SR, Sambrook JF, et al. Affinity panning of a library of peptides displayed on bacteriophages reveals the binding specificity of BiP. Cell. 1993 Nov 19;75(4):717–28.

72. Schuermann JP, Jiang J, Cuellar J, Llorca O, Wang L, Gimenez LE, et al. Structure of the Hsp110:Hsc70 nucleotide exchange machine. Mol Cell. 2008 Jul 25;31(2):232–43.
73. Raviol H, Sadlish H, Rodriguez F, Mayer MP, Bukau B. Chaperone network in the yeast cytosol: Hsp110 is revealed as an Hsp70 nucleotide exchange factor. EMBO J. 2006 Jun 7;25(11):2510–8.
74. Easton DP, Kaneko Y, Subjeck JR. The hsp110 and Grp1 70 stress proteins: newly recognized relatives of the Hsp70s. Cell Stress Chaperones. 2000 Oct;5(4):276–90.
75. Lüders J, Demand J, Papp O, Höhfeld J. Distinct isoforms of the cofactor BAG-1 differentially affect Hsc70 chaperone function. J Biol Chem. 2000 May 19;275(20):14817–23.
76. Höhfeld J, Jentsch S. GrpE-like regulation of the hsc70 chaperone by the anti-apoptotic protein BAG-1. EMBO J. 1997 Oct 15;16(20):6209–16.
77. Gassler CS, Wiederkehr T, Brehmer D, Bukau B, Mayer MP. Bag-1M accelerates nucleotide release for human Hsc70 and Hsp70 and can act concentration-dependent as positive and negative cofactor. J Biol Chem. 2001 Aug 31;276(35):32538–44.
78. Gamerdinger M, Hajieva P, Kaya AM, Wolfrum U, Hartl FU, Behl C. Protein quality control during aging involves recruitment of the macroautophagy pathway by BAG3. EMBO J. 2009 Apr 8;28(7):889–901.
79. Minoia M, Boncoraglio A, Vinet J, Morelli FF, Brunsting JF, Poletti A, et al. BAG3 induces the sequestration of proteasomal clients into cytoplasmic puncta. Autophagy. 2014 Sep 1;10(9):1603–21.
80. Oh WK, Song J. Cooperative interaction of Hsp40 and TPR1 with Hsp70 reverses Hsp70-HspBp1 complex formation. Mol Cells. 2003 Aug 31;16(1):84–91.
81. Gowda NKC, Kaimal JM, Kityk R, Daniel C, Liebau J, Öhman M, et al. Nucleotide exchange factors Fes1 and HspBP1 mimic substrate to release misfolded proteins from Hsp70. Nat Struct Mol Biol. 2018 Jan;25(1):83–9.
82. Kanelakis KC, Murphy PJ, Galigniana MD, Morishima Y, Takayama S, Reed JC, et al. hsp70 interacting protein Hip does not affect glucocorticoid receptor folding by the hsp90-based chaperone machinery except to oppose the effect of BAG-1. Biochemistry. 2000 Nov 21;39(46):14314–21.
83. Böttinger L, Oeljeklaus S, Guiard B, Rospert S, Warscheid B, Becker T. Mitochondrial Heat Shock Protein (Hsp) 70 and Hsp10 Cooperate in the Formation of Hsp60 Complexes. J Biol Chem. 2015 May 1;290(18):11611–22.
84. Roh SH, Kasembeli M, Bakthavatsalam D, Chiu W, Tweardy DJ. Contribution of the Type II Chaperonin, TRiC/CCT, to Oncogenesis. Int J Mol Sci. 2015 Nov 6;16(11):26706–20.
85. Rosenzweig R, Nillegoda NB, Mayer MP, Bukau B. The Hsp70 chaperone network. Nat Rev Mol Cell Biol. 2019 Nov;20(11):665–80.
86. Zhang H, Amick J, Chakravarti R, Santarriaga S, Schlanger S, McGlone C, et al. A bipartite interaction between Hsp70 and CHIP regulates ubiquitination of chaperoned client proteins. Struct Lond Engl 1993. 2015 Mar 3;23(3):472–82.
87. Calloni G, Chen T, Schermann SM, Chang HC, Genevaux P, Agostini F, et al. DnaK functions as a central hub in the E. coli chaperone network. Cell Rep. 2012 Mar 29;1(3):251–64.
88. Srinivasan SR, Gillies AT, Chang L, Thompson AD, Gestwicki JE. Molecular chaperones DnaK and DnaJ share predicted binding sites on most proteins in the E. coli proteome. Mol Biosyst. 2012 Sep;8(9):2323–33.

89. Behnke J, Mann MJ, Scruggs FL, Feige MJ, Hendershot LM. Members of the Hsp70 Family Recognize Distinct Types of Sequences to Execute ER Quality Control. Mol Cell. 2016 Sep 1;63(5):739–52.
90. Mayer MP, Bukau B. Hsp70 chaperones: cellular functions and molecular mechanism. Cell Mol Life Sci CMLS. 2005 Mar;62(6):670–84.
91. Johnson OT, Gestwicki JE. Multivalent protein–protein interactions are pivotal regulators of eukaryotic Hsp70 complexes. Cell Stress Chaperones. 2022 Jul;27(4):397–415.
92. Liu B, Han Y, Qian SB. Cotranslational response to proteotoxic stress by elongation pausing of ribosomes. Mol Cell. 2013 Feb 7;49(3):453–63.
93. Shalgi R, Hurt JA, Krykbaeva I, Taipale M, Lindquist S, Burge CB. Widespread Regulation of Translation by Elongation Pausing in Heat Shock. Mol Cell. 2013 Feb;49(3):439–52.
94. Xing Y, Böcking T, Wolf M, Grigorieff N, Kirchhausen T, Harrison SC. Structure of clathrin coat with bound Hsc70 and auxilin: mechanism of Hsc70-facilitated disassembly. EMBO J. 2010 Feb 3;29(3):655–65.
95. Mosser DD, Caron AW, Bourget L, Meriin AB, Sherman MY, Morimoto RI, et al. The chaperone function of hsp70 is required for protection against stress-induced apoptosis. Mol Cell Biol. 2000 Oct;20(19):7146–59.
96. Nollen EA, Brunsting JF, Roelofsen H, Weber LA, Kampinga HH. In vivo chaperone activity of heat shock protein 70 and thermotolerance. Mol Cell Biol. 1999 Mar;19(3):2069–79.
97. Lindquist S, Kim G. Heat-shock protein 104 expression is sufficient for thermotolerance in yeast. Proc Natl Acad Sci U S A. 1996 May 28;93(11):5301–6.
98. Parsell DA, Taulien J, Lindquist S, Viitanen P, Jaenicke R, Horwich A, et al. The Role of Heat-Shock Proteins in Thermotolerance [and Discussion]. Philos Trans Biol Sci. 1993;339(1289):279–86.
99. Alagar Boopathy LR, Beadle E, Xiao AR, Garcia-Bueno Rico A, Alecki C, Garcia de-Andres I, et al. The ribosome quality control factor Asc1 determines the fate of HSP70 mRNA on and off the ribosome. Nucleic Acids Res. 2023 Jul 7;51(12):6370–88.
100. Queitsch C, Hong SW, Vierling E, Lindquist S. Heat Shock Protein 101 Plays a Crucial Role in Thermotolerance in Arabidopsis. Plant Cell. 2000 Apr;12(4):479–92.
101. Schirmer EC, Lindquist S, Vierling E. An Arabidopsis heat shock protein complements a thermotolerance defect in yeast. Plant Cell. 1994 Dec;6(12):1899–909.
102. Parsell DA, Lindquist S. The function of heat-shock proteins in stress tolerance: degradation and reactivation of damaged proteins. Annu Rev Genet. 1993;27:437–96.
103. Crippa V, Sau D, Rusmini P, Boncoraglio A, Onesto E, Bolzoni E, et al. The small heat shock protein B8 (HspB8) promotes autophagic removal of misfolded proteins involved in amyotrophic lateral sclerosis (ALS). Hum Mol Genet. 2010 Sep 1;19(17):3440–56.
104. Ganassi M, Mateju D, Bigi I, Mediani L, Poser I, Lee HO, et al. A Surveillance Function of the HSPB8-BAG3-HSP70 Chaperone Complex Ensures Stress Granule Integrity and Dynamism. Mol Cell. 2016 Sep 1;63(5):796–810.
105. Shorter J. The Mammalian Disaggregase Machinery: Hsp110 Synergizes with Hsp70 and Hsp40 to Catalyze Protein Disaggregation and Reactivation in a Cell-Free System. PLoS ONE. 2011 Oct 14;6(10):e26319.
106. Arndt V, Daniel C, Nastainczyk W, Alberti S, Höhfeld J. BAG-2 Acts as an Inhibitor of the Chaperone-associated Ubiquitin Ligase CHIP. Mol Biol Cell. 2005 Dec;16(12):5891–900.

107. Demand J, Alberti S, Patterson C, Höhfeld J. Cooperation of a ubiquitin domain protein and an E3 ubiquitin ligase during chaperone/proteasome coupling. Curr Biol. 2001 Oct 16;11(20):1569–77.
108. Bercovich B, Stancovski I, Mayer A, Blumenfeld N, Laszlo A, Schwartz AL, et al. Ubiquitin-dependent degradation of certain protein substrates in vitro requires the molecular chaperone Hsc70. J Biol Chem. 1997 Apr 4;272(14):9002–10.
109. Ballinger CA, Connell P, Wu Y, Hu Z, Thompson LJ, Yin LY, et al. Identification of CHIP, a novel tetratricopeptide repeat-containing protein that interacts with heat shock proteins and negatively regulates chaperone functions. Mol Cell Biol. 1999 Jun;19(6):4535–45.
110. Lüders J, Demand J, Höhfeld J. The Ubiquitin-related BAG-1 Provides a Link between the Molecular Chaperones Hsc70/Hsp70 and the Proteasome *. J Biol Chem. 2000 Feb 18;275(7):4613–7.
111. Kopito RR. Aggresomes, inclusion bodies and protein aggregation. Trends Cell Biol. 2000 Dec;10(12):524–30.
112. Ravikumar B, Duden R, Rubinsztein DC. Aggregate-prone proteins with polyglutamine and polyalanine expansions are degraded by autophagy. Hum Mol Genet. 2002 May 1;11(9):1107–17.
113. Gamerdinger M, Kaya AM, Wolfrum U, Clement AM, Behl C. BAG3 mediates chaperone-based aggresome-targeting and selective autophagy of misfolded proteins. EMBO Rep. 2011 Feb;12(2):149–56.
114. Theodorakis NG, Drujan D, Maio AD. Thermotolerant Cells Show an Attenuated Expression of Hsp70 after Heat Shock *. J Biol Chem. 1999 Apr 23;274(17):12081–6.
115. Theodorakis NG, Morimoto RI. Posttranscriptional regulation of hsp70 expression in human cells: effects of heat shock, inhibition of protein synthesis, and adenovirus infection on translation and mRNA stability. Mol Cell Biol. 1987 Dec;7(12):4357–68.
116. Rubtsova MP, Sizova DV, Dmitriev SE, Ivanov DS, Prassolov VS, Shatsky IN. Distinctive Properties of the 5′-Untranslated Region of Human Hsp70 mRNA*. J Biol Chem. 2003 Jun 20;278(25):22350–6.
117. Vivinus S, Baulande S, Zanten M van, Campbell F, Topley P, Ellis JH, et al. An element within the 5′ untranslated region of human Hsp70 mRNA which acts as a general enhancer of mRNA translation. Eur J Biochem. 2001;268(7):1908–17.
118. Hess MA, Duncan RF. Sequence and structure determinants of Drosophila Hsp70 mRNA translation: 5'UTR secondary structure specifically inhibits heat shock protein mRNA translation. Nucleic Acids Res. 1996 Jun 15;24(12):2441–9.
119. McGarry TJ, Lindquist S. The preferential translation of Drosophila hsp70 mRNA requires sequences in the untranslated leader. Cell. 1985 Oct 1;42(3):903–11.
120. Petersen RB, Lindquist S. Regulation of HSP70 synthesis by messenger RNA degradation. Cell Regul. 1989 Nov;1(1):135–49.
121. Shi Y, Mosser DD, Morimoto RI. Molecularchaperones as HSF1-specific transcriptional repressors. Genes Dev. 1998 Mar 1;12(5):654–66.
122. Hershey JWB, Sonenberg N, Mathews MB. Principles of Translational Control. Cold Spring Harb Perspect Biol. 2019 Sep 1;11(9):a032607.
123. Holcik M, Sonenberg N. Translational control in stress and apoptosis. Nat Rev Mol Cell Biol. 2005 Apr;6(4):318–27.
124. Alagar Boopathy LR, Beadle E, Garcia-Bueno Rico A, Vera M. Proteostasis regulation through ribosome quality control and no-go-decay. WIREs RNA. 2023;14(6):e1809.

125. Sitron CS, Park JH, Brandman O. Asc1, Hel2, and Slh1 couple translation arrest to nascent chain degradation. RNA N Y N. 2017 May;23(5):798–810.
126. Becker T, Armache JP, Jarasch A, Anger AM, Villa E, Sieber H, et al. Structure of the no-go mRNA decay complex Dom34-Hbs1 bound to a stalled 80S ribosome. Nat Struct Mol Biol. 2011 Jun;18(6):715–20.
127. Doma MK, Parker R. Endonucleolytic cleavage of eukaryotic mRNAs with stalls in translation elongation. Nature. 2006 Mar;440(7083):561–4.
128. Ikeuchi K, Inada T. Ribosome-associated Asc1/RACK1 is required for endonucleolytic cleavage induced by stalled ribosome at the 3′ end of nonstop mRNA. Sci Rep. 2016 Jun 17;6(1):28234.
129. Wang J, Zhou J, Yang Q, Grayhack EJ. Multi-protein bridging factor 1(Mbf1), Rps3 and Asc1 prevent stalled ribosomes from frameshifting. Green R, Manley JL, editors. eLife. 2018 Nov 22;7:e39637.
130. Sinha NK, Ordureau A, Best K, Saba JA, Zinshteyn B, Sundaramoorthy E, et al. EDF1 coordinates cellular responses to ribosome collisions. Sonenberg N, Manley JL, Sonenberg N, editors. eLife. 2020 Aug 3;9:e58828.
131. Melamed D, Bar-Ziv L, Truzman Y, Arava Y. Asc1 Supports Cell-Wall Integrity Near Bud Sites by a Pkc1 Independent Mechanism. PLOS ONE. 2010 Jun 30;5(6):e11389.
132. Wong ED, Miyasato SR, Aleksander S, Karra K, Nash RS, Skrzypek MS, et al. Saccharomyces genome database update: server architecture, pan-genome nomenclature, and external resources. Genetics. 2023 May 4;224(1):iyac191.
133. Juszkiewicz S, Chandrasekaran V, Lin Z, Kraatz S, Ramakrishnan V, Hegde RS. ZNF598 Is a Quality Control Sensor of Collided Ribosomes. Mol Cell. 2018 Nov 1;72(3):469-481.e7.
134. Li Z, Lee I, Moradi E, Hung NJ, Johnson AW, Marcotte EM. Rational Extension of the Ribosome Biogenesis Pathway Using Network-Guided Genetics. PLOS Biol. 2009 Oct 6;7(10):e1000213.
135. Starosta AL, Wilson DN. Ribosome rescue, nearing the end. Cell. 2014 Feb 27;156(5):866–7.
136. Buskirk AR, Green R. Ribosome pausing, arrest and rescue in bacteria and eukaryotes. Philos Trans R Soc B Biol Sci. 2017 Mar 19;372(1716):20160183.
137. Matsuo Y, Ikeuchi K, Saeki Y, Iwasaki S, Schmidt C, Udagawa T, et al. Ubiquitination of stalled ribosome triggers ribosome-associated quality control. Nat Commun. 2017 Jul 31;8(1):159.
138. Ikeuchi K, Tesina P, Matsuo Y, Sugiyama T, Cheng J, Saeki Y, et al. Collided ribosomes form a unique structural interface to induce Hel2-driven quality control pathways. EMBO J. 2019 Mar 1;38(5):e100276.
139. Matsuo Y, Inada T. The ribosome collision sensor Hel2 functions as preventive quality control in the secretory pathway. Cell Rep. 2021 Mar;34(12):108877.
140. Best K, Ikeuchi K, Kater L, Best D, Musial J, Matsuo Y, et al. Structural basis for clearing of ribosome collisions by the RQT complex. Nat Commun. 2023 Feb 17;14(1):921.
141. T S, S L, M K, K I, A I, Y M, et al. Sequential Ubiquitination of Ribosomal Protein uS3 Triggers the Degradation of Non-functional 18S rRNA. Cell Rep [Internet]. 2019 Mar 19 [cited 2023 Mar 19];26(12). Available from: https://pubmed.ncbi.nlm.nih.gov/30893611/

142. Juszkiewicz S, Slodkowicz G, Lin Z, Freire-Pritchett P, Peak-Chew SY, Hegde RS. Ribosome collisions trigger cis-acting feedback inhibition of translation initiation. Topisirovic I, Pfeffer SR, Topisirovic I, editors. eLife. 2020 Jul 13;9:e60038.
143. Hickey KL, Dickson K, Cogan JZ, Replogle JM, Schoof M, D'Orazio KN, et al. GIGYF2 and 4EHP Inhibit Translation Initiation of Defective Messenger RNAs to Assist Ribosome-Associated Quality Control. Mol Cell. 2020 Sep 17;79(6):950-962.e6.
144. Hendrick JL, Wilson PG, Edelman II, Sandbaken MG, Ursic D, Culbertson MR. Yeast frameshift suppressor mutations in the genes coding for transcription factor Mbf1p and ribosomal protein S3: evidence for autoregulation of S3 synthesis. Genetics. 2001 Mar;157(3):1141–58.
145. Garí E, Volpe T, Wang H, Gallego C, Futcher B, Aldea M. Whi3 binds the mRNA of the G1 cyclin CLN3 to modulate cell fate in budding yeast. Genes Dev. 2001 Nov 1;15(21):2803–8.
146. Gilbert WV, Zhou K, Butler TK, Doudna JA. Cap-Independent Translation Is Required for Starvation-Induced Differentiation in Yeast. Science. 2007;317(5842):1224–7.
147. Zhang XR, Zhao L, Suo F, Gao Y, Wu Q, Qi X, et al. An improved auxin-inducible degron system for fission yeast. G3 Bethesda Md. 2022 Jan 4;12(1):jkab393.
148. Nishimura K, Fukagawa T, Takisawa H, Kakimoto T, Kanemaki M. An auxin-based degron system for the rapid depletion of proteins in nonplant cells. Nat Methods. 2009 Dec;6(12):917–22.
149. Kanke M, Nishimura K, Kanemaki M, Kakimoto T, Takahashi TS, Nakagawa T, et al. Auxin-inducible protein depletion system in fission yeast. BMC Cell Biol. 2011 Feb 11;12:8.
150. Feder JH, Rossi JM, Solomon J, Solomon N, Lindquist S. The consequences of expressing hsp70 in Drosophila cells at normal temperatures. Genes Dev. 1992 Aug 1;6(8):1402–13.
151. Kumar S, Stokes J, Singh UP, Gunn KS, Acharya A, Manne U, et al. Targeting Hsp70: A possible therapy for cancer. Cancer Lett. 2016 Apr 28;374(1):156–66.
152. Joshi CP, Nguyen HT. 5' untranslated leader sequences of eukaryotic mRNAs encoding heat shock induced proteins. Nucleic Acids Res. 1995 Feb 25;23(4):541–9.
153. Kozak M. An analysis of vertebrate mRNA sequences: intimations of translational control. J Cell Biol. 1991 Nov;115(4):887–903.
154. Kozak M. Structural features in eukaryotic mRNAs that modulate the initiation of translation. J Biol Chem. 1991 Oct 25;266(30):19867–70.
155. Zhang Y, Feigenblum D, Schneider RJ. A late adenovirus factor induces eIF-4E dephosphorylation and inhibition of cell protein synthesis. J Virol. 1994 Nov;68(11):7040–50.
156. Pelletier J, Sonenberg N. Internal initiation of translation of eukaryotic mRNA directed by a sequence derived from poliovirus RNA. Nature. 1988 Jul;334(6180):320–5.
157. Jang SK, Kräusslich HG, Nicklin MJ, Duke GM, Palmenberg AC, Wimmer E. A segment of the 5' nontranslated region of encephalomyocarditis virus RNA directs internal entry of ribosomes during in vitro translation. J Virol. 1988 Aug;62(8):2636–43.
158. Joshi-Barve S, Benedetti AD, Rhoads RE. Preferential translation of heat shock mRNAs in HeLa cells deficient in protein synthesis initiation factors eIF-4E and eIF-4 gamma. J Biol Chem. 1992 Oct 15;267(29):21038–43.

159. Chahal J, Gebert LFR, Gan HH, Camacho E, Gunsalus KC, MacRae IJ, et al. miR-122 and Ago interactions with the HCV genome alter the structure of the viral 5' terminus. Nucleic Acids Res. 2019 Jun 4;47(10):5307–24.
160. Perera R, Daijogo S, Walter BL, Nguyen JHC, Semler BL. Cellular Protein Modification by Poliovirus: the Two Faces of Poly(rC)-Binding Protein. J Virol. 2007 Sep;81(17):8919–32.
161. Ma LY, Wang L, Liang J, Huo L. Investigating the neuroprotective potential of rAAV2-PCBP1-EGFP gene therapy against a 6-OHDA-induced model of Parkinson's disease. Brain Behav. 2024;14(1):e3376.
162. Macejak DG, Sarnow P. Internal initiation of translation mediated by the 5′ leader of a cellular mRNA. Nature. 1991 Sep;353(6339):90–4.
163. Pelham HR. Speculations on the functions of the major heat shock and glucose-regulated proteins. Cell. 1986 Sep 26;46(7):959–61.
164. Lee AS. Coordinated regulation of a set of genes by glucose and calcium ionophores in mammalian cells. Trends Biochem Sci. 1987 Jan 1;12:20–3.
165. Lee AS. Mammalian stress response: induction of the glucose-regulated protein family. Curr Biol. 1992 Apr;2(4):191.
166. Sarnow P. Translation of glucose-regulated protein 78/immunoglobulin heavy-chain binding protein mRNA is increased in poliovirus-infected cells at a time when cap-dependent translation of cellular mRNAs is inhibited. Proc Natl Acad Sci U S A. 1989 Aug;86(15):5795–9.
167. Gülow K, Bienert D, Haas IG. BiP is feed-back regulated by control of protein translation efficiency. J Cell Sci. 2002 Jun 1;115(11):2443–52.
168. Le SY, Chen JH, Konings D, Maizel JV. Discovering well-ordered folding patterns in nucleotide sequences. Bioinforma Oxf Engl. 2003 Feb 12;19(3):354–61.
169. Xia X, Holcik M. Strong eukaryotic IRESs have weak secondary structure. PloS One. 2009;4(1):e4136.
170. Spriggs KA, Cobbold LC, Jopling CL, Cooper RE, Wilson LA, Stoneley M, et al. Canonical initiation factor requirements of the Myc family of internal ribosome entry segments. Mol Cell Biol. 2009 Mar;29(6):1565–74.
171. Bastide A, Karaa Z, Bornes S, Hieblot C, Lacazette E, Prats H, et al. An upstream open reading frame within an IRES controls expression of a specific VEGF-A isoform. Nucleic Acids Res. 2008 Apr;36(7):2434–45.
172. Lewis SM, Veyrier A, Hosszu Ungureanu N, Bonnal S, Vagner S, Holcik M. Subcellular Relocalization of a Trans-acting Factor Regulates XIAP IRES-dependent Translation. Mol Biol Cell. 2007 Apr;18(4):1302–11.
173. Shi Y, Frost PJ, Hoang BQ, Benavides A, Sharma S, Gera JF, et al. IL-6-induced stimulation of c-myc translation in multiple myeloma cells is mediated by myc internal ribosome entry site function and the RNA-binding protein, hnRNP A1. Cancer Res. 2008 Dec 15;68(24):10215–22.
174. Ungureanu NH, Cloutier M, Lewis SM, de Silva N, Blais JD, Bell JC, et al. Internal ribosome entry site-mediated translation of Apaf-1, but not XIAP, is regulated during UV-induced cell death. J Biol Chem. 2006 Jun 2;281(22):15155–63.
175. Stoneley M, Paulin FE, Quesne JPL, Chappell SA, Willis AE. C-Myc 5′ untranslated region contains an internal ribosome entry segment. Oncogene. 1998 Jan;16(3):423–8.

176. Holcik M, Korneluk RG. Functional Characterization of the X-Linked Inhibitor of Apoptosis (XIAP) Internal Ribosome Entry Site Element: Role of La Autoantigen in XIAP Translation. Mol Cell Biol. 2000 Jul;20(13):4648–57.
177. Kim YK, Back SH, Rho J, Lee SH, Jang SK. La autoantigen enhances translation of BiP mRNA. Nucleic Acids Res. 2001 Dec 15;29(24):5009–16.
178. Komar AA, Hatzoglou M. Cellular IRES-mediated translation. Cell Cycle. 2011 Jan 15;10(2):229–40.
179. Spahn CMT, Jan E, Mulder A, Grassucci RA, Sarnow P, Frank J. Cryo-EM visualization of a viral internal ribosome entry site bound to human ribosomes: the IRES functions as an RNA-based translation factor. Cell. 2004 Aug 20;118(4):465–75.
180. Muhs M, Hilal T, Mielke T, Skabkin MA, Sanbonmatsu KY, Pestova TV, et al. Cryo-EM of ribosomal 80S complexes with termination factors reveals the translocated cricket paralysis virus IRES. Mol Cell. 2015 Feb 5;57(3):422–32.
181. Akirtava C, May GE, McManus CJ. False-positive IRESes from Hoxa9 and other genes resulting from errors in mammalian 5′ UTR annotations. Proc Natl Acad Sci. 2022 Sep 6;119(36):e2122170119.
182. Yang Y, Wang Z. IRES-mediated cap-independent translation, a path leading to hidden proteome. J Mol Cell Biol. 2019 Sep 3;11(10):911–9.
183. Milner CM, Duncan Campbell R. Structure and expression of the three MHC-linked HSP70 genes. Immunogenetics. 1990 Oct 1;32(4):242–51.
184. Jan E, Sarnow P. Factorless ribosome assembly on the internal ribosome entry site of cricket paralysis virus. J Mol Biol. 2002 Dec 13;324(5):889–902.
185. Somero GN. RNA thermosensors: how might animals exploit their regulatory potential? J Exp Biol. 2018 Feb 22;221(4):jeb162842.
186. Kortmann J, Narberhaus F. Bacterial RNA thermometers: molecular zippers and switches. Nat Rev Microbiol. 2012 Apr;10(4):255–65.
187. Torrent M, Chalancon G, de Groot NS, Wuster A, Madan Babu M. Cells alter their tRNA abundance to selectively regulate protein synthesis during stress conditions. Sci Signal. 2018 Sep 4;11(546):eaat6409.
188. Saikia M, Wang X, Mao Y, Wan J, Pan T, Qian SB. Codon optimality controls differential mRNA translation during amino acid starvation. RNA. 2016 Nov;22(11):1719–27.
189. Bouveret E, Rigaut G, Shevchenko A, Wilm M, Séraphin B. A Sm-like protein complex that participates in mRNA degradation. EMBO J. 2000 Apr 3;19(7):1661–71.
190. Tharun S, He W, Mayes AE, Lennertz P, Beggs JD, Parker R. Yeast Sm-like proteins function in mRNA decapping and decay. Nature. 2000 Mar 30;404(6777):515–8.
191. Bonnerot C, Boeck R, Lapeyre B. The two proteins Pat1p (Mrt1p) and Spb8p interact in vivo, are required for mRNA decay, and are functionally linked to Pab1p. Mol Cell Biol. 2000 Aug;20(16):5939–46.
192. Zid BM, O'Shea EK. Promoter sequences direct cytoplasmic localization and translation of mRNAs during starvation in yeast. Nature. 2014 Oct;514(7520):117–21.
193. Trcek T, Larson DR, Moldón A, Query CC, Singer RH. Single-molecule mRNA decay measurements reveal promoter- regulated mRNA stability in yeast. Cell. 2011 Dec 23;147(7):1484–97.
194. Tkach JM, Yimit A, Lee AY, Riffle M, Costanzo M, Jaschob D, et al. Dissecting DNA damage response pathways by analysing protein localization and abundance changes during DNA replication stress. Nat Cell Biol. 2012 Sep;14(9):966–76.

195. Loll-Krippleber R, Brown GW. P-body proteins regulate transcriptional rewiring to promote DNA replication stress resistance. Nat Commun. 2017 Sep 15;8(1):558.
196. DiDomenico BJ, Bugaisky GE, Lindquist S. Heat shock and recovery are mediated by different translational mechanisms. Proc Natl Acad Sci. 1982 Oct 1;79(20):6181–5.
197. Didomenico BJ, Bugaisky GE, Lindquist S. The heat shock response is self-regulated at both the transcriptional and posttranscriptional levels. Cell. 1982 Dec 1;31(3, Part 2):593–603.
198. Jolly C, Morimoto RI. Role of the heat shock response and molecular chaperones in oncogenesis and cell death. J Natl Cancer Inst. 2000 Oct 4;92(19):1564–72.
199. Murphy ME. The HSP70 family and cancer. Carcinogenesis. 2013 Jun;34(6):1181–8.
200. Dankner M, Caron M, Al-Saadi T, Yu W, Ouellet V, Ezzeddine R, et al. Invasive growth associated with cold-inducible RNA-binding protein expression drives recurrence of surgically resected brain metastases. Neuro-Oncol. 2021 Sep 1;23(9):1470–80.
201. Dankner M, Savage P, Rose A, Lajoie M, Diaz R, Park M, et al. TMOD-41. ORTHOTOPIC PATIENT-DERIVED XENOGRAFT MODELS OF BRAIN METASTASIS: PLATFORMS FOR PRECISION ONCOLOGY AND UNDERSTANDING TUMOR BIOLOGY. Neuro-Oncol. 2019 Nov 11;21(Supplement_6):vi272.
202. Dankner M, Lam S, Degenhard T, Garzia L, Guiot MC, Petrecca K, et al. The Underlying Biology and Therapeutic Vulnerabilities of Leptomeningeal Metastases in Adult Solid Cancers. Cancers. 2021 Feb 10;13(4):732.
203. Zhao K, Zhou G, Liu Y, Zhang J, Chen Y, Liu L, et al. HSP70 Family in Cancer: Signaling Mechanisms and Therapeutic Advances. Biomolecules. 2023 Apr;13(4):601.

6. APPENDIX

APPENDIX 1: Asc1p modulation of *SSA4* mRNA stability during recovery from stress in Saccharomyces cerevisiae

Authors: Lokha R Alagar Boopathy, Kevin Munoz Portocarrero, Jessamine Mattson, Maria Vera Ugalde.

ABSTRACT

Organisms react to environmental stress by increasing the production of a group of proteins referred to as heat shock proteins (HSPs); more specifically, to HSP70 since it is one of the most functionally significant upon stress. This study delves into the regulatory mechanisms underlying the stability of *SSA4* mRNA, a member of the Stress Seventy sub-family A (Ssa) in budding yeast, during recovery from heat shock. The investigation focuses on the role of Asc1p, a scaffold protein, in mediating the decay of *SSA4* mRNA through potential binding sites within SSA4 3'UTR, promoter, and 5'UTR regions. Surprisingly, our results challenge our initial hypothesis that Asc1p directly influences *SSA4* mRNA stability through binding to specific regions. Swapping the 3'UTR, promoter, and 5'UTR of SSA4 with those of a constitutively expressed gene, SSA2, did not significantly alter mRNA turnover. However, the deletion of Asc1p led to a substantial increase in *SSA4* mRNA half-life during recovery, consistent with previous findings. Thus, the study proposes that Asc1p may indirectly modulate mRNA decay, potentially through its role in promoting the formation of cytoplasmic granules known as P-bodies. Future research aims to investigate P-body formation during recovery and further elucidate the intricate pathways through which Asc1p influences *SSA4* mRNA stability.

INTRODUCTION

Organisms respond to environmental stressors by upregulating a set of proteins known as heat shock proteins (HSPs) (1). These molecular chaperones play a crucial role in various biological activities, particularly in the reconfiguration of misfolded proteins, contributing to the maintenance of cellular homeostasis (2,3). HSPs are classified into families based on their apparent molecular weight. Among the ATP-dependent chaperones, HSP70 and HSP90 stand out as the most functionally significant in cellular processes (4). Additionally, HSPs are further categorized into constitutive and inducible groups based on their steady-state expression levels, with the inducible HSP70 genes demonstrating rapid and heightened expression (5). Fast resolution of the stress response is imperative, as prolonged expression of inducible HSP70 under basal conditions has been associated with cancer cells and tumorigenesis (6). In addition, prolonged expression of HSP70 has shown detrimental growth in Drosophila (7). Thus, HSP70 transcripts must transition from a state of high stability during stress to high instability during the recovery phase (8). For that reason, it is very important to study the mechanisms responsible for its mRNA decay.

In budding yeast, the Stress Seventy sub-family A (Ssa) consists of four members: Ssa1-4 (8,9). While the viability of the organism does not depend on any of these subfamilies, SSA4 (the focus of this investigation) is crucial (9). Ssa1 and SSA2 are constitutive, whereas SSA4 is minimally expressed under normal conditions and undergoes rapid and significant upregulation following exposure to heat shock (8,9). This is one of the reasons that SSA4 will be subjected to further analysis in this paper.

Previous literature reveals that Asc1p, a scaffold protein situated at the forefront of the 40S subunit, plays a major role in destabilizing *SSA4* mRNA during recovery from heat stress (8). Nevertheless, the exact process on how Asc1p activates downstream factors to signal the

degradation of *SSA4* mRNA is still poorly understood; thus, we aim to investigate this process. We hypothesize that Asc1p binds to a particular region of the *SSA4* mRNA which activates downstream factors to signal its decay. To test this hypothesis, we decided to look into the effects of Asc1p binding to the 3'UTR, Promoter and 5'UTR of *SSA4* mRNA.

In the first place, earlier studies indicate that the stability of many eukaryotic mRNAs is regulated by adenosine/uridine-rich elements (AREs) located in their 3'UTR sequences (10,11). These ARE sequences facilitate mRNA decay in response to various specific signals both within and outside the cell (12). In addition, the 3'UTR sequence contains the poly(A) tail whose deadenylation is often tightly coupled with mRNA decapping and decay (13,14,15). Moreover, 53 motifs, found in the 3'UTR of *Saccharomyces cerevisiae* genes, have been associated in the regulation of mRNA turnover (15,16). Thus, we hypothesize that Asc1p binds to the 3'UTR sequence of *SSA4* mRNA signaling to its degradation. To test this hypothesis, we swapped the 3'UTR of SSA4 with the one from SSA2 and we further studied the mRNA decay during recovery upon stress. Accordingly, we found that there is no significant difference in mRNA stability between the WT/*asc1Δ* and its corresponding swapped strains. Thus, Asc1p does not regulate *SSA4* mRNA stability through binding to SSA4 3'UTR.

Furthermore, previous work found that the stability of mRNA can be influenced by a promoter through the co-transcriptional loading of an accessory protein onto the mRNA (17). More specifically, they found that promoter-dependent activity directly determines the manner and timing of cytoplasmic degradation for a specific subset of budding yeast mRNAs (18). Therefore, we suspected that Asc1p binds to the promoter of *SSA4* mRNA signaling to its degradation. We tested the influence of SSA4 promoter on the stability of *SSA4* mRNA by replacing it with the promoter region of constitutively expressed SSA2 gene to study the effect on mRNA turnover

during recovery from stress. However, this replacement had no effect on either the WT/*asc1Δ* or its corresponding swapped strains. Thus, Asc1p does not regulate *SSA4* mRNA stability through binding to SSA4 promoter sequence.

Finally, we were able to observe a short poly(A) repeat located in the 5'UTR of *SSA4* mRNA. The SSA4 gene sequence was extracted from the SGD database and mapped on snapGene. As mentioned earlier, the deadenylation of the poly(A) tail is tightly coupled with mRNA degradation (13,14,15). Thus, we decided to further analyze Asc1p's role in binding to the 5'UTR of SSA4 and regulating its stability. On that note, we tested the influence of SSA4 5'UTR on the stability of *SSA4* mRNA by replacing it with the 5'UTR region of constitutively expressed SSA2 gene to study the effect on mRNA turnover during recovery from stress. Nevertheless, this replacement had no significant effect on either the WT/*asc1Δ* or its corresponding swapped strains. Thus, Asc1 does not regulate *SSA4* mRNA stability through binding to SSA4 5'UTR sequence.

MATERIALS AND METHODS

Yeast Culture

All yeast strains originate from the parental strain BY4741 and were cultivated in yeast extract peptone dextrose (YPD) medium. The cultivation was carried out at 25°C with continuous shaking at 250 rpm. Modified strains involving knock-ins and deletions were developed through homologous recombination of the parental strain. This process involved transforming a PCR-amplified fragment from a plasmid containing selection-specific markers. To confirm gene deletions and knock-ins, PCR assays were conducted on genomic DNA extracted from individual colonies.

Heat Shock and recovery

Yeast cells in the logarithmic growth phase (optical density at 600 nm (OD600): 0.4–0.6) were heat shocked in a 42°C water bath with constant shaking at 150 rpm for 30 minutes. Immediately after heat shock, the heated medium was replaced with the same volume of room temperature (RT) medium. The culture flasks were then placed in a 25°C incubator with continuous shaking (250 rpm) until cultures were collected for recovery at 15', 30', 60', and 90' minutes. Recovered yeast (5 ml) was centrifuged at 4000 × g for 3 min at RT and left at -80°C for downstream processing.

RNA extraction and Northern Blotting

In the given procedure, all centrifugations were carried out at 12,000 × g. The cell pellets were suspended in 500 µl of RNA extraction lysis buffer (composed of 10 mM Tris–HCl pH 8.5, 5 mM EDTA, 2% SDS, 2% stock 2-mercaptoethanol) and moved to 1.5 ml tubes. To induce cell lysis, the tubes were incubated in a heat block at 83°C for 20 minutes. Following a 5-minute centrifugation, the resulting supernatant was transferred to a new tube marked in red, containing 550 µl of phenol pH 8.0. After a 30-second vortex and 2-minute centrifugation, the upper layer was transferred to a fresh tube labeled in blue. To the red-labeled tube, 250 µl of RNA extraction lysis buffer was added and briefly vortexed. Subsequently, an equal volume (250 µl) of chloroform was introduced, followed by vortexing and centrifugation, and the upper layer was transferred to the blue-labeled tube. An additional 550 µl of phenol pH 8.0 was added to the blue-labeled tube, vortexed, and spun as previously described, and the upper layer was transferred to a new tube containing 550 µl of acid phenol–chloroform, pH 4.5 (Cat# AM9720, Thermofisher Scientific, St. Austin, TX, USA). After a brief vortex and spin, 450 µl of the upper layer was transferred to a new set of tubes containing 200 µl of 0.6 M sodium acetate + 600 µl Acid Phenol-Chloroform, pH 4.5.

These tubes were vortexed and centrifuged as before. Approximately 350 µl of the upper layer was once again transferred to new tubes containing 1.1 ml of 99% ethanol and 30 µl of 5 M ammonium acetate. Following thorough mixing, the samples were stored at −20°C overnight. On the subsequent day, the samples underwent centrifugation at 4°C for 15 minutes, and the supernatant was discarded. The pellet underwent two washes with 80% ethanol, was air-dried, and then dissolved in 40 µl of RNase-free water for RNA quantification. Twelve micrograms (12 µg) of RNA were dispensed into new tubes and dried in a SpeedVac for 45 minutes at 45°C. Subsequently, the samples were reconstituted in 5 µl of RNase-free water and combined with 7 µl of homemade RNA loading dye. The RNA samples were electrophoresed on a 1% denaturing gel in 1 × MESA buffer. Capillary electrophoresis was utilized for the overnight setup of the transfer to zeta probe nylon membranes. The membrane underwent UV crosslinking at 1200 mJ, followed by staining for total RNA, prehybridization, hybridization, exposure to a phosphor screen, and development using a phosphorimager.

mRNA half-lives calculations

The calculation of mRNA half-life involved quantifying Northern blots with ImageJ and normalizing the results based on corresponding methylene blue staining. The intensity of the heat shock sample at the 0-minute time point was designated as 100% induction. Subsequently, the relative intensity for recovery samples at timepoints 15, 30, 60, and 90 minutes was computed. To model the decay over time, a polynomial curve was generated, plotting time against the percentage of mRNA decayed. The equation of the polynomial curve was determined, and using the what-if analysis feature in Microsoft Excel, the equation was solved for X, with the condition that Y represents 50. This analytical approach allowed for the estimation of the time at which mRNA decay reaches 50%, providing a measure of mRNA half-life in the experimental context.

RESULTS

Asc1p does not affect *SSA4* mRNA stability through 3'UTR binding during recovery from heat shock

To explore Asc1p's role in binding to the 3'UTR to regulate *SSA4* mRNA stability during recovery, we performed a 3'UTR swap by replacing the SSA4 3'UTR with the SSA2 3'UTR in both WT and *asc1Δ* strains. SSA2, a constitutive gene, served as a control in northern blot analysis. The yeast cells were collected at 25°C (RT), after heat shock (42°C), and after recovery for 15, 30, 60, and 90 minutes to follow the stability of the mRNAs. Detection of full-length *SSA4* and *SSA2* mRNAs was achieved using radioactive probes (**Figure 6.1.1A**). Probes for the 3'UTR swap strains were generated through PCR amplification, with a forward primer flanking the end of the *SSA4* coding sequence and a reverse primer flanking a few base pairs of SSA2 3'UTR. In the WT strain, *SSA4* mRNA exhibited high induction during heat shock, returning rapidly to basal levels during recovery, consistent with expectations. On the contrary, *asc1Δ* showed prolonged induction post-heat shock which was anticipated since published data already supported Asc1p's role in regulating *SSA4* mRNA stability during recovery (8).

Notably, there was no significant difference in *SSA4* mRNA expression between WT and WT 3'UTR swap strains during recovery. Similarly, no significant difference was observed in *SSA4* mRNA levels between *asc1Δ* and *asc1Δ* 3'UTR swap strains during recovery. Finally, we plotted the intensities of *SSA4* mRNA bands and calculated their half-lives using non-linear regression (**Figure 6.1.1B**). As expected, we observed a 2.2-fold increase in its half-life upon deletion of Asc1p. Nevertheless, we did not observe a significant change in the half-life of the WT 3'UTR swap strain (0.88-fold) relative to the WT. On that note, we also did not observe a significant change in the half-life of the *asc1Δ* 3'UTR swap strain (0.77-fold) relative to the *asc1Δ*.

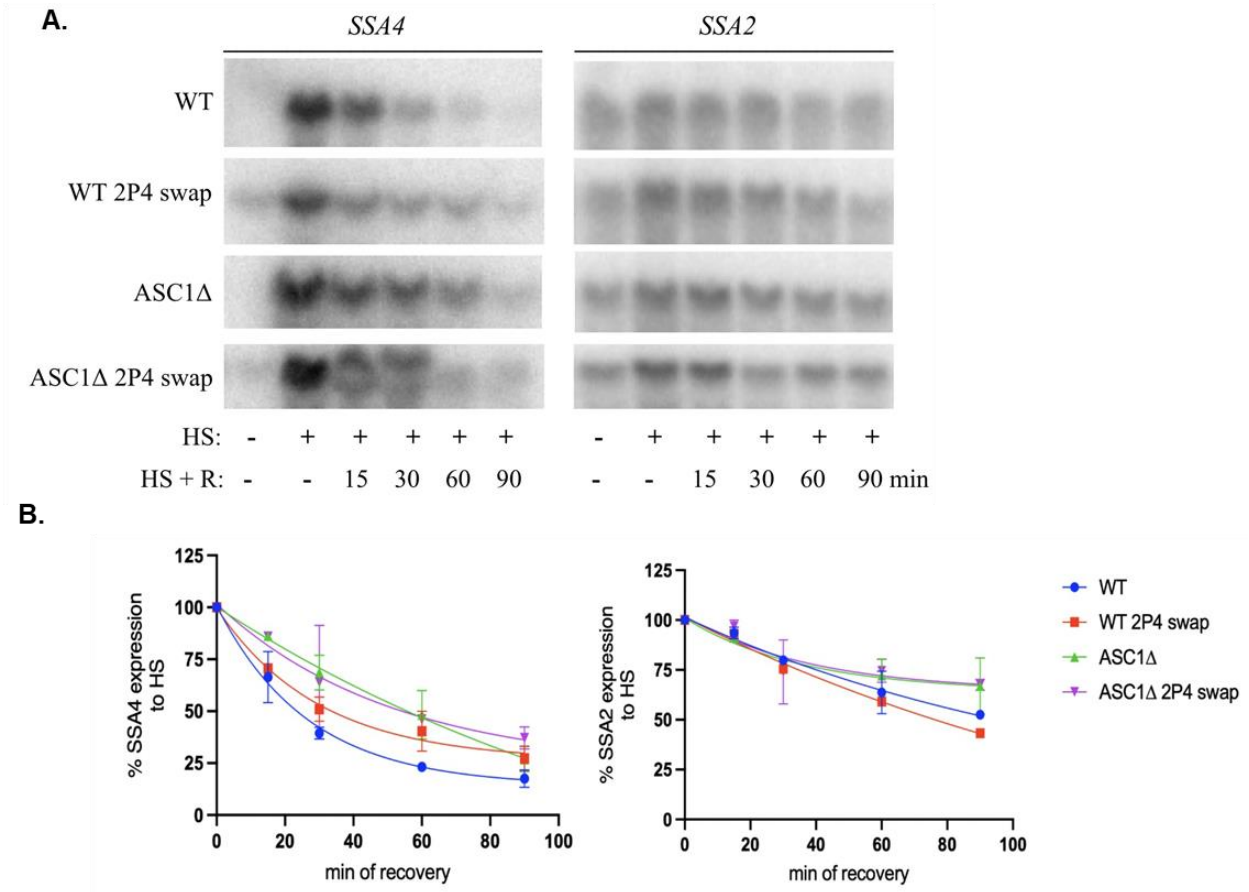

Figure 6.1.1. Asc1p does not affect *SSA4* mRNA stability through 3'UTR binding during recovery from heat shock. (A) Northern blots to assess the expression of SSA4 and *SSA2* mRNAs in the WT, WT 3'UTR swap, *asc1Δ* and *asc1Δ* 3'UTR swap strains at RT conditions, after 30 minutes of heat shock at 42°C (HS), and at the indicated recovery time stamps (R). **(B)** Decay plots of SSA4 and *SSA2* mRNAs throughout recovery. Band intensities were corrected to the methylene blue staining and are expressed relative to the HS band for each strain (considered to be 100% expression) to obtain decay curves and calculate half-lives *(t1/2 of SSA4* mRNA*: WT 26', WT 3'UTR swap 23', asc1Δ 57' and asc1Δ 3'UTR swap 44').*

Asc1p does not affect *SSA4* mRNA stability through promoter binding during recovery from heat shock

To determine whether Asc1p is binding to the promoter to regulate SSA4's mRNA stability during recovery, we performed a promoter swap by replacing the SSA4 promoter with the SSA2 promoter (referred to as 2P4) in both WT and *asc1Δ* strains (**Figure 6.1.2A**). The yeast cells were collected at 25°C (RT), after heat shock (42°C), and after recovery for 15, 30, 60, and 90 minutes

to follow the stability of the mRNAs. From the northern blot results, the *SSA4* mRNA in WT strain exhibited high induction during heat shock, returning rapidly to basal levels during recovery, consistent with expectations. On the other hand, the prolonged induction observed in *asc1Δ* after heat shock was expected, given the existing published data that supports Asc1p's role in the regulation of *SSA4* mRNA stability during the recovery phase (8). Notably, there was no significant difference in *SSA4* mRNA expression between WT and WT 2P4 swap strains during recovery. Similarly, no significant difference was observed in *SSA4* mRNA levels between *asc1Δ* and *asc1Δ* 2P4 swap strains during recovery. Finally, we plotted the intensities of *SSA4* mRNA bands and calculated their half-lives using non-linear regression (**Figure 6.1.2B**). As expected, we observed a 2.2-fold increase in its half-life upon deletion of *ASC1*. Nevertheless, we did not observe a significant change in the half-life of the WT 2P4 swap strain (1.2-fold) relative to the WT. On that note, we also did not observe a significant change in the half-life of the *asc1Δ* 2P4 swap strain (0.89-fold) relative to the *asc1Δ*.

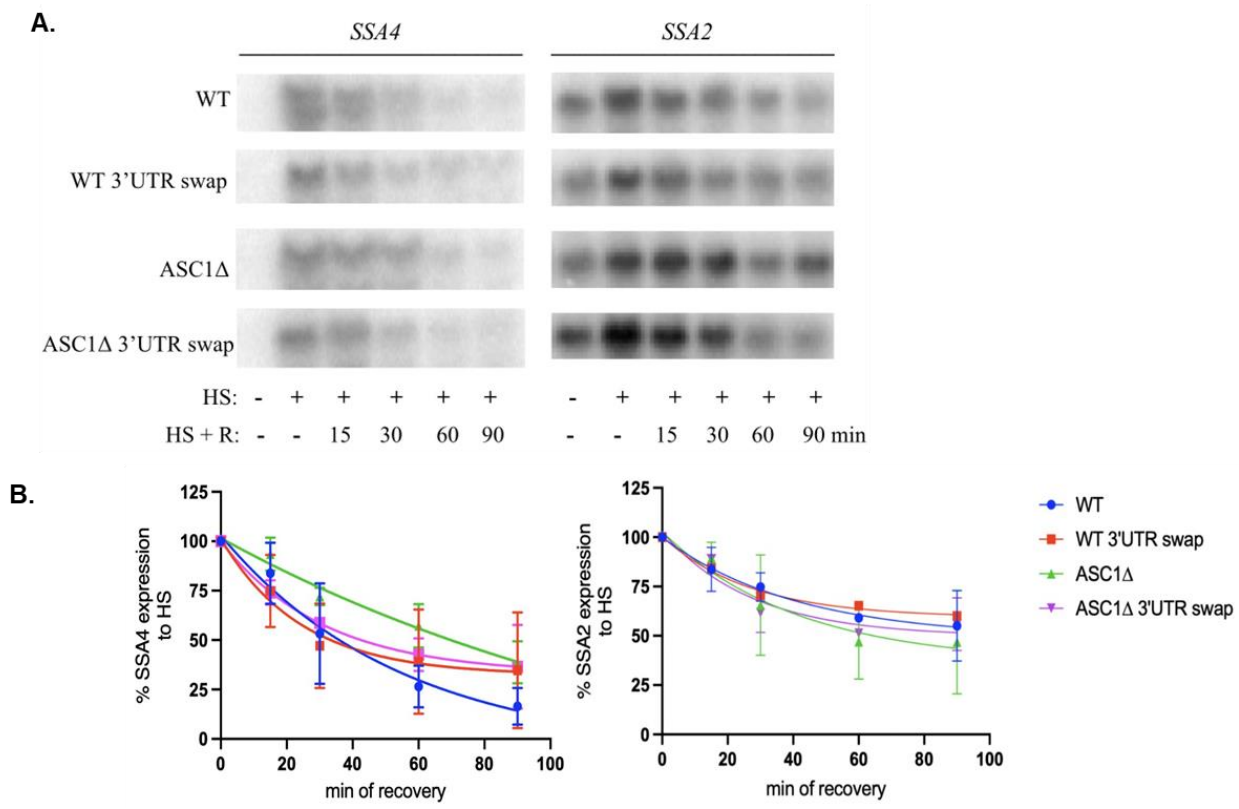

Figure 6.1.2. Asc1p does not affect *SSA4* mRNA stability through promoter binding during recovery from heat shock. (A) Northern blots to assess the expression of SSA4 and *SSA2* mRNAs in the WT, WT 2P4 swap, *asc1Δ* and *asc1Δ* 2P4 swap strains at RT conditions, after 30 minutes of heat shock at 42°C (HS), and at the indicated recovery time stamps (R). **(B)** Decay plots of SSA4 and *SSA2* mRNAs throughout recovery. Band intensities were corrected to the methylene blue staining and are expressed relative to the HS band for each strain (considered to be 100% expression) to obtain decay curves and calculate half-lives *(t1/2 of SSA4* mRNA*: WT 26', WT 2P4 swap 31', asc1Δ 56' and asc1Δ 2P4 swap 50').*

Asc1p does not affect *SSA4* mRNA stability through 5'UTR binding during recovery from heat shock

To explore Asc1p's role in binding to the 5'UTR to regulate SSA4's mRNA stability during recovery, we performed a 5'UTR swap by replacing the SSA4 5'UTR with the SSA2 5'UTR in both WT and *asc1Δ* strains. To assess the stability of *SSA4* mRNA levels, we performed northern blot by collect yeast cells under control, HS, HS followed by 15, 30, 60 and 90 minutes of recovery

(**Figure 6.1.3A**). In the WT strain, *SSA4* mRNA exhibited the expected pattern of high induction during heat shock, returning rapidly to basal levels during recovery. On the other hand, *asc1Δ* showed prolonged induction post-heat shock which was anticipated since published data already supported Asc1's role in regulating *SSA4* mRNA stability during recovery (8).

Notably, there was no significant difference in *SSA4* mRNA expression between WT and WT 5'UTR swap strains during recovery. Similarly, no significant difference was observed in *SSA4* mRNA levels between *asc1Δ* and *asc1Δ* 5'UTR swap strains during recovery. Finally, we plotted the intensities of *SSA4* mRNA bands and calculated their half-lives using non-linear regression (**Figure 6.1.3B**). As expected, we observed a 2.1-fold increase in its half-life upon deletion of Asc1p. Nevertheless, we did not observe a significant change in the half-life of the WT 5'UTR swap strain (0.89-fold) relative to the WT. Similarly, we also did not observe a significant change in the half-life of the *asc1Δ* 3'UTR swap strain (0.73-fold) relative to the *asc1Δ*.

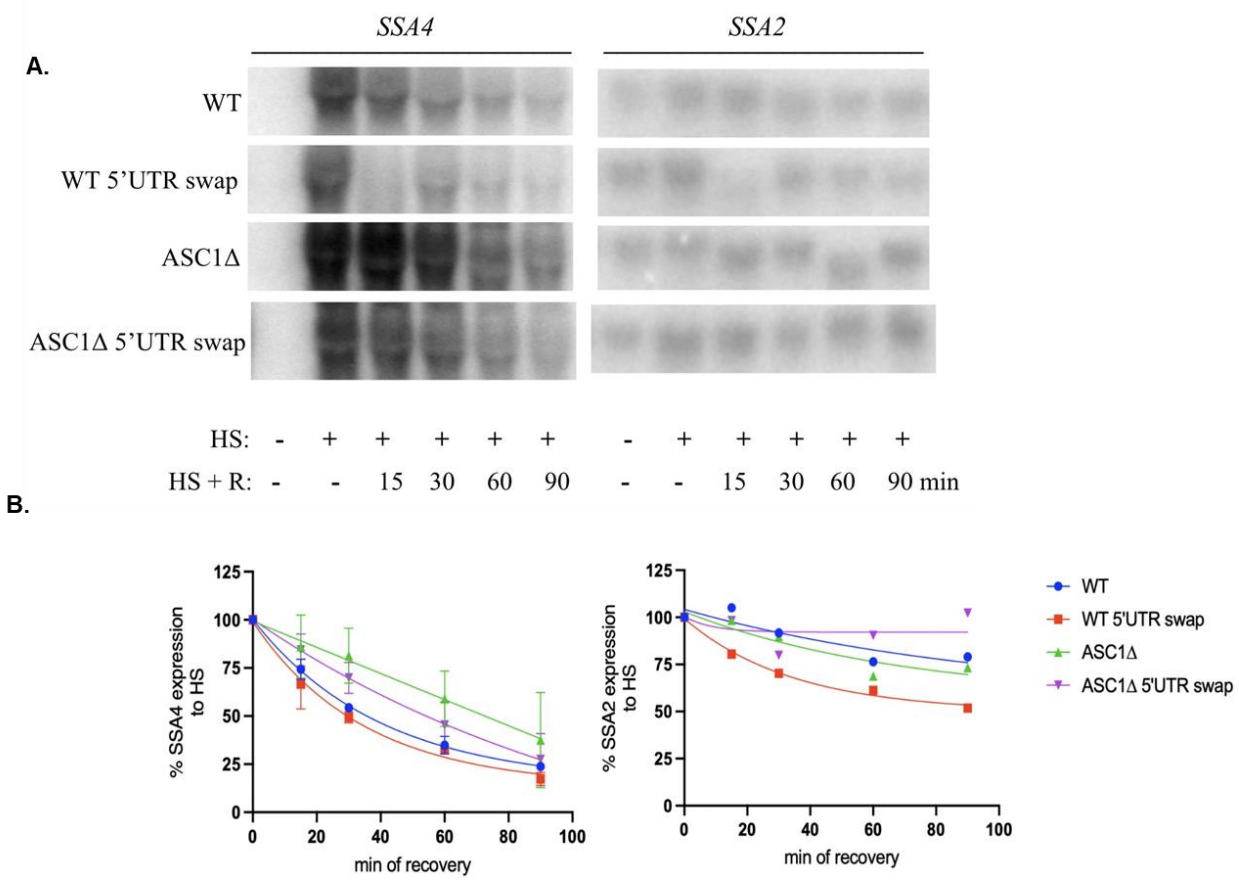

Figure 6.1.3. Asc1p does not affect *SSA4* mRNA stability through 5'UTR binding during recovery from heat shock. (A) Northern blots to assess the expression of SSA4 and *SSA2* mRNAs in the WT, WT 5'UTR swap, *asc1Δ* and *asc1Δ* 5'UTR swap strains at RT conditions, after 30 minutes of heat shock at 42°C (HS), and at the indicated recovery time stamps (R). **(B)** Decay plots of SSA4 and *SSA2* mRNAs throughout recovery. Band intensities were corrected to the methylene blue staining and are expressed relative to the HS band for each strain (considered to be 100% expression) to obtain decay curves and calculate half-lives *(t1/2 of SSA4* mRNA*: WT 36', WT 3'UTR swap 32', asc1Δ 75' and asc1Δ 3'UTR swap 55').*

DISCUSSION

The investigation aimed to elucidate the role of Asc1p in regulating the stability of *SSA4* mRNA during recovery from heat shock, focusing on potential binding sites within the 3'UTR, promoter, and 5'UTR regions. The results obtained provide insights into the molecular mechanisms underlying the decay of *SSA4* mRNA during recovery from stress. Our results demonstrated that replacing the 3'UTR of SSA4 with that of the constitutively expressed SSA2 did not alter *SSA4* mRNA stability. We were very surprised by the outcome of these results since researchers have

widely associated the function of 3'UTRs to mRNA decay (10-16). In a similar fashion, our work revealed that replacing the SSA4 promoter with the constitutively expressed SSA2 promoter did not affect mRNA turnover. Thus, the SSA4 promoter does not play a major role in its mRNA stability. An interesting observation to comment is that we were able to see some mRNA expression in the WT 2P4 swap control sample. As stated before, SSA4 is an inducible gene; thus, its expression should not be seen in control conditions but only upon stress (8,9). Nevertheless, due to the fact that the promoter was swapped to the one of SSA2 (constitutive gene), we were able to observe some expression even in control conditions. Lastly, our work disclosed that replacing the 5'UTR of *SSA4* with that of *SSA2* mRNA did not significantly impact *SSA4* mRNA stability. On that note, these findings refuted our original hypothesis which established Asc1p regulating *SSA4* mRNA stability through binding to a specific region of *SSA4* mRNA.

The observed increase in *SSA4* mRNA half-life upon *ASC1* deletion is consistent with previous findings, affirming Asc1p's role in modulating *SSA4* mRNA stability during recovery from heat shock. However, the lack of significant changes in mRNA stability in the swapped strains suggests that Asc1p may influence mRNA decay indirectly rather than direct binding to a single region. More specifically, previous literature has linked Asc1p promoting cytoplasmic granule formation during stress (19). These cytoplasmic granules known as P-bodies emerge in eukaryotic cells as a reaction to various stresses (19,20). These structures function as locations for the degradation of some mRNA molecules (19-21). In addition, it has been found that these P-bodies contain all the necessary components for the mRNA degradation machinery such as the 5'−3' exonuclease Xrn1p (20,21). Furthermore, previous studies have shown that *SSA4* mRNA's half-life is vastly increased in strains depleted from Xrn1p in comparison to WT (8). Thus, Xrn1p plays a crucial role in the degradation of *SSA4* mRNA during recovery (8). For the reasons outlined

before and the results obtained in this study, we believe that Asc1p might mitigate *SSA4* mRNA stability indirectly through P-bodies rather than a direct binding to a specific region of *SSA4* mRNA. To test this hypothesis in the future, we aim to start by transforming a plasmid containing a fluorescent tag for P-bodies into our yeast strains in order to observe them under the microscope and assess P-body formation during recovery. In conclusion, while our initial hypotheses regarding the direct involvement of the 3'UTR, promoter, and 5'UTR in Asc1p-mediated regulation of *SSA4* mRNA stability were not supported, the study opens avenues for future research to unravel the intricate web of interactions governing *SSA4* mRNA decay in response to environmental stressors.

REFERENCES

1. Mühlhofer,M., Berchtold,E., Stratil,C.G., Csaba,G., Kunold,E., Bach,N.C., Sieber,S.A., Haslbeck,M., Zimmer,R. and Buchner,J. (2019). The heat shock response in yeast maintains protein homeostasis by chaperoning and replenishing proteins. Cell Rep., 29, 4593–4607.
2. Shan Q, Ma F, Wei J, Li H, Ma H, Sun P. (2020). Physiological Functions of Heat Shock Proteins. Bentham Science, 21, 751-760.
3. Craig, E. A., Gambill, B. D., & Nelson, R. J. (1993). Heat shock proteins: molecular chaperones of protein biogenesis. Microbiological reviews, 57, 402–414.
4. Rosenzweig, R., Nillegoda, N.B., Mayer, M.P., and Bukau, B. (2019). The Hsp70 chaperone network. Nature reviews molecular cell biology, 20, 665-680.
5. Kampinga,H.H., Hageman,J., Vos,M.J., Kubota,H., Tanguay,R.M., Bruford,E.A., Cheetham,M.E., Chen,B. and Hightower,L.E. (2009). Guidelines for the nomenclature of the human heat shock proteins. Cell Stress Chaperones, 14, 105–111.
6. Kumar,S., Stokes,J., Singh,U.P., Gunn,K.S., Acharya,A., Manne,U. and Mishra,M. (2016) Targeting Hsp70: a possible therapy for cancer. Cancer Lett., 374, 156–166
7. Feder,J.H., Rossi,J.M., Solomon,J., Solomon,N. and Lindquist,S. (1992). The consequences of expressing hsp70 in Drosophila cells at normal temperatures. Genes Dev., 6, 1402–1413.
8. Alagar Boopathy, L. R., Beadle, E., Xiao, A. R., Garcia-Bueno Rico, A., Alecki, C., Garcia de-Andres, I., Edelmeier, K., Lazzari, L., Amiri, M., & Vera, M. (2023). The ribosome quality control factor Asc1p determines the fate of HSP70 mRNA on and off the ribosome. Nucleic acids research, 51, 6370–6388.
9. Boorstein, W. R., & Craig, E. A. (1990). Structure and regulation of the SSA4 HSP70 gene of Saccharomyces cerevisiae. The Journal of biological chemistry, 265, 18912–18921.
10. Prouteau, M., Daugeron, M. C., & Séraphin, B. (2008). Regulation of ARE transcript 3' end processing by the yeast Cth2 mRNA decay factor. The EMBO journal, 27, 2966–2976.

11. Laroia, G., Cuesta, R., Brewer, G., & Schneider, R. J. (1999). Control of mRNA decay by heat shock-ubiquitin-proteasome pathway. Science, 284, 499–502.
12. Mignone, F., Gissi, C., Liuni, S. et al. Untranslated regions of mRNAs. (2002). Genome Biol, 3.
13. Mayya Vinay K., Duchaine T. Ciphers and Executioners: How 3′-Untranslated Regions Determine the Fate of Messenger RNAs. (2019). Frontiers in Genetics, 10, 1-18.
14. Anderson, J. S., & Parker, R. P. (1998). The 3' to 5' degradation of yeast mRNAs is a general mechanism for mRNA turnover that requires the SKI2 DEVH box protein and 3' to 5' exonucleases of the exosome complex. The EMBO journal, 17, 1497–1506.
15. Savinov, A., Brandsen, B. M., Angell, B. E., Cuperus, J. T., & Fields, S. (2021). Effects of sequence motifs in the yeast 3' untranslated region determined from massively parallel assays of random sequences. Genome biology, 22, 1-27.
16. Shalgi, R., Lapidot, M., Shamir, R., & Pilpel, Y. (2005). A catalog of stability-associated sequence elements in 3' UTRs of yeast mRNAs. Genome biology, 6, 1-15.
17. Zid, B., O'Shea, E. (2014). Promoter sequences direct cytoplasmic localization and translation of mRNAs during starvation in yeast. Nature, 117–121.
18. Trcek, T., Larson, D. R., Moldón, A., Query, C. C., & Singer, R. H. (2011). Single-molecule mRNA decay measurements reveal promoter- regulated mRNA stability in yeast. Cell, 147, 1484–1497.
19. Loll-Krippleber, R., Brown, G.W. (2017). P-body proteins regulate transcriptional rewiring to promote DNA replication stress resistance. Nat Commun, 8, 1-15.
20. Wang, C., Schmich, F., Srivatsa, S., Weidner, J., Beerenwinkel, N., & Spang, A. (2018). Context-dependent deposition and regulation of mRNAs in P-bodies. eLife, 7, 1-25.
21. Walters, R. W., Muhlrad, D., Garcia, J., & Parker, R. (2015). Differential effects of Ydj1 and Sis1 on Hsp70-mediated clearance of stress granules in Saccharomyces cerevisiae. RNA, 21, 1660–1671.

APPENDIX 2: Chapter 3 supplementary tables

Supplementary table 2.1: table of plasmids

Plasmid	Reference
pSH62-EBD	Addgene 49455
pSH47 gal Ura Cre	Genbank AF298782
YCplac111	GenBank X75457, L26350
YCplac211	GenBank X75462, L26358
pFA6a-kanMX6	Euroscarf
pFA6-hphNT1	Euroscarf
p415-3xHA-12V6WT	pMV54
pUC57+OPTSSA4	pMV157
pSH47-OPTSSA4	pMV-AX005
pFN6+Hygro SSA4+MUT 3'UTR	pMV183
pRS416-Asc1M1x	pMV195
pRS416-Asc1DY	pMV196
pFA6a-kanMX6-3xFlag	pMV189
YCplac111+pGPD-GFP-K12 (AAAAAG)-FLAG-HIS	pMV234 (recloned from Dimitrova and Inada 2009)
YCplac111+pGPD-GFP-R12-FLAG-HIS	pMV235 (recloned from Dimitrova and Inada 2009)
p415GPDp-RPS20 WT	Matsuo Nat Commun 2017
p415GPDp-RPS20 K6R K8R	Matsuo Nat Commun 2017
pFA6-Halo-HISMX6+3XHA-SSA4	pMV237

Supplementary table 2.2: table of primers

Primer	Sequence
SSA4nbF	GAGTAAATTTTACGGAGCTGC
SSA4nbR	CTCTGGCTTATGACGATGAG
SSA3nbF	ATCCATGCCCAACTCGGGTGC
SSA3nbR	GAAGTGTGCGTTACTCTCGGAC
SSA2nbF	GAAGGCTGAAGAAACTATTGCTTGG
SSA2nbR	CTTTTCGGATATTTTACAGGGCG
SSA1nbF	CGATGACAAGTTGAAGGAGTTG
SSA1nbR	CATTAGTGTTAGCGATAATCAAG
DOANBF	GCT AAA CAG TCA CAG AAT TTG GC
DOANBR	GAT TAT TTG CTA TCT AGA CAT TAT GTG
SSA4OPTF	GGA AGG TGT TGC CAA TCC AAT CAT G
MS2V6R Northern	ATG CCG ATA TTC TGC ACC
SSA4F for 3xHA-12MS2V6 integration	CAGGAGCAGGCCCAGTTCCGGGTGCTGGAGCAGGCCCCACTGGAGCACCAGACAACG GCCCAACGGTTGAAGAGGT GTTTACCCATACGATGTTCCTG
SSA4R for 3xHA-12MS2V6 integration	TATATACTTATAAAAAGTTGTTAAGAGGGAAAACTAAGAAATTCTCATCGCATCTTTG TATTTAT CACTAGTGGATCTGATATCACC
SSA2F for 3xHA-12MS2V6 integration	GCAGCTCCAGGTGGTTTCCCAGGTGGTGCTCCTCCAGCTCCAGAAGCTGAAGGTCCAA CTGTCGAAGAAGTTGAT GTTTACCCATACGATGTTCCTG
SSA2R for 3xHA-12MS2V6 integration	CGTAAAAAAATTAAAAAATACAGAGGAAAGCAAAAGTAAAACTTTTCGGATATTTTA CAGGGCGATCGCTAAGC CACTAGTGGATCTGATATCACC
SSA3F for 3xHA-12MS2V6 integration	GGATTCCCCGGATCCATGCCCAACTCGGGTGCTACGGGAGGTGGAGAAGATACAGGT CCAACAGTGGAAGAGGTTGAT GTTTACCCATACGATGTTCCTG
SSA3R for 3xHA-12MS2V6 integration	CATCATGGATAGATTACCCGCCATCGTATAAAAGGTTAAACATAAAAAGTAGCTAAA TAGAACACTATAGAAGAATAA CACTAGTGGATCTGATATCACC
SSA1F for 3xHA-12MS2V6 integration	CAGGTGGTGCTCCAGGCGGTTTCCCAGGTGGTGCTCCTCCAGCTCCAGAGGCTGAAGG TCCAACCGTTGAAGAAGTTGAT GTTTACCCATACGATGTTCCTG
SSA1R for 3xHA-12MS2V6 integration	CGGAAAATTCCTCATTATACCCAGATCATTAAAAGACATTTTCGTTATTATCAATTGCC GCACCAATTGGC CACTAGTGGATCTGATATCACC
DOA for 3xHA-12MS2V6 integration	CTTGGCTTGCAAACATCAAAAGGAGCTATGGGAACGTGCCAAGGTTTAAGGATATTTT CGACGATCTC TCCGTTTACCCATACGATGTTCCTG
DOA for 3xHA-12MS2V6 integration	CAGAAAGAATTTTAAAGATTATTTGCTATCTAGACATTATGTGTTTTATATGATTGCTG TAAAAGTA CACTAGTGGATCTGATATCACC
SSA4-OPTMS2V6F	GCCGGTCCAGTTCCAGGTGCTGGTGCCGGTCCTACGGGCGCACCAGACAACGGTCCA ACTGTCGAAGAAGTCGATGTTTACCCATACGATGTTCCTG
Mutated3SSA4F	TGAAGAGGTTGATTAGATAAATACAAAGATGCGATGTTGATGCAGCATCGAATTTCTT AG
Mutated3SSA4R	TTTAAATTATGATTGCTGTACATTTCCGAGCTAAACTC
Asc1HisF	GGTTTTCCTAACTCGTTCTCTCTCTCTTTTTTTTTTCCAAAAAATCCTTATAACACACTA AAGTAAATAAAGTGAAAAATGACAGAGCAGAAAGCCCTAG
Asc1HisR	TATAGAAATTATTTTCTTTATTTTTACCATTTTAAACATGACCAATAACTAGAAGATAC ATAAAAGAACAAATGAACTTTATACATATTCCTACATAAGAACACCTTTGG
Hel2HygroF	AAAAAGATCCATAAAGTGCATTTTGATACAGTCTCTTTCGTCGAAAAAATAGTGGC TATACTTCTTTTCAAGAATTAGGATGGGTAAAAAGCCTGAACTC
Hel2HygroR	TATCGGAATTTTATTTAAGACTTTCATTTCTCTAATGCTATTGTCAGTTACAGGTTAGA AATATATTTCCAATCGTTAAAGCCTTCGAGCGTCCCAAAACC
STE20FHygro	CTTGGCTTGCAAACATCAAAAGGAGCTATGGGAACGTGCCAAGGTTTAAGGATATTTT CGACGATCTC TCCGTTTACCCATACGATGTTCCTG
STE20RHygro	CAGAAAGAATTTTAAAGATTATTTGCTATCTAGACATTATGTGTTTTATATGATTGCTG TAAAAGTA CACTAGTGGATCTGATATCACC
Edc3URAF	GCCGGTCCAGTTCCAGGTGCTGGTGCCGGTCCTACGGGCGCACCAGACAACGGTCCA ACTGTCGAAGAAGTCGATGTTTACCCATACGATGTTCCTG
Edc3URAR	GGTTTTCCTAACTCGTTCTCTCTCTCTTTTTTTTTTCCAAAAAATCCTTATAACACACTA AAGTAAATAAAGTGAAAAATGACAGAGCAGAAAGCCCTAG

RPS28AURAF	TATAGAAATTATTTTCTTTATTTTTACCATTTTAAACATGACCAATAACTAGAAGATAC ATAAAAGAACAAATGAACTTTATACATATTCCTACATAAGAACACCTTTGG
RPS28AURAF	AAAAAGATCCATAAAGTGCATTTTGATACAGTCTCTTTCGTCGAAAAAATAGTGGC TATACTTCTTTTCAAGAATTAGGATGGGTAAAAAGCCTGAACTC
Dom34HisF	AGATCCCAAAAAATTAAGCATTCGTTGCTGCATCGTTGTCATTTTGTTCAATTATCGCA TTCCTATCATAGCAAAAATATGACAGAGCAGAAAGCCCTAG
Dom34HisR	GAAGTAAAGAGAATAATCCGATTTATTATAGGGTTGCAAATTTTATGTGTACATTACT TTTTTCTTACATAGTAAATCTACATAAGAACACCTTTGGTGG
Hbs1HisF	AATAAGCAATTTAAAAAGAGTTAAGTACAGCTTGGAGACACCCAAAGGCTTCTGCTT CGACAACTATTGACTATCGAGATGACAGAGCAGAAAGCCCTAG
Hbs1HisR	GATCGCTATTAATGTGTAGAAATTGAAAAAATTACATACAGAAGCGTATAAAATTCTT ATCATCTATTTTCACCCTTCTACATAAGAACACCTTTGGTGG
AscHygroDepF	AGATCCCAAAAAATTAAGCATTCGTTGCTGCATCGTTGTCATTTTGTTCAATTATCGCA TTCCTATCATAGCAAAAATATGACAGAGCAGAAAGCCCTAG
AscHygroDepR	GAAGTAAAGAGAATAATCCGATTTATTATAGGGTTGCAAATTTTATGTGTACATTACT TTTTTCTTACATAGTAAATCTACATAAGAACACCTTTGGTGG
Ski7Fint	GAGACCCTTCTACAATACACGTACGAGGAGGTGGTCTTCGAAACTTACAGTACCACCT GACATGACAGAGCAGAAAGCCC
Ski7Rint	ATATATTAAACAATAAGTATGAATGCCTAGTATAATTTCTTAGTTGTAGGA CTACATA AGAACACCTTTGGTGG
dhh1URAF	GAAGTAAAGAGAATAATCCGATTTATTATAGGGTTGCAAATTTTATGTGTACATTACT TTTTTCTTACATAGTAAATCTACATAAGAACACCTTTGGTGG
dhh1URAR	GAGACCCTTCTACAATACACGTACGAGGAGGTGGTCTTCGAAACTTACAGTACCACCT GACATGACAGAGCAGAAAGCCC
NotHygroF	ATATATTAAACAATAAGTATGAATGCCTAGTATAATTTCTTAGTTGTAGGA CTACATA AGAACACCTTTGGTGG
NotHygroR	GAAGTAAAGAGAATAATCCGATTTATTATAGGGTTGCAAATTTTATGTGTACATTACT TTTTTCTTACATAGTAAATCTACATAAGAACACCTTTGGTGG
RPS19BURAF	GAAATTTTAAAGTGGGATTTTTGTGAATATTGACAACAAAGGTATAGAACCAAAGAT AATAAAGatgtcgaaagctacatataagg
RPS19BURAR	CGATAATACTATAGTATAATGATAATATTAATAAAAATCTTAGCTTTTTATTTTTAACA ACTCGCttagttttgctggccgcatcttctc
RPS28AURAF	ATTTATTGTAAATTACAGTTGTGTTCGTTTTCGATTCTTCTCAAAAGCAGAAAACCAAG CTAGCAATCatgtcgaaagctacatataagg
RPS28AURAR	AAAAGGCACAAATATATAAGATAGATTTTGTATAGCTGCAACCTTCAATCTGCAAATA AGCTTCCttagttttgctggccgcatcttctc
Mbf1UraF	GCTTCCATAACTGTAAAAGCTAATAAGCTAGAAAACAAAAAAGTTAACGAGCAAAAT CGTAAAGAAAA atgtcgaaagctacatataagg
Mbf1UraR	TAATGTACATTATTAAGAATGCTTCATTGATGACATGCAGTGCGAAAAGAAAGGAAC AAATGAAAGAAGACCTCT ttagttttgctggccgcatcttctc
Ltn1PFint	ACTGAAGAAGTCCTTCTTAATAGTTCAAATCTGCTAAGCCATCAAAAAAAGTTCAAGC AATAGTTGGTTCTTAatgtcgaaagctacatataagg
Ltn1Print	ATTTGTAAGAGAGCACAATAATAAAAGGAACTTTGTTTAAAAAATGTAGTACATTTAT ATGAAATTTATATGCGATAGT ttagttttgctggccgcatcttctc
Rps7BUraF	TTGACTTTGTATATACAAACAGAAGAGAAACCAACACACTAAAGACTAGACACATAA CTGACCAatgtcgaaagctacatataagg
Rps7BuraR	TTATTATTTTTTCTTAATATTATTTTCTTTAAGTATGACAAATGATGAGAATGATAGTT ATCTCACTATttagttttgctggccgcatcttctc
MAG2FintLeu	TGCACTGATAAAATAAAGATATAGTAGTAGAATCTGTTACTAATCTTAACACTTTTGA TGGTAGAACCGGAC ATGTCTGCCCCTAAGAAGATCG
MAG2RintLeu	GAAATGATATAGAATAGGTCCTCCCACATTTCTGGCTTGGAAAGAGATTTTTAAGCAG AACATGCTGTAACC TTAAGCAAGGATTTTCTTAACTTC
Asc1FlagF	GGTCAAACTTTGTTTGCCGGTTACACCGACAACGTCATTAGAGTTTGGCAAGTTATGA CTGCTAAC ACG CTG CAG GTC GAC GAC TAC AAA
Asc1FlagRKan	ATTTTTACCATTTTAAACATGACCAATAACTAGAAGATACATAAAAGAACAAATGAA CTTTATACATA ACTGGATGGCGGCGTTAGTATC
SSA4OPT5UTRF	TATAAATTGAACGAAACTCAAGCCAATAAAGGAC
URAREVSSA43UTR	TGATTGTGTATCTTATATATATACTTATAAAAAGTTGTTAAGAGGGAAAACTAAGAAA TTCTCATCGCATCTTTGTATTT ttagttttgctggccgcatcttctc
Asc1CheckF	GCATTGGGCTATTCCTTTAATTGTG
HisR	CCTGTGTGGACGTTAATCACTTG

Hel2CheckF	GGCGGTCACTCTTAATAATAGC
HygroR2test	GTTTCAGGCAGGTCTTGCAACG
KanRevCheck	CGGGCTTCCCATACAATCG
NOPFcheck:	GCATATCAAGACGTGTACTACATAC
Edc3PCheckF	TGTAATTAGCTGCAATCATCTTG
UraRev check	GCAAATTTTCTGTCTTCGAAGAG
RPS28AF	GATGATTTATTGTAAATTACAG
Asc1Promoter F	CCTAACTCGTTCTCTCTCTC
LeuRCheck	CAACGAAGTCAGTACCTTTAGC
Ski7CheckF	GACCAGATTTACATTGGTGTAC
Dhh1checkF	CAGAGCTATCATCAACAAGCG
Xrn1FwdCheck	ACGTTGAGTGGTTCAACAAG
Hbs1CheckF	CTATTCAACCTGGTGAATCTTTGAC
P3mutFcheck	GATAAATACAAAGATGCGATGTTGAT
RPS19BF	GAACATTAGTGAAGATACAATCG
RPS28AF	GATGATTTATTGTAAATTACAG
Mbf1pFcheck	CGCTTAACCAATAATAGTTTCATG
Ltn1CheckF	GTACTTCTTACCTCCAGCTTGAC
SSA4NTHAF	CATGTCAGTTTACCCATACGATG
SSA45F	ggatccGAGCTC TTGAACGAAACTCAAGCCAA
SSA4PFHindIII	ATTCCGAAGCTT CGAGGTTTACACGAAAGATATC
PSSA4HARev	TGAGGAAATTTCTTCTGGAGTAAATG
Rps20WT PF	ccatgtctgactttcaaaaggaaaag
Rps20K68R mut PF	ccatgtctgactttcaaagagaaaga
RPS20 Rev	cgagttagttggaagcaacaacaac
RPS28PF2	CTTGGTCGTTGAACTACTTGG
RPS28 ORF REV	CAATAGTTCTGGAAGTGTCTTCC
Rps7bcheck	CACGTTCCACACAGTTTGGG
MAG2FCheck	CTATATCGTAAACACCGTTGG
3Xflag tagF	tcgacGACTACAAAGACGATGACGACAAGGACTACAAAG ACGATGACGACAAG GAC TAC AAA GACGATGACGACAAGTAGc
3Xflag tagR	ccgggCTACTTGTCGTCATCGTCTTTGTAGTCCTTGTCGTCATCGTCTTTGTAGTCCTTGT CGTCATCGTCTTTGTAGTCg
Mutated3SSA4FHindIII	ATATATAAGCTTTGAAGAGGTTGATTAGATAAATACAAAGATGCGATGTTGATGCAG C
Mutated3SSA4RBamHI	ATATATGGATCCTTTAAATTATGATTGCTGTAC
RTT105F	TATTTATACAATGTACAGCAATCATAATTTAAATTCGG
RTT105R	GTCTTCCAAATCCTCGTTGTTTTGCC
RTTPromoterEcoRV	ATATATGATATCTATAATACTCTCTTATTTAAGTTACTTCTATTCTTCAATTGATTAATT CCAACAGATCAAGCAGATTTTATACAGAAATATTTATACAATGTACAGC
SSA4OPTPSt1	ATATATCTGCAGTATAAATTGAACGAAACTCAAGCC
SSA4OPTRevXbaI	ATATATTCTAGAAATCGACTTCTTCGACAGTTGG
Asc1FPFBlp1	CATACATATTCAATGAGCTGAGC
Asc13RevSpeI	atatatactagtCCTTTCTTTCATTACTTCGAAATCTATGACG
Asc1FQPCR	ATGTTTGGCCACTTTGTTGG
Asc1RQPCR	GTTACCGGCAGAAATGATGG
SNR24FQPCR	TTGCTACTTCAGATGGAACTTTG
SNR24RQPCR	TCAGAGATCTTGGTGATAATTGG
ACTFQPCR	TTCTGAGGTTGCTGCTTTGG
ACTRQPCR	CTTGGTGTCTTGGTCTACCG
SSA4optFqpcr	GACAAGATGGTTGCTGAAGC
SSA4optRqpcr	CTAGCGTCTTCTTCACCTAC
SSA4FQPCR	CTATAAATTGGTTAGATGCTTCGC
SSA4 Rev QPCR	CAACCGTTGGGCCGTTGTCTGG

APPENDIX 3: References to Chapter 1.2

1. Gasch AP, Spellman PT, Kao CM, Carmel-Harel O, Eisen MB, Storz G, et al. Genomic expression programs in the response of yeast cells to environmental changes. Mol Biol Cell. 2000 Dec;11(12):4241–57.
2. van Oosten-Hawle P, Morimoto RI. Organismal proteostasis: role of cell-nonautonomous regulation and transcellular chaperone signaling. Genes Dev. 2014 Jul 15;28(14):1533–43.
3. de la Fuente M, Valera S, Martínez-Guitarte JL. ncRNAs and thermoregulation: A view in prokaryotes and eukaryotes. FEBS Lett. 2012 Nov 30;586(23):4061–9.
4. Protter DSW, Parker R. Principles and Properties of Stress Granules. Trends Cell Biol. 2016 Sep;26(9):668–79.
5. Pohl C, Dikic I. Cellular quality control by the ubiquitin-proteasome system and autophagy. Science. 2019 Nov 15;366(6467):818–22.
6. Pomatto LCD, Davies KJA. The role of declining adaptive homeostasis in ageing. J Physiol. 2017 Dec 15;595(24):7275–309.
7. Yasuda S, Tsuchiya H, Kaiho A, Guo Q, Ikeuchi K, Endo A, et al. Stress- and ubiquitylation-dependent phase separation of the proteasome. Nature. 2020 Feb 13;578(7794):296–300.
8. Tomanek L. The Importance of Physiological Limits in Determining Biogeographical Range Shifts due to Global Climate Change: The Heat-Shock Response. Physiol Biochem Zool. 2008 Nov;81(6):709–17.
9. Kassahn KS, Crozier RH, Pörtner HO, Caley MJ. Animal performance and stress: responses and tolerance limits at different levels of biological organisation. Biol Rev. 2009 May;84(2):277–92.
10. Sengupta P, Garrity P. Sensing temperature. Curr Biol CB. 2013 Apr 22;23(8):R304-307.
11. Somero GN. The cellular stress response and temperature: Function, regulation, and evolution. J Exp Zool Part Ecol Integr Physiol. 2020 Jul;333(6):379–97.
12. Parsell DA, Lindquist S. The function of heat-shock proteins in stress tolerance: degradation and reactivation of damaged proteins. Annu Rev Genet. 1993;27:437–96.
13. Kültz D. MOLECULAR AND EVOLUTIONARY BASIS OF THE CELLULAR STRESS RESPONSE. Annu Rev Physiol. 2005 Mar 17;67(1):225–57.
14. Daugaard M, Rohde M, Jäättelä M. The heat shock protein 70 family: Highly homologous proteins with overlapping and distinct functions. FEBS Lett. 2007 Jul 31;581(19):3702–10.
15. Rosenzweig R, Nillegoda NB, Mayer MP, Bukau B. The Hsp70 chaperone network. Nat Rev Mol Cell Biol. 2019 Nov;20(11):665–80.
16. Morimoto RI. The Heat Shock Response: Systems Biology of Proteotoxic Stress in Aging and Disease. Cold Spring Harb Symp Quant Biol. 2011 Jan 1;76(0):91–9.
17. Wang Y, Le W-D. Autophagy and Ubiquitin-Proteasome System. Adv Exp Med Biol. 2019;1206:527–50.
18. Jayaraj GG, Hipp MS, Hartl FU. Functional Modules of the Proteostasis Network. Cold Spring Harb Perspect Biol. 2020 Jan 2;12(1):a033951.
19. Kampinga HH, Hageman J, Vos MJ, Kubota H, Tanguay RM, Bruford EA, et al. Guidelines for the nomenclature of the human heat shock proteins. Cell Stress Chaperones. 2009 Jan;14(1):105–11.

20. Abisambra JF, Blair LJ, Hill SE, Jones JR, Kraft C, Rogers J, et al. Phosphorylation Dynamics Regulate Hsp27-Mediated Rescue of Neuronal Plasticity Deficits in Tau Transgenic Mice. J Neurosci. 2010 Nov 17;30(46):15374–82.
21. Gamerdinger M, Hajieva P, Kaya AM, Wolfrum U, Hartl FU, Behl C. Protein quality control during aging involves recruitment of the macroautophagy pathway by BAG3. EMBO J. 2009 Apr 8;28(7):889–901.
22. Kumar P, Ambasta RK, Veereshwarayya V, Rosen KM, Kosik KS, Band H, et al. CHIP and HSPs interact with beta-APP in a proteasome-dependent manner and influence Abeta metabolism. Hum Mol Genet. 2007 Apr 1;16(7):848–64.
23. Lindquist S. The heat-shock response. Annu Rev Biochem. 1986;55:1151–91.
24. Lindquist S, Craig EA. The heat-shock proteins. Annu Rev Genet. 1988;22:631–77.
25. Liu Q, Liang C, Zhou L. Structural and functional analysis of the Hsp70/Hsp40 chaperone system. Protein Sci. 2020;29(2):378–90.
26. Petrucelli L, Dickson D, Kehoe K, Taylor J, Snyder H, Grover A, et al. CHIP and Hsp70 regulate tau ubiquitination, degradation and aggregation. Hum Mol Genet. 2004 Apr 1;13(7):703–14.
27. Ritossa F. A new puffing pattern induced by temperature shock and DNP in drosophila. Experientia. 1962 Dec 1;18(12):571–3.
28. Sørensen JG, Kristensen TN, Loeschcke V. The evolutionary and ecological role of heat shock proteins: Heat shock proteins. Ecol Lett. 2003 Nov;6(11):1025–37.
29. Brocchieri L, Conway de Macario E, Macario AJ. hsp70 genes in the human genome: Conservation and differentiation patterns predict a wide array of overlapping and specialized functions. BMC Evol Biol. 2008 Jan 23;8:19.
30. Petesch SJ, Lis JT. Rapid, Transcription-Independent Loss of Nucleosomes over a Large Chromatin Domain at Hsp70 Loci. Cell. 2008 Jul 11;134(1):74–84.
31. Anckar J, Sistonen L. Regulation of HSF1 Function in the Heat Stress Response: Implications in Aging and Disease. Annu Rev Biochem. 2011 Jul 7;80(1):1089–115.
32. Vihervaara A, Sistonen L. HSF1 at a glance. J Cell Sci. 2014 Jan 15;127(2):261–6.
33. Björk JK, Sistonen L. Regulation of the members of the mammalian heat shock factor family. FEBS J. 2010 Oct;277(20):4126–39.
34. Gomez-Pastor R, Burchfiel ET, Thiele DJ. Regulation of heat shock transcription factors and their roles in physiology and disease. Nat Rev Mol Cell Biol. 2018 Jan;19(1):4–19.
35. Guettouche T, Boellmann F, Lane WS, Voellmy R. Analysis of phosphorylation of human heat shock factor 1 in cells experiencing a stress. BMC Biochem. 2005 Mar 11;6(1):4.
36. Nakai A. Molecular basis of HSF regulation. Nat Struct Mol Biol. 2016 Feb;23(2):93–5.
37. Boellmann F, Guettouche T, Guo Y, Fenna M, Mnayer L, Voellmy R. DAXX interacts with heat shock factor 1 during stress activation and enhances its transcriptional activity. Proc Natl Acad Sci U S A. 2004 Mar 23;101(12):4100–5.
38. Hietakangas V, Anckar J, Blomster HA, Fujimoto M, Palvimo JJ, Nakai A, et al. PDSM, a motif for phosphorylation-dependent SUMO modification. Proc Natl Acad Sci U S A. 2006 Jan 3;103(1):45–50.
39. Westerheide SD, Anckar J, Stevens SM, Sistonen L, Morimoto RI. Stress-Inducible Regulation of Heat Shock Factor 1 by the Deacetylase SIRT1. Science. 2009 Feb 20;323(5917):1063–6.

40. Krakowiak J, Zheng X, Patel N, Feder ZA, Anandhakumar J, Valerius K, et al. Hsf1 and Hsp70 constitute a two-component feedback loop that regulates the yeast heat shock response. eLife. 7:e31668.
41. Zheng X, Krakowiak J, Patel N, Beyzavi A, Ezike J, Khalil AS, et al. Dynamic control of Hsf1 during heat shock by a chaperone switch and phosphorylation. eLife. 5:e18638.
42. Shamovsky I, Ivannikov M, Kandel ES, Gershon D, Nudler E. RNA-mediated response to heat shock in mammalian cells. Nature. 2006 Mar;440(7083):556–60.
43. Chen Y, Chen J, Yu J, Yang G, Temple E, Harbinski F, et al. Identification of mixed lineage leukemia 1(MLL1) protein as a coactivator of heat shock factor 1(HSF1) protein in response to heat shock protein 90 (HSP90) inhibition. J Biol Chem. 2014 Jul 4;289(27):18914–27.
44. Jonkers I, Lis JT. Getting up to speed with transcription elongation by RNA polymerase II. Nat Rev Mol Cell Biol. 2015 Mar;16(3):167–77.
45. Mason PB, Lis JT. Cooperative and competitive protein interactions at the hsp70 promoter. J Biol Chem. 1997 Dec 26;272(52):33227–33.
46. Park JM, Werner J, Kim JM, Lis JT, Kim YJ. Mediator, not holoenzyme, is directly recruited to the heat shock promoter by HSF upon heat shock. Mol Cell. 2001 Jul;8(1):9–19.
47. Takii R, Fujimoto M, Matsumoto M, Srivastava P, Katiyar A, Nakayama KI, et al. The pericentromeric protein shugoshin 2 cooperates with HSF1 in heat shock response and RNA Pol II recruitment. EMBO J. 2019 Dec 16;38(24):e102566.
48. Lis JT, Mason P, Peng J, Price DH, Werner J. P-TEFb kinase recruitment and function at heat shock loci. Genes Dev. 2000 Apr 1;14(7):792–803.
49. Marshall NF, Peng J, Xie Z, Price DH. Control of RNA Polymerase II Elongation Potential by a Novel Carboxyl-terminal Domain Kinase*. J Biol Chem. 1996 Oct 25;271(43):27176–83.
50. Khanna N, Hu Y, Belmont AS. HSP70 transgene directed motion to nuclear speckles facilitates heat shock activation. Curr Biol CB. 2014 May 19;24(10):1138–44.
51. Vera M, Singer RH. Gene Regulation: The HSP70 Gene Jumps When Shocked. Curr Biol. 2014 May 19;24(10):R396–8.
52. Chowdhary S, Kainth AS, Gross DS. Heat Shock Protein Genes Undergo Dynamic Alteration in Their Three-Dimensional Structure and Genome Organization in Response to Thermal Stress. Mol Cell Biol. 2017 Dec 15;37(24):e00292-17.
53. Vihervaara A, Duarte FM, Lis JT. Molecular mechanisms driving transcriptional stress responses. Nat Rev Genet. 2018 Jun;19(6):385–97.
54. Mueller B, Mieczkowski J, Kundu S, Wang P, Sadreyev R, Tolstorukov MY, et al. Widespread changes in nucleosome accessibility without changes in nucleosome occupancy during a rapid transcriptional induction. Genes Dev. 2017 Mar 1;31(5):451–62.
55. Vihervaara A, Mahat DB, Guertin MJ, Chu T, Danko CG, Lis JT, et al. Transcriptional response to stress is pre-wired by promoter and enhancer architecture. Nat Commun. 2017 Aug 15;8:255.
56. Ray J, Munn PR, Vihervaara A, Lewis JJ, Ozer A, Danko CG, et al. Chromatin conformation remains stable upon extensive transcriptional changes driven by heat shock. Proc Natl Acad Sci U S A. 2019 Sep 24;116(39):19431–9.

57. Li L, Lyu X, Hou C, Takenaka N, Nguyen HQ, Ong C-T, et al. Widespread rearrangement of 3D chromatin organization underlies Polycomb-mediated stress-induced silencing. Mol Cell. 2015 Apr 16;58(2):216–31.
58. Allen TA, Von Kaenel S, Goodrich JA, Kugel JF. The SINE-encoded mouse B2 RNA represses mRNA transcription in response to heat shock. Nat Struct Mol Biol. 2004 Sep;11(9):816–21.
59. Espinoza CA, Allen TA, Hieb AR, Kugel JF, Goodrich JA. B2 RNA binds directly to RNA polymerase II to repress transcript synthesis. Nat Struct Mol Biol. 2004 Sep;11(9):822–9.
60. Mariner PD, Walters RD, Espinoza CA, Drullinger LF, Wagner SD, Kugel JF, et al. Human Alu RNA Is a Modular Transacting Repressor of mRNA Transcription during Heat Shock. Mol Cell. 2008 Feb;29(4):499–509.
61. Ji Q, Zong X, Mao Y, Qian S-B. A heat shock–responsive lncRNA Heat acts as a HSF1-directed transcriptional brake via m 6 A modification. Proc Natl Acad Sci. 2021 Jun 22;118(25):e2102175118.
62. Cugusi S, Mitter R, Kelly GP, Walker J, Han Z, Pisano P, et al. Heat shock induces premature transcript termination and reconfigures the human transcriptome. Mol Cell. 2022 Feb;S1097276522000077.
63. Tutucci E, Stutz F. Keeping mRNPs in check during assembly and nuclear export. Nat Rev Mol Cell Biol. 2011 Jun;12(6):377–84.
64. Zander G, Hackmann A, Bender L, Becker D, Lingner T, Salinas G, et al. mRNA quality control is bypassed for immediate export of stress-responsive transcripts. Nature. 2016 Dec;540(7634):593–6.
65. Lindquist S. Varying patterns of protein synthesis in Drosophila during heat shock: Implications for regulation. Dev Biol. 1980 Jun 15;77(2):463–79.
66. Holcik M, Sonenberg N. Translational control in stress and apoptosis. Nat Rev Mol Cell Biol. 2005 Apr;6(4):318–27.
67. Weissbach H, Brot N. The role of protein factors in the biosynthesis of proteins. Cell. 1974 Jul 1;2(3):137–43.
68. Bresson S, Shchepachev V, Spanos C, Turowski TW, Rappsilber J, Tollervey D. Stress-Induced Translation Inhibition through Rapid Displacement of Scanning Initiation Factors. Mol Cell. 2020 Nov;80(3):470-484.e8.
69. Alluri RK, Li Z, McCrae KR. Stress Granule-Mediated Oxidized RNA Decay in P-Body: Hypothetical Role of ADAR1, Tudor-SN, and STAU1. Front Mol Biosci. 2021 Jun 4;8:672988.
70. Kedersha N, Stoecklin G, Ayodele M, Yacono P, Lykke-Andersen J, Fritzler MJ, et al. Stress granules and processing bodies are dynamically linked sites of mRNP remodeling. J Cell Biol. 2005 Jun 20;169(6):871–84.
71. Hubstenberger A, Courel M, Bénard M, Souquere S, Ernoult-Lange M, Chouaib R, et al. P-Body Purification Reveals the Condensation of Repressed mRNA Regulons. Mol Cell. 2017 Oct 5;68(1):144-157.e5.
72. Aitken CE, Lorsch JR. A mechanistic overview of translation initiation in eukaryotes. Nat Struct Mol Biol. 2012 Jun;19(6):568–76.
73. Hinnebusch AG, Lorsch JR. The Mechanism of Eukaryotic Translation Initiation: New Insights and Challenges. Cold Spring Harb Perspect Biol. 2012 Oct 1;4(10):a011544–a011544.

74. Preiss T, W Hentze M. Starting the protein synthesis machine: eukaryotic translation initiation. BioEssays News Rev Mol Cell Dev Biol. 2003 Dec;25(12):1201–11.
75. Sonenberg N, Hinnebusch AG. Regulation of Translation Initiation in Eukaryotes: Mechanisms and Biological Targets. Cell. 2009 Feb 20;136(4):731–45.
76. Taniuchi S, Miyake M, Tsugawa K, Oyadomari M, Oyadomari S. Integrated stress response of vertebrates is regulated by four eIF2α kinases. Sci Rep. 2016 Sep 16;6(1):32886.
77. Bonanou-Tzedaki SA, Smith KE, Sheeran BA, Arnstein HRV. The High-Temperature Inactivation of Rabbit Reticulocyte Lysates by a Haemin-Independent Mechanism. Eur J Biochem. 1978 Mar;84(2):591–600.
78. Chen J-J. Translational Control by Heme-Regulated eIF2α Kinase during Erythropoiesis. Curr Opin Hematol. 2014 May;21(3):172–8.
79. Chung J, Chen C, Paw BH. Heme Metabolism and Erythropoiesis. Curr Opin Hematol. 2012 May;19(3):156–62.
80. Costa-Mattioli M, Walter P. The integrated stress response: From mechanism to disease. Science [Internet]. 2020 Apr 24 [cited 2021 Aug 3];368(6489). Available from: https://science.sciencemag.org/content/368/6489/eaat5314
81. Suragani RNVS, Zachariah RS, Velazquez JG, Liu S, Sun C-W, Townes TM, et al. Heme-regulated eIF2α kinase activated Atf4 signaling pathway in oxidative stress and erythropoiesis. Blood. 2012 May 31;119(22):5276–84.
82. Farabaugh KT, Majumder M, Guan B-J, Jobava R, Wu J, Krokowski D, et al. Protein Kinase R Mediates the Inflammatory Response Induced by Hyperosmotic Stress. Mol Cell Biol. 2017 Feb 15;37(4):e00521-16.
83. Kimball SR. Regulation of translation initiation by amino acids in eukaryotic cells. Prog Mol Subcell Biol. 2001;26:155–84.
84. Deng J, Harding HP, Raught B, Gingras A-C, Berlanga JJ, Scheuner D, et al. Activation of GCN2 in UV-Irradiated Cells Inhibits Translation. Curr Biol. 2002 Aug 6;12(15):1279–86.
85. JIANG H-Y, WEK RC. GCN2 phosphorylation of eIF2α activates NF-κB in response to UV irradiation. Biochem J. 2005 Jan 7;385(2):371–80.
86. Gale M, Tan S-L, Katze MG. Translational Control of Viral Gene Expression in Eukaryotes. Microbiol Mol Biol Rev. 2000 Jun;64(2):239–80.
87. Ron D. Translational control in the endoplasmic reticulum stress response. J Clin Invest. 2002 Nov 15;110(10):1383–8.
88. Wang R, McGrath BC, Kopp RF, Roe MW, Tang X, Chen G, et al. Insulin Secretion and Ca2+ Dynamics in β-Cells Are Regulated by PERK (EIF2AK3) in Concert with Calcineurin *. J Biol Chem. 2013 Nov 22;288(47):33824–36.
89. Kubarenko AV, Sergiev PV, Rodnina MV. [GTPases of translational apparatus. Mol Biol (Mosk). 2005 Sep 1;39(5):746–61.
90. Kimball S.R., Fabian J.R., Pavitt G.D., Hinnebusch A.G., Jefferson L.S. Regulation of Guanine Nucleotide Exchange through Phosphorylation of Eukaryotic Initiation Factor eIF2α J. Biol. Chem. 1998;273:12841–12845.
91. Yoshizawa F, Kimball SR, Jefferson LS. Modulation of translation initiation in rat skeletal muscle and liver in response to food intake. Biochem Biophys Res Commun. 1997 Nov 26;240(3):825–31.
92. Aktas B.H., Chen T. In: Translation and its Regulation in Cancer Biology and Medicine [Internet] Parsyan A., editor. Springer Netherlands; Dordrecht: 2014. The eIF2 Complex and eIF2α pp. 195–221.

93. Pelletier J, Sonenberg N. The Organizing Principles of Eukaryotic Ribosome Recruitment. Annu Rev Biochem. 2019;88(1):307–35.
94. Gingras A.-C., Raught B., Sonenberg N. In: TOR: Target of Rapamycin [Internet] Thomas G., Sabatini D.M., Hall M.N., editors. Springer; Berlin, Heidelberg: 2004. mTOR signaling to translation; pp. 169–197. (Current Topics in Microbiology and Immunology)
95. Korneeva NL, Song A, Gram H, Edens MA, Rhoads RE. Inhibition of Mitogen-activated Protein Kinase (MAPK)-interacting Kinase (MNK) Preferentially Affects Translation of mRNAs Containing Both a 5′-Terminal Cap and Hairpin*. J Biol Chem. 2016 Feb 12;291(7):3455–67.
96. Ma XM, Blenis J. Molecular mechanisms of mTOR-mediated translational control. Nat Rev Mol Cell Biol. 2009 May;10(5):307–18.
97. Ruoff R, Katsara O, Kolupaeva V. Cell type-specific control of protein synthesis and proliferation by FGF-dependent signaling to the translation repressor 4E-BP. Proc Natl Acad Sci. 2016 Jul 5;113(27):7545–50.
98. Alain T, Morita M, Fonseca BD, Yanagiya A, Siddiqui N, Bhat M, et al. eIF4E/4E-BP Ratio Predicts the Efficacy of mTOR Targeted Therapies. Cancer Res. 2012 Dec 15;72(24):6468–76.
99. Laplante M, Sabatini DM. mTOR Signaling in Growth Control and Disease. Cell. 2012 Apr 13;149(2):274–93.
100. Teleman AA. 4E-BP functions as a metabolic brake used under stress conditions but not during normal growth. Genes Dev. 2005 Aug 15;19(16):1844–8.
101. Vries RGJ, Flynn A, Patel JC, Wang X, Denton RM, Proud CG. Heat Shock Increases the Association of Binding Protein-1 with Initiation Factor 4E *. J Biol Chem. 1997 Dec 26;272(52):32779–84.
102. Cuesta R, Laroia G, Schneider RJ. Chaperone Hsp27 inhibits translation during heat shock by binding eIF4G and facilitating dissociation of cap-initiation complexes. Genes Dev. 2000 Jun 15;14(12):1460–70.
103. Dever TE, Dinman JD, Green R. Translation Elongation and Recoding in Eukaryotes. Cold Spring Harb Perspect Biol. 2018 Aug 1;10(8):a032649.
104. Dever TE, Green R. The elongation, termination, and recycling phases of translation in eukaryotes. Cold Spring Harb Perspect Biol. 2012 Jul 1;4(7):a013706.
105. Sokabe M, Fraser CS. Toward a Kinetic Understanding of Eukaryotic Translation. Cold Spring Harb Perspect Biol. 2019 Feb 1;11(2):a032706.
106. Wang X, Li W, Williams M, Terada N, Alessi DR, Proud CG. Regulation of elongation factor 2 kinase by p90(RSK1) and p70 S6 kinase. EMBO J. 2001 Aug 15;20(16):4370–9.
107. Carlberg U, Nilsson A, Nygård O. Functional properties of phosphorylated elongation factor 2. Eur J Biochem. 1990;191(3):639–45.
108. Dumont-Miscopein A, Lavergne J-P, Guillot D, Sontag B, Reboud J-P. Interaction of phosphorylated elongation factor EF-2 with nucleotides and ribosomes. FEBS Lett. 1994;356(2–3):283–6.
109. Ryazanov AG, Shestakova EA, Natapov PG. Phosphorylation of elongation factor 2 by EF-2 kinase affects rate of translation. Nature. 1988 Jul;334(6178):170–3.
110. Ryazanov AG, Davydova EK. Mechanism of elongation factor 2 (EF-2) inactivation upon phosphorylation Phosphorylated EF-2 is unable to catalyze translocation. FEBS Lett. 1989;251(1–2):187–90.

111. Suzuki K., Monteggia L.M. In: Duman R.S., Krystal J.H., editors. Vol. 89. Academic Press; Cambridge, MA: 2020. The role of eEF2 kinase in the rapid antidepressant actions of ketamine; pp. 79–99. (Advances in Pharmacology [Internet]). Rapid Acting Antidepressants.
112. Browne GJ, Proud CG. A Novel mTOR-Regulated Phosphorylation Site in Elongation Factor 2 Kinase Modulates the Activity of the Kinase and Its Binding to Calmodulin. Mol Cell Biol. 2004 Apr 1;24(7):2986–97.
113. Knebel A, Morrice N, Cohen P. A novel method to identify protein kinase substrates: eEF2 kinase is phosphorylated and inhibited by SAPK4/p38delta. EMBO J. 2001 Aug 15;20(16):4360–9.
114. Liu R, Proud CG. Eukaryotic elongation factor 2 kinase as a drug target in cancer, and in cardiovascular and neurodegenerative diseases. Acta Pharmacol Sin. 2016 Mar;37(3):285–94.
115. Beckmann RP, Mizzen LE, Welch WJ. Interaction of Hsp 70 with newly synthesized proteins: implications for protein folding and assembly. Science. 1990 May 18;248(4957):850–4.
116. Nelson RJ, Ziegelhoffer T, Nicolet C, Werner-Washburne M, Craig EA. The translation machinery and 70 kd heat shock protein cooperate in protein synthesis. Cell. 1992 Oct 2;71(1):97–105.
117. Liu B, Han Y, Qian S-B. Cotranslational response to proteotoxic stress by elongation pausing of ribosomes. Mol Cell. 2013 Feb 7;49(3):453–63.
118. Shalgi R, Hurt JA, Krykbaeva I, Taipale M, Lindquist S, Burge CB. Widespread Regulation of Translation by Elongation Pausing in Heat Shock. Mol Cell. 2013 Feb;49(3):439–52.
119. Khong A, Matheny T, Jain S, Mitchell SF, Wheeler JR, Parker R. The Stress Granule Transcriptome Reveals Principles of mRNA Accumulation in Stress Granules. Mol Cell. 2017 Nov 16;68(4):808-820.e5.
120. Matheny T, Rao BS, Parker R. Transcriptome-Wide Comparison of Stress Granules and P-Bodies Reveals that Translation Plays a Major Role in RNA Partitioning. Mol Cell Biol. 39(24):e00313-19.
121. Vandelli A, Cid Samper F, Torrent Burgas M, Sanchez de Groot N, Tartaglia GG. The Interplay Between Disordered Regions in RNAs and Proteins Modulates Interactions Within Stress Granules and Processing Bodies. J Mol Biol. 2021 Jul 16;167159.
122. Franzmann TM, Alberti S. Protein Phase Separation as a Stress Survival Strategy. Cold Spring Harb Perspect Biol. 2019 Jan 7;a034058.
123. Banani SF, Lee HO, Hyman AA, Rosen MK. Biomolecular condensates: organizers of cellular biochemistry. Nat Rev Mol Cell Biol. 2017 May;18(5):285–98.
124. Luo Y, Na Z, Slavoff SA. P-Bodies: Composition, Properties, and Functions. Biochemistry. 2018 May 1;57(17):2424–31.
125. Standart N, Weil D. P-Bodies: Cytosolic Droplets for Coordinated mRNA Storage. Trends Genet. 2018 Aug 1;34(8):612–26.
126. Riback JA, Katanski CD, Kear-Scott JL, Pilipenko EV, Rojek AE, Sosnick TR, et al. Stress-Triggered Phase Separation Is an Adaptive, Evolutionarily Tuned Response. Cell. 2017 Mar;168(6):1028-1040.e19.
127. Teixeira D., Sheth U., Valencia-sanchez M.A., Brengues M., Parker R. Processing bodies require RNA for assembly and contain nontranslating mRNAs. RNA. 2005;11:371–382.

128. Brengues M, Teixeira D, Parker R. Movement of Eukaryotic mRNAs Between Polysomes and Cytoplasmic Processing Bodies. Science. 2005 Oct 21;310(5747):486–9.
129. Franks TM, Lykke-Andersen J. The Control of mRNA Decapping and P-Body Formation. Mol Cell. 2008 Dec 5;32(5):605–15.
130. Parker R, Sheth U. P bodies and the control of mRNA translation and degradation. Mol Cell. 2007 Mar 9;25(5):635–46.
131. Anderson P, Kedersha N. Stressful initiations. J Cell Sci. 2002 Aug 15;115(Pt 16):3227–34.
132. Kedersha NL, Gupta M, Li W, Miller I, Anderson P. RNA-Binding Proteins Tia-1 and Tiar Link the Phosphorylation of Eif-2α to the Assembly of Mammalian Stress Granules. J Cell Biol. 1999 Dec 27;147(7):1431–42.
133. Dang Y, Kedersha N, Low W-K, Romo D, Gorospe M, Kaufman R, et al. Eukaryotic initiation factor 2alpha-independent pathway of stress granule induction by the natural product pateamine A. J Biol Chem. 2006 Oct 27;281(43):32870–8.
134. Low W-K, Dang Y, Schneider-Poetsch T, Shi Z, Choi NS, Merrick WC, et al. Inhibition of Eukaryotic Translation Initiation by the Marine Natural Product Pateamine A. Mol Cell. 2005 Dec 9;20(5):709–22.
135. Mazroui R, Sukarieh R, Bordeleau M-E, Kaufman RJ, Northcote P, Tanaka J, et al. Inhibition of Ribosome Recruitment Induces Stress Granule Formation Independently of Eukaryotic Initiation Factor 2α Phosphorylation. Mol Biol Cell. 2006 Oct;17(10):4212–9.
136. Mokas S, Mills JR, Garreau C, Fournier M-J, Robert F, Arya P, et al. Uncoupling Stress Granule Assembly and Translation Initiation Inhibition. Mol Biol Cell. 2009 Jun 1;20(11):2673–83.
137. Tauber D, Tauber G, Khong A, Van Treeck B, Pelletier J, Parker R. Modulation of RNA Condensation by the DEAD-Box Protein eIF4A. Cell. 2020 Feb 6;180(3):411-426.e16.
138. Kedersha N, Chen S, Gilks N, Li W, Miller IJ, Stahl J, et al. Evidence that ternary complex (eIF2-GTP-tRNA(i)(Met))-deficient preinitiation complexes are core constituents of mammalian stress granules. Mol Biol Cell. 2002 Jan;13(1):195–210.
139. Kimball SR, Horetsky RL, Ron D, Jefferson LS, Harding HP. Mammalian stress granules represent sites of accumulation of stalled translation initiation complexes. Am J Physiol Cell Physiol. 2003 Feb;284(2):C273-284.
140. Adivarahan S, Livingston N, Nicholson B, Rahman S, Wu B, Rissland OS, et al. Spatial Organization of Single mRNPs at Different Stages of the Gene Expression Pathway. Mol Cell. 2018 15;72(4):727-738.e5.
141. Khong A, Parker R. mRNP architecture in translating and stress conditions reveals an ordered pathway of mRNP compaction. J Cell Biol. 2018 03;217(12):4124–40.
142. Bley N, Lederer M, Pfalz B, Reinke C, Fuchs T, Glaß M, et al. Stress granules are dispensable for mRNA stabilization during cellular stress. Nucleic Acids Res. 2015 Feb 27;43(4):e26–e26.
143. Moon SL, Morisaki T, Khong A, Lyon K, Parker R, Stasevich TJ. Multicolor single-molecule tracking of mRNA interactions with RNP granules. 2019;21.
144. Ohn T, Kedersha N, Hickman T, Tisdale S, Anderson P. A functional RNAi screen links O-GlcNAc modification of ribosomal proteins to stress granule and processing body assembly. Nat Cell Biol. 2008 Oct;10(10):1224–31.

145. Jobava R, Mao Y, Guan B-J, Hu D, Krokowski D, Chen C-W, et al. Adaptive translational pausing is a hallmark of the cellular response to severe environmental stress. Mol Cell. 2021 Oct;81(20):4191-4208.e8.
146. Mateju D, Eichenberger B, Voigt F, Eglinger J, Roth G, Chao JA. Single-Molecule Imaging Reveals Translation of mRNAs Localized to Stress Granules. Cell. 2020 Dec 23;183(7):1801-1812.e13.
147. Kedersha N, Anderson P. Stress granules: sites of mRNA triage that regulate mRNA stability and translatability. Biochem Soc Trans. 2002 Nov 1;30(6):963–9.
148. Yost HJ, Petersen RB, Linquist S. RNA metabolism: strategies for regulation in the heat shock response. Trends Genet. 1990 Jan 1;6:223–7.
149. Klemenz R, Hultmark D, Gehring WJ. Selective translation of heat shock mRNA in Drosophila melanogaster depends on sequence information in the leader. EMBO J. 1985 Aug;4(8):2053–60.
150. McGarry TJ, Lindquist S. The preferential translation of Drosophila HSP70 mRNA requires sequences in the untranslated leader. Cell. 1985 Oct 1;42(3):903–11.
151. Jang SK, Kräusslich HG, Nicklin MJ, Duke GM, Palmenberg AC, Wimmer E. A segment of the 5' nontranslated region of encephalomyocarditis virus RNA directs internal entry of ribosomes during in vitro translation. J Virol. 1988 Aug;62(8):2636–43.
152. Pelletier J, Sonenberg N. Internal initiation of translation of eukaryotic mRNA directed by a sequence derived from poliovirus RNA. Nature. 1988 Jul;334(6180):320–5.
153. Macejak DG, Sarnow P. Internal initiation of translation mediated by the 5' leader of a cellular mRNA. Nature. 1991 Sep 5;353(6339):90–4.
154. Bonneau AM, Sonenberg N. Involvement of the 24-kDa cap-binding protein in regulation of protein synthesis in mitosis. J Biol Chem. 1987 Aug 15;262(23):11134–9.
155. Huang J, Schneider RJ. Adenovirus inhibition of cellular protein synthesis involves inactivation of cap-binding protein. Cell. 1991 Apr 19;65(2):271–80.
156. Joshi-Barve S, Benedetti AD, Rhoads RE. Preferential translation of heat shock mRNAs in HeLa cells deficient in protein synthesis initiation factors eIF-4E and eIF-4 gamma. J Biol Chem. 1992 Oct 15;267(29):21038–43.
157. Rubtsova MP, Sizova DV, Dmitriev SE, Ivanov DS, Prassolov VS, Shatsky IN. Distinctive Properties of the 5′-Untranslated Region of Human HSP70 mRNA*. J Biol Chem. 2003 Jun 20;278(25):22350–6.
158. Vivinus S, Baulande S, Zanten M van, Campbell F, Topley P, Ellis JH, et al. An element within the 5′ untranslated region of human HSP70 mRNA which acts as a general enhancer of mRNA translation. Eur J Biochem. 2001;268(7):1908–17.
159. Yueh A, Schneider RJ. Translation by ribosome shunting on adenovirus and HSP70 mRNAs facilitated by complementarity to 18S rRNA. Genes Dev. 2000 Feb 15;14(4):414–21.
160. Sun J, Conn CS, Han Y, Yeung V, Qian S-B. PI3K-mTORC1 Attenuates Stress Response by Inhibiting Cap-independent Hsp70 Translation. J Biol Chem. 2011 Feb 25;286(8):6791–800.
161. Meyer KD, Patil DP, Zhou J, Zinoviev A, Skabkin MA, Elemento O, et al. 5′ UTR m6A Promotes Cap-Independent Translation. Cell. 2015 Nov;163(4):999–1010.
162. Zhou J, Wan J, Gao X, Zhang X, Jaffrey SR, Qian S-B. Dynamic m6A mRNA methylation directs translational control of heat shock response. Nature. 2015 Oct;526(7574):591–4.

163. Coots RA, Liu X-M, Mao Y, Dong L, Zhou J, Wan J, et al. m6A Facilitates eIF4F-Independent mRNA Translation. Mol Cell. 2017 Nov 2;68(3):504-514.e7.
164. Zhang X, Shu XE, Qian S-B. O-GlcNAc modification of eIF4GI acts as a translational switch in heat shock response. Nat Chem Biol. 2018 Oct;14(10):909–16.
165. Zhang X, Gao X, Coots RA, Conn CS, Liu B, Qian S-B. Translational control of the cytosolic stress response by mitochondrial ribosomal protein L18. Nat Struct Mol Biol. 2015 May;22(5):404–10.
166. Zid BM, O'Shea EK. Promoter sequences direct cytoplasmic localization and translation of mRNAs during starvation in yeast. Nature. 2014 Oct;514(7520):117–21.
167. Vera M., Pani B., Griffiths L.A., Muchardt C., Abbott C.M., Singer R.H., Nudler E. The translation elongation factor eEF1A1 couples transcription to translation during heat shock response. Elife. 2014;3
168. Iserman C, Desroches Altamirano C, Jegers C, Friedrich U, Zarin T, Fritsch AW, et al. Condensation of Ded1p Promotes a Translational Switch from Housekeeping to Stress Protein Production. Cell. 2020 May 14;181(4):818-831.e19.
169. Bond U. Stressed out! Effects of environmental stress on mRNA metabolism. FEMS Yeast Res. 2006 Mar 1;6(2):160–70.
170. Buchan JR, Parker R. Eukaryotic Stress Granules: The Ins and Outs of Translation. Mol Cell. 2009 Dec 24;36(6):932–41.
171. DiDomenico BJ, Bugaisky GE, Lindquist S. The heat shock response is self-regulated at both the transcriptional and posttranscriptional levels. Cell. 1982 Dec;31(3 Pt 2):593–603.
172. Petersen R, Lindquist S. The Drosophila hsp70 message is rapidly degraded at normal temperatures and stabilized by heat shock. Gene. 1988 Dec 10;72(1):161–8.
173. Simcox AA, Cheney CM, Hoffman EP, Shearn A. A deletion of the 3' end of the Drosophila melanogaster hsp70 gene increases stability of mutant mRNA during recovery from heat shock. Mol Cell Biol. 1985 Dec;5(12):3397–402.
174. Feder JH, Rossi JM, Solomon J, Solomon N, Lindquist S. The consequences of expressing hsp70 in Drosophila cells at normal temperatures. Genes Dev. 1992 Aug 1;6(8):1402–13.
175. Kumar S, Stokes J, Singh UP, Gunn KS, Acharya A, Manne U, et al. Targeting Hsp70: A possible therapy for cancer. Cancer Lett. 2016 Apr 28;374(1):156–66.
176. DiDomenico BJ, Bugaisky GE, Lindquist S. Heat Shock and Recovery are Mediated by Different Translational Mechanisms. Proc Natl Acad Sci U S A. 1982;79(20):6181–5.
177. Petersen RB, Lindquist S. Differential mRNA Stability: A Regulatory Strategy for Hsp70 Synthesis. In: McCarthy JEG, Tuite MF, editors. Post-Transcriptional Control of Gene Expression. Berlin, Heidelberg: Springer; 1990. p. 83–91. (NATO ASI Series).
178. Bunch TA, Grinblat Y, Goldstein LS. Characterization and use of the Drosophila metallothionein promoter in cultured Drosophila melanogaster cells. Nucleic Acids Res. 1988 Feb 11;16(3):1043–61.
179. Mokdad R, Debec A, Wegnez M. Metallothionein Genes in Drosophila melanogaster Constitute a Dual System. Proc Natl Acad Sci U S A. 1987;84(9):2658–62.
180. Theodorakis NG, Morimoto RI. Posttranscriptional regulation of hsp70 expression in human cells: effects of heat shock, inhibition of protein synthesis, and adenovirus infection on translation and mRNA stability. Mol Cell Biol. 1987 Dec;7(12):4357–68.
181. Petersen RB, Lindquist S. Regulation of HSP70 synthesis by messenger RNA degradation. Cell Regul. 1989 Nov;1(1):135–49.

182. Zhao M, Tang D, Lechpammer S, Hoffman A, Asea A, Stevenson MA, et al. Double-stranded RNA-dependent protein kinase (pkr) is essential for thermotolerance, accumulation of HSP70, and stabilization of ARE-containing HSP70 mRNA during stress. J Biol Chem. 2002 Nov 15;277(46):44539–47.
183. Bönisch C, Temme C, Moritz B, Wahle E. Degradation of hsp70 and Other mRNAs in Drosophila via the 5′–3′ Pathway and Its Regulation by Heat Shock *. J Biol Chem. 2007 Jul 27;282(30):21818–28.
184. Deka K, Singh A, Chakraborty S, Mukhopadhyay R, Saha S. Protein arginylation regulates cellular stress response by stabilizing HSP70 and HSP40 transcripts. Cell Death Discov. 2016 Oct 3;2(1):1–8.
185. Rebeaud ME, Mallik S, Goloubinoff P, Tawfik DS. On the evolution of chaperones and cochaperones and the expansion of proteomes across the Tree of Life. Proc Natl Acad Sci U S A. 2021 May 25;118(21):e2020885118.
186. Shemesh N, Jubran J, Dror S, Simonovsky E, Basha O, Argov C, et al. The landscape of molecular chaperones across human tissues reveals a layered architecture of core and variable chaperones. Nat Commun. 2021 Apr 12;12(1):2180.
187. Sweeny EA, Shorter J. Mechanistic and Structural Insights into the Prion-Disaggregase Activity of Hsp104. J Mol Biol. 2016 May 8;428(9 Pt B):1870–85.
188. Bukau B. Regulation of the Escherichia coli heat-shock response. Mol Microbiol. 1993 Aug;9(4):671–80.
189. Harrison AF, Shorter J. RNA-binding proteins with prion-like domains in health and disease. Biochem J. 2017 Apr 7;474(8):1417–38.
190. Kirstein J, Arnsburg K, Scior A, Szlachcic A, Guilbride DL, Morimoto RI, et al. In vivo properties of the disaggregase function of J-proteins and Hsc70 in Caenorhabditis elegans stress and aging. Aging Cell. 2017 Dec;16(6):1414–24.
191. Nillegoda NB, Kirstein J, Szlachcic A, Berynskyy M, Stank A, Stengel F, et al. Crucial HSP70 co-chaperone complex unlocks metazoan protein disaggregation. Nature. 2015 Aug;524(7564):247–51.
192. Gao X, Carroni M, Nussbaum-Krammer C, Mogk A, Nillegoda NB, Szlachcic A, et al. Human Hsp70 Disaggregase Reverses Parkinson's-Linked α-Synuclein Amyloid Fibrils. Mol Cell. 2015 Sep;59(5):781–93.
193. Clos J, Rabindran S, Wisniewski J, Wu C. Induction temperature of human heat shock factor is reprogrammed in a Drosophila cell environment. Nature. 1993 Jul 15;364(6434):252–5.
194. Hentze N, Le Breton L, Wiesner J, Kempf G, Mayer MP. Molecular mechanism of thermosensory function of human heat shock transcription factor Hsf1. eLife. 2016 Jan 19;5:e11576.
195. Hammel HT. Regulation of internal body temperature. Annu Rev Physiol. 1968;30:641–710.
196. Tomanek L. Proteomics to study adaptations in marine organisms to environmental stress. J Proteomics. 2014 Jun;105:92–106.
197. Tomanek L. Variation in the heat shock response and its implication for predicting the effect of global climate change on species' biogeographical distribution ranges and metabolic costs. J Exp Biol. 2010 Mar 15;213(6):971–9.
198. Hofmann GE. Patterns of Hsp gene expression in ectothermic marine organisms on small to large biogeographic scales. Integr Comp Biol. 2005 Apr;45(2):247–55.

199. Macario AJ, Lange M, Ahring BK, Conway de Macario E. Stress genes and proteins in the archaea. Microbiol Mol Biol Rev MMBR. 1999 Dec;63(4):923–67, table of contents.
200. Ahmed R, Duncan RF. Translational Regulation of Hsp90 mRNA. J Biol Chem. 2004 Nov;279(48):49919–30.
201. Morán Luengo T, Kityk R, Mayer MP, Rüdiger SGD. Hsp90 Breaks the Deadlock of the Hsp70 Chaperone System. Mol Cell. 2018 May;70(3):545-552.e9.
202. Nava R, Zuhl MN. Heat acclimation-induced intracellular HSP70 in humans: a meta-analysis. Cell Stress Chaperones. 2020 Jan;25(1):35–45.
203. Chao Y-C, Merritt M, Schaefferkoetter D, Evans TG. High-throughput quantification of protein structural change reveals potential mechanisms of temperature adaptation in Mytilus mussels. BMC Evol Biol. 2020 Dec;20(1):28.
204. Berger MS, Emlet RB. Heat-shock response of the upper intertidal barnacle Balanus glandula: thermal stress and acclimation. Biol Bull. 2007 Jun;212(3):232–41.
205. Domnauer M, Zheng F, Li L, Zhang Y, Chang CE, Unruh JR, et al. Proteome plasticity in response to persistent environmental change. Mol Cell. 2021 Aug;81(16):3294-3309.e12.
206. Morimoto RI. Cell-Nonautonomous Regulation of Proteostasis in Aging and Disease. Cold Spring Harb Perspect Biol. 2020 Apr 1;12(4):a034074.
207. Amin V, Cumming DVE, Coffin RS, Latchman DS. The degree of protection provided to neuronal cells by a pre-conditioning stress correlates with the amount of heat shock protein 70 it induces and not with the similarity of the subsequent stress. Neurosci Lett. 1995 Nov;200(2):85–8.
208. Teranishi KS, Stillman JH. A cDNA microarray analysis of the response to heat stress in hepatopancreas tissue of the porcelain crab Petrolisthes cinctipes. Comp Biochem Physiol Part D Genomics Proteomics. 2007 Mar;2(1):53–62.
209. Currie RW, Karmazyn M, Kloc M, Mailer K. Heat-shock response is associated with enhanced postischemic ventricular recovery. Circ Res. 1988 Sep;63(3):543–9.
210. Gray CC, Amrani M, Yacoub MH. Heat stress proteins and myocardial protection: experimental model or potential clinical tool? Int J Biochem Cell Biol. 1999 May;31(5):559–73.
211. Alzahrani SM, Ebert PR. Stress pre-conditioning with temperature, UV and gamma radiation induces tolerance against phosphine toxicity. Shelden EA, editor. PLOS ONE. 2018 Apr 19;13(4):e0195349.
212. Das M, Das DK. Molecular mechanism of preconditioning. IUBMB Life. 2008 Apr;60(4):199–203.
213. Prahlad V, Cornelius T, Morimoto RI. Regulation of the cellular heat shock response in Caenorhabditis elegans by thermosensory neurons. Science. 2008 May 9;320(5877):811–4.
214. Fawcett TW, Sylvester SL, Sarge KD, Morimoto RI, Holbrook NJ. Effects of neurohormonal stress and aging on the activation of mammalian heat shock factor 1. J Biol Chem. 1994 Dec 23;269(51):32272–8.
215. Hipp MS, Kasturi P, Hartl FU. The proteostasis network and its decline in ageing. Nat Rev Mol Cell Biol. 2019 Jul;20(7):421–35.
216. Batulan Z, Shinder GA, Minotti S, He BP, Doroudchi MM, Nalbantoglu J, et al. High threshold for induction of the stress response in motor neurons is associated with failure to activate HSF1. J Neurosci Off J Soc Neurosci. 2003 Jul 2;23(13):5789–98.

217. Dugger BN, Dickson DW. Pathology of Neurodegenerative Diseases. Cold Spring Harb Perspect Biol. 2017 Jul 5;9(7).
218. Penke B, Bogár F, Crul T, Sántha M, Tóth ME, Vígh L. Heat Shock Proteins and Autophagy Pathways in Neuroprotection: from Molecular Bases to Pharmacological Interventions. Int J Mol Sci. 2018 Jan 22;19(1).
219. Gil R.S., Cox D., McAlary L., Berg T., Walker A.K., Yerbury J.J., Ooi L., Ecroyd H. Neurodegenerative disease-associated protein aggregates are poor inducers of the heat shock response in neuronal-like cells. J. Cell Sci. 2020 doi: 10.1242/jcs.243709.
220. Hoshino T, Murao N, Namba T, Takehara M, Adachi H, Katsuno M, et al. Suppression of Alzheimer's disease-related phenotypes by expression of heat shock protein 70 in mice. J Neurosci Off J Soc Neurosci. 2011 Apr 6;31(14):5225–34.
221. Bobkova NV, Garbuz DG, Nesterova I, Medvinskaya N, Samokhin A, Alexandrova I, et al. Therapeutic effect of exogenous hsp70 in mouse models of Alzheimer's disease. J Alzheimers Dis JAD. 2014;38(2):425–35.
222. Evgen'ev MB, Krasnov GS, Nesterova IV, Garbuz DG, Karpov VL, Morozov AV, et al. Molecular Mechanisms Underlying Neuroprotective Effect of Intranasal Administration of Human Hsp70 in Mouse Model of Alzheimer's Disease. J Alzheimers Dis JAD. 2017;59(4):1415–26.
223. Campanella C, Pace A, Caruso Bavisotto C, Marzullo P, Marino Gammazza A, Buscemi S, et al. Heat Shock Proteins in Alzheimer's Disease: Role and Targeting. Int J Mol Sci. 2018 Sep 1;19(9).
224. Kuta R, Larochelle N, Fernandez M, Pal A, Minotti S, Tibshirani M, et al. Depending on the stress, histone deacetylase inhibitors act as heat shock protein co-inducers in motor neurons and potentiate arimoclomol, exerting neuroprotection through multiple mechanisms in ALS models. Cell Stress Chaperones. 2020 Jan;25(1):173–91.
225. Ravikumar B, Duden R, Rubinsztein DC. Aggregate-prone proteins with polyglutamine and polyalanine expansions are degraded by autophagy. Hum Mol Genet. 2002 May 1;11(9):1107–17.
226. Webb JL, Ravikumar B, Atkins J, Skepper JN, Rubinsztein DC. Alpha-Synuclein is degraded by both autophagy and the proteasome. J Biol Chem. 2003 Jul 4;278(27):25009–13.
227. Rubinsztein DC, Codogno P, Levine B. Autophagy modulation as a potential therapeutic target for diverse diseases. Nat Rev Drug Discov. 2012 Sep;11(9):709–30.
228. Ghavami S, Shojaei S, Yeganeh B, Ande SR, Jangamreddy JR, Mehrpour M, et al. Autophagy and apoptosis dysfunction in neurodegenerative disorders. Prog Neurobiol. 2014 Jan;112:24–49.
229. Huang H, Zhu J, Li Y, Zhang L, Gu J, Xie Q, et al. Upregulation of SQSTM1/p62 contributes to nickel-induced malignant transformation of human bronchial epithelial cells. Autophagy. 2016 Oct 2;12(10):1687–703.
230. Wolff S, Weissman JS, Dillin A. Differential scales of protein quality control. Cell. 2014 Mar 27;157(1):52–64.
231. Sato H, Das S, Singer RH, Vera M. Imaging of DNA and RNA in Living Eukaryotic Cells to Reveal Spatiotemporal Dynamics of Gene Expression. Annu Rev Biochem. 2020 Jun 20;89:159–87.
232. Tutucci E, Livingston NM, Singer RH, Wu B. Imaging mRNA In Vivo, from Birth to Death. Annu Rev Biophys. 2018 May 20;47:85–106.

233. Pichon X, Lagha M, Mueller F, Bertrand E. A Growing Toolbox to Image Gene Expression in Single Cells: Sensitive Approaches for Demanding Challenges. Mol Cell. 2018 02;71(3):468–80.
234. Brandvold KR, Morimoto RI. The Chemical Biology of Molecular Chaperones--Implications for Modulation of Proteostasis. J Mol Biol. 2015 Sep 11;427(18):2931–47.
235. Brandman O, Stewart-Ornstein J, Wong D, Larson A, Williams CC, Li G-W, et al. A ribosome-bound quality control complex triggers degradation of nascent peptides and signals translation stress. Cell. 2012 Nov 21;151(5):1042–54.
236. Massey A, Kiffin R, Cuervo AM. Pathophysiology of chaperone-mediated autophagy. Int J Biochem Cell Biol. 2004 Dec;36(12):2420–34.
237. Majeski AE, Fred Dice J. Mechanisms of chaperone-mediated autophagy. Int J Biochem Cell Biol. 2004 Dec;36(12):2435–44.
238. Morano KA, Grant CM, Moye-Rowley WS. The response to heat shock and oxidative stress in Saccharomyces cerevisiae. Genetics. 2012 Apr;190(4):1157–95.
239. Snutch TP, Baillie DL. Alterations in the pattern of gene expression following heat shock in the nematode Caenorhabditis elegans. Can J Biochem Cell Biol Rev Can Biochim Biol Cell. 1983 Jun;61(6):480–7.
240. Candido EPM. The small heat shock proteins of the nematode Caenorhabditis elegans: structure, regulation and biology. Prog Mol Subcell Biol. 2002;28:61–78.
241. Velichko AK, Markova EN, Petrova NV, Razin SV, Kantidze OL. Mechanisms of heat shock response in mammals. Cell Mol Life Sci CMLS. 2013 Nov;70(22):4229–41.
242. Avila DS, Benedetto A, Au C, Bornhorst J, Aschner M. Involvement of heat shock proteins on Mn-induced toxicity in Caenorhabditis elegans. BMC Pharmacol Toxicol. 2016 Dec;17(1):54.
243. Han M-J, Lee SY. The Escherichia coli proteome: past, present, and future prospects. Microbiol Mol Biol Rev MMBR. 2006 Jun;70(2):362–439.
244. Mühlhofer M, Berchtold E, Stratil CG, Csaba G, Kunold E, Bach NC, et al. The Heat Shock Response in Yeast Maintains Protein Homeostasis by Chaperoning and Replenishing Proteins. Cell Rep. 2019 Dec;29(13):4593-4607.e8.
245. Verghese J, Abrams J, Wang Y, Morano KA. Biology of the heat shock response and protein chaperones: budding yeast (Saccharomyces cerevisiae) as a model system. Microbiol Mol Biol Rev MMBR. 2012 Jun;76(2):115–58.
246. Vazquez J, Pauli D, Tissières A. Transcriptional regulation in Drosophila during heat shock: a nuclear run-on analysis. Chromosoma. 1993 Mar;102(4):233–48.
247. Mahat DB, Salamanca HH, Duarte FM, Danko CG, Lis JT. Mammalian Heat Shock Response and Mechanisms Underlying Its Genome-wide Transcriptional Regulation. Mol Cell. 2016 Apr 7;62(1):63–78.
248. Yura T, Nagai H, Mori H. Regulation of the heat-shock response in bacteria. Annu Rev Microbiol. 1993;47:321–50.
249. McAlister L, Strausberg S, Kulaga A, Finkelstein DB. Altered patterns of protein synthesis induced by heat shock of yeast. Curr Genet. 1979 Dec;1(1):63–74.
250. Richter K, Haslbeck M, Buchner J. The heat shock response: life on the verge of death. Mol Cell. 2010 Oct 22;40(2):253–66.
251. de Benedetti A, Baglioni C. Translational regulation of the synthesis of a major heat shock protein in HeLa cells. J Biol Chem. 1986 Nov 25;261(33):15800–4.

252. Yura T. Regulation of the heat shock response in Escherichia coli: history and perspectives. Genes Genet Syst. 2019 Jul 27;94(3):103–8.
253. Grossman A.D., Straus D.B., Walter W.A., Gross C.A. Sigma 32 synthesis can regulate the synthesis of heat shock proteins in Escherichia coli. Genes Dev. 1987;1:179–184.

APPENDIX 4: References to Chapter 1.3

Alagar Boopathy, L. R., Beadle, E., Xiao, A., Rico, A. G.-B., Alecki, C., de-Andres, I. G., & Vera, M. (2022). *The ribosome quality control factors Asc1 and Hel2 regulate the expression of HSP70 during heat shock and recovery* (p. 2022.09.12.507689). bioRxiv. https://doi.org/10.1101/2022.09.12.507689

Alexaki, A., Kames, J., Holcomb, D. D., Athey, J., Santana-Quintero, L. V., Lam, P. V. N., Hamasaki-Katagiri, N., Osipova, E., Simonyan, V., Bar, H., Komar, A. A., & Kimchi-Sarfaty, C. (2019). Codon and Codon-Pair Usage Tables (CoCoPUTs): Facilitating Genetic Variation Analyses and Recombinant Gene Design. *Journal of Molecular Biology*, *431*(13), 2434–2441. https://doi.org/10.1016/j.jmb.2019.04.021

Alford, B. D., Tassoni-Tsuchida, E., Khan, D., Work, J. J., Valiant, G., & Brandman, O. (2021). ReporterSeq reveals genome-wide dynamic modulators of the heat shock response across diverse stressors. *ELife*, *10*, e57376. https://doi.org/10.7554/eLife.57376

Anazi, S., Maddirevula, S., Faqeih, E., Alsedairy, H., Alzahrani, F., Shamseldin, H. E., Patel, N., Hashem, M., Ibrahim, N., Abdulwahab, F., Ewida, N., Alsaif, H. S., Al sharif, H., Alamoudi, W., Kentab, A., Bashiri, F. A., Alnaser, M., AlWadei, A. H., Alfadhel, M., … Alkuraya, F. S. (2017). Clinical genomics expands the morbid genome of intellectual disability and offers a high diagnostic yield. *Molecular Psychiatry*, *22*(4), Article 4. https://doi.org/10.1038/mp.2016.113

Anderson, J. S., & Parker, R. P. (1998). The 3’ to 5’ degradation of yeast mRNAs is a general mechanism for mRNA turnover that requires the SKI2 DEVH box protein and 3’ to 5’ exonucleases of the exosome complex. *The EMBO Journal*, *17*(5), 1497–1506. https://doi.org/10.1093/emboj/17.5.1497

Arribere, J. A., & Fire, A. Z. (2018). Nonsense mRNA suppression via nonstop decay. *ELife*, *7*, e33292. https://doi.org/10.7554/eLife.33292

Artieri, C. G., & Fraser, H. B. (2014). Accounting for biases in riboprofiling data indicates a major role for proline in stalling translation. *Genome Research*, *24*(12), 2011–2021. https://doi.org/10.1101/gr.175893.114

Atkinson, G. C., Baldauf, S. L., & Hauryliuk, V. (2008). Evolution of nonstop, no-go and nonsense-mediated mRNA decay and their termination factor-derived components. *BMC Evolutionary Biology*, *8*, 290. https://doi.org/10.1186/1471-2148-8-290

Aviner, R., Lee, T.-T., Masto, V. B., Gestaut, D., Li, K. H., Andino, R., & Frydman, J. (2022). *Ribotoxic collisions on CAG expansions disrupt proteostasis and stress responses in Huntington’s Disease* (p. 2022.05.04.490528). bioRxiv. https://doi.org/10.1101/2022.05.04.490528

Becker, T., Armache, J.-P., Jarasch, A., Anger, A. M., Villa, E., Sieber, H., Motaal, B. A., Mielke, T., Berninghausen, O., & Beckmann, R. (2011). Structure of the no-go mRNA decay complex Dom34-Hbs1 bound to a stalled 80S ribosome. *Nature Structural & Molecular Biology*, *18*(6), Article 6. https://doi.org/10.1038/nsmb.2057

Bengtson, M. H., & Joazeiro, C. A. P. (2010). Role of a ribosome-associated E3 ubiquitin ligase in protein quality control. *Nature*, *467*(7314), 470–473. https://doi.org/10.1038/nature09371

Best, K., Ikeuchi, K., Kater, L., Best, D., Musial, J., Matsuo, Y., Berninghausen, O., Becker, T., Inada, T., & Beckmann, R. (2023). Structural basis for clearing of ribosome collisions by the RQT complex. *Nature Communications*, *14*(1), Article 1. https://doi.org/10.1038/s41467-023-36230-8

Bönisch, C., Temme, C., Moritz, B., & Wahle, E. (2007). Degradation of hsp70 and Other mRNAs in Drosophila via the 5′–3′ Pathway and Its Regulation by Heat Shock *. *Journal of Biological Chemistry*, *282*(30), 21818–21828. https://doi.org/10.1074/jbc.M702998200

Brandman, O., Stewart-Ornstein, J., Wong, D., Larson, A., Williams, C. C., Li, G.-W., Zhou, S., King, D., Shen, P. S., Weibezahn, J., Dunn, J. G., Rouskin, S., Inada, T., Frost, A., & Weissman, J. S. (2012). A ribosome-bound quality control complex triggers degradation of nascent peptides and signals translation stress. *Cell*, *151*(5), 1042–1054. https://doi.org/10.1016/j.cell.2012.10.044

Brewer, G. (2001). Misregulated Posttranscriptional Checkpoints. *The Journal of Experimental Medicine*, *193*(2), f1–f4.

Brickner, J. R., Soll, J. M., Lombardi, P. M., Vågbø, C. B., Mudge, M. C., Oyeniran, C., Rabe, R., Jackson, J., Sullender, M. E., Blazosky, E., Byrum, A. K., Zhao, Y., Corbett, M. A., Gécz, J., Field, M., Vindigni, A., Slupphaug, G., Wolberger, C., & Mosammaparast, N. (2017). A ubiquitin-dependent signalling axis specific for ALKBH-mediated DNA dealkylation repair. *Nature*, *551*(7680), Article 7680. https://doi.org/10.1038/nature24484

Buschauer, R., Matsuo, Y., Sugiyama, T., Chen, Y.-H., Alhusaini, N., Sweet, T., Ikeuchi, K., Cheng, J., Matsuki, Y., Nobuta, R., Gilmozzi, A., Berninghausen, O., Tesina, P., Becker, T., Coller, J., Inada, T., & Beckmann, R. (2020). The Ccr4-Not complex monitors the translating ribosome for codon optimality. *Science*, *368*(6488), Article 6488. https://doi.org/10.1126/science.aay6912

Chandrasekaran, V., Juszkiewicz, S., Choi, J., Puglisi, J. D., Brown, A., Shao, S., Ramakrishnan, V., & Hegde, R. S. (2019). Mechanism of ribosome stalling during translation of a poly(A) tail. *Nature Structural & Molecular Biology*, *26*(12), 1132–1140. https://doi.org/10.1038/s41594-019-0331-x

Chang, J. H., Jiao, X., Chiba, K., Oh, C., Martin, C. E., Kiledjian, M., & Tong, L. (2012). Dxo1 is a novel eukaryotic enzyme with both decapping and 5′-3′ exoribonuclease activity. *Nature Structural & Molecular Biology*, *19*(10), 1011–1017. https://doi.org/10.1038/nsmb.2381

Charneski, C. A., & Hurst, L. D. (2013). Positively Charged Residues Are the Major Determinants of Ribosomal Velocity. *PLOS Biology*, *11*(3), e1001508. https://doi.org/10.1371/journal.pbio.1001508

Chi, B., O'Connell, J. D., Iocolano, A. D., Coady, J. A., Yu, Y., Gangopadhyay, J., Gygi, S. P., & Reed, R. (2018). The neurodegenerative diseases ALS and SMA are linked at the molecular

level via the ASC-1 complex. *Nucleic Acids Research*, *46*(22), 11939–11951. https://doi.org/10.1093/nar/gky1093

Chiabudini, M., Conz, C., Reckmann, F., & Rospert, S. (2012). Ribosome-associated complex and Ssb are required for translational repression induced by polylysine segments within nascent chains. *Molecular and Cellular Biology*, *32*(23), 4769–4779. https://doi.org/10.1128/MCB.00809-12

Choe, Y.-J., Park, S.-H., Hassemer, T., Körner, R., Vincenz-Donnelly, L., Hayer-Hartl, M., & Hartl, F. U. (2016). Failure of RQC machinery causes protein aggregation and proteotoxic stress. *Nature*, *531*(7593), Article 7593. https://doi.org/10.1038/nature16973

Chu, J., Hong, N. A., Masuda, C. A., Jenkins, B. V., Nelms, K. A., Goodnow, C. C., Glynne, R. J., Wu, H., Masliah, E., Joazeiro, C. A. P., & Kay, S. A. (2009). A mouse forward genetics screen identifies LISTERIN as an E3 ubiquitin ligase involved in neurodegeneration. *Proceedings of the National Academy of Sciences*, *106*(7), 2097–2103. https://doi.org/10.1073/pnas.0812819106

Cougot, N., van Dijk, E., Babajko, S., & Séraphin, B. (2004). 'Cap-tabolism.' *Trends in Biochemical Sciences*, *29*(8), 436–444. https://doi.org/10.1016/j.tibs.2004.06.008

de Almeida, S. F., & Carmo-Fonseca, M. (2010). Cotranscriptional RNA checkpoints. *Epigenomics*, *2*(3), 449–455. https://doi.org/10.2217/epi.10.21

De, S., & Mühlemann, O. (2022). A comprehensive coverage insurance for cells: Revealing links between ribosome collisions, stress responses and mRNA surveillance. *RNA Biology*, *19*(1), 609–621. https://doi.org/10.1080/15476286.2022.2065116

Decker, C. J., & Parker, R. (2002). mRNA decay enzymes: Decappers conserved between yeast and mammals. *Proceedings of the National Academy of Sciences of the United States of America*, *99*(20), 12512–12514. https://doi.org/10.1073/pnas.212518099

Defenouillère, Q., Yao, Y., Mouaikel, J., Namane, A., Galopier, A., Decourty, L., Doyen, A., Malabat, C., Saveanu, C., Jacquier, A., & Fromont-Racine, M. (2013). Cdc48-associated complex bound to 60S particles is required for the clearance of aberrant translation products. *Proceedings of the National Academy of Sciences of the United States of America*, *110*(13), 5046–5051. https://doi.org/10.1073/pnas.1221724110

Deshaies, R. J., & Joazeiro, C. A. P. (2009). RING domain E3 ubiquitin ligases. *Annual Review of Biochemistry*, *78*, 399–434. https://doi.org/10.1146/annurev.biochem.78.101807.093809

Dimitrova, L. N., Kuroha, K., Tatematsu, T., & Inada, T. (2009). Nascent Peptide-dependent Translation Arrest Leads to Not4p-mediated Protein Degradation by the Proteasome*. *Journal of Biological Chemistry*, *284*(16), 10343–10352. https://doi.org/10.1074/jbc.M808840200

Djumagulov, M., Demeshkina, N., Jenner, L., Rozov, A., Yusupov, M., & Yusupova, G. (2021). Accuracy mechanism of eukaryotic ribosome translocation. *Nature*, *600*(7889), Article 7889. https://doi.org/10.1038/s41586-021-04131-9

Doma, M. K., & Parker, R. (2006). Endonucleolytic cleavage of eukaryotic mRNAs with stalls in translation elongation. *Nature*, *440*(7083), Article 7083. https://doi.org/10.1038/nature04530

D'Orazio, K. N., & Green, R. (2021). Ribosome states signal RNA quality control. *Molecular Cell*, *81*(7), 1372–1383. https://doi.org/10.1016/j.molcel.2021.02.022

D'Orazio, K. N., Wu, C. C.-C., Sinha, N., Loll-Krippleber, R., Brown, G. W., & Green, R. (2019). The endonuclease Cue2 cleaves mRNAs at stalled ribosomes during No Go Decay. *ELife*, *8*, e49117. https://doi.org/10.7554/eLife.49117

Eberle, A. B., Lykke-Andersen, S., Mühlemann, O., & Jensen, T. H. (2009). SMG6 promotes endonucleolytic cleavage of nonsense mRNA in human cells. *Nature Structural & Molecular Biology*, *16*(1), 49–55. https://doi.org/10.1038/nsmb.1530

Frank, J. (2017). The translation elongation cycle—Capturing multiple states by cryo-electron microscopy. *Philosophical Transactions of the Royal Society B: Biological Sciences*, *372*(1716), 20160180. https://doi.org/10.1098/rstb.2016.0180

Frischmeyer, P. A., van Hoof, A., O'Donnell, K., Guerrerio, A. L., Parker, R., & Dietz, H. C. (2002). An mRNA surveillance mechanism that eliminates transcripts lacking termination codons. *Science (New York, N.Y.)*, *295*(5563), 2258–2261. https://doi.org/10.1126/science.1067338

Gamble, C. E., Brule, C. E., Dean, K. M., Fields, S., & Grayhack, E. J. (2016). Adjacent Codons Act in Concert to Modulate Translation Efficiency in Yeast. *Cell*, *166*(3), 679–690. https://doi.org/10.1016/j.cell.2016.05.070

Gandhi, R., Manzoor, M., & Hudak, K. A. (2008). Depurination of Brome mosaic virus RNA3 in vivo results in translation-dependent accelerated degradation of the viral RNA. *The Journal of Biological Chemistry*, *283*(47), 32218–32228. https://doi.org/10.1074/jbc.M803785200

Garneau, N. L., Wilusz, J., & Wilusz, C. J. (2007). The highways and byways of mRNA decay. *Nature Reviews Molecular Cell Biology*, *8*(2), Article 2. https://doi.org/10.1038/nrm2104

Garshott, D. M., Sundaramoorthy, E., Leonard, M., & Bennett, E. J. (2020). Distinct regulatory ribosomal ubiquitylation events are reversible and hierarchically organized. *ELife*, *9*, e54023. https://doi.org/10.7554/eLife.54023

Gatfield, D., & Izaurralde, E. (2004). Nonsense-mediated messenger RNA decay is initiated by endonucleolytic cleavage in Drosophila. *Nature*, *429*(6991), 575–578. https://doi.org/10.1038/nature02559

Gerbasi, V. R., Weaver, C. M., Hill, S., Friedman, D. B., & Link, A. J. (2004). Yeast Asc1p and mammalian RACK1 are functionally orthologous core 40S ribosomal proteins that repress gene expression. *Molecular and Cellular Biology*, *24*(18), 8276–8287. https://doi.org/10.1128/MCB.24.18.8276-8287.2004

Glover, M. L., Burroughs, A. Max., Monem, P. C., Egelhofer, T. A., Pule, M. N., Aravind, L., & Arribere, J. A. (2020). NONU-1 Encodes a Conserved Endonuclease Required for mRNA Translation Surveillance. *Cell Reports*, *30*(13), 4321-4331.e4. https://doi.org/10.1016/j.celrep.2020.03.023

Goldman, D. H., Livingston, N. M., Movsik, J., Wu, B., & Green, R. (2021). Live-cell imaging reveals kinetic determinants of quality control triggered by ribosome stalling. *Molecular Cell*, *81*(8), 1830-1840.e8. https://doi.org/10.1016/j.molcel.2021.01.029

Graille, M., Chaillet, M., & van Tilbeurgh, H. (2008). Structure of yeast Dom34: A protein related to translation termination factor Erf1 and involved in No-Go decay. *The Journal of Biological Chemistry*, *283*(11), 7145–7154. https://doi.org/10.1074/jbc.M708224200

Green, R. E., Lewis, B. P., Hillman, R. T., Blanchette, M., Lareau, L. F., Garnett, A. T., Rio, D. C., & Brenner, S. E. (2003). Widespread predicted nonsense-mediated mRNA decay of alternatively-spliced transcripts of human normal and disease genes. *Bioinformatics (Oxford, England)*, *19 Suppl 1*, i118-121. https://doi.org/10.1093/bioinformatics/btg1015

Guydosh, N. R., & Green, R. (2017). Translation of poly(A) tails leads to precise mRNA cleavage. *RNA (New York, N.Y.)*, *23*(5), 749–761. https://doi.org/10.1261/rna.060418.116

Halbach, F., Reichelt, P., Rode, M., & Conti, E. (2013). The yeast ski complex: Crystal structure and RNA channeling to the exosome complex. *Cell*, *154*(4), 814–826. https://doi.org/10.1016/j.cell.2013.07.017

Hashimoto, S., Sugiyama, T., Yamazaki, R., Nobuta, R., & Inada, T. (2020). Identification of a novel trigger complex that facilitates ribosome-associated quality control in mammalian cells. *Scientific Reports*, *10*(1), Article 1. https://doi.org/10.1038/s41598-020-60241-w

Hayes, C. S., & Sauer, R. T. (2003). Cleavage of the A site mRNA codon during ribosome pausing provides a mechanism for translational quality control. *Molecular Cell*, *12*(4), 903–911. https://doi.org/10.1016/s1097-2765(03)00385-x

Hendrick, J. L., Wilson, P. G., Edelman, I. I., Sandbaken, M. G., Ursic, D., & Culbertson, M. R. (2001). Yeast frameshift suppressor mutations in the genes coding for transcription factor Mbf1p and ribosomal protein S3: Evidence for autoregulation of S3 synthesis. *Genetics*, *157*(3), 1141–1158. https://doi.org/10.1093/genetics/157.3.1141

Hershey, J. W. B., Sonenberg, N., & Mathews, M. B. (2019). Principles of Translational Control. *Cold Spring Harbor Perspectives in Biology*, *11*(9), a032607. https://doi.org/10.1101/cshperspect.a032607

Hickey, K. L., Dickson, K., Cogan, J. Z., Replogle, J. M., Schoof, M., D'Orazio, K. N., Sinha, N. K., Hussmann, J. A., Jost, M., Frost, A., Green, R., Weissman, J. S., & Kostova, K. K. (2020). GIGYF2 and 4EHP Inhibit Translation Initiation of Defective Messenger RNAs to Assist Ribosome-Associated Quality Control. *Molecular Cell*, *79*(6), 950-962.e6. https://doi.org/10.1016/j.molcel.2020.07.007

Hilal, T., Yamamoto, H., Loerke, J., Bürger, J., Mielke, T., & Spahn, C. M. T. (2016). Structural insights into ribosomal rescue by Dom34 and Hbs1 at near-atomic resolution. *Nature Communications*, *7*(1), Article 1. https://doi.org/10.1038/ncomms13521

Himeno, H., Sato, M., Tadaki, T., Fukushima, M., Ushida, C., & Muto, A. (1997). In vitro Trans Translation mediated by alanine-charged 10sa RNA11Edited by D.E. Draper. *Journal of Molecular Biology*, *268*(5), 803–808. https://doi.org/10.1006/jmbi.1997.1011

Hoek, T. A., Khuperkar, D., Lindeboom, R. G. H., Sonneveld, S., Verhagen, B. M. P., Boersma, S., Vermeulen, M., & Tanenbaum, M. E. (2019). Single-Molecule Imaging Uncovers Rules Governing Nonsense-Mediated mRNA Decay. *Molecular Cell*, *75*(2), 324-339.e11. https://doi.org/10.1016/j.molcel.2019.05.008

Holcik, M., & Sonenberg, N. (2005). Translational control in stress and apoptosis. *Nature Reviews Molecular Cell Biology*, *6*(4), 318–327. https://doi.org/10.1038/nrm1618

Hosoda, N., Kobayashi, T., Uchida, N., Funakoshi, Y., Kikuchi, Y., Hoshino, S., & Katada, T. (2003). Translation termination factor eRF3 mediates mRNA decay through the regulation of deadenylation. *The Journal of Biological Chemistry*, *278*(40), 38287–38291. https://doi.org/10.1074/jbc.C300300200

Houston, L., Platten, E. M., Connelly, S. M., Wang, J., & Grayhack, E. J. (2022). Frameshifting at collided ribosomes is modulated by elongation factor eEF3 and by integrated stress response regulators Gcn1 and Gcn20. *RNA*, *28*(3), 320–339. https://doi.org/10.1261/rna.078964.121

Hsu, C. L., & Stevens, A. (1993). Yeast cells lacking 5'→3' exoribonuclease 1 contain mRNA species that are poly(A) deficient and partially lack the 5' cap structure. *Molecular and Cellular Biology*, *13*(8), 4826–4835. Scopus. https://doi.org/10.1128/MCB.13.8.4826

Ikeuchi, K., & Inada, T. (2016). Ribosome-associated Asc1/RACK1 is required for endonucleolytic cleavage induced by stalled ribosome at the 3′ end of nonstop mRNA. *Scientific Reports*, *6*(1), Article 1. https://doi.org/10.1038/srep28234

Ikeuchi, K., Izawa, T., & Inada, T. (2019a). Recent Progress on the Molecular Mechanism of Quality Controls Induced by Ribosome Stalling. *Frontiers in Genetics*, *9*. https://www.frontiersin.org/articles/10.3389/fgene.2018.00743

Ikeuchi, K., Izawa, T., & Inada, T. (2019b). Recent Progress on the Molecular Mechanism of Quality Controls Induced by Ribosome Stalling. *Frontiers in Genetics*, *9*. https://www.frontiersin.org/articles/10.3389/fgene.2018.00743

Ikeuchi, K., Tesina, P., Matsuo, Y., Sugiyama, T., Cheng, J., Saeki, Y., Tanaka, K., Becker, T., Beckmann, R., & Inada, T. (2019). Collided ribosomes form a unique structural interface to induce Hel2-driven quality control pathways. *The EMBO Journal*, *38*(5), e100276. https://doi.org/10.15252/embj.2018100276

Ikeuchi, K., Yazaki, E., Kudo, K., & Inada, T. (2016). Conserved functions of human Pelota in mRNA quality control of nonstop mRNA. *FEBS Letters*, *590*(18), 3254–3263. https://doi.org/10.1002/1873-3468.12366

Inada, T. (2020). Quality controls induced by aberrant translation. *Nucleic Acids Research*, *48*(3), Article 3. https://doi.org/10.1093/nar/gkz1201

Ingolia, N. T., Ghaemmaghami, S., Newman, J. R. S., & Weissman, J. S. (2009). Genome-wide analysis in vivo of translation with nucleotide resolution using ribosome profiling. *Science (New York, N.Y.)*, *324*(5924), 218–223. https://doi.org/10.1126/science.1168978

Ishimura, R., Nagy, G., Dotu, I., Zhou, H., Yang, X.-L., Schimmel, P., Senju, S., Nishimura, Y., Chuang, J. H., & Ackerman, S. L. (2014). RNA function. Ribosome stalling induced by

mutation of a CNS-specific tRNA causes neurodegeneration. *Science (New York, N.Y.)*, *345*(6195), 455–459. https://doi.org/10.1126/science.1249749

Ito-Harashima, S., Kuroha, K., Tatematsu, T., & Inada, T. (2007). Translation of the poly(A) tail plays crucial roles in nonstop mRNA surveillance via translation repression and protein destabilization by proteasome in yeast. *Genes & Development*, *21*(5), 519–524. https://doi.org/10.1101/gad.1490207

Izawa, T., Park, S.-H., Zhao, L., Hartl, F. U., & Neupert, W. (2017). Cytosolic Protein Vms1 Links Ribosome Quality Control to Mitochondrial and Cellular Homeostasis. *Cell*, *171*(4), 890-903.e18. https://doi.org/10.1016/j.cell.2017.10.002

Joazeiro, C. A. P. (2017). Ribosomal Stalling During Translation: Providing Substrates for Ribosome-Associated Protein Quality Control. *Annual Review of Cell and Developmental Biology*, *33*, 343–368. https://doi.org/10.1146/annurev-cellbio-111315-125249

Joazeiro, C. A. P. (2019). Mechanisms and functions of ribosome-associated protein quality control. *Nature Reviews. Molecular Cell Biology*, *20*(6), 368–383. https://doi.org/10.1038/s41580-019-0118-2

Juszkiewicz, S., Chandrasekaran, V., Lin, Z., Kraatz, S., Ramakrishnan, V., & Hegde, R. S. (2018). ZNF598 Is a Quality Control Sensor of Collided Ribosomes. *Molecular Cell*, *72*(3), 469-481.e7. https://doi.org/10.1016/j.molcel.2018.08.037

Juszkiewicz, S., & Hegde, R. S. (2017). Initiation of Quality Control during Poly(A) Translation Requires Site-Specific Ribosome Ubiquitination. *Molecular Cell*, *65*(4), 743-750.e4. https://doi.org/10.1016/j.molcel.2016.11.039

Juszkiewicz, S., Slodkowicz, G., Lin, Z., Freire-Pritchett, P., Peak-Chew, S.-Y., & Hegde, R. S. (2020). Ribosome collisions trigger cis-acting feedback inhibition of translation initiation. *ELife*, *9*, e60038. https://doi.org/10.7554/eLife.60038

Juszkiewicz, S., Speldewinde, S. H., Wan, L., Svejstrup, J. Q., & Hegde, R. S. (2020). The ASC-1 Complex Disassembles Collided Ribosomes. *Molecular Cell*, *79*(4), 603-614.e8. https://doi.org/10.1016/j.molcel.2020.06.006

Karamyshev, A. L., & Karamysheva, Z. N. (2018). Lost in Translation: Ribosome-Associated mRNA and Protein Quality Controls. *Frontiers in Genetics*, *9*. https://www.frontiersin.org/articles/10.3389/fgene.2018.00431

Keene, J. D. (2007). RNA regulons: Coordination of post-transcriptional events. *Nature Reviews Genetics*, *8*(7), Article 7. https://doi.org/10.1038/nrg2111

Keiler, K. C., Waller, P. R., & Sauer, R. T. (1996). Role of a peptide tagging system in degradation of proteins synthesized from damaged messenger RNA. *Science (New York, N.Y.)*, *271*(5251), 990–993. https://doi.org/10.1126/science.271.5251.990

Kim, S. J., Yoon, J. S., Shishido, H., Yang, Z., Rooney, L. A., Barral, J. M., & Skach, W. R. (2015). Protein folding. Translational tuning optimizes nascent protein folding in cells. *Science (New York, N.Y.)*, *348*(6233), 444–448. https://doi.org/10.1126/science.aaa3974

Klauer, A. A., & van Hoof, A. (2012). Degradation of mRNAs that lack a stop codon: A decade of nonstop progress. *Wiley Interdisciplinary Reviews. RNA*, *3*(5), 649–660. https://doi.org/10.1002/wrna.1124

Kobayashi, K., Kikuno, I., Kuroha, K., Saito, K., Ito, K., Ishitani, R., Inada, T., & Nureki, O. (2010). Structural basis for mRNA surveillance by archaeal Pelota and GTP-bound EF1α complex. *Proceedings of the National Academy of Sciences of the United States of America*, *107*(41), 17575–17579. https://doi.org/10.1073/pnas.1009598107

Komine, Y., Kitabatake, M., Yokogawa, T., Nishikawa, K., & Inokuchi, H. (1994). A tRNA-like structure is present in 10Sa RNA, a small stable RNA from *Escherichia coli*. *Proceedings of the National Academy of Sciences of the United States of America*, *91*(20), 9223–9227. https://doi.org/10.1073/pnas.91.20.9223

Kostova, K. K., Hickey, K. L., Osuna, B. A., Hussmann, J. A., Frost, A., Weinberg, D. E., & Weissman, J. S. (2017). CAT-tailing as a fail-safe mechanism for efficient degradation of stalled nascent polypeptides. *Science (New York, N.Y.)*, *357*(6349), 414–417. https://doi.org/10.1126/science.aam7787

Kuroha, K., Akamatsu, M., Dimitrova, L., Ito, T., Kato, Y., Shirahige, K., & Inada, T. (2010). Receptor for activated C kinase 1 stimulates nascent polypeptide-dependent translation arrest. *EMBO Reports*, *11*(12), 956–961. https://doi.org/10.1038/embor.2010.169

Labbadia, J., & Morimoto, R. I. (2015). The Biology of Proteostasis in Aging and Disease. *Annual Review of Biochemistry*, *84*, 435–464. https://doi.org/10.1146/annurev-biochem-060614-033955

Łabno, A., Tomecki, R., & Dziembowski, A. (2016). Cytoplasmic RNA decay pathways—Enzymes and mechanisms. *Biochimica et Biophysica Acta (BBA) - Molecular Cell Research*, *1863*(12), 3125–3147. https://doi.org/10.1016/j.bbamcr.2016.09.023

Lanza, A. M., Curran, K. A., Rey, L. G., & Alper, H. S. (2014). A condition-specific codon optimization approach for improved heterologous gene expression in Saccharomyces cerevisiae. *BMC Systems Biology*, *8*(1), 33. https://doi.org/10.1186/1752-0509-8-33

Letzring, D. P., Dean, K. M., & Grayhack, E. J. (2010). Control of translation efficiency in yeast by codon–anticodon interactions. *RNA*, *16*(12), Article 12. https://doi.org/10.1261/rna.2411710

Letzring, D. P., Wolf, A. S., Brule, C. E., & Grayhack, E. J. (2013). Translation of CGA codon repeats in yeast involves quality control components and ribosomal protein L1. *RNA (New York, N.Y.)*, *19*(9), 1208–1217. https://doi.org/10.1261/rna.039446.113

Li, S., Ikeuchi, K., Kato, M., Buschauer, R., Sugiyama, T., Adachi, S., Kusano, H., Natsume, T., Berninghausen, O., Matsuo, Y., Becker, T., Beckmann, R., & Inada, T. (2022). Sensing of individual stalled 80S ribosomes by Fap1 for nonfunctional rRNA turnover. *Molecular Cell*, *82*(18), 3424-3437.e8. https://doi.org/10.1016/j.molcel.2022.08.018

Li, T., Shi, Y., Wang, P., Guachalla, L. M., Sun, B., Joerss, T., Chen, Y.-S., Groth, M., Krueger, A., Platzer, M., Yang, Y.-G., Rudolph, K. L., & Wang, Z.-Q. (2015). Smg6/Est1 licenses

embryonic stem cell differentiation via nonsense-mediated mRNA decay. *The EMBO Journal*, *34*(12), 1630–1647. https://doi.org/10.15252/embj.201489947

Li, Z., Lee, I., Moradi, E., Hung, N.-J., Johnson, A. W., & Marcotte, E. M. (2009). Rational Extension of the Ribosome Biogenesis Pathway Using Network-Guided Genetics. *PLOS Biology*, *7*(10), e1000213. https://doi.org/10.1371/journal.pbio.1000213

Limoncelli, K. A., Merrikh, C. N., & Moore, M. J. (2017). ASC1 and RPS3: New actors in 18S nonfunctional rRNA decay. *RNA (New York, N.Y.)*, *23*(12), Article 12. https://doi.org/10.1261/rna.061671.117

Liu, H., Rodgers, N. D., Jiao, X., & Kiledjian, M. (2002). The scavenger mRNA decapping enzyme DcpS is a member of the HIT family of pyrophosphatases. *EMBO Journal*, *21*(17), 4699–4708. Scopus. https://doi.org/10.1093/emboj/cdf448

Lu, J., & Deutsch, C. (2008). Electrostatics in the ribosomal tunnel modulate chain elongation rates. *Journal of Molecular Biology*, *384*(1), 73–86. https://doi.org/10.1016/j.jmb.2008.08.089

Maity, P., & Iben, S. (2022). Collisions and protein aggregations ahead: How aging affects ribosomal elongation dynamics. *Signal Transduction and Targeted Therapy*, *7*(1), Article 1. https://doi.org/10.1038/s41392-022-01001-2

Maquat, L. E. (2004). Nonsense-mediated mRNA decay: Splicing, translation and mRNP dynamics. *Nature Reviews Molecular Cell Biology*, *5*(2), Article 2. https://doi.org/10.1038/nrm1310

Matsuo, Y., Ikeuchi, K., Saeki, Y., Iwasaki, S., Schmidt, C., Udagawa, T., Sato, F., Tsuchiya, H., Becker, T., Tanaka, K., Ingolia, N. T., Beckmann, R., & Inada, T. (2017). Ubiquitination of stalled ribosome triggers ribosome-associated quality control. *Nature Communications*, *8*(1), Article 1. https://doi.org/10.1038/s41467-017-00188-1

Matsuo, Y., Tesina, P., Nakajima, S., Mizuno, M., Endo, A., Buschauer, R., Cheng, J., Shounai, O., Ikeuchi, K., Saeki, Y., Becker, T., Beckmann, R., & Inada, T. (2020). RQT complex dissociates ribosomes collided on endogenous RQC substrate SDD1. *Nature Structural & Molecular Biology*, *27*(4), Article 4. https://doi.org/10.1038/s41594-020-0393-9

Matsuo, Y., Uchihashi, T., & Inada, T. (2022). *Decoding of the ubiquitin code for clearance of colliding ribosomes by the RQT complex* (p. 2022.09.12.507701). bioRxiv. https://doi.org/10.1101/2022.09.12.507701

Mendell, J. T., Sharifi, N. A., Meyers, J. L., Martinez-Murillo, F., & Dietz, H. C. (2004). Nonsense surveillance regulates expression of diverse classes of mammalian transcripts and mutes genomic noise. *Nature Genetics*, *36*(10), 1073–1078. https://doi.org/10.1038/ng1429

Meydan, S., & Guydosh, N. R. (2020). Disome and Trisome Profiling Reveal Genome-wide Targets of Ribosome Quality Control. *Molecular Cell*, *79*(4), 588-602.e6. https://doi.org/10.1016/j.molcel.2020.06.010

Meyer, C., Garzia, A., Morozov, P., Molina, H., & Tuschl, T. (2020). The G3BP1-Family-USP10 Deubiquitinase Complex Rescues Ubiquitinated 40S Subunits of Ribosomes Stalled in

Translation from Lysosomal Degradation. *Molecular Cell*, *77*(6), 1193-1205.e5. https://doi.org/10.1016/j.molcel.2019.12.024

Morita, M., Ler, L. W., Fabian, M. R., Siddiqui, N., Mullin, M., Henderson, V. C., Alain, T., Fonseca, B. D., Karashchuk, G., Bennett, C. F., Kabuta, T., Higashi, S., Larsson, O., Topisirovic, I., Smith, R. J., Gingras, A.-C., & Sonenberg, N. (2012). A novel 4EHP-GIGYF2 translational repressor complex is essential for mammalian development. *Molecular and Cellular Biology*, *32*(17), 3585–3593. https://doi.org/10.1128/MCB.00455-12

Morris, C., Cluet, D., & Ricci, E. P. (2021). Ribosome dynamics and mRNA turnover, a complex relationship under constant cellular scrutiny. *Wiley Interdisciplinary Reviews. RNA*, *12*(6), e1658. https://doi.org/10.1002/wrna.1658

Muhlrad, D., Decker, C. J., & Parker, R. (1994). Deadenylation of the unstable mRNA encoded by the yeast MFA2 gene leads to decapping followed by 5'—>3' digestion of the transcript. *Genes & Development*, *8*(7), 855–866. https://doi.org/10.1101/gad.8.7.855

Muhlrad, D., Decker, C. J., & Parker, R. (1995). Turnover mechanisms of the stable yeast PGK1 mRNA. *Molecular and Cellular Biology*, *15*(4), 2145–2156. Scopus. https://doi.org/10.1128/MCB.15.4.2145

Muto, H., & Ito, K. (2008). Peptidyl-prolyl-tRNA at the ribosomal P-site reacts poorly with puromycin. *Biochemical and Biophysical Research Communications*, *366*(4), 1043–1047. https://doi.org/10.1016/j.bbrc.2007.12.072

Narita, M., Denk, T., Matsuo, Y., Sugiyama, T., Kikuguchi, C., Ito, S., Sato, N., Suzuki, T., Hashimoto, S., Machová, I., Tesina, P., Beckmann, R., & Inada, T. (2022). A distinct mammalian disome collision interface harbors K63-linked polyubiquitination of uS10 to trigger hRQT-mediated subunit dissociation. *Nature Communications*, *13*(1), Article 1. https://doi.org/10.1038/s41467-022-34097-9

Navickas, A., Chamois, S., Saint-Fort, R., Henri, J., Torchet, C., & Benard, L. (2020). No-Go Decay mRNA cleavage in the ribosome exit tunnel produces 5′-OH ends phosphorylated by Trl1. *Nature Communications*, *11*(1), Article 1. https://doi.org/10.1038/s41467-019-13991-9

Osuna, B. A., Howard, C. J., KC, S., Frost, A., & Weinberg, D. E. (2017). In vitro analysis of RQC activities provides insights into the mechanism and function of CAT tailing. *ELife*, *6*, e27949. https://doi.org/10.7554/eLife.27949

Park, H., & Subramaniam, A. R. (2019). Inverted translational control of eukaryotic gene expression by ribosome collisions. *PLOS Biology*, *17*(9), e3000396. https://doi.org/10.1371/journal.pbio.3000396

Passos, D. O., Doma, M. K., Shoemaker, C. J., Muhlrad, D., Green, R., Weissman, J., Hollien, J., & Parker, R. (2009). Analysis of Dom34 and Its Function in No-Go Decay. *Molecular Biology of the Cell*, *20*(13), 3025–3032. https://doi.org/10.1091/mbc.e09-01-0028

Pavlov, M. Y., Watts, R. E., Tan, Z., Cornish, V. W., Ehrenberg, M., & Forster, A. C. (2009). Slow peptide bond formation by proline and other N-alkylamino acids in translation.

Proceedings of the National Academy of Sciences of the United States of America, *106*(1), 50–54. https://doi.org/10.1073/pnas.0809211106

Pedersen, K., Zavialov, A. V., Pavlov, M. Y., Elf, J., Gerdes, K., & Ehrenberg, M. (2003). The bacterial toxin RelE displays codon-specific cleavage of mRNAs in the ribosomal A site. *Cell*, *112*(1), 131–140. https://doi.org/10.1016/s0092-8674(02)01248-5

Pisareva, V. P., Skabkin, M. A., Hellen, C. U. T., Pestova, T. V., & Pisarev, A. V. (2011a). Dissociation by Pelota, Hbs1 and ABCE1 of mammalian vacant 80S ribosomes and stalled elongation complexes. *The EMBO Journal*, *30*(9), Article 9. https://doi.org/10.1038/emboj.2011.93

Pisareva, V. P., Skabkin, M. A., Hellen, C. U. T., Pestova, T. V., & Pisarev, A. V. (2011b). Dissociation by Pelota, Hbs1 and ABCE1 of mammalian vacant 80S ribosomes and stalled elongation complexes. *The EMBO Journal*, *30*(9), 1804–1817. https://doi.org/10.1038/emboj.2011.93

Pochopien, A. A., Beckert, B., Kasvandik, S., Berninghausen, O., Beckmann, R., Tenson, T., & Wilson, D. N. (2021). Structure of Gcn1 bound to stalled and colliding 80S ribosomes. *Proceedings of the National Academy of Sciences*, *118*(14), e2022756118. https://doi.org/10.1073/pnas.2022756118

Powers, K. T., Szeto, J.-Y. A., & Schaffitzel, C. (2020). New insights into no-go, non-stop and nonsense-mediated mRNA decay complexes. *Current Opinion in Structural Biology*, *65*, 110–118. https://doi.org/10.1016/j.sbi.2020.06.011

Rom, E., Kim, H. C., Gingras, A. C., Marcotrigiano, J., Favre, D., Olsen, H., Burley, S. K., & Sonenberg, N. (1998). Cloning and characterization of 4EHP, a novel mammalian eIF4E-related cap-binding protein. *The Journal of Biological Chemistry*, *273*(21), 13104–13109. https://doi.org/10.1074/jbc.273.21.13104

Rubio, A., Ghosh, S., Mülleder, M., Ralser, M., & Mata, J. (2021). Ribosome profiling reveals ribosome stalling on tryptophan codons and ribosome queuing upon oxidative stress in fission yeast. *Nucleic Acids Research*, *49*(1), 383–399. https://doi.org/10.1093/nar/gkaa1180

Saito, K., Horikawa, W., & Ito, K. (2015). Inhibiting K63 Polyubiquitination Abolishes No-Go Type Stalled Translation Surveillance in Saccharomyces cerevisiae. *PLOS Genetics*, *11*(4), e1005197. https://doi.org/10.1371/journal.pgen.1005197

Saito, K., Kratzat, H., Campbell, A., Buschauer, R., Burroughs, A. M., Berninghausen, O., Aravind, L., Green, R., Beckmann, R., & Buskirk, A. R. (2022). Ribosome collisions induce mRNA cleavage and ribosome rescue in bacteria. *Nature*, *603*(7901), Article 7901. https://doi.org/10.1038/s41586-022-04416-7

Schmidt, S. A., Foley, P. L., Jeong, D.-H., Rymarquis, L. A., Doyle, F., Tenenbaum, S. A., Belasco, J. G., & Green, P. J. (2015). Identification of SMG6 cleavage sites and a preferred RNA cleavage motif by global analysis of endogenous NMD targets in human cells. *Nucleic Acids Research*, *43*(1), 309–323. https://doi.org/10.1093/nar/gku1258

Schmitt, K., Smolinski, N., Neumann, P., Schmaul, S., Hofer-Pretz, V., Braus, G. H., & Valerius, O. (2017). Asc1p/RACK1 Connects Ribosomes to Eukaryotic Phosphosignaling. *Molecular and Cellular Biology*, *37*(3), e00279-16. https://doi.org/10.1128/MCB.00279-16

Shao, S., Brown, A., Santhanam, B., & Hegde, R. S. (2015). Structure and assembly pathway of the ribosome quality control complex. *Molecular Cell*, *57*(3), 433–444. https://doi.org/10.1016/j.molcel.2014.12.015

Shao, S., & Hegde, R. S. (2014). Reconstitution of a minimal ribosome-associated ubiquitination pathway with purified factors. *Molecular Cell*, *55*(6), 880–890. https://doi.org/10.1016/j.molcel.2014.07.006

Shao, S., von der Malsburg, K., & Hegde, R. S. (2013). Listerin-dependent nascent protein ubiquitination relies on ribosome subunit dissociation. *Molecular Cell*, *50*(5), 637–648. https://doi.org/10.1016/j.molcel.2013.04.015

Shen, P. S., Park, J., Qin, Y., Li, X., Parsawar, K., Larson, M. H., Cox, J., Cheng, Y., Lambowitz, A. M., Weissman, J. S., Brandman, O., & Frost, A. (2015). Protein synthesis. Rqc2p and 60S ribosomal subunits mediate mRNA-independent elongation of nascent chains. *Science (New York, N.Y.)*, *347*(6217), 75–78. https://doi.org/10.1126/science.1259724

Shoemaker, C. J., Eyler, D. E., & Green, R. (2010a). Dom34:Hbs1 promotes subunit dissociation and peptidyl-tRNA drop off to initiate no-go decay. *Science (New York, N.Y.)*, *330*(6002), Article 6002. https://doi.org/10.1126/science.1192430

Shoemaker, C. J., Eyler, D. E., & Green, R. (2010b). Dom34:Hbs1 promotes subunit dissociation and peptidyl-tRNA drop off to initiate no-go decay. *Science (New York, N.Y.)*, *330*(6002), 369–372. https://doi.org/10.1126/science.1192430

Shoemaker, C. J., & Green, R. (2011a). Kinetic analysis reveals the ordered coupling of translation termination and ribosome recycling in yeast. *Proceedings of the National Academy of Sciences of the United States of America*, *108*(51), Article 51. https://doi.org/10.1073/pnas.1113956108

Shoemaker, C. J., & Green, R. (2011b). Kinetic analysis reveals the ordered coupling of translation termination and ribosome recycling in yeast. *Proceedings of the National Academy of Sciences of the United States of America*, *108*(51), E1392-1398. https://doi.org/10.1073/pnas.1113956108

Shoemaker, C. J., & Green, R. (2012). Translation drives mRNA quality control. *Nature Structural & Molecular Biology*, *19*(6), Article 6. https://doi.org/10.1038/nsmb.2301

Simms, C. L., Hudson, B. H., Mosior, J. W., Rangwala, A. S., & Zaher, H. S. (2014). An active role for the ribosome in determining the fate of oxidized mRNA. *Cell Reports*, *9*(4), 1256–1264. https://doi.org/10.1016/j.celrep.2014.10.042

Simms, C. L., Kim, K. Q., Yan, L. L., Qiu, J., & Zaher, H. S. (2018). Interactions between the mRNA and Rps3/uS3 at the entry tunnel of the ribosomal small subunit are important for no-go decay. *PLOS Genetics*, *14*(11), e1007818. https://doi.org/10.1371/journal.pgen.1007818

Simms, C. L., Yan, L. L., Qiu, J. K., & Zaher, H. S. (2019). Ribosome Collisions Result in +1 Frameshifting in the Absence of No-Go Decay. *Cell Reports*, *28*(7), 1679-1689.e4. https://doi.org/10.1016/j.celrep.2019.07.046

Simms, C. L., Yan, L. L., & Zaher, H. S. (2017). Ribosome Collision Is Critical for Quality Control during No-Go Decay. *Molecular Cell*, *68*(2), 361-373.e5. https://doi.org/10.1016/j.molcel.2017.08.019

Simms, C. L., & Zaher, H. S. (2016). Quality control of chemically damaged RNA. *Cellular and Molecular Life Sciences: CMLS*, *73*(19), Article 19. https://doi.org/10.1007/s00018-016-2261-7

Sinha, N. K., Ordureau, A., Best, K., Saba, J. A., Zinshteyn, B., Sundaramoorthy, E., Fulzele, A., Garshott, D. M., Denk, T., Thoms, M., Paulo, J. A., Harper, J. W., Bennett, E. J., Beckmann, R., & Green, R. (2020). EDF1 coordinates cellular responses to ribosome collisions. *ELife*, *9*, e58828. https://doi.org/10.7554/eLife.58828

Sitron, C. S., & Brandman, O. (2019). CAT tails drive degradation of stalled polypeptides on and off the ribosome. *Nature Structural & Molecular Biology*, *26*(6), 450–459. https://doi.org/10.1038/s41594-019-0230-1

Sitron, C. S., & Brandman, O. (2020). Detection and Degradation of Stalled Nascent Chains via Ribosome-Associated Quality Control. *Annual Review of Biochemistry*, *89*, 417–442. https://doi.org/10.1146/annurev-biochem-013118-110729

Sitron, C. S., Park, J. H., & Brandman, O. (2017). Asc1, Hel2, and Slh1 couple translation arrest to nascent chain degradation. *RNA (New York, N.Y.)*, *23*(5), 798–810. https://doi.org/10.1261/rna.060897.117

Starosta, A. L., & Wilson, D. N. (2014). Ribosome rescue, nearing the end. *Cell*, *156*(5), 866–867. https://doi.org/10.1016/j.cell.2014.02.028

Stein, K. C., Morales-Polanco, F., van der Lienden, J., Rainbolt, T. K., & Frydman, J. (2022). Ageing exacerbates ribosome pausing to disrupt cotranslational proteostasis. *Nature*, *601*(7894), Article 7894. https://doi.org/10.1038/s41586-021-04295-4

Stoneley, M., Harvey, R. F., Mulroney, T. E., Mordue, R., Jukes-Jones, R., Cain, K., Lilley, K. S., Sawarkar, R., & Willis, A. E. (2022). Unresolved stalled ribosome complexes restrict cell-cycle progression after genotoxic stress. *Molecular Cell*, *82*(8), 1557-1572.e7. https://doi.org/10.1016/j.molcel.2022.01.019

Sundaramoorthy, E., Leonard, M., Mak, R., Liao, J., Fulzele, A., & Bennett, E. J. (2017). ZNF598 and RACK1 Regulate Mammalian Ribosome-Associated Quality Control Function by Mediating Regulatory 40S Ribosomal Ubiquitylation. *Molecular Cell*, *65*(4), 751-760.e4. https://doi.org/10.1016/j.molcel.2016.12.026

T, S., S, L., M, K., K, I., A, I., Y, M., & T, I. (2019). Sequential Ubiquitination of Ribosomal Protein uS3 Triggers the Degradation of Non-functional 18S rRNA. *Cell Reports*, *26*(12). https://doi.org/10.1016/j.celrep.2019.02.067

Tesina, P., Lessen, L. N., Buschauer, R., Cheng, J., Wu, C. C., Berninghausen, O., Buskirk, A. R., Becker, T., Beckmann, R., & Green, R. (2020). Molecular mechanism of translational

stalling by inhibitory codon combinations and poly(A) tracts. *The EMBO Journal*, *39*(3), e103365. https://doi.org/10.15252/embj.2019103365

Tharun, S., & Parker, R. (2001). Targeting an mRNA for Decapping: Displacement of Translation Factors and Association of the Lsm1p–7p Complex on Deadenylated Yeast mRNAs. *Molecular Cell*, *8*(5), 1075–1083. https://doi.org/10.1016/S1097-2765(01)00395-1

Tomomatsu, S., Watanabe, A., Tesina, P., Hashimoto, S., Ikeuchi, K., Li, S., Matsuo, Y., Beckmann, R., & Inada, T. (2023). Two modes of Cue2-mediated mRNA cleavage with distinct substrate recognition initiate no-go decay. *Nucleic Acids Research*, *51*(1), 253–270. https://doi.org/10.1093/nar/gkac1172

Tsao, D., Shabalina, S. A., Gauthier, J., Dokholyan, N. V., & Diatchenko, L. (2011). Disruptive mRNA folding increases translational efficiency of catechol-O-methyltransferase variant. *Nucleic Acids Research*, *39*(14), 6201–6212. https://doi.org/10.1093/nar/gkr165

Tsuboi, T., Kuroha, K., Kudo, K., Makino, S., Inoue, E., Kashima, I., & Inada, T. (2012). Dom34:Hbs1 Plays a General Role in Quality-Control Systems by Dissociation of a Stalled Ribosome at the 3′ End of Aberrant mRNA. *Molecular Cell*, *46*(4), 518–529. https://doi.org/10.1016/j.molcel.2012.03.013

Tu, G.-F., Reid, G. E., Zhang, J.-G., Moritz, R. L., & Simpson, R. J. (1995). C-terminal Extension of Truncated Recombinant Proteins in *Escherichia coli* with a 10Sa RNA Decapeptide *. *Journal of Biological Chemistry*, *270*(16), 9322–9326. https://doi.org/10.1074/jbc.270.16.9322

Tuck, A. C., Rankova, A., Arpat, A. B., Liechti, L. A., Hess, D., Iesmantavicius, V., Castelo-Szekely, V., Gatfield, D., & Bühler, M. (2020). Mammalian RNA Decay Pathways Are Highly Specialized and Widely Linked to Translation. *Molecular Cell*, *77*(6), 1222-1236.e13. https://doi.org/10.1016/j.molcel.2020.01.007

Tucker, M., & Parker, R. (2000). Mechanisms And Control Of mRNA Decapping in Saccharomyces cerevisiae. *Annual Review of Biochemistry*, *69*(1), 571–595. https://doi.org/10.1146/annurev.biochem.69.1.571

Udagawa, T., Seki, M., Okuyama, T., Adachi, S., Natsume, T., Noguchi, T., Matsuzawa, A., & Inada, T. (2021). Failure to Degrade CAT-Tailed Proteins Disrupts Neuronal Morphogenesis and Cell Survival. *Cell Reports*, *34*(1). https://doi.org/10.1016/j.celrep.2020.108599

Unterholzner, L., & Izaurralde, E. (2004). SMG7 Acts as a Molecular Link between mRNA Surveillance and mRNA Decay. *Molecular Cell*, *16*(4), 587–596. https://doi.org/10.1016/j.molcel.2004.10.013

Ushida, C., Himeno, H., Watanabe, T., & Muto, A. (1994). TRNA-like structures in 10Sa RNAs of Mycoplasma capricolum and Bacillus subtilis. *Nucleic Acids Research*, *22*(16), 3392–3396. https://doi.org/10.1093/nar/22.16.3392

van den Elzen, A. M. G., Schuller, A., Green, R., & Séraphin, B. (2014). Dom34-Hbs1 mediated dissociation of inactive 80S ribosomes promotes restart of translation after stress. *The EMBO Journal*, *33*(3), 265–276. https://doi.org/10.1002/embj.201386123

van Hoof, A., Frischmeyer, P. A., Dietz, H. C., & Parker, R. (2002). Exosome-mediated recognition and degradation of mRNAs lacking a termination codon. *Science (New York, N.Y.)*, *295*(5563), Article 5563. https://doi.org/10.1126/science.1067272

Veltri, A. J., D'Orazio, K. N., Lessen, L. N., Loll-Krippleber, R., Brown, G. W., & Green, R. (2022). Distinct elongation stalls during translation are linked with distinct pathways for mRNA degradation. *ELife*, *11*, e76038. https://doi.org/10.7554/eLife.76038

Verma, R., Reichermeier, K. M., Burroughs, A. M., Oania, R. S., Reitsma, J. M., Aravind, L., & Deshaies, R. J. (2018). Vms1 and ANKZF1 peptidyl-tRNA hydrolases release nascent chains from stalled ribosomes. *Nature*, *557*(7705), Article 7705. https://doi.org/10.1038/s41586-018-0022-5

Vidya, E., & Duchaine, T. F. (2022). Eukaryotic mRNA Decapping Activation. *Frontiers in Genetics*, *13*, 832547. https://doi.org/10.3389/fgene.2022.832547

Wang, J., Zhou, J., Yang, Q., & Grayhack, E. J. (2018). Multi-protein bridging factor 1(Mbf1), Rps3 and Asc1 prevent stalled ribosomes from frameshifting. *ELife*, *7*, e39637. https://doi.org/10.7554/eLife.39637

Webster, M. W., Chen, Y.-H., Stowell, J. A. W., Alhusaini, N., Sweet, T., Graveley, B. R., Coller, J., & Passmore, L. A. (2018). MRNA Deadenylation Is Coupled to Translation Rates by the Differential Activities of Ccr4-Not Nucleases. *Molecular Cell*, *70*(6), Article 6. https://doi.org/10.1016/j.molcel.2018.05.033

Weinberg, D. E., Shah, P., Eichhorn, S. W., Hussmann, J. A., Plotkin, J. B., & Bartel, D. P. (2016). Improved Ribosome-Footprint and mRNA Measurements Provide Insights into Dynamics and Regulation of Yeast Translation. *Cell Reports*, *14*(7), 1787–1799. https://doi.org/10.1016/j.celrep.2016.01.043

Williams, K. P., Martindale, K. A., & Bartel, D. P. (1999). Resuming translation on tmRNA: A unique mode of determining a reading frame. *The EMBO Journal*, *18*(19), 5423–5433. https://doi.org/10.1093/emboj/18.19.5423

Winz, M.-L., Peil, L., Turowski, T. W., Rappsilber, J., & Tollervey, D. (2019). Molecular interactions between Hel2 and RNA supporting ribosome-associated quality control. *Nature Communications*, *10*(1), 563. https://doi.org/10.1038/s41467-019-08382-z

Wolf, A. S., & Grayhack, E. J. (2015). Asc1, homolog of human RACK1, prevents frameshifting in yeast by ribosomes stalled at CGA codon repeats. *RNA (New York, N.Y.)*, *21*(5), 935–945. https://doi.org/10.1261/rna.049080.114

Wu, C. C.-C., Peterson, A., Zinshteyn, B., Regot, S., & Green, R. (2020). Ribosome Collisions Trigger General Stress Responses to Regulate Cell Fate. *Cell*, *182*(2), 404-416.e14. https://doi.org/10.1016/j.cell.2020.06.006

Yan, L. L., Simms, C. L., McLoughlin, F., Vierstra, R. D., & Zaher, H. S. (2019). Oxidation and alkylation stresses activate ribosome-quality control. *Nature Communications*, *10*(1), 5611. https://doi.org/10.1038/s41467-019-13579-3

Yan, L. L., & Zaher, H. S. (2021). Ribosome-quality control antagonizes the activation of the integrated-stress response on colliding ribosomes. *Molecular Cell*, *81*(3), 614-628.e4. https://doi.org/10.1016/j.molcel.2020.11.033

Yip, M. C. J., & Shao, S. (2021). Detecting and Rescuing Stalled Ribosomes. *Trends in Biochemical Sciences*, *46*(9), 731–743. https://doi.org/10.1016/j.tibs.2021.03.008

Yonashiro, R., Tahara, E. B., Bengtson, M. H., Khokhrina, M., Lorenz, H., Chen, K.-C., Kigoshi-Tansho, Y., Savas, J. N., Yates, J. R., III, Kay, S. A., Craig, E. A., Mogk, A., Bukau, B., & Joazeiro, C. A. (2016). The Rqc2/Tae2 subunit of the ribosome-associated quality control (RQC) complex marks ribosome-stalled nascent polypeptide chains for aggregation. *ELife*, *5*, e11794. https://doi.org/10.7554/eLife.11794

Young, D. J., & Guydosh, N. R. (2022). Rebirth of the translational machinery: The importance of recycling ribosomes. *BioEssays: News and Reviews in Molecular, Cellular and Developmental Biology*, *44*(4), e2100269. https://doi.org/10.1002/bies.202100269

Young, D. J., Guydosh, N. R., Zhang, F., Hinnebusch, A. G., & Green, R. (2015). Rli1/ABCE1 Recycles Terminating Ribosomes and Controls Translation Reinitiation in 3'UTRs In Vivo. *Cell*, *162*(4), 872–884. https://doi.org/10.1016/j.cell.2015.07.041

Yu, C.-H., Dang, Y., Zhou, Z., Wu, C., Zhao, F., Sachs, M. S., & Liu, Y. (2015). Codon Usage Influences the Local Rate of Translation Elongation to Regulate Co-translational Protein Folding. *Molecular Cell*, *59*(5), 744–754. https://doi.org/10.1016/j.molcel.2015.07.018

Zhao, T., Chen, Y.-M., Li, Y., Wang, J., Chen, S., Gao, N., & Qian, W. (2021). Disome-seq reveals widespread ribosome collisions that promote cotranslational protein folding. *Genome Biology*, *22*(1), 16. https://doi.org/10.1186/s13059-020-02256-0

Zuberek, J., Kubacka, D., Jablonowska, A., Jemielity, J., Stepinski, J., Sonenberg, N., & Darzynkiewicz, E. (2007). Weak binding affinity of human 4EHP for mRNA cap analogs. *RNA (New York, N.Y.)*, *13*(5), 691–697. https://doi.org/10.1261/rna.453107

Zurita Rendón, O., Fredrickson, E. K., Howard, C. J., Van Vranken, J., Fogarty, S., Tolley, N. D., Kalia, R., Osuna, B. A., Shen, P. S., Hill, C. P., Frost, A., & Rutter, J. (2018). Vms1p is a release factor for the ribosome-associated quality control complex. *Nature Communications*, *9*(1), Article 1. https://doi.org/10.1038/s41467-018-04564-3

Permissions to use copyright material

Mechanisms tailoring the expression of heat shock proteins to proteostasis challenges

Lokha R Alagar Boopathy, Suleima Jacob-Tomas, Célia Alecki, and Maria Vera.

Copyright © 2022 The Authors

This is an open access article under the CC BY-NC-ND license (http://creativecommons.org/licenses/by-nc-nd/4.0/).

Proteostasis regulation through ribosome quality control and no-go-decay.

Lokha R Alagar Boopathy, Emma Beadle, Aitana Garcia-Bueno Rico, and Maria Vera.

This is an open access article under the CC BY-NC-ND license.

The ribosome quality control factor Asc1 determines the fate of HSP70 mRNA on and off the ribosome.

Lokha R Alagar Boopathy, Emma Beadle, Alan RuoChen Xiao, Aitana Garcia-Bueno Rico, Celia Alecki, Irene Garcia de-Andres, Kyla Edelmeier, Luca Lazzari, Mehdi Amiri, and Maria Vera.